

University of Alberta

Neonatal Cardiac Fatty Acid Metabolism

by

Victoria Hol Mun Lam

A thesis submitted to the Faculty of Graduate Studies and Research
in partial fulfillment of the requirements for the degree of

Doctor of Philosophy
Medical Sciences - Pediatrics

©Victoria Hol Mun Lam

Spring 2012

Edmonton, Alberta

Permission is hereby granted to the University of Alberta Libraries to reproduce single copies of this thesis and to lend or sell such copies for private, scholarly or scientific research purposes only. Where the thesis is converted to, or otherwise made available in digital form, the University of Alberta will advise potential users of the thesis of these terms.

The author reserves all other publication and other rights in association with the copyright in the thesis and, except as herein before provided, neither the thesis nor any substantial portion thereof may be printed or otherwise reproduced in any material form whatsoever without the author's prior written permission.

Dedication

With gratitude, this thesis is dedicated to my grandparents, Tim and Kwen Ying Lam and Albert and Sup Wai Lee, and parents, Victor and Elizabeth Lam.

Abstract

The surgical repair of congenital heart defects (CHDs) often requires a bloodless/motionless field achieved by arresting the neonatal heart and exposing it to a period of ischemia. Metabolic manipulation, such as suppression of fatty acid (FA) oxidation, improves post-ischemic functional recovery in adult hearts. However, the metabolic profile of a neonatal heart differs dramatically from that of an adult. The neonatal heart is highly dependent on FA oxidation while glucose metabolic rates remain low until weaning. Since the neonatal myocardium is a FA-centered metabolism, then, unlike the adult heart, augmenting FA oxidation may improve its post-ischemic function recovery by increasing ATP available to the myocardium. In these studies, hearts were isolated from relevant neonatal rabbit models to study insulin's effect, neonatal volume-overload hypertrophy, neonatal cardiac hypertrophy treated with a peroxisome proliferator activated-receptor- α (PPAR α) agonist. The hearts were perfused *ex vivo* to assess changes in cardiac metabolism and post-ischemic functional recovery associated with each treatment. The results demonstrate that high fat alters the neonatal heart's response to insulin to increase FA oxidation and improve post-ischemic functional recovery. In contrast, neonatal cardiac hypertrophy downregulates FA metabolism and is associated with poor post-ischemic functional recovery. The administration of a PPAR α agonist upregulated the FA metabolic pathway; therefore, FA metabolism increased and rescued the metabolic phenotype associated with cardiac hypertrophy and normalized post-ischemic functional

recovery. In conclusion, augmenting FA oxidation with clinical levels of insulin in the normal neonatal heart and or a PPAR α agonist in hypertrophied neonatal hearts improves post-ischemic functional recovery and may be a viable therapy of ischemia-reperfusion protection.

Acknowledgement

I would like to thank my supervisors, Dr. Gary Lopaschuk and Dr. Ivan Rebeyka, for mentoring me in your laboratories, for the opportunities to participate in the process of research, the many grilling sessions that have improved my presentation and query skills, and for their patience and support.

Thank you, Dr. Jason Dyck, for always asking for more and giving me insightful input and advice during my committee meetings.

Many thanks to my examiners, Dr. Zamaneh Kassiri, Dr. Peter Light, and Dr. Thomas Scholz, for their patience and insightful input.

Thank you, Donna Beker and Sandy Kelly, for your technical and emotional support. Nothing could have been achieved without their encouragement, help, and attentive ears.

I am indebted to Dr. Jagdip Jaswal and Dr. Wendy Keung for your continuous support throughout my graduate studies from advising, to active teaching, to editing, they contributed extensively my education and experience.

Many thanks to Joanne Zhao, Panakkezhum Thomas, and Ken Strynadka for your expertise in RT-PCR and HPLC.

My deepest appreciation goes to Mary-Jo Boeglin and Cheryl Meriot for both of your hard work in getting me through the paper work and meetings during my graduate studies. Most of all, thank you for your friendships.

To my family, especially my grandparents and parents, who this thesis is for, this thesis is a testimony to your prayers, love, support, patience, and inspiration. You have each taught me to seek more knowledge and given me the emotional and intellectual tools to do it. This thesis is as much mine as it is yours.

To my best friend, Po-Yee Chan, thank you for your patience and support all these years. Thank you for listening and praying for and with me all these years.

Thank you, Shu-Wei Lee, for your love. You have upheld our relationship with prayer, a supportive attitude, and patience. I would not have experienced life without you as part of it.

To my many friends I have made at the lab and in the Heritage Medical Research Centre: Dr. Tatsujiro Oka, Virgilio Cadete, Dr. John Ussher, Brandon Tanner, Dr. Joanna Lucy Stanley, Linn Moore, Vijay Kandalam, Dr. Ratnadeep Basu, Brandi

Sidlick, Shannon Lang, Dr. Miranda Sung, Cory Wagg, Dr. Wei Wang and many more. Thank you all.

Table of Content

1	Introduction	1
1.1	Neonatal Heart Energy metabolism	2
1.2	Neonatal Carbohydrate Metabolism	3
1.3	Fatty Acid Transport and Oxidation	7
1.4	Mechanisms in Cardiac Metabolic Maturation	9
1.5	Peroxisome Proliferator-Activated Receptor α in the Heart	13
1.6	Hypoxia-Inducible Factor- α in the Heart	15
1.7	Ischemia-Reperfusion Injury and the Neonatal Heart	16
1.8	Ischemia-Reperfusion Injury	17
1.9	Ischemia-Reperfusion Injury in the Neonatal Myocardium	20
1.10	Cardiac Hypertrophy and Energy Metabolism	24
1.11	Peroxisome Proliferator-Activated Receptor α in Cardiac Hypertrophy	26
1.12	Hypoxia Inducible Factor-1 α and Glucose Metabolism in Cardiac Hypertrophy	30
1.13	Neonatal Cardiac Hypertrophy	33
1.14	The Neonatal Rabbit Model	35
1.15	General Hypothesis	38
1.16	References	39
1.17	Figures	87

2	Supra-physiological Insulin Levels Elevate Palmitate Oxidation to Improve Neonatal Rabbit Heart Ischemia-Reperfusion Recovery	99
2.1	Introduction	101
2.2	Materials and Methods	104
	<i>Animals</i>	104
	<i>Isolated working-heart perfusion using the 7-day-old rabbit model</i>	104
	<i>Quantifying Fatty Acid Oxidation, Glucose Oxidation, and Glycolysis</i>	106
	<i>Steady State ATP production</i>	108
	<i>Quantifying Plasma Membrane CD36 and GLUT4 Content</i>	109
	<i>Triacylglycerol (TG) Quantification</i>	109
	<i>Immunoblot Assay</i>	110
	<i>Statistical Analysis</i>	111
2.3	Results	111
	<i>Benefits of a High Fat Concentration on Cardiac Function</i>	111
	<i>Effects of 0.1 or 10 U/L Insulin on Cardiac Function</i>	112
	<i>Control of Metabolism in Ischemic-Reperfused Neonatal Hearts</i>	113
2.4	Discussion	114
	<i>High Fatty Acids are Beneficial to the Neonatal Heart During Reperfusion</i>	115
	<i>10 U/L insulin Improves Post-ischemic Cardiac Recovery Only in the Presence of 1.2 mM Palmitate</i>	117
2.5	Limitations	122
2.6	References	126
2.7	Figures	133

2.8	Tables	144
3	Neonatal Rabbit Aorto-Caval Shunt Volume-Overload Cardiac Hypertrophy Model	145
3.1	Introduction	147
3.2	Materials and Methods	148
	<i>Animals</i>	148
	<i>The Aorto-caval Shunt</i>	149
	<i>Echocardiography Evaluation of the Aorta-Caval Shunt and of Cardiac Size and Function</i>	151
3.3	Results	152
	<i>Shunt Success Rates were Different Between the Two Models</i>	152
	<i>Shunt Patency Detection by Ultrasound Increased IVC Diameter</i>	153
	<i>Volume-overload Cardiac Hypertrophy Resulted from the Shunt Procedure</i>	153
3.4	Discussion	154
3.5	Limitations	158
3.6	References	164
3.7	Figures	171
3.8	Tables	180
4	Cardiac Hypertrophy in the Newborn Delays the Maturation of Fatty Acid β-Oxidation and Compromises Post-ischemic Functional Recovery	183
4.1	Introduction	186
4.2	Methods and Material	189
	<i>Animals</i>	189
	<i>Induction of volume-overload via production of an aorto-caval fistula in newborn rabbits</i>	189

	<i>Echocardiography</i>	190
	<i>Isolated Bi-ventricular Heart Perfusion Model</i>	191
	<i>Mechanical Measurements in Isolated Rabbit Bi-ventricular Working Heart</i>	192
	<i>Tissue Sample Preparation for Immunoblot Analysis</i>	193
	<i>Immunoblot Analysis</i>	193
	<i>Pyruvate Dehydrogenase Activity Assay</i>	194
	<i>Citrate Synthase Activity Assay</i>	196
	<i>β-hydroxyacyl CoA Dehydrogenase Activity Assay (β-HAD)</i>	197
	<i>Malonyl-CoA Dehydrogenase (MCD) Activity Assay</i>	197
	<i>Peroxisome Proliferator Activated Receptor (PPAR)-α PPAR-α mRNA Expression</i>	199
	<i>Statistical Analyses</i>	200
4.3	Results	200
	<i>Establishing and Assessing Cardiac Hypertrophy by Echocardiography</i>	200
	<i>Aerobic Cardiac Function in Isolated Bi-ventricular Working Hearts</i>	201
	<i>Impact of Ischemia on Hypertrophied Hearts</i>	202
	<i>Metabolism in Aerobically-Perfused Hypertrophied Newborn Rabbit Hearts</i>	203
	<i>Control of Fatty Acid Oxidation in Hypertrophied Hearts</i>	204
	<i>HIF-1α Expression and PPARα Expression and Activity in Control and Hypertrophied Hearts</i>	205
4.4	Discussion	206
4.5	Conclusion	212
4.6	Limitations	213
4.7	References	219
4.7	Figures	229
4.8	Tables	244

5	Activating Peroxisome Proliferator-Activated Receptor α Prevents Post-Ischemic Contractile Dysfunction in the Hypertrophied Neonatal Heart	249
5.1	Introduction	251
5.2	Materials and Methods	254
	<i>Animals</i>	254
	<i>Induction of Volume-overload via Production of an Aorto-caval Fistula in Neonatal Rabbits and GW7647 Treatment</i>	254
	<i>Isolated Bi-ventricular Heart Perfusion Model</i>	255
	<i>Tissue Sample Preparation for Immunoblot Analysis</i>	256
	<i>PPAR-α mRNA Expression</i>	257
	<i>Triglycerol (TG) Quantification</i>	258
	<i>Carnitine Palmitoyl Transferase-1 (CPT-1) Activity Assay</i>	258
5.3	Results	259
	<i>The Effects of GW7467 Treatment</i>	259
	<i>GW7467 Rescues Post-ischemic Cardiac Dysfunction in Hypertrophied Hearts</i>	261
	<i>GW7467 Increased ATP Production Rates</i>	261
	<i>GW7467 Altered Gene Transcription</i>	263
	<i>GW7467 Removed CPT-1 Inhibition in Hypertrophied Hearts</i>	264
	<i>Intracellular Triacylglycerol (TG) Storage Altered by Hypertrophy and GW7467 treatment</i>	265
	<i>Glucose Uptake and Metabolism</i>	266
5.4	Discussion	268
	<i>The Hypertrophied Neonatal Heart and Tolerance to Ischemia-Reperfusion</i>	269
	<i>GW7647 Normalizes the Regulatory Pathway on FA Oxidation in Hypertrophied Neonatal Myocardium</i>	272
	<i>GW7647 Altered FA Uptake and Utilization</i>	275
	<i>GW7647 Suppresses HIF-1α and Downstream Effectors</i>	277

	<i>GW7647 Effects on Cardiac Hypertrophy and Implications on Cardiac Surgery</i>	279
5.5	Conclusion	281
5.6	Limitations	281
5.7	References	285
5.8	Figures	301
5.9	Tables	320
6	General discussion	321
6.1	Increasing FA Oxidation Improved Normal Neonatal Cardiac Post-ischemic Contractile Recovery	323
6.2	A Model of Neonatal Cardiac Pathological Hypertrophy	325
6.3	Neonatal Cardiac Hypertrophy Alters Cardiac Metabolism	329
6.4	Rescuing the Ischemic-Reperfused Neonatal Heart	332
6.5	Conclusion	335
6.6	Future Directions	336
6.7	References	339

Lists of Tables

Table 2-1: Comparison of rates of glycolysis and glucose oxidation when perfused with 0.4 mM or 1.2 mM palmitate	144
Table 2-2: Average pre- and post-ischemia cardiac hemodynamic parameters	144
Table 2-3: Metabolic rates of hearts perfused with 0.4 mM palmitate treated with 0.1 or 10 U/L insulin	144
Table 3-1: Success rates of aorto-caval shunt operation	180
Table 3-2: Physical and Cardiac Parameters in 20-day-old rabbits with sham or model A (single puncture) aorto-caval shunt operation	180
Table 3-3: Physical and Cardiac Parameters in 20-day-old rabbits with sham or model B (triple puncture) aorto-caval shunt operation	181
Table 4-1 Physical and Cardiac Parameters in 20-day-old rabbits and hypertrophy rabbits	244
Table 4-2: Cardiac function and corresponding ATP:AMP ratios in 21-day-old control and hypertrophy hearts under aerobic bi-ventricular perfusion or ischemic reperfusion	245
Table 4-3: Percent contribution to ATP production	246
Table 4-4: PDH, citrate synthase and β HAD activity in 1-day, 7-day, 21-day control and 21-day hypertrophy	247
Table 5-1: Physical and Cardiac Parameters in vehicle- or GW7647-treated 20-day-old rabbits with of sham or aorto-caval fistula operation	320

Lists of Figures

Figure 1-1: Changes in Cardiac Metabolism Capacity During the Neonatal Period.	89
Figure 1-2: CD36 Translocation Signalling.	91
Figure 1-3: Schematic of the Process of Long Chain Fatty Acid Transport for Fatty Acid β -Oxidation.	93
Figure 1-4: Insulin Signalling in the Neonatal Period.	95
Figure 1-5: Hypoxia-Inducible Factor-1 α (HIF-1 α) in Normoxia and Hypoxia.	97
Figure 2-1: Neonatal Cardiac Function and Metabolism in 0.4 mM Palmitate or 1.2 mM Palmitate Without the Effects of Insulin.	135
Figure 2-2: Neonatal Cardiac Function in 0.4 mM Palmitate or 1.2 mM Palmitate Treated with Either 0.1 or 10 U/L Insulin.	137
Figure 2-3: The Metabolic Effects of 0.1 and 10 U/L Insulin in Neonatal Hearts Perfused With 1.2 mM Palmitate.	139
Figure 2-4: 10 U/L insulin Activates Akt and Inhibits AMPK Activation Without Affecting ACC Phosphorylation in 1.2 mM Palmitate-Perfused Hearts.	141
Figure 2-5: Cardiac Plasma Membrane CD36 is Increased in the Presence of 10 U/L Insulin Stimulation While Perfused with 1.2 mM Palmitate.	143
Figure 3-1: Schematic of the aorto-caval shunt models A and B	173
Figure 3-2: Timeline of events.	175
Figure 3-3: Ultrasound of the Aorto-Caval Shunt.	177
Figure 3-4: Representative M-mode Images.	179
Figure 4-1: Aorto-caval Fistula Validation and Volume-Overload Cardiac Hypertrophy Assessment.	231

Figure 4-2: Comparison of 21-day-old control and hypertrophy LV cardiac functions during 30 min aerobic left ventricular followed by 30 min bi-ventricular perfusion.	233
Figure 4-3: Metabolic Effects of Neonatal Volume-Overload Cardiac Hypertrophy.	235
Figure 4-4: MCD Expression and Activity and Malonyl-CoA Levels in Control and Hypertrophied Neonatal Hearts.	237
Figure 4-5: AMPK expression and phosphorylation do not change in hypertrophied hearts compared to controls in left (LV) or right (RV) ventricles	239
Figure 4-6: Cardiac HIF-1 α Expression and PPAR- α Activity Change with Age and Hypertrophy.	241
Figure 4-7: Post-Ischemic Metabolic Rates From Control and Hypertrophied Hearts Subjected to 25 minutes of Ischemia.	243
Figure 5-1: Bi-ventricular Perfusion of 21-day-old Rabbit Hearts.	303
Figure 5-2: Pre-Ischemic and Post-ischemic Metabolic Rates Measured During Bi-ventricular Isolated Heart Perfusions.	305
Figure 5-3: Calculated Steady State ATP and Acetyl-CoA Production Rates of Control, Hypertrophied, and GW7647-Treated Hypertrophied Hearts.	307
Figure 5-4: Expression of PPAR α and HIF-1 α in Control, Hypertrophied, and GW7647-Treated Hypertrophied Hearts.	309
Figure 5-5: GW7467 Removes CPT-1 Inhibition in Hypertrophied Hearts.	311
Figure 5-6: Malonyl-CoA Levels are Reflective of Collective Changes in MCD and ACC.	313
Figure 5-7: GW7647 Decreases Triacylglycerol Pools in the LV and RV Relative to Altered Enzyme Expression.	315

Figure 5-8: Effects of Hypertrophy and GW7647 Treatment on Regulators of Glucose Metabolism in the LV and RV in Control, Hypertrophied, and GW7647-Treated Hypertrophied Hearts. 317

Figure 5-9: The Rate-Limiting Step to Glucose Oxidation is Controlled by PDH Activity. 319

List of Abbreviations

%EF	Percent ejection fraction
ACC	Acetyl-CoA carboxylase
ADP	Adenosine diphosphate
AICAR	5-aminoimidazole-4-carboxamide-1-beta-D-ribofuranoside
Akt	Protein Kinase B
AMPK	5'-adenosine monophosphate activated protein kinase
Ang II	Angiotensin II
ANOVA	Analysis of Variance
AoPSP	Aortic Peak Systolic Pressure
ASD	Atrial septal defect
ATGL	Adipose triacylglycerol lipase
ATP	Adenosine Triphosphate
AU	Arbitrary Unit
AVSD	Atrioventral Septal Defect
β HAD	β -hydroxyacyl CoA dehydrogenase
BSA	Bovine serum albumin
BW	Body weight
CAT	Carnitine acyl-translocase
CD36	Cluster of Differentiation 36
CHD	Congenital heart disease
CMR	Cardiac magnetic resonance imaging
CO ₂	Carbon dioxide
CPT	Carnitine palmitoyltransferase
CPT-1	Carnitine palmitoyltransferase-1
CPT-2	Carnitine palmitoyltransferase-2
CS	Citrate synthase
dAo	Descending Aorta
DCA	Dichloroacetate
DHAP	Dihydroxyacetone phosphate
DMSO	Dimethylsulfoxide
ECG	Electrocardiogram
Echo	Echocardiography
ED	Embryonic day
F2,6-BP	Fructose 2, 6-bisphosphate
FA	Fatty acid
FABP	FA binding protein
FABP _{pm}	Plasma membrane fatty acid binding protein
FADH ₂	Reduced Flavin Adenine Dinucleotide
FAT/CD36	Fatty acid translocase
FATP	Fatty acid transport protein
FFA	Free fatty acid

GIK	Glucose-Insulin-Potassium
GLUT1	Glucose transporter 1
GLUT2	Glucose transporter 2
GPAT	Glycerol-phosphate acyltransferase
HIF	Hypoxia-inducible factor
HIF-1 α	Hypoxia-inducible factor-1 α
HK	Hexokinase
HK-I	Hexokinase-I
HK-II	Hexokinase-II
HR	Heart Rate
IR	Ischemic-reperfusion
IVC	Inferior vena cava
IVS	Interventricular septum
LCFA	Long-chain fatty acid
L-CPT-1	Liver-Carnitine Palmitoyltransferase-1
LDH	Lactate dehydrogenase
LKB1	Liver Kinase B1
L-NAME	L-N ^G -Nitroarginine methyl ester
LPL	Lipoprotein lipase
LTCC	L-type calcium channels
LV	Left ventricle
LV:BW	Left ventricular weight to body weight ratio
LVIDd	Left ventricular internal diameter, diastole
LVPW	Left ventricular posterior wall
MCAD	Medium chain acyl-CoA dehydrogenase
MCD	Malonyl-CoA decarboxylase
M-CPT-1	Muscle-Carnitine Palmitoyltransferase-1
MCT	Monocarboxylate transporter
MPT	Mitochondrial transition permeability
mRNA	Messenger ribonucleic acid
mTOR	mammalian target of rapamycin
NADH	Nicotinamide adenine dinucleotide
NCX	Na ⁺ -Ca ²⁺ anti-porter
NHE	Na ⁺ -H ⁺ exchanger
P-ACC	Phosphorylated acetyl-CoA carboxylase
P-AMPK	Phosphorylated 5'-adenosine monophosphate activated protein kinase
PCI	Percutaneous coronary intervention
PDA	Patent ductus arteriosus
PDH	Pyruvate dehydrogenase
PDK	Pyruvate dehydrogenase kinase
PDK4	Pyruvate dehydrogenase-4
PFK	Phosphofructokinase

PFK-1	6-phosphofructosekinase-1
PFK-2	6-phosphofructosekinase-2
PGC-1 α	Peroxisome proliferator-activated receptor gamma coactivator 1-alpha
PHD	Prolyl-Hydroxylase Demain-containing enzymes
PI3 Kinase	Phosphoinositol-3-kinase
PPAR	Peroxisome proliferator-activated receptor
PPAR γ	Peroxisome proliferator-activated receptor- γ
PPAR α	Peroxisome proliferator agonist receptor- α
PPAR β	Peroxisome proliferator-activated receptor- β
PPAR δ	Peroxisome proliferator-activated receptor- δ
PSP	Peak Systolic Pressure
PVPSP	Pulmonary Venous Peak Systolic Pressure
PW	Posterior Wall
RT	Room Temperature
RV	Right ventricle
RV: BW	Right ventricular weight to body weight ratio
RVD	Right ventricular diameter
RVIDd	Right ventricular internal diameter, diastole
RXR	Retinoid X Receptor
SEM	Standard Error of the Mean
Sep	Septum
SEP: BW	Septum weight to body weight ratio
SERCA	Sarcoplasmic Reticulum Ca ²⁺ -ATPase
SR	Sarcoplasmic Reticulum
T-ACC	Total acetyl-CoA carboxylase
T-AMPK	Total 5'-adenosine monophosphate activated protein kinase
TCA cycle	Tricarboxylic acid cycle
TG	Triacylglycerol
VHL	von-Hippel Lindau
VSD	Ventricular septal defect
WT	Wild Type

Chapter 1

Introduction

1.1 Neonatal Heart Energy Metabolism and Pathological Alterations

The heart's energy demands are met through several catabolic pathways: glycolysis, glucose oxidation, Fatty acid (FA) oxidation (mostly oleic and palmitic acids), and lactate oxidation (fig 1-1). The adult heart derives 50-70% of its required ATP from FA oxidation (1-3). In contrast, the fetal heart relies heavily on anaerobic glycolysis to meet its energy demands (4-6). Approximately 44% of total ATP production in the fetal heart is derived from glycolysis (6) while FA oxidation contributes ~15% (6). Over the neonatal period, the heart adapts to a high-fat milk diet as a new source of energy substrate (7). In rabbits, by 7 days old, the heart's glycolytic rate drops to 5% and FA oxidation rates increase 10 folds making it the primary supply of ATP (8). Within this neonatal period, the myocardium undergoes drastic hemodynamic, structural, and metabolic modifications. Therefore, the neonatal myocardium responds to ischemia-reperfusion much differently compared to the adult heart. The neonatal hearts that are subjected to ischemia-reperfusion are often those with a congenital heart defect (CHD) requiring cardiac surgery. The defect itself is capable of altering hemodynamics sufficiently to cause pressure- or volume-overload cardiac hypertrophy. As cardiac hypertrophy modifies cardiac metabolism in the adult heart, the hypertrophied neonatal myocardium may also have distorted metabolism and consequently an altered response to ischemia-reperfusion. However, the disparity between adult and neonatal heart metabolism prevents the translation of adult cardiac therapies to the neonatal population. Herein,

focus will be placed on the neonatal metabolic transition, ischemia-reperfusion injury, and cardiac hypertrophy.

1.2 Neonatal Carbohydrate Metabolism

The maturation of myocardial glucose metabolism is multi-faceted and includes changes to glucose uptake and trapping, glycolysis, and glucose oxidation. This transition occurs over the neonatal period, but full maturation of the glucose oxidation pathway cannot be appreciated until after weaning (6,7).

Glucose uptake is controlled by the glucose transporters embedded within the plasma membrane. While GLUT1 is constitutively present in the plasma membrane and is responsible for basal glucose uptake, GLUT4 translocation to the plasma membrane is controlled by insulin stimulation. This regulation of glucose uptake fine-tunes coordination of alternate substrate metabolism to the metabolic needs of the heart. GLUT1 is the predominant glucose transporter found in the fetal heart and remains so in the immediate newborn heart (9-12). In the neonatal period, GLUT1 expression decreases as GLUT4 expression increases (9-12). Hexokinase (HK)-I is part of the basal glucose uptake along with GLUT1 expression. HK phosphorylates glucose molecules to generate glucose-6-phosphate, preventing its expulsion from the cytoplasm to provide a negative gradient that further draws glucose into the cytoplasm. As GLUT1 to GLUT4 expressional dominance changes, HK-I expression subsides and the expression of HK-II, often found in insulin-sensitive tissues (13,14), increases in the neonatal

period (9,10). These expression changes could be thought of as increased insulin sensitivity and control over glucose uptake.

However, in bovine hearts, coinciding with GLUT4 upregulation, the number of insulin and insulin-like-growth factor-1 receptors may be decreased during this period (12). Whole-body insulin resistance is also apparent in neonatal dogs in which liver glucose production is incompletely decreased upon insulin stimulation compared to an adult (15). Insulin receptor binding affinity does not differ greatly between adult and neonatal canine hearts (16). Therefore, it has been hypothesized that insulin resistance in the neonatal myocardium may exist due to a post-receptor mechanism (15,16). Hence, though the switch to GLUT4-predominant glucose uptake occurs, insulin control over metabolism may play a lesser role than that found in the adult heart. Simultaneous to this insulin-resistant state, plasma insulin levels decrease in the neonatal period (7). These changes help promote the development and the dependence of the neonatal heart on FA oxidation.

Downstream to glucose uptake and its activation into glucose-6-phosphate by HK, glycolysis and glucose (pyruvate) oxidation metabolize glucose into energy units. The ATP contribution from glycolysis in the heart drops dramatically during the neonatal period due to altered expression of glycolytic enzyme expression (5,17-19) and regulatory signaling proteins (20,21). Fetal cardiac glycolytic rates are in excess compared to that found in the normal adult heart; and these rates

persist in the immediate newborn as found in 1-day old rabbit hearts (6). In contrast, the glycolytic rates in 7-day-old rabbit hearts decrease to levels found in the adult heart and supply less than 10% of the necessary ATP (6,8). This change is largely the product of altered phosphofructokinase (PFK)-1 isozyme expression (20,21). PFK1 is a key glycolytic enzyme that is heavily regulated to control the rate of glycolysis as it catalyzes the formation of fructose 1,6-bisphosphate from fructose-6-phosphate. PFK1 is allosterically inhibited by ATP, a process which is potentiated by citrate. On the other hand, PFK1 activity can be stimulated by fructose 2, 6-bisphosphate (F2,6-BP) produced by PFK2. During the neonatal period, the expression of the muscle PFK1 isoform is increased compared to the fetal level (21). Fetal PFK1 is more sensitive to F2,6-BP stimulation and less sensitive to ATP inhibition, while that of the adult is more sensitive to changes in ATP and citrate levels compared to F2,6-BP stimulation (20). Therefore, during maturation, as PFK1 isoforms switch, glycolysis becomes increasingly regulated and sensitive to changes in ATP and citrate produced from alternative substrates, such as FA, and therefore more easily suppressed as FA oxidation predominates.

The metabolic fate of glycolytic products also changes with maturation. In order for glycolysis to produce a meaningful energy equivalent, NADH must be converted into ATP in the mitochondria. This conversion requires the malate-aspartate shuttle to transfer the NADH into the mitochondria in order that the electron transport chain converts it to ATP. In maturation, the malate-aspartate

shuttle capacity decreases during the neonatal period (22,23). In porcine hearts, this decline occurs within 35 days of birth (23) and parallels the decline in glycolysis simultaneous to increased FA oxidation rates.

Another end product of glycolysis is pyruvate. In the fetal heart, much of the pyruvate produced from anaerobic glycolysis is converted into lactate rather than undergo oxidation (4). In turn, the fetal heart readily oxidizes lactate (17,24). Incidentally, lactate oxidation accounts for most of the fetal myocardial oxygen consumed (17,24,25). Low glucose oxidation rates, dependence on glycolysis and lactate oxidation reflect the low tricarboxylic acid cycle activity (17,26) and low mitochondria content in the fetal heart (18). Following birth, as lactate levels drop from 5-7 mM to adult levels of approximately 0.5 mM (27), myocardial lactate oxidation rates decrease significantly to proportionately contribute less ATP to the neonatal heart. In contrast, as the neonatal myocardium increases dependence on oxidative phosphorylation, namely through FA oxidation; the number, size, and complexity of mitochondria also increase (28).

Although the elements of the glucose metabolic pathway mature in the newborn period, the contribution of glucose oxidation to ATP production in the myocardium does not fully mature until weaning (6,7). This maintained immaturity may be a consequence of relative insulin resistance in the neonatal heart, increased sensitivity to ATP inhibition, and a rise in FA oxidation.

Therefore, as the heart transitions from the fetal state to the neonatal state, cardiac metabolism become highly dependent on FA metabolism until adulthood.

1.3 Fatty Acid Transport and Oxidation

FA oxidation is limited by its rate of transport into both the cell and the mitochondrial matrix. Numerous theories have been hypothesized regarding the movement of FAs into the cytoplasm, such as the “flip-flop” model, whereby extracellular FAs are integrated momentarily into the plasma membrane and extruded into the cytoplasm. On the other hand, CD36, fatty acid transport protein (FATP), and plasma membrane-associated FA-binding proteins have been shown to facilitate long chain FA (LCFA) transport into the cytoplasm (29). This FA transporter and its translocation process is described in fig 1-2. CD36 is mostly found in the recyclable endosomal pool (30). Its translocation to the plasma membrane is stimulated by insulin, adiponectin, or myocyte contraction (31,32). Little is known about CD36/FATP in the neonatal heart, but alongside the decreased circulating insulin, adiponectin levels increase (33) as with adiponectin receptor-1 mRNA expression (34) in the neonatal period in order that the heart metabolically matures to depend on FA oxidation. Adiponectin increases CD36 recruitment to the plasma membrane and increases FA uptake; it also causes 5'-AMP-kinase (AMPK) phosphorylation to increase FA oxidation (32).

Therefore, CD36 may play an important role in cardiac metabolic maturation as its presence may play a vital role in FA uptake into the cytoplasm.

Mitochondrial FA uptake is the rate-limiting step to FA oxidation (1,35-37). The gatekeeper of FA transport into the mitochondria is carnitine palmitoyltransferase (CPT-1). Shown in fig 1-3, cytoplasmic FA is first activated by acyl-CoA synthetase into an acyl-CoA. On the outer mitochondrial membrane, CPT-1 transfers the fat moiety from acyl-CoA to carnitine and is, in turn, transported via a translocase to the inner mitochondria matrix where CPT-2, located at the matrix side of the inner mitochondrial membrane, reconverts the acyl-carnitine into acyl-CoA. The reconstituted acyl-CoA is directed to FA β -oxidation. The released carnitine may diffuse across the mitochondria membrane and is recycled to bind to another acyl-moiety for transport. Alternatively, carnitine may also bind to an acetyl group to form acetylcarnitine by carnitine acetylcarnitine translocase, which also catalyzes its transport out of the mitochondria. Short- and medium-chain FAs are thought to freely diffuse across the mitochondria membrane and their oxidation is not rate limited. Meanwhile, CPT-1 regulates the transport of LCFA as CPT-1 is subjected to inhibition by allosterically binding to malonyl-CoA, an intermediary product in the process of FA synthesis. Malonyl-CoA is synthesized by acetyl CoA carboxylase from acetyl-CoA and metabolized by malonyl-CoA decarboxylase (MCD); it is the resultant product of the dynamic between the two enzymes that causes CPT-1 inhibition.

1.4 Mechanisms in Cardiac Metabolic Maturation

In contrast to glucose metabolic maturation, cardiac FA metabolic maturation reaches adult levels early on in life. Less than 0.1 mM of free FAs circulate in fetal blood, but immediately following birth, free FA levels rise to those seen in adults (0.2-0.4 mM) (27,38,39). In the 1-day-old rabbit heart, FA oxidation provides only 10% of the ATP required by the heart to reflect fetal FA oxidation rates (8,40). Within 7 days of birth, FA oxidation rates increase 10 fold in the neonatal rabbit heart (8). The transition from reliance on glycolysis to FA oxidation is attributed to a change in diet and hormones that coincide with transcriptional changes.

Increased substrate availability partially drives the switch from glycolysis to FA oxidation. As the neonate consumes milk, dietary FAs increase leading to an increased supply of FA to the heart. *In utero*, fetal nutrition is largely composed of carbohydrates (~70%) (7). Although in some species (humans, rabbits, rats) the placenta readily allows the diffusion of lipid-soluble substances, much of the fat that crosses the placenta is stored in the liver and adipose tissue (7). Though oxygen may be thought of as limited as the fetus resides in a relatively hypoxic state, its oxygen extraction capacity is much greater than that of the adult due to fetal hemoglobin. The fetal heart undergoes high rates of lactate oxidation (18) to demonstrate a well oxygenated fetus. Whether the fetal heart oxidative capacity is oxygen-limited is debatable. However, the oxygen-rich environment of neonates, combined with increased circulating FA means that the substrates

required to facilitate the early and rapid maturation of FA oxidation are available. In human neonates, dietary fats increased to supply nearly 50% of the neonate's total calories consumed (7). The dietary fats are supplied by the mother's milk of which 95% of the fat is contained in triacylglycerol (TG) (7). In human milk, a large proportion of these TGs are unsaturated LCFA while 5-15% are medium-chain FA (7); and in rabbit, cow, and goat milk, the proportion of medium-chain FAs is 30-40% (7). Additionally, in the immediate newborn, prior to establishing suckling, the newborn is dependent on endogenous adipose tissue fat stores. These adipose tissues are predominantly composed of palmitate and oleate-containing TGs (54-55%) (7) and are mobilized to increase plasma FFA in the immediate newborn. In contrast, as suckling rats are weaned from fat-rich milk to a high carbohydrate diet, hepatic rates of FA oxidation decrease significantly due to coordinated changes in plasma FFA and the liver's response to substrate availability (7).

Hormonally, in the immediate newborn period, circulating insulin levels decrease (7,41) while adiponectin rises (33). Acetyl-CoA carboxylase (ACC) produces malonyl-CoA which strongly inhibits CPT-1 (fig 1-3 and fig 1-4). In the immediate newborn, as insulin levels rise, AMPK expression and activity are increased to phosphorylate and inhibit ACC so that malonyl-CoA synthesis is inhibited (35,41). Simultaneous to lowered ACC activity/expression, cardiac MCD expression/activity increases (42-46) following birth. This accelerates the rate at which malonyl-CoA is decarboxylated and removed. Consequently, the

fetal/newborn high malonyl-CoA levels drop rapidly within days, post-partum (35,41). Although this adaptation may allow for the myocardium to normalize wall stress, intolerance to ischemia reperfusion is increased as well (47-49).

As malonyl-CoA levels drop, CPT-1 inhibition is lifted to increase FAs influx for oxidation. This critical drop in malonyl-CoA levels drives FA oxidation maturation and is due to both a decrease in synthesis and an increase in degradation. During this transition, CPT-1 expression also switches from the liver (L)-CPT-1/CPT-1a isoform to the muscle (M) CPT-1/CPT-1b isoform, which accounts for 90% of all CPT-1 activity in the adult heart (50). Interestingly, intrinsic to M-CPT-1, with the isoform switching, the rate of FA oxidation is now subjected to an increased sensitivity to malonyl-CoA inhibition. There is no evidence to suggest that this increased sensitivity decreases FA oxidation rates. To add, this occurs simultaneously to a significant drop in malonyl-CoA levels to further suggest that the switch causes increased fine-tuning of metabolic pathways, which occurs in the midst of downregulated regulatory signaling.

Pyruvate dehydrogenase (PDH) is the enzyme that catalyzes the committed, irreversible reaction in glucose oxidation. Coincident to the changes that decrease glycolysis and FA oxidation, mitochondrial PDH expression and activity increases during the first 10 days of life (51) and should equate to increased pyruvate oxidative capacity. However, pyruvate dehydrogenase kinase (PDK), which covalently modifies PDH to inhibit PDH activity, also rises within the

neonatal period (52). Elevated FA oxidation rates increase acetyl-CoA levels to inhibit PDH activity alongside the PDK modifications (6,53). Hence, glucose oxidation rates remain low (6) and its maturation is postponed until after weaning (7).

Transcriptionally, two major nuclear receptor pathways control the maturation of cardiac metabolism: 1) hypoxia-induced factor-1 α (HIF-1 α) and 2) peroxisome proliferators activated receptor α (PPAR α). HIF-1 α regulates hypoxia-induced expression of various genes involved in anaerobic glycolysis by binding to the HIF-1 α response element. HIF-1 α increases the expression of genes such as PDK1 (54,55), GLUT1 (56-58), hexokinase 1 (56), and lactate dehydrogenase-A (56,57). We have found that HIF-1 α levels are high in the 1-day-old rabbit heart and rapidly decrease over the neonatal period (unpublished data) mirroring the fetal ovine heart profile (59). Subsequently, during the neonatal period, glycolytic pathway genes may decrease, ultimately decreasing glycolytic rates.

PPAR α seems to act reciprocally to HIF-1 α . PPAR α regulates genes involved in FA metabolism (60,61). Activating the PPAR α response element increases expression of fatty acyl-CoA synthase (62), CPT-1 (62-64), medium-, and long-chain acyl-CoA dehydrogenase (62,65,66). Our lab has correlated corresponding changes to FA oxidation rates to PPAR α up-(67) or down-regulation (68). In the neonatal period, PPAR α expression increases in the heart (69) but metabolic rates have not been quantified.

1.5 Peroxisome Proliferator-Activated Receptor α in the Heart

Peroxisome proliferator-activated receptors (PPAR) are a group of ligand-activated transcription factors that control expression of genes responsible for FA metabolism. There are three subtypes: PPAR α , β , and γ . Upon activation by a ligand, the PPAR forms a heterodimer with the retinoid X receptor and binds to the PPAR response element located at the promoter regions of the target genes. PPARs have a wide range of synthetic and natural ligands. Synthetic PPAR ligands include hypolipidemic drugs often used clinically to reduce plasma lipids (eg fibrates and gemfibrozil); these display preferential binding to PPAR α ; thiazolidinediones are anti-hyperglycaemic agents (eg Glitazones) which have a propensity towards PPAR γ ; and other synthetic PPAR δ ligands which have yet to find their clinical application (L165041 or GW0742X)(70). Additionally, FAs of varying chain lengths act as endogenous ligands to these PPARs (71-73).

Of the three subtypes, PPAR α has been the most studied and is highly expressed in organs that undergo high rates of FA catabolism such as the heart, skeletal muscle, liver, kidneys, pancreas, and intestinal mucosa (74,75). PPAR γ is mostly found in adipose tissue and is expressed at lower levels in the heart, liver, skeletal and vascular smooth muscle, endothelial and bone marrow (76-78). PPAR δ is expressed in greater quantities and is more ubiquitous relative to the other two subtypes (74). However, regardless of distribution, the differential

binding of varying ligands and co-factors/repressors make each subtype of PPAR multi-functional (79,80).

In the fetal heart at embryonic day (ED) 54 and 125, PPAR mRNA levels have been quantified to show timely expressional fluxes (81) that are implicated in coordinated cell differentiation and proliferation (82) outlining PPAR α 's importance in cardiomyocyte metabolic and overall maturation. The activation of PPAR α , but not PPAR β or γ promotes embryonic stem cell differentiation into cardiomyocytes (82). According with fetal cardiac metabolism comprising of high glycolytic rates and an underdeveloped FA oxidation pathway, PPAR α , β , and γ are expressed at low levels compared to that observed in the adult equivalent and changes very little with fetal age (81). In contrast, mRNA of PPAR α , β , and γ are significantly upregulated to that of adult levels at 7-days old in neonatal rat hearts compared to 0-days old (34). This illustrates the dramatic transcriptional change that occurs simultaneously to the enzymatic and metabolic changes during the neonatal period. For instance, medium chain acyl-CoA dehydrogenase (MCAD) and other FA oxidation enzymes are expressed at low quantities in the prenatal period and rise rapidly to levels seen in adults during the immediate newborn period (83-85). Therefore, PPAR's transcriptional control plays a vital role in the metabolic transition between fetal and neonatal cardiac FA metabolism.

1.6 Hypoxia-Inducible Factor- α in the Heart

Hypoxia-inducible factor-1 α (HIF-1 α) is a transcription factor regulating over 100 genes involved in glycolysis, metabolism, apoptosis, angiogenesis, and cell cycling (86) in response to changes in oxygenation (fig 1-5). Although constitutively expressed, in a well oxygenated cell, a prolyl-hydroxylase domain (PHD)-containing enzyme hydroxylates HIF-1 α making it prone to polyubiquitination by von-Hippel Lindau (VHL) E3 ubiquitin ligase (87) and destined for proteasomal degradation. In contrast, hypoxia (typically below 3%–5% O₂) (88) suppresses PHD activity and reduces HIF-1 α hydroxylation and interaction with VHL (89,90). Decreased degradation allows HIF-1 α to interact in a heterodimer with other HIF factors, translocate into the nucleus, and increase transcription of target genes such as GLUT1 (56-58), PDK1 (54,55), HK-I (56,91), HK-II (91) and lactate dehydrogenase (LDH)-A (56,57).

HIF-1 α protein levels are relatively high in the fetal ovine heart and decrease dramatically and immediately in the post-natal period as with α -enolase, LDH-A, and PFK1 (59). Vital to cardiovascular development, HIF-1 α knockout mice demonstrate disturbed cardiac looping predisposing the heart to ventricular deformation (92,93). HIF-1 α downregulation is also associated with folic acid deficiency-related CHDs (94). Correct cardiac morphogenesis in mice requires a hypoxic environment, which elevates HIF-1 α at ED 8.5-10 (93). In turn, the genetic changes affect metabolism and therefore survival. In HIF-1 α knockout

mice, HK-I expression is severely diminished (92). Hyperglycemia failed to rescue these embryos, but hyperoxia prolonged their survival and abolished findings of growth inhibition demonstrating that the loss of HIF-1 α during embryo development prompts inappropriate and untimely oxidative metabolism. Therefore, its cyclical activations during crucial periods in embryonic development contribute to appropriate morphological and metabolic cardiac development.

1.7 Ischemia-Reperfusion Injury and the Neonatal Heart

In Canada, approximately 6000 infants are born with congenital heart disease every year and about one-third will require surgical intervention within the first month of life to survive. Surgical intervention requires the cardioplegic arrest of the neonatal heart in order to attain a bloodless and motionless field for operation. This exposes the neonatal heart to ischemic periods that can exceed one hour (95). Post-operative myocardial functional recovery is not only reliant upon optimal surgical techniques, but also on perioperative interventions. However, in spite of superior surgical techniques (96-101), inadequate cardioprotection remains a major contributor to mortality (i.e. mortality ~4%) (102) following surgical repair (98,103-105). Depressed contractile function manifests in up to 20% of pediatric patients following surgical correction of CHDs (106), and is the most common cause of post-surgical death in these patients (107-109). Though the incidence of depressed contractile function can be

decreased through inotropic support (110), increased inotropic support is associated with increased mortality (111,112).

Ischemic injury remains a major contributor to post-surgical morbidity and mortality. Elevated circulating lactate has been correlated to poor clinical outcome and high mortality in patients undergoing correctional surgery for CHDs (113-117). Elevated lactate levels result from prolonged cardio-pulmonary bypass time and clamp duration, and higher inotropic score (118). A recent study reported mortality rates of 10% associated with elevated lactic acid levels, and thus prolonged ischemic time (118). Taken together, these clinical correlates demonstrate that prolonged surgery and ischemic time contributes to adverse outcome as a result of ischemia-reperfusion injury. Although energy substrate metabolism may be a therapeutic target to attenuate myocardial ischemia reperfusion injury (119), there are marked differences between the neonatal and the adult heart. Furthermore, cardiac hypertrophy may develop secondary to the CHD-induced pressure- or volume-overload to alter cardiac metabolism. Therefore, understanding hypertrophied neonatal cardiac metabolism during and following ischemia-reperfusion will aid the development of new strategic approaches to protect the neonatal heart during cardiac surgery.

1.8 Ischemia-Reperfusion Injury

Myocardial ischemia-reperfusion (IR) injury is related to the balance between energy supply and demand; a topic that has been extensively reviewed (120-

126). During ischemia, O_2 and extracellular substrates are limited or depleted resulting in a dramatic reduction in glucose and FA oxidation. Consequently, ATP is generated from anaerobic glycolysis of intracellular glycogen to meet the metabolic demands of the heart. As ischemia activates AMPK, malonyl-CoA production decreases to release CPT-1 inhibition. Along with ischemia-induced increased plasma FA levels (127), increased FA uptake occurs and residual amounts of FA oxidation occur generating acetyl-CoA and elevating NADH:NAD⁺ ratio that activates PDK, which in turn, inhibits PDH alongside of depleting residual oxygen, and hence, inhibit glucose oxidation. Glycolysis becomes uncoupled from glucose oxidation causing an accumulation of cytosolic H⁺ resulting in intracellular acidosis due to the absence of coronary flow waste removal. The H⁺ gradient obligates the exchange of 1 Na⁺ for 1 H⁺ via the Na⁺-H⁺ exchanger (NHE). The NHE therefore plays a vital role regulating cellular pH and has been shown to contribute to IR injury (128). Indeed, genetic deletion of the NHE in cardiomyocytes is cardioprotective against IR injury (129). Intracellular Na⁺ builds up, obligating the reversal of the Na⁺-Ca²⁺ anti-porter (NCX) to now expel 3 Na⁺ in exchange for 1 Ca²⁺ ion (130) leading to intracellular Ca²⁺ overload and further of ATP in attempts to restore intracellular ionic homeostasis (125,131). Male mice with an overexpression of NCX1 show greater susceptibility to IR injury (132). Ca²⁺ overload may be caused by several mechanisms during ischemia and reperfusion (133), including opening of voltage-gated L-type calcium channels (LTCC) during ischemia. Therefore, Ca²⁺ overload may be

attributed in part to opening of these LTCC channels. However, in human trials, LTCC blockers have shown either to reduce cellular damage or no cardioprotective effects (134-136). In addition, the sarcoplasmic reticulum (SR) also becomes impaired (137) and impedes Ca^{2+} reuptake via SR Ca^{2+} -ATPase (SERCA) (138,139).

During ischemia the intracellular Ca^{2+} overload, in turn, activates the mitochondrial permeability transition (MPT) that opens the MPT pore. However, intracellular acidosis during ischemia inhibits the MPT pore from opening; but during reperfusion, as pH is normalized, the MPT pore opens, allowing solutes to freely enter the mitochondrial matrix and for the release of cytochrome C from the intramitochondrial space into the cytoplasm. Cytochrome C can then activate caspases and initiated apoptosis. Excess Ca^{2+} also activates Ca^{2+} -dependent proteases and phospholipases (137,140). During reperfusion, reoxygenation also causes production of reactive oxygen species that further cause reperfusion injury.

During reperfusion following ischemia, the primary source of ATP in the adult heart originates from accelerated rates of FA oxidation (127,141). Increased circulating levels of FA during ischemia (127) and altered cellular control over FA oxidation (40,142) drive the acceleration of FA oxidation. In a non-diabetic heart, FA oxidation rates can increase to provide 80-90% of the heart's total energy needs (120,143,144). As above, in reperfusion, FA oxidation produces copious

amounts of acetyl-CoA and increases NADH:NAD⁺ ratio to activate PDK, which phosphorylates and inhibits PDH as part of the Randle cycle (145). Glycolysis continues to produce H⁺ uncoupled from the neutralization of glucose oxidation, but O₂ consumption increases to maintain cardiac energy inefficiency (125). Consequently, global contractile dysfunction ensues during reperfusion (125,144).

A large proportion of ATP is continually diverted towards restoring ionic homeostasis and removal of metabolic byproducts during reperfusion in the midst of lowered cardiac efficiency (124,146). This process diverts ATP away from the energy needed to initiate and maintain immediate contractile function (1,125,147,148). With the ischemic ionic imbalance, reperfusion, while removing the accumulated extracellular ions and waste products, generates an osmotic gradient that favours cell swelling. The rapid pH restoration causes further ionic imbalances that exacerbate intracellular Ca²⁺ accumulation. Numerous components of either phase overlap and ultimately bring about cell death by necrosis, apoptosis, and/or autophagy.

1.9 Ischemia-Reperfusion Injury in the Neonatal Myocardium

The relative ability of the neonatal heart to withstand ischemia-reperfusion has been a controversial topic. While some studies have demonstrated the intolerance of the neonatal heart to ischemia-reperfusion (149-155), others have demonstrated an increased tolerance (156-162) relative to that of the adult

heart. The latter camp also provides evidence to demonstrate the tolerance to ischemia is inversely related to age; therefore, with age, tolerance to ischemia diminishes. However, ischemic intolerance relative to adult hearts has been gauged using parameters that are adult-specific and have been criticized for their accuracy relative to the biochemical and physical immaturity of the neonatal heart (162-165). Therefore, interpretation of age comparison studies must be executed with caution.

As H^+ accumulation and acidosis are highly correlated to ischemia reperfusion injury in adult hearts, several studies have shown that this holds true in the neonatal equivalent. Neonatal hearts subjected to ischemia-reperfusion have excessive lactate and H^+ accumulation compared to adult hearts subjected to similar lengths of ischemia-reperfusion (166-168). However, in these studies, the increased H^+ accumulation was not correlated to cardiac function. Clinically, elevated lactate levels correspond to poorer outcomes and increased mortality after CHD correctional surgery (113-117). However, Milerova et al (169) demonstrated that mitochondria extracted from isolated perfused normal neonatal rat hearts subjected to ischemia reperfusion are less susceptible to Ca^{2+} induced swelling. This suggests that normal neonatal cardiomyocyte mitochondria are less sensitive to MPT opening and are more tolerant of ischemia-reperfusion injury in spite of acidosis, which may develop more rapidly in the neonatal heart. Furthermore, normal working 7-day-old rabbit heart have been proven to be more resilient with an 87% functional recovery compared to

an adult heart, which recovered to only 47% of its pre-ischemic function after being exposed to the same length of ischemic time (163).

Ischemia suppresses oxidative phosphorylation in both the adult and neonatal heart due to the lack of adequate oxygenation. During post-ischemic reperfusion, rates of FA oxidation recover rapidly in the adult heart and in turn continue to suppress glucose oxidation (1,170-172). These elevated rates of FA oxidation during reperfusion are detrimental to the adult heart. Augmenting glucose metabolism, promoting re-coupling of glucose oxidation to glycolysis (173-175), or inhibiting FA oxidation (176,177) are methods that aid the adult heart's recovery from ischemia. However, due to the metabolic disparity between the adult and the neonatal heart, these cardioprotective strategies cannot be extrapolated to the neonatal heart.

Neonatal hearts are vulnerable to an energy deficit during ischemia-reperfusion. The longer the duration of ischemia, the more depleted glycogen stores and high energy phosphate pools become (178). Consequently, the more severe functional deficit occurs in neonatal hearts. Torrance et al (178) have further shown in newborn hearts that better recovery from ischemia is associated with higher levels of available high energy phosphates and reducing equivalents. Energy deficiency correlating to post-ischemic cardiac dysfunction has been documented in canine models of neonatal cardiac ischemia-reperfusion injury (179) and clinically (180). Therefore, while metabolic substrate selectivity is

crucial to prevent further ischemia-reperfusion injury and improve functional recovery in the adult heart, non-selectively increasing energy equivalents take precedence in the neonatal myocardium. In fact, in contrast to the adult heart, elevated post-ischemic FA oxidation rates are cardioprotective to the neonatal heart (181). Furthermore, the increase of pyruvate oxidation is equally protective for the neonatal heart (182,183), showing that non-selective substrate supplementation is equally effective. The non-selective nature of substrate metabolism is likely due to the increased resistance of the normal neonatal myocardium against acidosis and mitochondrial damages elicited by ischemia-reperfusion compared to the adult myocardium.

Unfortunately, most neonatal animal studies of cardiac ischemia-reperfusion injuries use normal animals. These models do not take into account the abnormal anatomy, biochemistry, and hemodynamics of the hearts in the children undergoing corrective surgery for their CHD. Therefore, it is difficult to compare the findings from these studies to the clinical correlate. Placed into context, children with elevated plasma lactate levels have poorer outcomes and are likely to have hearts with abnormal biochemistry unable to cope with the acidosis, unlike the normal heart. Therefore, it is crucial to elucidate the biochemical changes in a model relevant to CHDs, such as that of a hypertrophic heart model. By understanding the biochemical changes, more relevant cardiac protection strategies can be elicited.

1.10 Cardiac Hypertrophy and Energy Metabolism

Cardiac hypertrophy is an adaptive response to increased cardiac workload to normalize wall stress. In adult hearts, terminally differentiated cardiomyocytes non-proliferatively increase in mass and volume. However, progressive cardiac hypertrophy can become maladaptive leading to heart failure. In the adult heart, cardiac hypertrophy is associated with numerous protein expression changes such as a switch from α -myosin to β -myosin heavy chain (184-186), decreased M-CPT-1 (187), increased LDH-A (188,189), a switch towards fetal-type creatine kinase (190), increased GLUT1 (191), a downregulation of MCAD and, increased PFK expressions (192). These expression changes are conducive to metabolic remodeling towards a fetal metabolic profile whereby the myocardium becomes heavily dependent on glycolytic metabolism and less on oxidative phosphorylation (186,189,193,194). Cardiac hypertrophy is associated with deranged cardiac metabolism, be it a consequence of acquired or congenital cardiomyopathy (195-197). We and others have demonstrated that glycolysis increases (198) while FA oxidation decreases in pressure- and volume-overloaded hearts (199,200). Furthermore, these genes are under the regulation of PPAR α and HIF-1 α ; hypertrophy-related changes have been associated with altered PPAR α (201-204) and HIF-1 α expression/activity (192,205-207).

PPAR α is implicated in the metabolic switch observed in cardiac hypertrophy in which the fetal metabolic phenotype is revived at the expense of FA oxidation

(185,189,208-213). In cardiac hypertrophy, different PPARs play a different role to contribute to the hypertrophic phenotype. The inactivation of PPAR α and PPAR β/δ downregulates the FA oxidation pathway while the inactivation of PPAR γ leads to the development of hypertrophy (214) to show that the metabolic phenotype is largely a result of PPAR α changes. In a pressure-overload hypertrophy model, PPAR α expression is downregulated in the heart alongside several genes involved in PPAR α controlled genes involved in FA metabolism, such as M-CPT-1, MCAD, acyl-CoA oxidase (187,215), and uncoupling protein-3 (215,216).

Equally, HIF-1 α itself (192) and HIF-1 α -regulated genes controlling glycolysis are upregulated: namely GLUT1 (191), LDH-A (188,189), PFK2 (192) and monocarboxylate transporter (MCT)-4 (217,218). Physiologically, FA oxidation requires 10% more O₂ compared to glucose oxidation (219). The metabolic changes associated with cardiac hypertrophy is thought to be adaptive (220) as FA oxidation requires more oxygen to metabolize than glucose. In hypertrophied hearts, rates of FA oxidation can be nearly 30-40% lower than that in normal hearts (199,221). Therefore, this adaptation makes the heart more energy efficient. However, FA oxidation of medium FA chain, such as palmitate, produces 105 mol of ATP. In contrast, glycolysis produces 2 ATP per molecule of glucose and complete oxidation of glucose produces only 31 mol of ATP. While increasing metabolic efficiency, the ATP producing capacity of the heart is downregulated. The elevated rates of glycolysis are not accompanied by

increased pyruvate oxidation (198,222-224). Rates of pyruvate oxidation are lower in hypertrophied hearts compared to normal hearts (223). In fact, glucose metabolism is unable to completely compensate for the decreased FA oxidation. When challenged with increased workloads, without the ability to increase ATP production, the now metabolically inflexible heart, fails.

1.11 Peroxisome Proliferator-Activated Receptor α in Cardiac Hypertrophy

The metabolic switch occurs via a downregulation of the FA oxidation pathways as well as altered expression of key enzymes that act as metabolic switches between glucose and FA metabolism. PDK4 is one such gene. It is under the transcriptional control of PPAR α (225). PDK4 acts as a metabolic switch to toggle between FA and glucose oxidation due to its ability to phosphorylate and inhibit PDH, therefore favouring FA oxidation. In cardiac hypertrophy, along with decreased FA oxidation, PDK4 is downregulated (226), thus permitting glucose metabolism to predominate in the hypertrophied myocardium (227). Alone, its upregulation does not alter cardiac function, but it can exacerbate pre-existing cardiomyopathy by intensifying cardiac necrosis and fibrosis (228) likely by inhibiting PDH without a parallel increase in FA oxidation. This may lead to an energy deficiency or even crisis which underlies the exacerbated necrosis. Furthermore, decreased PDK4 may also decrease ischemia-reperfusion

tolerance, which requires copious amounts of ATP for successfully functional recovery that minimizes myocardial damage.

Meanwhile, extracellular FA uptake may be diminished. In the spontaneous hypertensive rat, cardiac hypertrophy develops between 8-12 weeks of age secondary to hypertension (229-231). CD36 is downregulated in these rats simultaneously to increased intracellular lipid accumulation due to impaired FA oxidation (232). This downregulation is also observed following angiotensin II (Ang II)-induced cardiac hypertrophy, CD36 is also downregulated (233). In humans, children with congenital CD36 defects develop cardiomyopathies (234,235). Yet, in hypertrophied caveolin-3 KO hearts (236), transgenic mice overexpressing a truncated form of troponin (237), and age-related cardiac hypertrophy of mice hearts (238) all have normal or increased CD36 expression. The diversity of CD36 phenotypes suggests that CD36 may exhibit differential expression due to temporal, species, and pathological differences between these models of cardiac hypertrophy and alone may not induced hypertrophy. Yet, in association with increased PPAR α expression (239), FA continues to accumulate in various human and animal models of cardiac hypertrophy including: pressure-overload (240), volume-overload, diabetic cardiomyopathy (241-243), and other idiopathic cardiomyopathies (240,244,245). In a model of volume-overload hypertrophy, lipid accumulation is associated with myocardial dysfunction that can be corrected by administration of rosiglitazone, a PPAR γ agonist, which decreased triacylglycerol (TG) accumulation and improved contractile function.

Intramyocyte lipid accumulation was first reported in 1858 in patients with congestive heart failure (246). This pathology has been termed lipotoxicity due to the resulting lipid-induced apoptosis and may contribute to contractile dysfunction in the hypertrophied heart. This process has been extensively reviewed (247). TG accumulation may or may not occur simultaneous to an increased FA uptake by CD36 as indicated by the varying CD36 phenotypes. This is further affirmed by studies in myocytes overexpressing CD36 in which FA uptake increased alongside corresponding FA oxidation with no increased TG synthesis (248). Therefore, while CD36 facilitates increased FA uptake, CD36 upregulation is not necessary for TG accumulation in a hypertrophied myocardium; rather the context of increased glycolysis and decreased rates of FA oxidation in which the altered CD36 expression occurs determines the detriments it causes.

In the hypertrophied heart, rates of glycolysis are elevated, which encourages the formation of TG and therefore its accumulation. The increased rates of glycolysis increase substrate for glycerol-3-phosphate production via glycerol-3-phosphostate dehydrogenase from dihydroxyacetone phosphate, a glycolysis intermediary. Increased glycerol-3-phosphate facilitates TG synthesis by providing substrate for glycerol-phosphate acyltransferase (GPAT), the rate limiting enzyme for de novo TG synthesis (249). Hence, though alone, the expressional changes of CD36 may not alter TG accumulation and lipotoxicity, the underlying elevated glycolysis is conducive to increased TG synthesis.

Furthermore, hypertrophy downregulates mitochondrial FA uptake to effectively reduce rates of FA oxidation, rates that cannot be compensated by increased glucose metabolism (250). CPT-1 is downregulated in several models of cardiac hypertrophy (240,251-253). It has been observed that the pharmacological activation of PPAR α prevents the reduction in CPT-1 expression along with other enzymes in the FA oxidation pathway in a hypertrophied heart to curb the progression towards heart failure and improves survival (202,254,255). In association with M-CPT-1 downregulation, the removal of its allosteric inhibitor by MCD is also decreased in cardiac hypertrophy. In pressure-overload rat models of cardiac hypertrophy, MCD expression/activity decreased significantly together with reduced PPAR α expression (256) allowing malonyl-CoA to accumulate and inhibit CPT-1 transport of FA into the mitochondria for oxidation. In contrast to PPAR α transcriptional control, the activation of PPAR γ decreases MCD expression (256). This further illustrates the cause-and-effect relationship between specifically PPAR α and cardiac metabolism in a hypertrophied heart.

The relevance of CPT-1 inhibition is further exemplified by altered AMPK and ACC activity in cardiac hypertrophy. The genetic deletion of LKB1, the upstream kinase that phosphorylates AMPK, also induces cardiac hypertrophy (257). In both an Ang II-stimulated cultured cardiomyocyte and murine pressure-overload model of cardiac hypertrophy, AMPK phosphorylation was significantly decreased without altered AMPK expression (258). In fact, in mice expressing a

mutant form of AMPK it was observed that AMPK deficiency exacerbates obesity-induced cardiac hypertrophy and cardiac dysfunction (259). These findings were accompanied by decreased ACC phosphorylation and increased GLUT4 translocation to the plasma membrane (258). Interestingly, in various cultured cardiomyocyte models of cardiac hypertrophy, incubation with an AMPK stimulator, 5-aminoimidazole-4-carboxamide-1-beta-D-ribofuranoside (AICAR) (258,260) or metformin (259), prevented cardiac hypertrophy. Metformin-treated rats with aortic banding also exhibited lessened cardiac hypertrophy, an effect abrogated by co-treating with L-NAME, a nitric oxide synthase inhibitor (259). The sum of decreased M-CPT-1 expression and its increased inhibition decreases FA transport into the mitochondria for oxidation in the hypertrophied heart. Furthermore, mitochondrial FA uptake and subsequent FA oxidation play a key role in the development of cardiac hypertrophy and may represent a potential therapeutic target to modify the course of cardiac hypertrophy and heart failure.

1.12 Hypoxia Inducible Factor-1 α and Glucose Metabolism in Cardiac Hypertrophy

The deranged metabolism in a hypertrophied heart is partly a result of the dynamic relationship between PPAR α and HIF-1 α , whereby elevated activity of one is associated with diminished activity of the other. In cases of hypoxia, PPAR α activity and expression are downregulated while that of HIF-1 α is

upregulated in order to equilibrate metabolism in response to altered substrate availability, namely oxygen (252,261). In cardiac hypertrophy, HIF-1 α alters metabolism in coordination with PPAR α changes by directly interacting with PPAR α as well as regulating processes that facilitate both glucose and FA metabolic pathways.

HIF-1 α participates in a dynamic relationship with PPAR α . Intriguingly, the PPAR α gene contains a consensus motif that is under HIF-1 α transcriptional regulation (261). Upon hypoxia-induced HIF-1 α nuclear accumulation, HIF-1 α binding to the consensus sequence on the PPAR α gene is increased and PPAR α expression and binding activity is decreased. Additionally, HIF-1 α may also interrupt the interaction between PPAR α and the retinoid X receptor to prevent PPAR α induced transcription (252). This increases lipid accumulation in cardiomyocytes and limits FA oxidation (252). In contrast, despite the presence of hypoxia, when HIF-1 α gene is depleted the anti-sense oligonucleotide, HIF-1 α binding to the PPAR α gene is prevented and PPAR α becomes upregulated (261). In the midst of metabolic distortion, cardiac hypertrophy can be averted when HIF-1 α is deleted. Indeed, transaortic constriction or unilateral renal ligation fails to provoke cardiac hypertrophy in HIF-1 α knockout mice (240). It is likely that persistent normal cardiac metabolism accompanies this phenotype.

In the hypertrophied heart, increased HIF-1 α augments anaerobic glycolysis as the heart decreases its reliance on oxidative phosphorylation coupled with

defective mitochondrial biosynthesis (252,262). The upregulation of HIF-1 α alone is sufficient to stimulate cardiac hypertrophy (240). The hypertrophied heart is predominantly dependent on glucose metabolism, but the rate of glycolysis occurs disproportionately higher than the rate of glucose oxidation (194,263). This occurs as GLUT1, PFK1, PFK2, and HK-I are upregulated, as is PDK1 (54,55). The switch towards GLUT1 expression increases glucose uptake in the hypertrophied heart (264,265). The increased expression of PFK1 facilitates a metabolic vacuum to metabolize increased glucose supply by elevating glycolysis rates. PFK2 is also upregulated to increase F-2,6-BP, which further stimulates PFK1 activity.

Meanwhile, PDK1 phosphorylates and inhibits the conversion of the glycolytic end-product into acetyl-CoA (54,55), thus reducing substrates entering into the TCA cycle, or glucose oxidation. The pyruvate may accumulate and become a substrate for LDH for the conversion into lactate. The increased LDH-A expression, characteristic of the hypertrophic and fetal phenotype (188), further facilitates lactate metabolism as pyruvate is directed away from oxidation. However, this lactate is not oxidized. Rather, the increased expression of MCT-4 increases under HIF-1 α control to expel excess lactate into the extracellular space (217). The removal of excess lactate prevents the inhibition of glycolysis through acidification as lactate dissociates into lactate anion and H⁺ at physiological pH.

Upregulated HIF-1 α expression and glycolysis also impact TG synthesis (252). In animal models of HIF-1 α overexpression, or in VHL knockout mice, excessive TG accumulates in the heart (252,262). It has been hypothesized that preventing the conversion of pyruvate to acetyl-CoA encourages anabolic use of glycolytic products in the de novo synthesis of FA (266). As glycolysis increases, so do levels of dihydroxyacetone phosphate (DHAP). DHAP is converted to glycerol-3-phosphate by glycerol-3-phosphate dehydrogenase and serves as the substrate for glycerol-3-phosphate acyltransferase, the rate-limiting step of de novo TG synthesis. Krishnan et al (2009) demonstrated that a portion of glucose that undergoes glycolysis during upregulated HIF-1 α expression, is directed into the increasing TG pool (240). While FA oxidation is diminished, the free FA uptaken into the hypertrophied myocardium (267) is channeled into TG synthesis, prompted by increased HIF-1 α expression. Hence, the interplay between PPAR α and HIF-1 α plays a large part in altering cardiac metabolism in the hypertrophied heart by regulating key pathways in hypertrophy pathology.

1.13 Neonatal Cardiac Hypertrophy

In the post-natal period, cardiomyocyte proliferation occurs at near undetectable rates (268). Therefore the heart undergoes physiological hypertrophy in order to adapt to the life *ex utero*. During this transition, the left ventricle encounters added resistance and is solely responsible for peripheral circulation. Meanwhile, the right ventricle is now exclusive to the pulmonary

circulation and subjected to less resistance. With the dynamic pressure changes encountered by the left and right ventricles, the left ventricle undergoes physiological hypertrophy while the right involutes. Meanwhile, Akt activity increases during this rapid newborn maturational period (269). Akt, when activated acutely for two weeks in cardiac-specific Akt1-transgenic mice of 12-weeks of age, causes physiologic hypertrophy with no activation of fetal genes; the hypertrophy is also reversible when the transgene is repressed (270). Akt plays an important role in the development of physiological hypertrophy through the PI3K/Akt/mTOR pathway (271-273). Additionally, Akt also mediates the upregulation of the GLUT4 gene (274). When Akt is chronically stimulated for 6 weeks leads to pathological hypertrophy (270). Therefore, the transition between physiological and pathological hypertrophy may be a difference in duration of heightened Akt activity.

Pathological hypertrophy can develop secondary to CHD(s) that cause pressure- or volume-overload (275). While numerous studies catalogue the development of normal neonatal myocardium, little is known about neonatal cardiac hypertrophy. Prior studies have suggested that cardiac hypertrophy in the neonate alters cardiac metabolism. AMPK activity and expression are decreased in a porcine model of patent ductus arteriosus volume-overload hypertrophy (276). Consequently, ACC activity remained elevated as well as high malonyl-CoA levels, favorable to inhibiting FA oxidation and its pathway development. HIF-1 α mRNA and protein levels normally decrease in the first week of life in newborn

sheep (59); however, in rabbits that have received aortic banding at 10 days of age or housed in a hypoxic chamber, cardiac HIF-1 α expression is significantly higher compared to control animals (205). Neonatal piglets with pulmonary artery banding-induced right ventricular hypertrophy show an increase in enolase α expression (277). This may consequently affect glycolysis. However, to what extent cardiac hypertrophy affects neonatal heart metabolism and more importantly, the impact of these alterations on myocardial ischemia-reperfusion tolerance has yet to be fully understood.

1.14 The Neonatal Rabbit Model

The neonatal rabbit model is a widely accepted model of several pediatric diseases (eg. pulmonary hypertension, PDA, hypoxia). Neonatal rabbit cardiovascular biology has been extensively examined and has a similar metabolic maturational profile to that of humans (7). Reviews that examine adult cardiac models have highlighted the advantages of the rabbit model (278-280). Electrophysiologically, adult rabbit hearts have a conduction system similar to that found in human and dog hearts (281). This is further exemplified by a similar underlying cardiomyocyte Ca²⁺ transport between rabbits and humans. The removal/sequestration of the Ca²⁺ at the restart of the contraction cycle in the rat heart is mainly derived from the sarcoplasmic reticulum (92%) to where it is re-sequestered (282). In contrast, the rabbit heart is more consistent to that of the human heart where a considerable amount of Ca²⁺ originates extracellularly

and is only 70% dependent on the sarcoplasmic reticulum. ~30% of the intracellular Ca^{2+} is therefore extruded by Na^+ - Ca^{2+} exchanger in rabbit and human cardiomyocytes (282,283). This correlates to a prolonged action potential in the rabbit and human heart, as with most mammalian hearts, with a prominent plateau phase, which is lacking in the rat and mouse ventricles (280).

Another advantage of using a rabbit cardiac model relates to the contractile components. As with adult humans, the adult rabbit heart expresses the β -myosin heavy chain, an attribute of slow-twitching muscles (284) (285). In contrast, rat and mouse ventricles predominantly express the α -myosin that contributes to fast-twitch muscles (286). Moreover, the development of the rabbit heart, in respect to myosin differential expression, is also similar to that of human heart development. In the fetal rabbit heart, both α - and β -myosins are expressed; this expression pattern favours α -myosin expression in neonatal cardiac development, which is later dominated by β -myosin in adult life (287). Relative to a fetal/neonatal model, the rabbit heart development would follow a closer pattern to that of a human heart.

Interestingly, as a model related to ischemia-reperfusion, the rabbit heart has less collateral coronary circulation relative to the human or even a canine heart model whereby the circumflex supplies most of the LV free wall as compared that of the left anterior descending artery (288,289). The impact of fewer collaterals may not be appreciated across species, but may decrease the rabbit

heart's tolerance to hypertrophy as well as ischemia and reperfusion injuries and produce a more pronounced reaction to the insult of volume-overload. Therefore, the rabbit model may be more efficient at dissecting out the impact of ischemia on cardiac function.

Logistically, the size of the neonatal rabbit and its heart is appropriate for surgical manipulation as well as isolated heart perfusion and adds to decrease obstacles encountered when attempting to experiment on neonatal models. Therefore, developmentally and physiologically, the rabbit heart model is an appropriate model to study and appreciate neonatal cardiac morphology and pathology.

1.15 General Hypothesis

Rationale: Ischemia and reperfusion alters cardiac metabolism, which is a major determinant of post-ischemic functional recovery. In the adult heart, a glucose-centered metabolism, achieved by increasing glucose oxidation to match rates of glycolysis, and inhibiting FA oxidation are methods successfully employed to rescue the ischemic heart. However, the neonatal myocardium is critically different not only in size, but metabolic profile from the adult heart. The neonatal heart is largely dependent on FA oxidation as glucose metabolism develops in the background and occurs at unappreciable rates. Therefore, when subjected to ischemia and reperfusion, the neonatal myocardium may be less tolerant compared to the adult heart and treatments employed in the adult setting may be detrimental.

Hypothesis: If FA oxidation is augmented in the normal or hypertrophied neonatal heart, then post-ischemic functional recovery would be improved compared to the controls because of the FA oxidation-centered metabolism of the neonatal heart.

1.16 References

1. Lopaschuk GD, Belke DD, Gamble J, Itoi T, Schonekess BO. Regulation of fatty acid oxidation in the mammalian heart in health and disease. *Biochim Biophys Acta* 1994;1213:263-76.
2. Stanley WC, Recchia FA, Lopaschuk GD. Myocardial substrate metabolism in the normal and failing heart. *Physiol Rev* 2005;85:1093-129.
3. Lopaschuk GD, Ussher JR, Folmes CD, Jaswal JS, Stanley WC. Myocardial fatty acid metabolism in health and disease. *Physiol Rev* 2010;90:207-58.
4. Hoerter JA, Opie LH. Perinatal changes in glycolytic function in response to hypoxia in the incubated or perfused rat heart. *Biol Neonate* 1978;33:144-61.
5. Rolph TP, Jones CT. Regulation of glycolytic flux in the heart of the fetal guinea pig. *J Dev Physiol* 1983;5:31-49.
6. Lopaschuk GD, Spafford MA, Marsh DR. Glycolysis is predominant source of myocardial ATP production immediately after birth. *Am J Physiol* 1991;261:H1698-705.
7. Girard J, Ferre P, Pegorier JP, Duee PH. Adaptations of glucose and fatty acid metabolism during perinatal period and suckling-weaning transition. *Physiol Rev* 1992;72:507-62.

8. Lopaschuk GD, Spafford MA. Energy substrate utilization by isolated working hearts from newborn rabbits. *Am J Physiol* 1990;258:H1274-80.
9. Santalucia T, Camps M, Castello A, et al. Developmental regulation of GLUT-1 (erythroid/Hep G2) and GLUT-4 (muscle/fat) glucose transporter expression in rat heart, skeletal muscle, and brown adipose tissue. *Endocrinology* 1992;130:837-46.
10. Postic C, Leturque A, Printz RL, et al. Development and regulation of glucose transporter and hexokinase expression in rat. *Am J Physiol* 1994;266:E548-59.
11. Castello A, Rodriguez-Manzaneque JC, Camps M, et al. Perinatal hypothyroidism impairs the normal transition of GLUT4 and GLUT1 glucose transporters from fetal to neonatal levels in heart and brown adipose tissue. Evidence for tissue-specific regulation of GLUT4 expression by thyroid hormone. *J Biol Chem* 1994;269:5905-12.
12. Hocquette JF, Sauerwein H, Higashiyama Y, Picard B, Abe H. Prenatal developmental changes in glucose transporters, intermediary metabolism and hormonal receptors related to the IGF/insulin-glucose axis in the heart and adipose tissue of bovines. *Reprod Nutr Dev* 2006;46:257-72.

13. Osawa H, Printz RL, Whitesell RR, Granner DK. Regulation of hexokinase II gene transcription and glucose phosphorylation by catecholamines, cyclic AMP, and insulin. *Diabetes* 1995;44:1426-32.
14. Osawa H, Sutherland C, Robey RB, Printz RL, Granner DK. Analysis of the signaling pathway involved in the regulation of hexokinase II gene transcription by insulin. *J Biol Chem* 1996;271:16690-4.
15. Kliegman R, Trindade C, Huang M, Hulman S. Effect of euglycemic hyperinsulinemia on neonatal canine hepatic and muscle metabolism. *Pediatr Res* 1989;25:124-9.
16. Johnston V, Frazzini V, Davidheiser S, Przybylski RJ, Kliegman RM. Insulin receptor number and binding affinity in newborn dogs. *Pediatr Res* 1991;29:611-4.
17. Fisher DJ, Heymann MA, Rudolph AM. Myocardial oxygen and carbohydrate consumption in fetal lambs in utero and in adult sheep. *Am J Physiol* 1980;238:H399-405.
18. Lopaschuk GD, Collins-Nakai RL, Itoi T. Developmental changes in energy substrate use by the heart. *Cardiovasc Res* 1992;26:1172-80.
19. Makinde AO, Kantor PF, Lopaschuk GD. Maturation of fatty acid and carbohydrate metabolism in the newborn heart. *Mol Cell Biochem* 1998;188:49-56.

20. Bristow J, Bier DM, Lange LG. Regulation of adult and fetal myocardial phosphofructokinase. Relief of cooperativity and competition between fructose 2,6-bisphosphate, ATP, and citrate. *J Biol Chem* 1987;262:2171-5.
21. Thrasher JR, Cooper MD, Dunaway GA. Developmental changes in heart and muscle phosphofructokinase isozymes. *J Biol Chem* 1981;256:7844-8.
22. Scholz TD, Koppenhafer SL. Reducing equivalent shuttles in developing porcine myocardium: enhanced capacity in the newborn heart. *Pediatr Res* 1995;38:221-7.
23. Scholz TD, Koppenhafer SL, tenEyck CJ, Schutte BC. Ontogeny of malate-aspartate shuttle capacity and gene expression in cardiac mitochondria. *Am J Physiol* 1998;274:C780-8.
24. Werner JC, Sicard RE. Lactate metabolism of isolated, perfused fetal, and newborn pig hearts. *Pediatr Res* 1987;22:552-6.
25. Itoi T, Lopaschuk GD. The contribution of glycolysis, glucose oxidation, lactate oxidation, and fatty acid oxidation to ATP production in isolated biventricular working hearts from 2-week-old rabbits. *Pediatr Res* 1993;34:735-41.

26. Werner JC, Whitman V, Musselman J, Schuler HG. Perinatal changes in mitochondrial respiration of the rabbit heart. *Biol Neonate* 1982;42:208-16.
27. Medina JM. The role of lactate as an energy substrate for the brain during the early neonatal period. *Biol Neonate* 1985;48:237-44.
28. Smith HE, Page E. Ultrastructural changes in rabbit heart mitochondria during the perinatal period. Neonatal transition to aerobic metabolism. *Dev Biol* 1977;57:109-17.
29. Luiken JJ, Koonen DP, Willems J, et al. Insulin stimulates long-chain fatty acid utilization by rat cardiac myocytes through cellular redistribution of FAT/CD36. *Diabetes* 2002;51:3113-9.
30. Fischer Y, Thomas J, Sevilla L, et al. Insulin-induced recruitment of glucose transporter 4 (GLUT4) and GLUT1 in isolated rat cardiac myocytes. Evidence of the existence of different intracellular GLUT4 vesicle populations. *J Biol Chem* 1997;272:7085-92.
31. Schwenk RW, Luiken JJ, Bonen A, Glatz JF. Regulation of sarcolemmal glucose and fatty acid transporters in cardiac disease. *Cardiovasc Res* 2008;79:249-58.

32. Fang X, Palanivel R, Cresser J, et al. An APPL1-AMPK signaling axis mediates beneficial metabolic effects of adiponectin in the heart. *Am J Physiol Endocrinol Metab* 2010;299:E721-9.
33. Onay-Besikci A, Altarejos JY, Lopaschuk GD. gAd-globular head domain of adiponectin increases fatty acid oxidation in newborn rabbit hearts. *J Biol Chem* 2004;279:44320-6.
34. Steinmetz M, Quentin T, Poppe A, Paul T, Jux C. Changes in expression levels of genes involved in fatty acid metabolism: upregulation of all three members of the PPAR family (alpha, gamma, delta) and the newly described adiponectin receptor 2, but not adiponectin receptor 1 during neonatal cardiac development of the rat. *Basic Res Cardiol* 2005;100:263-9.
35. Lopaschuk GD, Witters LA, Itoi T, Barr R, Barr A. Acetyl-CoA carboxylase involvement in the rapid maturation of fatty acid oxidation in the newborn rabbit heart. *J Biol Chem* 1994;269:25871-8.
36. Lopaschuk GD, Spafford MA. Differences in myocardial ischemic tolerance between 1- and 7-day-old rabbits. *Can J Physiol Pharmacol* 1992;70:1315-23.

37. Kunau WH, Dommes V, Schulz H. beta-oxidation of fatty acids in mitochondria, peroxisomes, and bacteria: a century of continued progress. *Prog Lipid Res* 1995;34:267-342.
38. Knopp RH, Warth MR, Charles D, et al. Lipoprotein metabolism in pregnancy, fat transport to the fetus, and the effects of diabetes. *Biol Neonate* 1986;50:297-317.
39. Portman OW, Behrman RE, Soltys P. Transfer of free fatty acids across the primate placenta. *Am J Physiol* 1969;216:143-7.
40. Kudo N, Gillespie JG, Kung L, et al. Characterization of 5'AMP-activated protein kinase activity in the heart and its role in inhibiting acetyl-CoA carboxylase during reperfusion following ischemia. *Biochim Biophys Acta* 1996;1301:67-75.
41. Makinde AO, Gamble J, Lopaschuk GD. Upregulation of 5'-AMP-activated protein kinase is responsible for the increase in myocardial fatty acid oxidation rates following birth in the newborn rabbit. *Circ Res* 1997;80:482-9.
42. Sakamoto J, Barr RL, Kavanagh KM, Lopaschuk GD. Contribution of malonyl-CoA decarboxylase to the high fatty acid oxidation rates seen in the diabetic heart. *Am J Physiol Heart Circ Physiol* 2000;278:H1196-204.

43. Dyck JR, Berthiaume LG, Thomas PD, et al. Characterization of rat liver malonyl-CoA decarboxylase and the study of its role in regulating fatty acid metabolism. *Biochem J* 2000;350 Pt 2:599-608.
44. Lee GY, Kim NH, Zhao ZS, Cha BS, Kim YS. Peroxisomal-proliferator-activated receptor alpha activates transcription of the rat hepatic malonyl-CoA decarboxylase gene: a key regulation of malonyl-CoA level. *Biochem J* 2004;378:983-90.
45. Yoda-Murakami M, Taniguchi M, Takahashi K, et al. Change in expression of GBP28/adiponectin in carbon tetrachloride-administrated mouse liver. *Biochem Biophys Res Commun* 2001;285:372-7.
46. Dyck JR, Barr AJ, Barr RL, Kolattukudy PE, Lopaschuk GD. Characterization of cardiac malonyl-CoA decarboxylase and its putative role in regulating fatty acid oxidation. *Am J Physiol* 1998;275:H2122-9.
47. Anderson PG, Allard MF, Thomas GD, Bishop SP, Digerness SB. Increased ischemic injury but decreased hypoxic injury in hypertrophied rat hearts. *Circ Res* 1990;67:948-59.
48. Buser PT, Wikman-Coffelt J, Wu ST, Derugin N, Parmley WW, Higgins CB. Postischemic recovery of mechanical performance and energy metabolism in the presence of left ventricular hypertrophy. A ³¹P-MRS study. *Circ Res* 1990;66:735-46.

49. Hearse DJ, Stewart DA, Green DG. Myocardial susceptibility to ischemic damage: a comparative study of disease models in the rat. *Eur J Cardiol* 1978;7:437-50.
50. Brown NF, Weis BC, Husti JE, Foster DW, McGarry JD. Mitochondrial carnitine palmitoyltransferase I isoform switching in the developing rat heart. *J Biol Chem* 1995;270:8952-7.
51. Onay-Besikci A, Campbell FM, Hopkins TA, Dyck JR, Lopaschuk GD. Relative importance of malonyl CoA and carnitine in maturation of fatty acid oxidation in newborn rabbit heart. *Am J Physiol Heart Circ Physiol* 2003;284:H283-9.
52. Sugden MC, Langdown ML, Harris RA, Holness MJ. Expression and regulation of pyruvate dehydrogenase kinase isoforms in the developing rat heart and in adulthood: role of thyroid hormone status and lipid supply. *Biochem J* 2000;352 Pt 3:731-8.
53. Spriet LL, Heigenhauser GJ. Regulation of pyruvate dehydrogenase (PDH) activity in human skeletal muscle during exercise. *Exerc Sport Sci Rev* 2002;30:91-5.
54. Papandreou I, Cairns RA, Fontana L, Lim AL, Denko NC. HIF-1 mediates adaptation to hypoxia by actively downregulating mitochondrial oxygen consumption. *Cell Metab* 2006;3:187-97.

55. Kim JW, Tchernyshyov I, Semenza GL, Dang CV. HIF-1-mediated expression of pyruvate dehydrogenase kinase: a metabolic switch required for cellular adaptation to hypoxia. *Cell Metab* 2006;3:177-85.
56. Iyer NV, Kotch LE, Agani F, et al. Cellular and developmental control of O₂ homeostasis by hypoxia-inducible factor 1 alpha. *Genes Dev* 1998;12:149-62.
57. Ryan HE, Lo J, Johnson RS. HIF-1 alpha is required for solid tumor formation and embryonic vascularization. *EMBO J* 1998;17:3005-15.
58. Wood SM, Wiesener MS, Yeates KM, et al. Selection and analysis of a mutant cell line defective in the hypoxia-inducible factor-1 alpha-subunit (HIF-1alpha). Characterization of hif-1alpha-dependent and -independent hypoxia-inducible gene expression. *J Biol Chem* 1998;273:8360-8.
59. Nau PN, Van Natta T, Ralphe JC, et al. Metabolic adaptation of the fetal and postnatal ovine heart: regulatory role of hypoxia-inducible factors and nuclear respiratory factor-1. *Pediatr Res* 2002;52:269-78.
60. Finck BN. The PPAR regulatory system in cardiac physiology and disease. *Cardiovasc Res* 2007;73:269-77.
61. Huss JM, Kelly DP. Nuclear receptor signaling and cardiac energetics. *Circ Res* 2004;95:568-78.

62. van der Lee KA, Vork MM, De Vries JE, et al. Long-chain fatty acid-induced changes in gene expression in neonatal cardiac myocytes. *J Lipid Res* 2000;41:41-7.
63. Brandt JM, Djouadi F, Kelly DP. Fatty acids activate transcription of the muscle carnitine palmitoyltransferase I gene in cardiac myocytes via the peroxisome proliferator-activated receptor alpha. *J Biol Chem* 1998;273:23786-92.
64. Mascaro C, Acosta E, Ortiz JA, Marrero PF, Hegardt FG, Haro D. Control of human muscle-type carnitine palmitoyltransferase I gene transcription by peroxisome proliferator-activated receptor. *J Biol Chem* 1998;273:8560-3.
65. Gulick T, Cresci S, Caira T, Moore DD, Kelly DP. The peroxisome proliferator-activated receptor regulates mitochondrial fatty acid oxidative enzyme gene expression. *Proc Natl Acad Sci U S A* 1994;91:11012-6.
66. Leone TC, Weinheimer CJ, Kelly DP. A critical role for the peroxisome proliferator-activated receptor alpha (PPARalpha) in the cellular fasting response: the PPARalpha-null mouse as a model of fatty acid oxidation disorders. *Proc Natl Acad Sci U S A* 1999;96:7473-8.

67. Finck BN, Lehman JJ, Leone TC, et al. The cardiac phenotype induced by PPARalpha overexpression mimics that caused by diabetes mellitus. *J Clin Invest* 2002;109:121-30.
68. Campbell FM, Kozak R, Wagner A, et al. A role for peroxisome proliferator-activated receptor alpha (PPARalpha) in the control of cardiac malonyl-CoA levels: reduced fatty acid oxidation rates and increased glucose oxidation rates in the hearts of mice lacking PPARalpha are associated with higher concentrations of malonyl-CoA and reduced expression of malonyl-CoA decarboxylase. *J Biol Chem* 2002;277:4098-103.
69. Skarka L, Bardova K, Brauner P, et al. Expression of mitochondrial uncoupling protein 3 and adenine nucleotide translocase 1 genes in developing rat heart: putative involvement in control of mitochondrial membrane potential. *J Mol Cell Cardiol* 2003;35:321-30.
70. Michalik L, Auwerx J, Berger JP, et al. International Union of Pharmacology. LXI. Peroxisome proliferator-activated receptors. *Pharmacol Rev* 2006;58:726-41.
71. Gottlicher M, Widmark E, Li Q, Gustafsson JA. Fatty acids activate a chimera of the clofibric acid-activated receptor and the glucocorticoid receptor. *Proc Natl Acad Sci U S A* 1992;89:4653-7.

72. Kliewer SA, Sundseth SS, Jones SA, et al. Fatty acids and eicosanoids regulate gene expression through direct interactions with peroxisome proliferator-activated receptors alpha and gamma. *Proc Natl Acad Sci U S A* 1997;94:4318-23.
73. Xu L, Glass CK, Rosenfeld MG. Coactivator and corepressor complexes in nuclear receptor function. *Curr Opin Genet Dev* 1999;9:140-7.
74. Braissant O, Fougère F, Scotto C, Dauca M, Wahli W. Differential expression of peroxisome proliferator-activated receptors (PPARs): tissue distribution of PPAR-alpha, -beta, and -gamma in the adult rat. *Endocrinology* 1996;137:354-66.
75. Schoonjans K, Peinado-Onsurbe J, Lefebvre AM, et al. PPARalpha and PPARgamma activators direct a distinct tissue-specific transcriptional response via a PPRE in the lipoprotein lipase gene. *EMBO J* 1996;15:5336-48.
76. Staels B, Koenig W, Habib A, et al. Activation of human aortic smooth-muscle cells is inhibited by PPARalpha but not by PPARgamma activators. *Nature* 1998;393:790-3.
77. Chinetti G, Gbaguidi FG, Griglio S, et al. CLA-1/SR-BI is expressed in atherosclerotic lesion macrophages and regulated by activators of

- peroxisome proliferator-activated receptors. *Circulation* 2000;101:2411-7.
78. Escher P, Wahli W. Peroxisome proliferator-activated receptors: insight into multiple cellular functions. *Mutat Res* 2000;448:121-38.
79. Robinson E, Grieve DJ. Significance of peroxisome proliferator-activated receptors in the cardiovascular system in health and disease. *Pharmacol Ther* 2009;122:246-63.
80. Wagner KD, Wagner N. Peroxisome proliferator-activated receptor beta/delta (PPARbeta/delta) acts as regulator of metabolism linked to multiple cellular functions. *Pharmacol Ther* 2010;125:423-35.
81. Abbott BD, Wood CR, Watkins AM, Das KP, Lau CS. Peroxisome proliferator-activated receptors alpha, Beta, and gamma mRNA and protein expression in human fetal tissues. *PPAR Res* 2010;2010.
82. Sharifpanah F, Wartenberg M, Hannig M, Piper HM, Sauer H. Peroxisome proliferator-activated receptor alpha agonists enhance cardiomyogenesis of mouse ES cells by utilization of a reactive oxygen species-dependent mechanism. *Stem Cells* 2008;26:64-71.
83. Kelly DP, Gordon JI, Alpers R, Strauss AW. The tissue-specific expression and developmental regulation of two nuclear genes encoding rat

- mitochondrial proteins. Medium chain acyl-CoA dehydrogenase and mitochondrial malate dehydrogenase. *J Biol Chem* 1989;264:18921-5.
84. Nagao M, Parimoo B, Tanaka K. Developmental, nutritional, and hormonal regulation of tissue-specific expression of the genes encoding various acyl-CoA dehydrogenases and alpha-subunit of electron transfer flavoprotein in rat. *J Biol Chem* 1993;268:24114-24.
85. Disch DL, Rader TA, Cresci S, et al. Transcriptional control of a nuclear gene encoding a mitochondrial fatty acid oxidation enzyme in transgenic mice: role for nuclear receptors in cardiac and brown adipose expression. *Mol Cell Biol* 1996;16:4043-51.
86. Semenza GL. Hypoxia-inducible factor 1: oxygen homeostasis and disease pathophysiology. *Trends Mol Med* 2001;7:345-50.
87. Kaelin WG, Jr. Molecular basis of the VHL hereditary cancer syndrome. *Nat Rev Cancer* 2002;2:673-82.
88. Gordan JD, Thompson CB, Simon MC. HIF and c-Myc: sibling rivals for control of cancer cell metabolism and proliferation. *Cancer Cell* 2007;12:108-13.
89. Bruick RK, McKnight SL. A conserved family of prolyl-4-hydroxylases that modify HIF. *Science* 2001;294:1337-40.

90. Jaakkola P, Mole DR, Tian YM, et al. Targeting of HIF- α to the von Hippel-Lindau ubiquitylation complex by O₂-regulated prolyl hydroxylation. *Science* 2001;292:468-72.
91. Bhaskar PT, Nogueira V, Patra KC, et al. mTORC1 hyperactivity inhibits serum deprivation-induced apoptosis via increased hexokinase II and GLUT1 expression, sustained Mcl-1 expression, and glycogen synthase kinase 3 β inhibition. *Mol Cell Biol* 2009;29:5136-47.
92. Compernelle V, Brusselmans K, Franco D, et al. *Cardia bifida*, defective heart development and abnormal neural crest migration in embryos lacking hypoxia-inducible factor-1 α . *Cardiovasc Res* 2003;60:569-79.
93. Krishnan J, Ahuja P, Bodenmann S, et al. Essential role of developmentally activated hypoxia-inducible factor 1 α for cardiac morphogenesis and function. *Circ Res* 2008;103:1139-46.
94. Amati F, Diano L, Campagnolo L, et al. Hif1 α down-regulation is associated with transposition of great arteries in mice treated with a retinoic acid antagonist. *BMC Genomics* 2010;11:497.
95. Minich LL, Atz AM, Colan SD, et al. Partial and transitional atrioventricular septal defect outcomes. *Ann Thorac Surg* 2010;89:530-6.

96. Allen BS. The clinical significance of the reoxygenation injury in pediatric heart surgery. *Semin Thorac Cardiovasc Surg Pediatr Card Surg Annu* 2003;6:116-27.
97. Allen BS. Pediatric myocardial protection: a cardioplegic strategy is the "solution". *Semin Thorac Cardiovasc Surg Pediatr Card Surg Annu* 2004;7:141-54.
98. Allen BS, Barth MJ, Ilbawi MN. Pediatric myocardial protection: an overview. *Semin Thorac Cardiovasc Surg* 2001;13:56-72.
99. Amark K, Berggren H, Bjork K, et al. Blood cardioplegia provides superior protection in infant cardiac surgery. *Ann Thorac Surg* 2005;80:989-94.
100. Durandy Y. Pediatric myocardial protection. *Curr Opin Cardiol* 2008;23:85-90.
101. Hammon JW, Jr. Myocardial protection in the immature heart. *Ann Thorac Surg* 1995;60:839-42.
102. Welke KF, Diggs BS, Karamlou T, Ungerleider RM. Comparison of pediatric cardiac surgical mortality rates from national administrative data to contemporary clinical standards. *Ann Thorac Surg* 2009;87:216-22; discussion 222-3.
103. Allen BS. Pediatric myocardial protection: where do we stand? *J Thorac Cardiovasc Surg* 2004;128:11-3.

104. Bolling K, Kronon M, Allen BS, et al. Myocardial protection in normal and hypoxically stressed neonatal hearts: the superiority of hypocalcemic versus normocalcemic blood cardioplegia. *J Thorac Cardiovasc Surg* 1996;112:1193-200; discussion 1200-1.
105. Bolling K, Kronon M, Allen BS, Wang T, Ramon S, Feinberg H. Myocardial protection in normal and hypoxically stressed neonatal hearts: the superiority of blood versus crystalloid cardioplegia. *J Thorac Cardiovasc Surg* 1997;113:994-1003; discussion 1003-5.
106. Butler TL, Egan JR, Graf FG, et al. Dysfunction induced by ischemia versus edema: does edema matter? *J Thorac Cardiovasc Surg* 2009;138:141-7, 147 e1.
107. Modi P, Suleiman MS, Reeves B, et al. Myocardial metabolic changes during pediatric cardiac surgery: a randomized study of 3 cardioplegic techniques. *J Thorac Cardiovasc Surg* 2004;128:67-75.
108. Imura H, Caputo M, Parry A, Pawade A, Angelini GD, Suleiman MS. Age-dependent and hypoxia-related differences in myocardial protection during pediatric open heart surgery. *Circulation* 2001;103:1551-6.
109. Caputo M, Modi P, Imura H, et al. Cold blood versus cold crystalloid cardioplegia for repair of ventricular septal defects in pediatric heart

surgery: a randomized controlled trial. *Ann Thorac Surg* 2002;74:530-4; discussion 535.

110. Hoffman TM, Wernovsky G, Atz AM, et al. Efficacy and safety of milrinone in preventing low cardiac output syndrome in infants and children after corrective surgery for congenital heart disease. *Circulation* 2003;107:996-1002.
111. Gaies MG, Gurney JG, Yen AH, et al. Vasoactive-inotropic score as a predictor of morbidity and mortality in infants after cardiopulmonary bypass. *Pediatr Crit Care Med* 2010;11:234-8.
112. Scheurer MA, Thiagarajan RR. Vasoactive-inotropic score as a measure of pediatric cardiac surgical outcomes. *Pediatr Crit Care Med* 2010;11:307-8.
113. Basaran M, Sever K, Kafali E, et al. Serum lactate level has prognostic significance after pediatric cardiac surgery. *J Cardiothorac Vasc Anesth* 2006;20:43-7.
114. Cheifetz IM, Kern FH, Schulman SR, Greeley WJ, Ungerleider RM, Meliones JN. Serum lactates correlate with mortality after operations for complex congenital heart disease. *Ann Thorac Surg* 1997;64:735-8.
115. Hannan RL, Ybarra MA, White JA, Ojito JW, Rossi AF, Burke RP. Patterns of lactate values after congenital heart surgery and timing of

- cardiopulmonary support. *Ann Thorac Surg* 2005;80:1468-73; discussion 1473-4.
116. Siegel LB, Dalton HJ, Hertzog JH, Hopkins RA, Hannan RL, Hauser GJ. Initial postoperative serum lactate levels predict survival in children after open heart surgery. *Intensive Care Med* 1996;22:1418-23.
117. Munoz R, Laussen PC, Palacio G, Zienko L, Piercey G, Wessel DL. Changes in whole blood lactate levels during cardiopulmonary bypass for surgery for congenital cardiac disease: an early indicator of morbidity and mortality. *J Thorac Cardiovasc Surg* 2000;119:155-62.
118. Molina Hazan V, Gonen Y, Vardi A, et al. Blood lactate levels differ significantly between surviving and nonsurviving patients within the same risk-adjusted Classification for Congenital Heart Surgery (RACHS-1) group after pediatric cardiac surgery. *Pediatr Cardiol* 2010;31:952-60.
119. Lopaschuk GD, Ussher JR, Folmes CDL, Jaswal JS, Stanley WC. Myocardial fatty acid metabolism in health and disease. Submitted to *Physiol Rev* 2009.
120. Lopaschuk GD. Metabolic abnormalities in the diabetic heart. *Heart Fail Rev* 2002;7:149-59.

121. Scolletta S, Biagioli B. Energetic myocardial metabolism and oxidative stress: let's make them our friends in the fight against heart failure. *Biomed Pharmacother* 2010;64:203-7.
122. Lopaschuk GD. AMP-activated protein kinase control of energy metabolism in the ischemic heart. *Int J Obes (Lond)* 2008;32 Suppl 4:S29-35.
123. Taegtmeyer H, King LM, Jones BE. Energy substrate metabolism, myocardial ischemia, and targets for pharmacotherapy. *Am J Cardiol* 1998;82:54K-60K.
124. Ussher JR, Lopaschuk GD. Targeting malonyl CoA inhibition of mitochondrial fatty acid uptake as an approach to treat cardiac ischemia/reperfusion. *Basic Res Cardiol* 2009;104:203-10.
125. Liu B, el Alaoui-Talibi Z, Clanachan AS, Schulz R, Lopaschuk GD. Uncoupling of contractile function from mitochondrial TCA cycle activity and MVO₂ during reperfusion of ischemic hearts. *Am J Physiol* 1996;270:H72-80.
126. Taegtmeyer H, Goodwin GW, Doenst T, Frazier OH. Substrate metabolism as a determinant for postischemic functional recovery of the heart. *Am J Cardiol* 1997;80:3A-10A.

127. Kantor PF, Dyck JR, Lopaschuk GD. Fatty acid oxidation in the reperfused ischemic heart. *Am J Med Sci* 1999;318:3-14.
128. Karmazyn M, Sawyer M, Fliegel L. The Na(+)/H(+) exchanger: a target for cardiac therapeutic intervention. *Curr Drug Targets Cardiovasc Haematol Disord* 2005;5:323-35.
129. Wang Y, Meyer JW, Ashraf M, Shull GE. Mice with a null mutation in the NHE1 Na⁺-H⁺ exchanger are resistant to cardiac ischemia-reperfusion injury. *Circ Res* 2003;93:776-82.
130. Hinata M, Kimura J. Forefront of Na⁺/Ca²⁺ exchanger studies: stoichiometry of cardiac Na⁺/Ca²⁺ exchanger; 3:1 or 4:1? *J Pharmacol Sci* 2004;96:15-8.
131. Liu B, Clanachan AS, Schulz R, Lopaschuk GD. Cardiac efficiency is improved after ischemia by altering both the source and fate of protons. *Circ Res* 1996;79:940-8.
132. Cross HR, Lu L, Steenbergen C, Philipson KD, Murphy E. Overexpression of the cardiac Na⁺/Ca²⁺ exchanger increases susceptibility to ischemia/reperfusion injury in male, but not female, transgenic mice. *Circ Res* 1998;83:1215-23.
133. Talukder MA, Zweier JL, Periasamy M. Targeting calcium transport in ischaemic heart disease. *Cardiovasc Res* 2009;84:345-52.

134. Early treatment of unstable angina in the coronary care unit: a randomised, double blind, placebo controlled comparison of recurrent ischaemia in patients treated with nifedipine or metoprolol or both. Report of The Holland Interuniversity Nifedipine/Metoprolol Trial (HINT) Research Group. *Br Heart J* 1986;56:400-13.
135. Theroux P, Gregoire J, Chin C, Pelletier G, de Guise P, Juneau M. Intravenous diltiazem in acute myocardial infarction. Diltiazem as adjunctive therapy to activase (DATA) trial. *J Am Coll Cardiol* 1998;32:620-8.
136. Sheiban I, Tonni S, Chizzoni A, Marini A, Trevisani G. Recovery of left ventricular function following early reperfusion in acute myocardial infarction: a potential role for the calcium antagonist nisoldipine. *Cardiovasc Drugs Ther* 1997;11:5-16.
137. Andreadou I, Iliodromitis EK, Koufaki M, Kremastinos DT. Pharmacological pre- and post- conditioning agents: reperfusion-injury of the heart revisited. *Mini Rev Med Chem* 2008;8:952-9.
138. Talukder MA, Kalyanasundaram A, Zuo L, et al. Is reduced SERCA2a expression detrimental or beneficial to postischemic cardiac function and injury? Evidence from heterozygous SERCA2a knockout mice. *Am J Physiol Heart Circ Physiol* 2008;294:H1426-34.

139. Talukder MA, Yang F, Nishijima Y, et al. Reduced SERCA2a converts sub-lethal myocardial injury to infarction and affects postischemic functional recovery. *J Mol Cell Cardiol* 2009;46:285-7.
140. Ostadal B. The past, the present and the future of experimental research on myocardial ischemia and protection. *Pharmacol Rep* 2009;61:3-12.
141. Lopaschuk GD, Collins-Nakai R, Olley PM, et al. Plasma fatty acid levels in infants and adults after myocardial ischemia. *Am Heart J* 1994;128:61-7.
142. Kudo N, Barr AJ, Barr RL, Desai S, Lopaschuk GD. High rates of fatty acid oxidation during reperfusion of ischemic hearts are associated with a decrease in malonyl-CoA levels due to an increase in 5'-AMP-activated protein kinase inhibition of acetyl-CoA carboxylase. *J Biol Chem* 1995;270:17513-20.
143. Saddik M, Lopaschuk GD. Myocardial triglyceride turnover during reperfusion of isolated rat hearts subjected to a transient period of global ischemia. *J Biol Chem* 1992;267:3825-31.
144. Lopaschuk GD, Spafford MA, Davies NJ, Wall SR. Glucose and palmitate oxidation in isolated working rat hearts reperfused after a period of transient global ischemia. *Circ Res* 1990;66:546-53.

145. Randle PJ, Garland PB, Newsholme EA, Hales CN. The glucose fatty acid cycle in obesity and maturity onset diabetes mellitus. *Ann N Y Acad Sci* 1965;131:324-33.
146. Ruiz-Meana M, Garcia-Dorado D. Translational cardiovascular medicine (II). Pathophysiology of ischemia-reperfusion injury: new therapeutic options for acute myocardial infarction. *Rev Esp Cardiol* 2009;62:199-209.
147. Liu Q, Docherty JC, Rendell JC, Clanachan AS, Lopaschuk GD. High levels of fatty acids delay the recovery of intracellular pH and cardiac efficiency in post-ischemic hearts by inhibiting glucose oxidation. *J Am Coll Cardiol* 2002;39:718-25.
148. Tani M, Neely JR. Na⁺ accumulation increases Ca²⁺ overload and impairs function in anoxic rat heart. *J Mol Cell Cardiol* 1990;22:57-72.
149. Magovern JA, Pae WE, Jr., Miller CA, Waldhausen JA. The immature and the mature myocardium. Responses to multidose crystalloid cardioplegia. *J Thorac Cardiovasc Surg* 1988;95:618-24.
150. Parrish MD, Payne A, Fixler DE. Global myocardial ischemia in the newborn, juvenile, and adult isolated isovolumic rabbit heart. Age-related differences in systolic function, diastolic stiffness, coronary resistance, myocardial oxygen consumption, and extracellular pH. *Circ Res* 1987;61:609-15.

151. Pridjian AK, Levitsky S, Krukenkamp I, Silverman NA, Feinberg H. Developmental changes in reperfusion injury. A comparison of intracellular cation accumulation in the newborn, neonatal, and adult heart. *J Thorac Cardiovasc Surg* 1987;93:428-33.
152. Watanabe H, Yokosawa T, Eguchi S, Imai S. Functional and metabolic protection of the neonatal myocardium from ischemia. Insufficient protection by cardioplegia. *J Thorac Cardiovasc Surg* 1989;97:50-8.
153. Wittnich C, Peniston C, Ianuzzo D, Abel JG, Salerno TA. Relative vulnerability of neonatal and adult hearts to ischemic injury. *Circulation* 1987;76:V156-60.
154. Wittnich C, Belanger MP, Bandali KS. Newborn hearts are at greater 'metabolic risk' during global ischemia--advantages of continuous coronary washout. *Can J Cardiol* 2007;23:195-200.
155. Hammel JM, Caldarone CA, Van Natta TL, et al. Myocardial apoptosis after cardioplegic arrest in the neonatal lamb. *J Thorac Cardiovasc Surg* 2003;125:1268-75.
156. Baker JE, Boerboom LE, Olinger GN. Age-related changes in the ability of hypothermia and cardioplegia to protect ischemic rabbit myocardium. *J Thorac Cardiovasc Surg* 1988;96:717-24.

157. Bove EL, Stammers AH. Recovery of left ventricular function after hypothermic global ischemia. Age-related differences in the isolated working rabbit heart. *J Thorac Cardiovasc Surg* 1986;91:115-22.
158. Bove EL, Stammers AH, Gallagher KP. Protection of the neonatal myocardium during hypothermic ischemia. Effect of cardioplegia on left ventricular function in the rabbit. *J Thorac Cardiovasc Surg* 1987;94:115-23.
159. Coles JG, Watanabe T, Wilson GJ, et al. Age-related differences in the response to myocardial ischemic stress. *J Thorac Cardiovasc Surg* 1987;94:526-34.
160. Jarmakani JM, Nakazawa M, Nagatomo T, Langer GA. Effect of hypoxia on mechanical function in the neonatal mammalian heart. *Am J Physiol* 1978;235:H469-74.
161. Nishioka K, Jarmakani JM. Effect of ischemia on mechanical function and high-energy phosphates in rabbit myocardium. *Am J Physiol* 1982;242:H1077-83.
162. Yano Y, Braimbridge MV, Hearse DJ. Protection of the pediatric myocardium. Differential susceptibility to ischemic injury of the neonatal rat heart. *J Thorac Cardiovasc Surg* 1987;94:887-96.

163. Murashita T, Borgers M, Hearse DJ. Developmental changes in tolerance to ischaemia in the rabbit heart: disparity between interpretations of structural, enzymatic and functional indices of injury. *J Mol Cell Cardiol* 1992;24:1143-54.
164. Achterberg PW, Nieukoop AS, Schoutsen B, de Jong JW. Different ATP-catabolism in reperfused adult and newborn rat hearts. *Am J Physiol* 1988;254:H1091-8.
165. Riva E, Leopaldi D. Control of the cardiac consequences of myocardial ischemia and reperfusion by L-propionylcarnitine: age-response and dose-response studies in the rat heart. *Pediatr Res* 1993;34:465-70.
166. Wittnich C, Su J, Boscarino C, Belanger M. Age-related differences in myocardial hydrogen ion buffering during ischemia. *Mol Cell Biochem* 2006;285:61-7.
167. Wittnich C. Age-related differences in myocardial metabolism affects response to ischemia. Age in heart tolerance to ischemia. *Am J Cardiovasc Pathol* 1992;4:175-80.
168. Chiu RC, Bindon W. Why are newborn hearts vulnerable to global ischemia? The lactate hypothesis. *Circulation* 1987;76:V146-9.
169. Milerova M, Charvatova Z, Skarka L, et al. Neonatal cardiac mitochondria and ischemia/reperfusion injury. *Mol Cell Biochem* 2010;335:147-53.

170. Lopaschuk GD, Stanley WC. Glucose metabolism in the ischemic heart. *Circulation* 1997;95:313-5.
171. Stanley WC, Lopaschuk GD, McCormack JG. Regulation of energy substrate metabolism in the diabetic heart. *Cardiovasc Res* 1997;34:25-33.
172. Stanley WC, Lopaschuk GD, Hall JL, McCormack JG. Regulation of myocardial carbohydrate metabolism under normal and ischaemic conditions. Potential for pharmacological interventions. *Cardiovasc Res* 1997;33:243-57.
173. Itoi T, Huang L, Lopaschuk GD. Glucose use in neonatal rabbit hearts reperfused after global ischemia. *Am J Physiol* 1993;265:H427-33.
174. McVeigh JJ, Lopaschuk GD. Dichloroacetate stimulation of glucose oxidation improves recovery of ischemic rat hearts. *Am J Physiol* 1990;259:H1079-85.
175. Stanley WC, Hernandez LA, Spires D, Bringas J, Wallace S, McCormack JG. Pyruvate dehydrogenase activity and malonyl CoA levels in normal and ischemic swine myocardium: effects of dichloroacetate. *J Mol Cell Cardiol* 1996;28:905-14.

176. Fragasso G, Palloshi A, Puccetti P, et al. A randomized clinical trial of trimetazidine, a partial free fatty acid oxidation inhibitor, in patients with heart failure. *J Am Coll Cardiol* 2006;48:992-8.
177. Fragasso G, Perseghin G, De Cobelli F, et al. Effects of metabolic modulation by trimetazidine on left ventricular function and phosphocreatine/adenosine triphosphate ratio in patients with heart failure. *Eur Heart J* 2006;27:942-8.
178. Torrance SM, Belanger MP, Wallen WJ, Wittnich C. Metabolic and functional response of neonatal pig hearts to the development of ischemic contracture: is recovery possible? *Pediatr Res* 2000;48:191-9.
179. Julia P, Young HH, Buckberg GD, Kofsky ER, Bugyi HI. Studies of myocardial protection in the immature heart. IV. Improved tolerance of immature myocardium to hypoxia and ischemia by intravenous metabolic support. *J Thorac Cardiovasc Surg* 1991;101:23-32.
180. Hammon JW, Jr., Graham TP, Jr., Boucek RJ, Jr., Parrish MD, Merrill WH, Bender HW, Jr. Myocardial adenosine triphosphate content as a measure of metabolic and functional myocardial protection in children undergoing cardiac operation. *Ann Thorac Surg* 1987;44:467-70.

181. Ito M, Jaswal JS, Lam VH, et al. High levels of fatty acids increase contractile function of neonatal rabbit hearts during reperfusion following ischemia. *Am J Physiol Heart Circ Physiol* 2010;298:H1426-37.
182. Itoi T, Lopaschuk GD. Calcium improves mechanical function and carbohydrate metabolism following ischemia in isolated Bi-ventricular working hearts from immature rabbits. *J Mol Cell Cardiol* 1996;28:1501-14.
183. Saiki Y, Lopaschuk GD, Dodge K, Yamaya K, Morgan C, Rebeyka IM. Pyruvate augments mechanical function via activation of the pyruvate dehydrogenase complex in reperfused ischemic immature rabbit hearts. *J Surg Res* 1998;79:164-9.
184. Lorell BH, Grossman W. Cardiac hypertrophy: the consequences for diastole. *J Am Coll Cardiol* 1987;9:1189-93.
185. van Bilsen M, Smeets PJ, Gilde AJ, van der Vusse GJ. Metabolic remodelling of the failing heart: the cardiac burn-out syndrome? *Cardiovasc Res* 2004;61:218-26.
186. Razeghi P, Young ME, Alcorn JL, Moravec CS, Frazier OH, Taegtmeier H. Metabolic gene expression in fetal and failing human heart. *Circulation* 2001;104:2923-31.

187. Barger PM, Brandt JM, Leone TC, Weinheimer CJ, Kelly DP. Deactivation of peroxisome proliferator-activated receptor-alpha during cardiac hypertrophic growth. *J Clin Invest* 2000;105:1723-30.
188. Bishop SP, Altschuld RA. Increased glycolytic metabolism in cardiac hypertrophy and congestive failure. *Am J Physiol* 1970;218:153-9.
189. Taegtmeyer H, Overturf ML. Effects of moderate hypertension on cardiac function and metabolism in the rabbit. *Hypertension* 1988;11:416-26.
190. Ingwall JS. The hypertrophied myocardium accumulates the MB-creatine kinase isozyme. *Eur Heart J* 1984;5 Suppl F:129-39.
191. Morissette MR, Howes AL, Zhang T, Heller Brown J. Upregulation of GLUT1 expression is necessary for hypertrophy and survival of neonatal rat cardiomyocytes. *J Mol Cell Cardiol* 2003;35:1217-27.
192. Minchenko O, Opentanova I, Caro J. Hypoxic regulation of the 6-phosphofructo-2-kinase/fructose-2,6-bisphosphatase gene family (PFKFB-1-4) expression in vivo. *FEBS Lett* 2003;554:264-70.
193. Depre C, Shipley GL, Chen W, et al. Unloaded heart in vivo replicates fetal gene expression of cardiac hypertrophy. *Nat Med* 1998;4:1269-75.
194. Nascimben L, Ingwall JS, Lorell BH, et al. Mechanisms for increased glycolysis in the hypertrophied rat heart. *Hypertension* 2004;44:662-7.

195. DiMauro S, Hirano M. Mitochondria and heart disease. *Curr Opin Cardiol* 1998;13:190-7.
196. Piao L, Marsboom G, Archer SL. Mitochondrial metabolic adaptation in right ventricular hypertrophy and failure. *J Mol Med* 2010;88:1011-20.
197. Kato T, Niizuma S, Inuzuka Y, et al. Analysis of metabolic remodeling in compensated left ventricular hypertrophy and heart failure. *Circ Heart Fail* 2010;3:420-30.
198. Wambolt RB, Henning SL, English DR, Dyachkova Y, Lopaschuk GD, Allard MF. Glucose utilization and glycogen turnover are accelerated in hypertrophied rat hearts during severe low-flow ischemia. *J Mol Cell Cardiol* 1999;31:493-502.
199. el Alaoui-Talibi Z, Landormy S, Loireau A, Moravec J. Fatty acid oxidation and mechanical performance of volume-overloaded rat hearts. *Am J Physiol* 1992;262:H1068-74.
200. van der Vusse GJ, van Bilsen M, Glatz JF. Cardiac fatty acid uptake and transport in health and disease. *Cardiovasc Res* 2000;45:279-93.
201. Li R, Zheng W, Pi R, et al. Activation of peroxisome proliferator-activated receptor-alpha prevents glycogen synthase 3beta phosphorylation and inhibits cardiac hypertrophy. *FEBS Lett* 2007;581:3311-6.

202. Brigadeau F, Gele P, Wibaux M, et al. The PPARalpha activator fenofibrate slows down the progression of the left ventricular dysfunction in porcine tachycardia-induced cardiomyopathy. *J Cardiovasc Pharmacol* 2007;49:408-15.
203. Irukayama-Tomobe Y, Miyauchi T, Sakai S, et al. Endothelin-1-induced cardiac hypertrophy is inhibited by activation of peroxisome proliferator-activated receptor-alpha partly via blockade of c-Jun NH2-terminal kinase pathway. *Circulation* 2004;109:904-10.
204. Finck BN, Han X, Courtois M, et al. A critical role for PPARalpha-mediated lipotoxicity in the pathogenesis of diabetic cardiomyopathy: modulation by dietary fat content. *Proc Natl Acad Sci U S A* 2003;100:1226-31.
205. Choi YH, Cowan DB, Nathan M, et al. Myocardial hypertrophy overrides the angiogenic response to hypoxia. *PLoS One* 2008;3:e4042.
206. Shyu KG, Liou JY, Wang BW, Fang WJ, Chang H. Carvedilol prevents cardiac hypertrophy and overexpression of hypoxia-inducible factor-1alpha and vascular endothelial growth factor in pressure-overloaded rat heart. *J Biomed Sci* 2005;12:409-20.
207. Martin C, Yu AY, Jiang BH, et al. Cardiac hypertrophy in chronically anemic fetal sheep: Increased vascularization is associated with increased

- myocardial expression of vascular endothelial growth factor and hypoxia-inducible factor 1. *Am J Obstet Gynecol* 1998;178:527-34.
208. Finck BN, Lehman JJ, Barger PM, Kelly DP. Regulatory networks controlling mitochondrial energy production in the developing, hypertrophied, and diabetic heart. *Cold Spring Harb Symp Quant Biol* 2002;67:371-82.
209. Barger PM, Kelly DP. PPAR signaling in the control of cardiac energy metabolism. *Trends Cardiovasc Med* 2000;10:238-45.
210. Ventura-Clapier R, Garnier A, Veksler V. Energy metabolism in heart failure. *J Physiol* 2004;555:1-13.
211. Russell LK, Finck BN, Kelly DP. Mouse models of mitochondrial dysfunction and heart failure. *J Mol Cell Cardiol* 2005;38:81-91.
212. Davila-Roman VG, Vedala G, Herrero P, et al. Altered myocardial fatty acid and glucose metabolism in idiopathic dilated cardiomyopathy. *J Am Coll Cardiol* 2002;40:271-7.
213. Takeyama D, Kagaya Y, Yamane Y, et al. Effects of chronic right ventricular pressure overload on myocardial glucose and free fatty acid metabolism in the conscious rat. *Cardiovasc Res* 1995;29:763-7.
214. Pellieux C, Montessuit C, Papageorgiou I, Lerch R. Inactivation of peroxisome proliferator-activated receptor isoforms alpha, beta/delta,

and gamma mediate distinct facets of hypertrophic transformation of adult cardiac myocytes. *Pflugers Arch* 2007;455:443-54.

215. Purushothaman S, Renuka Nair R, Harikrishnan VS, Fernandez AC. Temporal relation of cardiac hypertrophy, oxidative stress, and fatty acid metabolism in spontaneously hypertensive rat. *Mol Cell Biochem* 2011;351:59-64.
216. Young ME, Patil S, Ying J, et al. Uncoupling protein 3 transcription is regulated by peroxisome proliferator-activated receptor (α) in the adult rodent heart. *FASEB J* 2001;15:833-45.
217. Ullah MS, Davies AJ, Halestrap AP. The plasma membrane lactate transporter MCT4, but not MCT1, is up-regulated by hypoxia through a HIF-1 α -dependent mechanism. *J Biol Chem* 2006;281:9030-7.
218. Evans RK, Schwartz DD, Gladden LB. Effect of myocardial volume overload and heart failure on lactate transport into isolated cardiac myocytes. *J Appl Physiol* 2003;94:1169-76.
219. Carley AN, Severson DL. Fatty acid metabolism is enhanced in type 2 diabetic hearts. *Biochim Biophys Acta* 2005;1734:112-26.
220. Frey N, Olson EN. Modulating cardiac hypertrophy by manipulating myocardial lipid metabolism? *Circulation* 2002;105:1152-4.

221. El Alaoui-Talibi Z, Guendouz A, Moravec M, Moravec J. Control of oxidative metabolism in volume-overloaded rat hearts: effect of propionyl-L-carnitine. *Am J Physiol* 1997;272:H1615-24.
222. Allard MF, Schonekess BO, Henning SL, English DR, Lopaschuk GD. Contribution of oxidative metabolism and glycolysis to ATP production in hypertrophied hearts. *Am J Physiol* 1994;267:H742-50.
223. Allard MF, Henning SL, Wambolt RB, Granleese SR, English DR, Lopaschuk GD. Glycogen metabolism in the aerobic hypertrophied rat heart. *Circulation* 1997;96:676-82.
224. Schonekess BO, Allard MF, Lopaschuk GD. Recovery of glycolysis and oxidative metabolism during postischemic reperfusion of hypertrophied rat hearts. *Am J Physiol* 1996;271:H798-805.
225. Wu P, Peters JM, Harris RA. Adaptive increase in pyruvate dehydrogenase kinase 4 during starvation is mediated by peroxisome proliferator-activated receptor alpha. *Biochem Biophys Res Commun* 2001;287:391-6.
226. Planavila A, Laguna JC, Vazquez-Carrera M. Nuclear factor-kappaB activation leads to down-regulation of fatty acid oxidation during cardiac hypertrophy. *J Biol Chem* 2005;280:17464-71.

227. Alvarez-Guardia D, Palomer X, Coll T, et al. The p65 subunit of NF-kappaB binds to PGC-1alpha, linking inflammation and metabolic disturbances in cardiac cells. *Cardiovasc Res* 2010;87:449-58.
228. Zhao G, Jeoung NH, Burgess SC, et al. Overexpression of pyruvate dehydrogenase kinase 4 in heart perturbs metabolism and exacerbates calcineurin-induced cardiomyopathy. *Am J Physiol Heart Circ Physiol* 2008;294:H936-43.
229. Kokubo M, Uemura A, Matsubara T, Murohara T. Noninvasive evaluation of the time course of change in cardiac function in spontaneously hypertensive rats by echocardiography. *Hypertens Res* 2005;28:601-9.
230. Zanchi A, Brunner HR, Hayoz D. Age-related changes of the mechanical properties of the carotid artery in spontaneously hypertensive rats. *J Hypertens* 1997;15:1415-22.
231. Iemitsu M, Miyauchi T, Maeda S, et al. Cardiac hypertrophy by hypertension and exercise training exhibits different gene expression of enzymes in energy metabolism. *Hypertens Res* 2003;26:829-37.
232. Hajri T, Ibrahimi A, Coburn CT, et al. Defective fatty acid uptake in the spontaneously hypertensive rat is a primary determinant of altered glucose metabolism, hyperinsulinemia, and myocardial hypertrophy. *J Biol Chem* 2001;276:23661-6.

233. Yamashita H, Bharadwaj KG, Ikeda S, Park TS, Goldberg IJ. Cardiac metabolic compensation to hypertension requires lipoprotein lipase. *Am J Physiol Endocrinol Metab* 2008;295:E705-13.
234. Teraguchi M, Ohkohchi H, Ikemoto Y, Higashino H, Kobayashi Y. CD36 deficiency and absent myocardial iodine-123-(R,S)-15-(p-iodophenyl)-3-methylpentadecanoic acid uptake in a girl with cardiomyopathy. *Eur J Pediatr* 2003;162:264-6.
235. Hirooka K, Yasumura Y, Ishida Y, et al. Improvement in cardiac function and free fatty acid metabolism in a case of dilated cardiomyopathy with CD36 deficiency. *Jpn Circ J* 2000;64:731-5.
236. Augustus AS, Buchanan J, Addya S, et al. Substrate uptake and metabolism are preserved in hypertrophic caveolin-3 knockout hearts. *Am J Physiol Heart Circ Physiol* 2008;295:H657-66.
237. Luedde M, Flogel U, Knorr M, et al. Decreased contractility due to energy deprivation in a transgenic rat model of hypertrophic cardiomyopathy. *J Mol Med* 2009;87:411-22.
238. Koonen DP, Febbraio M, Bonnet S, et al. CD36 expression contributes to age-induced cardiomyopathy in mice. *Circulation* 2007;116:2139-47.

239. Sharma S, Adroge JV, Golfman L, et al. Intramyocardial lipid accumulation in the failing human heart resembles the lipotoxic rat heart. *FASEB J* 2004;18:1692-700.
240. Krishnan J, Suter M, Windak R, et al. Activation of a HIF1alpha-PPARgamma axis underlies the integration of glycolytic and lipid anabolic pathways in pathologic cardiac hypertrophy. *Cell Metab* 2009;9:512-24.
241. Barouch LA, Berkowitz DE, Harrison RW, O'Donnell CP, Hare JM. Disruption of leptin signaling contributes to cardiac hypertrophy independently of body weight in mice. *Circulation* 2003;108:754-9.
242. Lee Y, Wang MY, Kakuma T, et al. Liporegulation in diet-induced obesity. The antisteatotic role of hyperleptinemia. *J Biol Chem* 2001;276:5629-35.
243. Zhou YT, Grayburn P, Karim A, et al. Lipotoxic heart disease in obese rats: implications for human obesity. *Proc Natl Acad Sci U S A* 2000;97:1784-9.
244. Tomita T, Wilson L, Chiga M. Idiopathic dilated cardiomyopathy--an evidence of abnormal lipid accumulation accumulation in myocardium. *Am J Cardiovasc Pathol* 1990;3:81-5.
245. Chiu HC, Kovacs A, Ford DA, et al. A novel mouse model of lipotoxic cardiomyopathy. *J Clin Invest* 2001;107:813-22.
246. Virchow RLK, Chance F. Cellular pathology as based upon physiological and pathological histology : twenty lectures delivered in the Pathological

Institute of Berlin during the months of February, March, and April, 1858.
Special ed. Birmingham, Ala.: Classics of Medicine Library, 1978.

247. Brindley DN, Kok BP, Kienesberger PC, Lehner R, Dyck JR. Shedding light on the enigma of myocardial lipotoxicity: the involvement of known and putative regulators of fatty acid storage and mobilization. *Am J Physiol Endocrinol Metab* 2010;298:E897-908.
248. Bastie CC, Hajri T, Drover VA, Grimaldi PA, Abumrad NA. CD36 in myocytes channels fatty acids to a lipase-accessible triglyceride pool that is related to cell lipid and insulin responsiveness. *Diabetes* 2004;53:2209-16.
249. Gonzalez-Baro MR, Lewin TM, Coleman RA. Regulation of Triglyceride Metabolism. II. Function of mitochondrial GPAT1 in the regulation of triacylglycerol biosynthesis and insulin action. *Am J Physiol Gastrointest Liver Physiol* 2007;292:G1195-9.
250. Sorokina N, O'Donnell JM, McKinney RD, et al. Recruitment of compensatory pathways to sustain oxidative flux with reduced carnitine palmitoyltransferase I activity characterizes inefficiency in energy metabolism in hypertrophied hearts. *Circulation* 2007;115:2033-41.

251. Schwarzer M, Faerber G, Rueckauer T, et al. The metabolic modulators, Etomoxir and NVP-LAB121, fail to reverse pressure overload induced heart failure in vivo. *Basic Res Cardiol* 2009;104:547-57.
252. Belanger AJ, Luo Z, Vincent KA, et al. Hypoxia-inducible factor 1 mediates hypoxia-induced cardiomyocyte lipid accumulation by reducing the DNA binding activity of peroxisome proliferator-activated receptor alpha/retinoid X receptor. *Biochem Biophys Res Commun* 2007;364:567-72.
253. Huss JM, Levy FH, Kelly DP. Hypoxia inhibits the peroxisome proliferator-activated receptor alpha/retinoid X receptor gene regulatory pathway in cardiac myocytes: a mechanism for O₂-dependent modulation of mitochondrial fatty acid oxidation. *J Biol Chem* 2001;276:27605-12.
254. Labinsky V, Bellomo M, Chandler MP, et al. Chronic activation of peroxisome proliferator-activated receptor-alpha with fenofibrate prevents alterations in cardiac metabolic phenotype without changing the onset of decompensation in pacing-induced heart failure. *J Pharmacol Exp Ther* 2007;321:165-71.
255. Linz W, Wohlfart P, Baader M, et al. The peroxisome proliferator-activated receptor-alpha (PPAR-alpha) agonist, AVE8134, attenuates the progression of heart failure and increases survival in rats. *Acta Pharmacol Sin* 2009;30:935-46.

256. Young ME, Goodwin GW, Ying J, et al. Regulation of cardiac and skeletal muscle malonyl-CoA decarboxylase by fatty acids. *Am J Physiol Endocrinol Metab* 2001;280:E471-9.
257. Ikeda Y, Sato K, Pimentel DR, et al. Cardiac-specific deletion of LKB1 leads to hypertrophy and dysfunction. *J Biol Chem* 2009;284:35839-49.
258. Stuck BJ, Lenski M, Bohm M, Laufs U. Metabolic switch and hypertrophy of cardiomyocytes following treatment with angiotensin II are prevented by AMP-activated protein kinase. *J Biol Chem* 2008;283:32562-9.
259. Turdi S, Kandadi MR, Zhao J, Huff AF, Du M, Ren J. Deficiency in AMP-activated protein kinase exaggerates high fat diet-induced cardiac hypertrophy and contractile dysfunction. *J Mol Cell Cardiol* 2011;50:712-22.
260. Chen BL, Ma YD, Meng RS, et al. Activation of AMPK inhibits cardiomyocyte hypertrophy by modulating of the FOXO1/MuRF1 signaling pathway in vitro. *Acta Pharmacol Sin* 2010;31:798-804.
261. Narravula S, Colgan SP. Hypoxia-inducible factor 1-mediated inhibition of peroxisome proliferator-activated receptor alpha expression during hypoxia. *J Immunol* 2001;166:7543-8.

262. Zhang H, Gao P, Fukuda R, et al. HIF-1 inhibits mitochondrial biogenesis and cellular respiration in VHL-deficient renal cell carcinoma by repression of C-MYC activity. *Cancer Cell* 2007;11:407-20.
263. Lydell CP, Chan A, Wambolt RB, et al. Pyruvate dehydrogenase and the regulation of glucose oxidation in hypertrophied rat hearts. *Cardiovasc Res* 2002;53:841-51.
264. Piao L, Fang YH, Cadete VJ, et al. The inhibition of pyruvate dehydrogenase kinase improves impaired cardiac function and electrical remodeling in two models of right ventricular hypertrophy: resuscitating the hibernating right ventricle. *J Mol Med* 2010;88:47-60.
265. Paternostro G, Clarke K, Heath J, Seymour AM, Radda GK. Decreased GLUT-4 mRNA content and insulin-sensitive deoxyglucose uptake show insulin resistance in the hypertensive rat heart. *Cardiovasc Res* 1995;30:205-11.
266. Lum JJ, Bui T, Gruber M, et al. The transcription factor HIF-1 α plays a critical role in the growth factor-dependent regulation of both aerobic and anaerobic glycolysis. *Genes Dev* 2007;21:1037-49.
267. Taylor M, Wallhaus TR, Degrado TR, et al. An evaluation of myocardial fatty acid and glucose uptake using PET with [18F]fluoro-6-thia-

- heptadecanoic acid and [18F]FDG in Patients with Congestive Heart Failure. *J Nucl Med* 2001;42:55-62.
268. Bergmann O, Bhardwaj RD, Bernard S, et al. Evidence for cardiomyocyte renewal in humans. *Science* 2009;324:98-102.
269. Shiojima I, Walsh K. Role of Akt signaling in vascular homeostasis and angiogenesis. *Circ Res* 2002;90:1243-50.
270. Shiojima I, Sato K, Izumiya Y, et al. Disruption of coordinated cardiac hypertrophy and angiogenesis contributes to the transition to heart failure. *J Clin Invest* 2005;115:2108-18.
271. McMullen JR, Shioi T, Zhang L, et al. Phosphoinositide 3-kinase(p110alpha) plays a critical role for the induction of physiological, but not pathological, cardiac hypertrophy. *Proc Natl Acad Sci U S A* 2003;100:12355-60.
272. McMullen JR, Shioi T, Huang WY, et al. The insulin-like growth factor 1 receptor induces physiological heart growth via the phosphoinositide 3-kinase(p110alpha) pathway. *J Biol Chem* 2004;279:4782-93.
273. Luo J, McMullen JR, Sobkiw CL, et al. Class IA phosphoinositide 3-kinase regulates heart size and physiological cardiac hypertrophy. *Mol Cell Biol* 2005;25:9491-502.

274. Hernandez R, Teruel T, Lorenzo M. Akt mediates insulin induction of glucose uptake and up-regulation of GLUT4 gene expression in brown adipocytes. *FEBS Lett* 2001;494:225-31.
275. Mehta AV, Chidambaram B. Ventricular septal defect in the first year of life. *Am J Cardiol* 1992;70:364-6.
276. Kantor PF, Robertson MA, Coe JY, Lopaschuk GD. Volume overload hypertrophy of the newborn heart slows the maturation of enzymes involved in the regulation of fatty acid metabolism. *J Am Coll Cardiol* 1999;33:1724-34.
277. Sheikh AM, Barrett C, Villamizar N, et al. Right ventricular hypertrophy with early dysfunction: A proteomics study in a neonatal model. *J Thorac Cardiovasc Surg* 2009;137:1146-53.
278. Hasenfuss G. Animal models of human cardiovascular disease, heart failure and hypertrophy. *Cardiovasc Res* 1998;39:60-76.
279. Pariaut R. Cardiovascular physiology and diseases of the rabbit. *Vet Clin North Am Exot Anim Pract* 2009;12:135-44, vii.
280. Pogwizd SM, Bers DM. Rabbit models of heart disease. *Drug Discovery Today: Disease Models* 2008;5:185-193.
281. James TN. Anatomy of the cardiac conduction system in the rabbit. *Circ Res* 1967;20:638-48.

282. Bers DM. Excitation-Contraction Coupling and Cardiac Contractile Force. 2nd ed. Dordrecht, Netherlands Kluwer Academic Publishers, 2001.
283. Pieske B, Kretschmann B, Meyer M, et al. Alterations in intracellular calcium handling associated with the inverse force-frequency relation in human dilated cardiomyopathy. *Circulation* 1995;92:1169-78.
284. Everett AW, Sinha AM, Umeda PK, Jakovcic S, Rabinowitz M, Zak R. Regulation of myosin synthesis by thyroid hormone: relative change in the alpha- and beta-myosin heavy chain mRNA levels in rabbit heart. *Biochemistry* 1984;23:1596-9.
285. Everett AW, Umeda PK, Sinha AM, Rabinowitz M, Zak R. Expression of myosin heavy chains during thyroid hormone-induced cardiac growth. *Fed Proc* 1986;45:2568-72.
286. Gorza L, Pauletto P, Pessina AC, Sartore S, Schiaffino S. Isomyosin distribution in normal and pressure-overloaded rat ventricular myocardium. An immunohistochemical study. *Circ Res* 1981;49:1003-9.
287. Lompre AM, Mercadier JJ, Wisnewsky C, et al. Species- and age-dependent changes in the relative amounts of cardiac myosin isoenzymes in mammals. *Dev Biol* 1981;84:286-90.

288. Coker SJ. Anesthetized rabbit as a model for ischemia- and reperfusion-induced arrhythmias: effects of quinidine and bretylium. *J Pharmacol Methods* 1989;21:263-79.
289. Ng GA, Cobbe SM, Smith GL. Non-uniform prolongation of intracellular Ca²⁺ transients recorded from the epicardial surface of isolated hearts from rabbits with heart failure. *Cardiovasc Res* 1998;37:489-502.
290. Semenza GL. HIF-1, O₂, and the 3 PHDs: how animal cells signal hypoxia to the nucleus. *Cell* 2001;107:1-3.

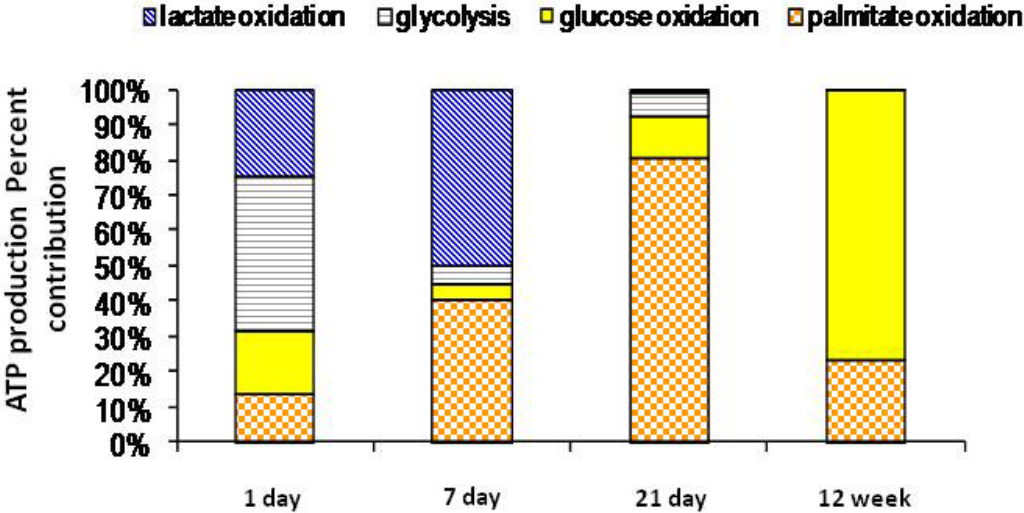
1. 17 Figures

Figure 1-1: Changes in Cardiac Metabolism Capacity During the Neonatal Period.

A) Comparison of metabolic profiles based on ATP production percent contributions from the metabolized lactate, glucose, and palmitate of hearts from 1-, 7-, and 21-day old rabbits. These values are compared to the partial profile of the adult rabbit heart (12 weeks old). B) An approximate of cardiac metabolic transition from fetal to adult cardiac metabolism.

Fig 1-1

A



B

Pathway	Fetus	Neonate	Adult
GOX	Low	Low	High
Glycolysis	High	Low	High
FAOX	Low	High	High

Figure 1-2: CD36 Translocation Signalling. CD36, a plasma membrane fatty acid transporter, is stored in intracellular vesicles. Their translocation can be stimulated by insulin and myocardial contraction in cardiomyocytes. Firstly, insulin acts on the insulin receptor to phosphorylate phosphoinositol-3-kinase (P-PI3 Kinase), which in turn phosphorylates Akt. Vesicles containing CD36 is stimulated to translocate an increase CD36 insertion into the plasma membrane. This equally occurs upon cardiomyocyte contraction, which increases the AMP:ATP ratio to activate AMP-activated protein kinase (AMPK). Downstream to AMPK, CD36-containing vesicles are directed towards the plasma membrane to translocate the CD36 into the plasma membrane as well. CD36 increases the uptake of free fatty acids (FFA) into the cytoplasm. Upon entering the cytoplasm, in order to maintain an uptake gradient, the FFA is bound to a FA binding protein (FABP) and brought into close proximity of the outer mitochondria membrane where acyl-CoA synthetase resides. Acyl-CoA synthetase, then catalyzes the formation of a fatty acyl-CoA. The fatty acyl-CoA may be directed towards triacylglycerol (TG) storage or enter the mitochondria via CPT-1 for oxidation.

Fig 1-2

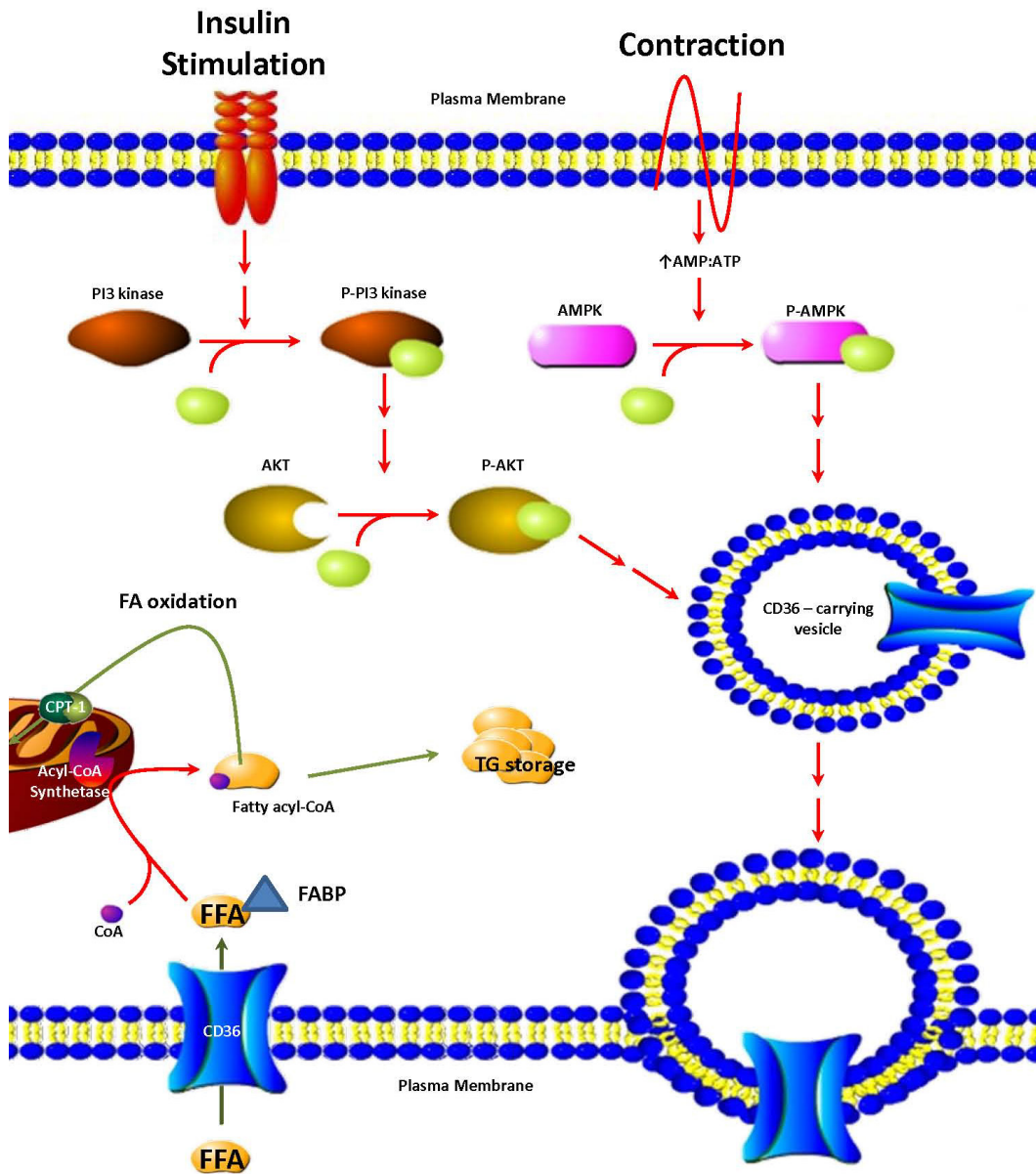


Figure 1-3: Schematic of Long Chain Fatty Acid Transport. The majority of long chain fatty acids (LCFAs) enter into the cytoplasm via CD36. As it enters into the cytoplasm, the LCFA is neutralized by its conversion to an acyl-CoA. To be oxidized, the acyl-CoA must enter the mitochondria in which the components of the oxidative pathway reside. Carnitine palmitoyl-transferase-1 (CPT-1) is located on the outer mitochondrial membrane. It is the rate-limited step for mitochondrial FA uptake and does so by transferring the acyl-moiety from a CoA to a carnitine group to make acyl-carnitine. The acyl-carnitine then is shuttled into the mitochondria via the carnitine acyl-translocase (CAT). CPT-2, residing in the inner mitochondrial membrane, catalyzes the transfer of the acyl- moiety back onto a CoA and allows the free carnitine to exit the mitochondria in exchange for another acyl-carnitine. The reconstituted fatty acyl-CoA in the mitochondria undergoes FA oxidation. The transport of fatty acyl-CoAs into the mitochondria can be inhibited by malonyl-CoA, which inhibits CPT-1, the rate-limiting step in mitochondria fatty acid uptake. Malonyl-CoA is the product of acyl-CoA carboxylase (ACC). It is degraded back into acetyl-CoA by malonyl-CoA decarboxylase (MCD). Insulin can inhibit FA oxidation by inhibiting mitochondrial fatty acyl-CoA uptake by decreasing the phosphorylation of 5-AMP-kinase (AMPK). Consequently, ACC is not phosphorylated and remains active. Upon removal of insulin, AMPK phosphorylation increases as with ACC phosphorylation, thus inhibiting the production of malonyl-CoA allowing increased fatty acyl-CoA uptake into the mitochondria for oxidation.

Fig 1-3

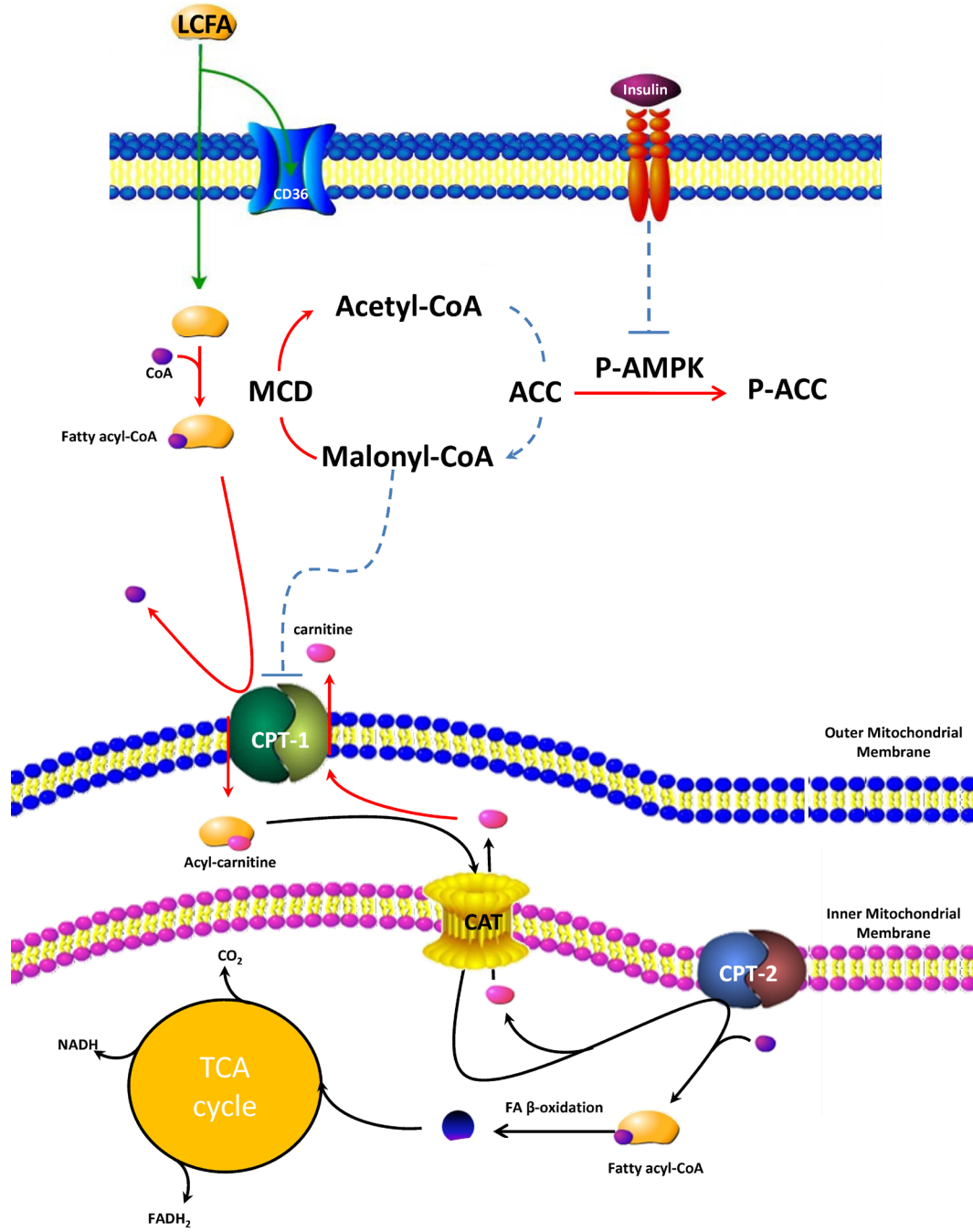


Figure 1-4: Insulin Signaling in the Neonatal Period. Decreased circulating insulin levels during the neonatal period encourages fatty acid (FA) oxidation maturation.

Fig 1-4

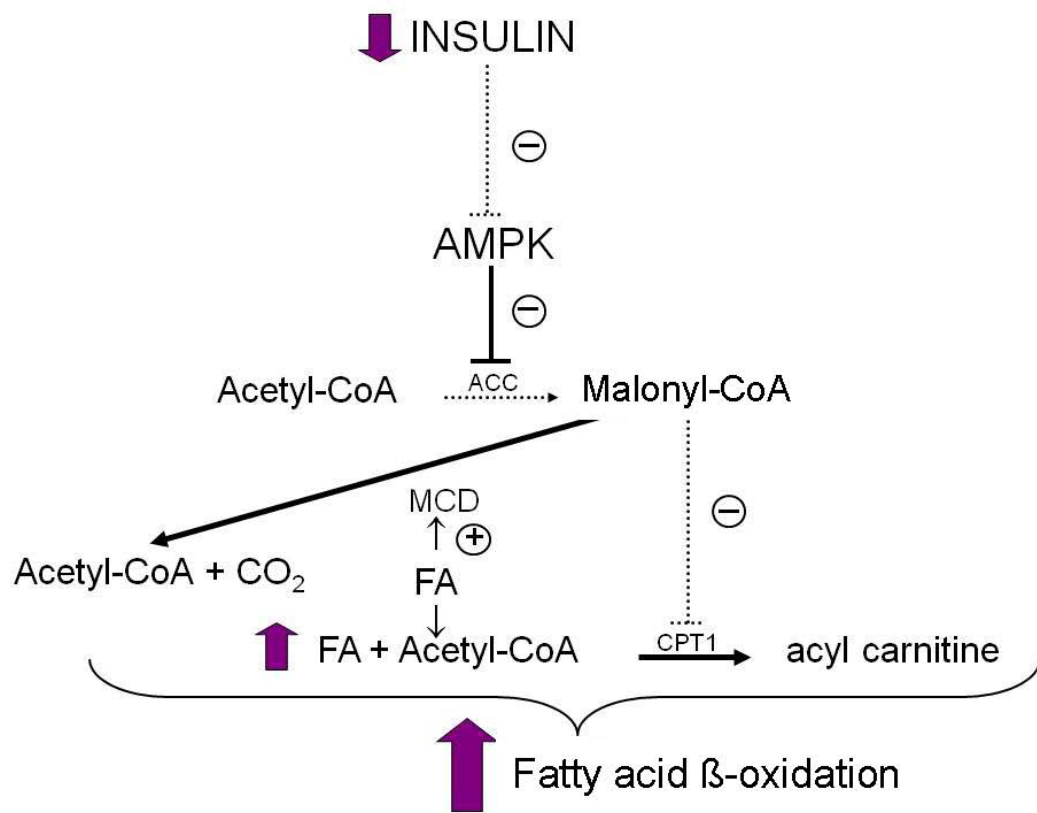
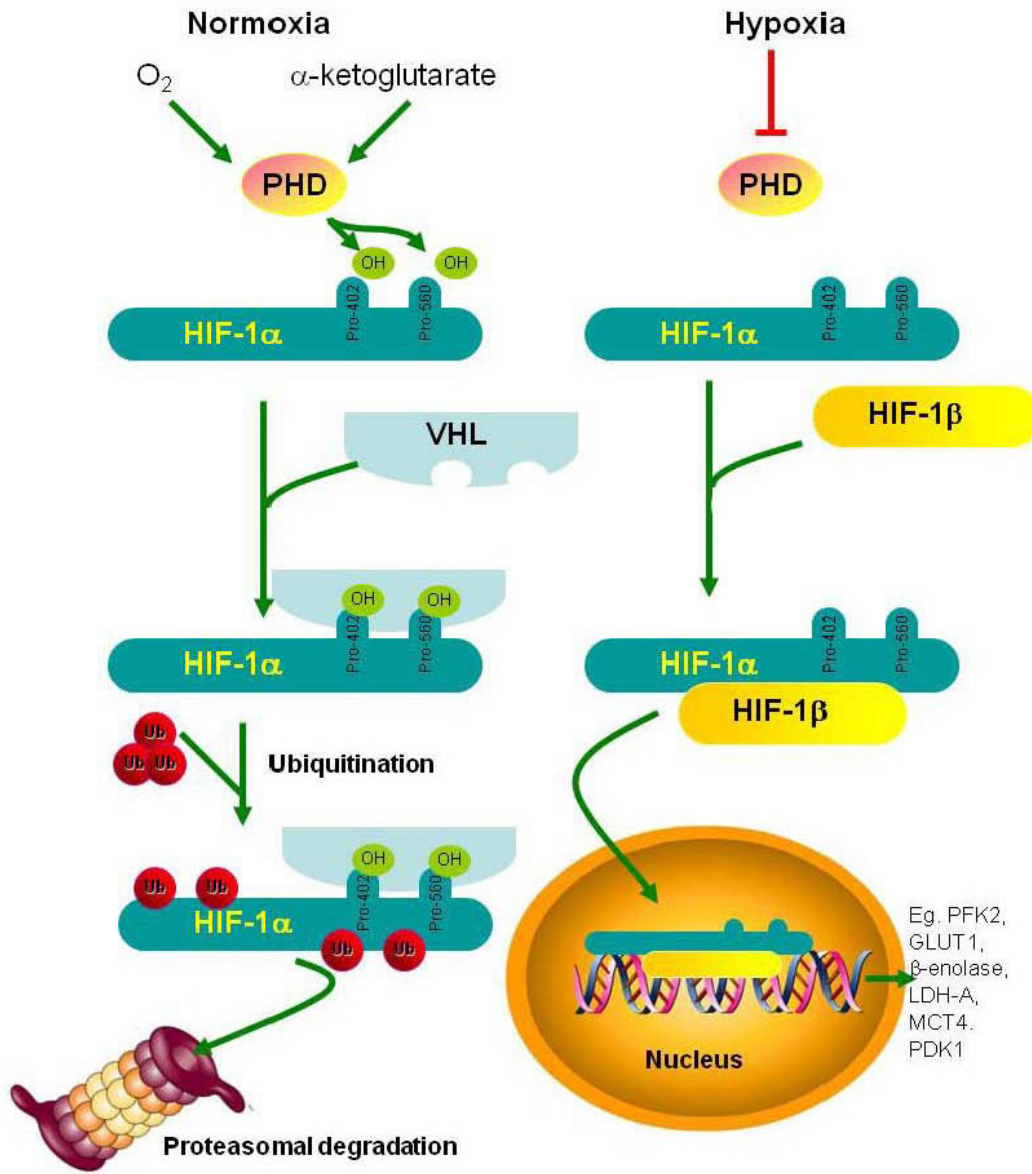


Figure 1-5: Hypoxia-Inducible Factor-1 α (HIF-1 α) in Normoxia and Hypoxia. HIF-1 α is a transcription factor that regulates over 100 genes involved in cell cycle regulation, apoptosis, glycolysis, metabolism, and angiogenesis (290). The HIF-1 α is highly regulated by prolyl-hydroxylase domain-containing enzymes (PHD). Under normoxic conditions, PHD enzymes hydroxylate HIF-1 α so that HIF-1 α may bind to and be polyubiquitinated by the E3 ubiquitin ligase von Hippel-Lindau (VHL) factor. The polyubiquitinated HIF-1 α is directed to the proteasome for degradation and therefore maintaining low HIF-1 α transcription levels under normoxia. Hypoxia inhibits the actions of PHD enzymes so that the HIF-1 α is unhydroxylated and cannot be bound to the VHL factor. Consequently, HIF-1 α 's accumulate to form a heterodimer complex with HIF-1 β and translocated from the cytoplasm to the nucleus. In the nucleus, the HIF-1 complex binds to the hypoxic response element to increase transcriptional transactivation.

Fig 1-5



Chapter 2

Supra-physiological Insulin Levels Elevate Palmitate Oxidation to Improve Neonatal Rabbit Heart Ischemia-Reperfusion Recovery

Supra-physiological Insulin Levels Elevate Palmitate Oxidation to Improve Neonatal Rabbit Heart Ischemia-Reperfusion Recovery

Victoria HM Lam, Brandon A Tanner, John R Ussher, Donna L Beker, Jagdip S Jaswal, Ivan M Rebeyka, and Gary D Lopaschuk

Cardiovascular Research Centre, Mazankowski Alberta Heart Institute, and Departments of Pediatrics and Surgery, University of Alberta, Edmonton, Canada

Abbreviated title: Supra-physiological insulin improves post-icshemic cardiac function

Contribution:

Victoria HM Lam: Isolated working heart perfusions, cell fractionation, Western blot, TG quantification, data analysis, primary author

Brandon A Tanner: Western blot

John R Ussher: Intellectual and editorial contribution

Donna L Beker: Isolated working heart perfusions and intellectual contribution

Jagdip S Jaswal: Intellectual and editorial contribution

Hypothesis:

Since insulin activates glucose metabolism and inhibits FA oxidation, graded increase in insulin given to neonatal hearts during cardioplegia is expected to cause correlated graded energy deficiencies manifested as poor cardiac function.

2.1 Introduction

Despite improved surgical techniques, post-operative mortality remains prevalent (1,2). Suboptimal cardioprotection may contribute to high mortality rates in both adults and neonatal cardiac surgery (3). Most cardioprotective strategies are targeted towards the adult heart. As neonatal hearts differ from adult hearts structurally, functionally, and metabolically, it is important to identify cardioprotective strategies unique to neonatal hearts, such as that which increases fatty acid (FA) oxidation (4)

In the adult heart, insulin is thought to enhance cardiac functional recovery following surgical ischemia through increasing glucose oxidation (5,6) and simultaneously inhibiting FA oxidation (7,8), which inter-inhibit each other as described by the Randle cycle. In so, insulin likely restores the coupling between glycolysis and glucose oxidation to prevent acidosis. As one of insulin's cardioprotective mechanisms, it is the basis for extrapolating insulin use in neonatal cardioplegia. However, the effects insulin has on neonatal cardiac metabolism and functional recovery are unknown and may differ from adults due to an immature glucose oxidation pathway and a greater reliance of the heart on FA oxidation in the post-natal period.

Mitochondrial FA uptake regulates the rate of FA oxidation (9-11). The gatekeeper of FA transport into the mitochondria for oxidation is carnitine

palmitoyltransferase (CPT)-1. Acetyl-CoA carboxylase (ACC) synthesizes malonyl-CoA to strongly inhibit CPT-1. During the neonatal period, the metabolism of the immature heart changes rapidly from dependence on fetal glycolysis and lactate oxidation to a dependence on FA oxidation, a more adult-like metabolic profile. By 7 days of age, a rabbit heart relies chiefly on FA oxidation for ATP production (12). This change is partly accomplished through a decrease in circulating insulin levels in the neonate (12) and simultaneous increase in glucagon (13), a phenomenon found in the humans, rabbits, rats, pigs, and sheep (13). Decreased circulating insulin causes ACC activity and, consequently, malonyl-CoA levels to decline. Decreased malonyl-CoA levels correlate with increased FA oxidation rates (12,14) as CPT-1 is released from its inhibition. Compared to 1-day old rabbit hearts, 7-day old rabbit hearts have 10-fold higher FA oxidation rates (15). In fact, we have previously demonstrated that increasing FA substrate to the neonatal myocardium improves post-ischemic contractile recovery (4)

In adults, insulin protects the myocardium from ischemia-reperfusion injury by acting through Akt and the 5'-AMP-activated protein kinase (AMPK)-ACC axis. AMPK (63 kDa) is a fuel gauge that activates during low energy states as signified by elevated AMP:ATP ratios. AMPK is an upstream regulator of multiple cellular pathways, one of which phosphorylates and inhibits ACC. Upon binding to insulin, the insulin receptor phosphorylates and activates phosphoinositide-3-kinase (PI3 kinase), which in turn leads to Akt phosphorylation (P-Akt), upstream

to AMPK. Through P-Akt, insulin increases GLUT4 translocation and stimulates glucose uptake and metabolism. By the Randle cycle, the elevated acetyl-CoA from increased glucose oxidation increases malonyl-CoA synthesis and inhibits CPT-1 (16). Insulin also inhibits AMPK phosphorylation via P-Akt (17,18) to prevent the phosphorylation and inhibition of ACC and therefore malonyl-CoA synthesis. Hence, as glucose oxidation is stimulated, FA oxidation is inhibited by insulin. Of interest, the AMPK response to insulin is attenuated and its cardioprotective effect lost in the presence of high FA (19).

Since increased FA substrate availability to the neonatal heart improves post-ischemic contractile recovery, but insulin activates glucose metabolism and inhibits FA oxidation, we hypothesize that a graded increase in insulin given to neonatal hearts during the ischemic period would cause graded energy deficiencies manifested as poor post-ischemic cardiac functional recovery. To study the relationship between insulin, cardiac function, and cardiac substrate metabolism, we perfused 7-day-old rabbit hearts with 0.4 mM palmitate and 1.2 mM palmitate and compared the influence of differing levels of insulin (0, 0.1, and 10 U/L) added 2 min prior to the onset of ischemia.

2.2 Methods and Materials

2.2.1 *Animals*

7-day-old New Zealand White rabbits of either gender were supplied by Vandermeer Farms, Edmonton, Alberta, Canada. All animal procedures were approved by the University of Alberta Health Sciences Animal Welfare Committee who adheres to the Canadian Counsel on Animal Care guidelines.

2.2.2 *Isolated working-heart perfusion using the 7-day-old rabbit model*

7-day old rabbits were separated from the doe in the morning of the day of the experiment. These rabbits, weighing 100-200g, were anesthetized with 60 mg/kg pentobarbital sodium, intraperitoneal injection. When the rabbit has achieved surgical plane of anaesthesia, signified by loss of all tactile sensation, its thoracic cavity was opened and its lungs and heart and respective vasculature were excised in its entirety and immersed in ice-cold Krebs-Henseleit solution. The aorta is immediately cannulated and retrogradely perfused in Langendorff mode with Krebs-Henseleit solution at 37⁰C, gassed with 95% O₂-5% CO₂, and delivered at a constant pressure of 50 mmHg. As the heart is retrogradely perfused, the pulmonary artery was severed open near its trunk to maintain patency. The lungs and excess tissue were removed and the left atrium was cannulated via the pulmonary venous opening.

After 10 minutes of retrograde perfusion to stabilize the beating heart, the flows into the heart were switched to the working heart mode by clamping off the inflow from the Langendorff reservoir and opening the inflow line from the oxygenator containing the oxygenated perfusate. 120 mL of recirculating perfusate was delivered to the left atrium of the spontaneously beating heart at the constant preload pressure of 7.5 mmHg and was ejected from the left ventricle against a constant afterload of 35 mmHg. Spontaneously beating hearts must generate an aerobic cardiac output of ≥ 30 mL/min to be included in this study.

Perfusate buffers were modified Krebs-Henseleit solution (118.5 mmol/L NaCl, 25 mmol/L NaHCO₃, 4.7 mmol/L KCl, 1.2 mmol/L KH₂PO₄, 1.2 mmol/L MgSO₄) containing either high fat (1.2 mmol/L palmitate) or low fat (0.4 mmol/L palmitate) with 11 mmol/L glucose, 2.5 mmol/L Ca²⁺, and 3% BSA. Palmitate was pre-bound to fat-free albumin overnight in dialysis tubing and equilibrated in Krebs-Henseleit solution. 0 U/L, 0.1 U/L or 10 U/L of insulin was added en bolus to the perfusate 2 min prior to global ischemia. The above solutions were oxygenated with 95% O₂ and kept at 37°C. The hearts were subjected to one of the following time protocols with a circulating perfusate volume of 120 mL: a) 30-min aerobic perfusion followed by a 30-min global no flow normothermic ischemia and 40 min of aerobic reperfusion; b) 30-min aerobic perfusion

followed by a 30-min global no flow normothermic ischemia; or c) 30 minutes of aerobic perfusion.

The AcqKnowledge[®] program recorded the heart rate, peak systolic pressure, cardiac output, and aortic afterload in the working mode. No recordings were made during Langendorff mode or during global ischemia. Heart rate and aortic pressure (mmHg) were measured using a Gould P21 pressure transducer (Harvard Apparatus; Gould Inc., Valley View, OH) connected to the aortic outflow line. Cardiac output and aortic flow ($\text{mL}\cdot\text{min}^{-1}$) were measured with Transonic T206 ultrasonic flow probes (Transonic Systems, Ithaca NY) placed in the preload and afterload lines, respectively. Coronary flow ($\text{mL}\cdot\text{min}^{-1}$) was calculated from the difference between the cardiac output and the aortic flow.

2.2.3 Quantifying Fatty Acid Oxidation, Glucose Oxidation, and Glycolysis

[5-³H]-glucose, [U-¹⁴C]-glucose, or [U-¹⁴C]-palmitate to determine glycolysis, glucose oxidation, and FA oxidation, respectively, were added to the perfusate in combinations of either [5-³H]-glucose and [U-¹⁴C]-glucose or [5-³H]-glucose and [U-¹⁴C]-palmitate. 5 mL of perfusate was sampled every 10 minutes. Samples were taken during 30 minutes of aerobic perfusion and the 40 minutes of reperfusion while no samples were taken during the ischemic period when the heart was at a no-flow state.

Total myocardial $^3\text{H}_2\text{O}$ production is used to determine myocardial glycolysis rates. The $^3\text{H}_2\text{O}$ present in the perfusate is separated from [5- ^3H]-glucose and [U- ^{14}C]-glucose or [1- ^{14}C]-palmitate via a vapor transfer method. To elaborate, 500 μL of distilled water is added to a 5 mL scintillation vial and a lidless 1.5 mL microcentrifuge tube is placed inside each 5 mL scintillation vial. 200 μL of buffer sample is added to the microcentrifuge tube and the scintillation vial is capped. The vials are incubated at 50°C for 24 hours to allow $^3\text{H}_2\text{O}$ in the liquid and gas forms to equilibrate. The vials are then taken out to cool at 4°C for another 24 hours. After cooling, the scintillation vials are uncapped, the microcentrifuge tube removed, scintillation fluid (ScintiSafe, Fisher Scientific) added and vials were counted in a scintillation counter.

Meanwhile, glucose and palmitate oxidation rates were measured by quantifying total myocardial $^{14}\text{CO}_2$ -production by summing the gaseous $^{14}\text{CO}_2$ trapped in hyamine hydroxide and the dissolved $^{14}\text{CO}_2$ found in the form of bicarbonate ions (HCO_3^-). Gaseous $^{14}\text{CO}_2$ is trapped in 15 mL of hyamine hydroxide through an exhaust line channeling all gaseous exhaust from a sealed perfusion system into the hyamine hydroxide. 300 μL of hyamine hydroxide and a replicate were sampled from the 15 mL hyamine hydroxide trap every 10 minutes during aerobic perfusion and reperfusion. To release gaseous $^{14}\text{CO}_2$ from the HCO_3^- , 1 mL of perfusate buffer is reacted with 1 mL of 4.5 mol/L H_2SO_4 every 10 minutes during aerobic perfusion and reperfusion. This step is also replicated at each

time point. As the $^{14}\text{CO}_2$ is released from the HCO_3^- , the gas is trapped with filter paper soaked with hyamine hydroxide in the central well of a 25-mL stopper flask. Perfusate was sampled at pre-determined time points (10, 20, 30, 60, 70, 80, 90, and 100min), and steady state rates (μmol [$5\text{-}^3\text{H}$]glucose, [$\text{U-}^{14}\text{C}$]glucose, and [$1\text{-}^{14}\text{C}$] palmitate metabolized per g dry wt $\cdot\text{min}^{-1}$), were calculated.

At the end of each perfusion protocol, heart ventricles were clamped, frozen with liquid nitrogen-cooled Wollenberger tongs, submerged in liquid nitrogen, and then stored at -80°C . The frozen tissues was weighed and powdered with a mortar and pestle while maintaining freezing temperatures by cooling tissue and apparatuses to liquid nitrogen temperature. The remaining heart atrial tissue was air dried for > 24 hrs and weighed. The weights of the dried atria and frozen ventricles and ventricular dry-to-wet ratio were used to determine the hearts' total dry weight.

2.2.4 Steady State ATP Production

Steady state ATP production rates were calculated from glucose oxidation, glycolysis, and palmitate oxidation assuming 2 ATP molecules are produced per molecule of glucose undergoing glycolysis, 31 ATP molecules per molecule of glucose oxidized, and 105 ATP molecules per molecule of palmitate oxidized.

2.2.5 Quantifying Plasma Membrane CD36 and GLUT4 Content

Serial cellular fractionation was prepared as previously described in (20,21). In brief, powdered frozen ventricular tissue was incubated in a high-salt buffer (2 M NaCl, 20 mM HEPES (pH 7.4), and 5 mM NaN₃) for 30 min at 4⁰C. The mixture was centrifuged for 5 min at 1000 x g and tissue pellet resuspended in 10% wt/vol homogenization buffer (20 mM HEPES (pH 7.4), 2 mM EDTA, 1 mM MgCl₂, and 250 mM sucrose). A protein assay was performed to normalize protein content here after. The tissue was then homogenized using handheld homogenizers (DUALL, Kontes) and the homogenate was serially centrifuged at 100 x g for 10 min and then at 5000 x g for 10 min to obtain the plasma membrane fraction. Equal amounts of plasma fraction was subjected to SDS-polyacrylamide gel electrophoresis and transferred to a nitrocellulose membrane for Western blotting with rabbit anti-Na⁺/K⁺ ATPase α_1 -subunit, anti-GLUT4, or anti-CD36 (1:1000, Cell Signaling Technology) using the immunoblot assay protocol as follows.

2.2.6 Triacylglycerol (TG) Quantification

20 mg of powdered frozen ventricular sample was homogenized in 20x chloroform:methanol (2:1) mixture for 30 sec. Methanol (amount equal to 0.2 x the homogenate volume) was then added and sample vortexed before the samples were centrifuged (10 min at 3500 rpm). Supernatant volume was collected and recorded. 0.2 x the volume of 0.04% CaCl₂ was added to the

supernatant and allowed to separate into 2 phases. Samples were then centrifuged (2400 rpm, 20 min). The upper phase was removed and the bottom phase was washed with 150 μ L of pure solvent (chloroform, methanol, and water mixture) and centrifuged again at 2400 rpm for 20 min. The wash was repeated twice. The upper phase was removed and 50 μ L of methanol was added to the lower phase, which contained the extracted TG, and each sample was heated to 60⁰C and dried under a stream of N₂ gas. Once dried, samples were re-dissolved in 50 μ L of 3:2 tertbutyl alcohol:triton X-100/methyl alcohol (1:1) mixture. At room temperature, the samples were left overnight. TG concentrations were determined by a Wako Triglyceride M kit on the day after.

2.2.7 Immunoblot Assay

Protein were extracted from tissue homogenates and subjected to SDS-PAGE in gel matrices containing either 5% or 8% acrylamide and transferred to nitrocellulose (15). The membranes were then blocked in 5% milk in 1XPBS/0.1% Tween 20 and then immunoblotted at 1:1000 dilution with (unless otherwise specified) with rabbit anti-phospho- α -AMPK (Thr 172), rabbit anti- α -AMPK, rabbit anti-phosho-acetyl CoA carboxylase (ACC) (Ser-79), rabbit anti-ACC, or peroxidase-labeled streptavidin (1:500 dilution) in 5% bovine serum albumn/1XPBS/0.1% Tween 20 overnight at 4⁰C.

After washing the membrane repeatedly, as needed, in 1XPBS/0.1% Tween 20, the membranes were incubated with peroxidase-conjugated goat anti-rabbit secondary antibody in 5% milk/1XPBS/0.1 Tween 20, except for the membrane immunoblotted for peroxidase-labeled streptavidin. After further washing in 1XPBS, the antibodies were visualized using PerkinElmer enhanced chemiluminescence Western blotting detection system.

2.2.8 Statistical Analysis

All values are presented as mean \pm SEM. Statistical significance of differences for multiple comparisons was estimated by One-way Analysis of Variance (ANOVA). Outliers were excluded based on the Grubb's test. If significant, selected data sets were compared by Bonferroni's Multiple Comparison Test. Differences were considered significant when $P < 0.05$.

2.3 Results

2.3.1 Benefits of a High Fat Concentration on Cardiac Function

Aerobic cardiac function was not affected by the presence of high FA. During aerobic perfusion, steady state cardiac output was 42.8 ± 1.8 and 46.2 ± 2.3 mL \cdot min⁻¹ with 0.4 mM palmitate and 1.2 mM palmitate, respectively when no (0 U/L) insulin is added (fig 2-1A). In contrast, 1.2 mM palmitate improved post-ischemic contractile recovery compared to hearts perfused in 0.4 mM palmitate

(fig 2-1A). Hearts perfused with 0.4 mM palmitate recovered to $41.2 \pm 4.2\%$ ($P < 0.05$) of aerobic function compared to $64.4 \pm 3.7\%$ when perfused with 1.2 mM palmitate ($P < 0.05$). Heart rate and peak systolic pressure were not significantly different between the two groups. 1.2 mM palmitate significantly increased pre- and post-ischemic palmitate oxidation rates compared to 0.4 mM palmitate (fig 2-1B). Meanwhile, differences in palmitate concentrations did not affect glucose oxidation or glycolysis (table 2-1).

The altered metabolic rates are reflected by calculated steady state ATP production rates (fig 2-1C). As palmitate oxidation contributed the greatest proportion to steady ATP production rates, overall steady state ATP production is increased in the presence of 1.2 mM palmitate compared to 0.4 mM palmitate. Hence, though performing the same amount of work prior to ischemia, with 1.2 mM palmitate, FA oxidation rates were much higher than in hearts given only 0.4 mM palmitate.

2.3.2 Effects of 0.1 or 10 U/L Insulin on Cardiac Function

To assess the relevance of pre-ischemic supra-physiological (10 U/L) insulin, 0.1 or 10 U/L insulin were used. To 0.4 mM palmitate or 1.2 mM palmitate perfusate, 0.1 or 10 U/L insulin was added at 28 minutes into the perfusion (fig 2-2), which is 2 min prior to ischemia. Cardiac output did not differ significantly throughout the perfusion between 0.1 and 10 U/L insulin when perfused with

0.4 mM palmitate (fig 2-2A). Likewise, no differences were found between insulin groups in the first 30 minutes of aerobic perfusion in the presence of 1.2 mM palmitate (fig 2-2B). However, 10 U/L insulin significantly improved cardiac output during the latter 40 minutes of reperfusion (fig 2-2B). All other cardiac hemodynamic parameters 0.1 U/L and 10 U/L insulin-treated hearts are shown in table 2-2.

As differing insulin concentrations did not affect cardiac function in 0.4 mM palmitate perfusions, neither did it affect cardiac metabolism (table 2-3). In contrast and unexpectedly, 10 U/L insulin significantly increased pre-ischemic and post-ischemic palmitate oxidation rates (pre: 0.75 ± 0.10 , post: 0.71 ± 0.06 $\mu\text{mol} \cdot \text{g dry wt}^{-1} \cdot \text{min}^{-1}$) in hearts perfused with 1.2 mM palmitate compared to 0.1 U/L insulin (pre: 0.58 ± 0.07 , post: 0.39 ± 0.06 $\mu\text{mol} \cdot \text{g dry wt}^{-1} \cdot \text{min}^{-1}$, $P > 0.05$) (fig 2-3A). Insulin did not affect glucose metabolism (fig 2-3B and 3C). The change in palmitate oxidation is reflected in the overall steady state ATP production rates (fig 2-3D). With 0.1 U/L insulin, overall post-ischemic steady state ATP production decreased compared to the pre-ischemic period. With 10 U/L insulin, ATP production rates were maintained.

2.3.3 Control of Metabolism in Ischemic-Reperfused Neonatal Hearts

Insulin increased Akt phosphorylation (fig 2-4A). Simultaneously, AMPK responded to 10 U/L insulin as phosphorylated AMPK significantly decreased

compared to 0.1 U/L insulin stimulation (fig 2-4B). However, as with Folmes et al (2005)(22), subsequent ACC response to changes in AMPK phosphorylation did not occur between 0.1 and 10 U/L insulin at reperfusion in high fat perfusions (fig 2-4C).

As FA oxidation rates surprisingly increased with supra-physiological insulin stimulation, transporter proteins for both glucose and FA were examined (fig 2-5A and 5B). The amount of GLUT4 situated in the plasma membrane did not increase in response to 10 U/L insulin treatment compared to 0.1 U/L (fig 2-5A). Conversely, 10 U/L insulin significantly increased plasma membrane CD36 compared to 0.1 U/L (fig 2-5B). The increased plasma membrane CD36 content was not accompanied by altered ventricular TG content (fig 2-5D)

2.4 Discussion

The metabolism of an immature heart is different from that of an adult (23). While the adult heart has the metabolic flexibility to derive ATP from glucose, lactate, and FA, the neonatal heart relies mostly on FA oxidation with the minor contributions from glycolysis and lactate oxidation. Meanwhile, glucose oxidation rates remain low in the neonatal period. In the neonatal period, circulating glucagon levels increase while insulin levels decrease (24). These hormonal changes are conducive to FA oxidation development. Unexpectedly, our findings demonstrated that supra-physiological levels of insulin, which are

often administered as part of the cardioplegia during cardiac surgery or peri-operatively (25-27), was cardioprotective. We showed that though supra-physiological insulin (10 U/L) did not improve contractile function in low fat-perfused 7-day-old hearts, it improved post-ischemic functional recovery when hearts were perfused with 1.2 mM palmitate. To our surprise, the improved contractile recovery is associated with increased FA oxidation rates in the absence of changes in glucose metabolism.

2.4.1 High Fatty Acids are Beneficial to the Neonatal Heart During Reperfusion

In the adult heart, during ischemia-reperfusion, circulating FA levels are elevated and flood the myocardium with excess substrate. Consequently, the predominant metabolite in the reperfused heart is FA. FA oxidation generates copious amounts of acetyl-CoA that inhibit pyruvate dehydrogenase (PDH) causing a mis-match between glycolysis and glucose oxidation. Acidosis is perpetuated during reperfusion causing cellular damage. Insulin is thought to be cardioprotective by inhibiting AMPK and subsequently inhibiting FA oxidation to normalize glucose oxidation. However, clinical findings in the glucose-insulin-potassium (GIK) trials have been controversial as to whether insulin can truly protect the myocardium (28-30).

The neonatal heart quickly develops the ability to oxidize FA from its fetal glycolysis-dependent metabolism. In previous studies, we demonstrated that

increasing FA availability to the immature heart, in contrast to the adult heart, is beneficial during reperfusion (4). This previous study used 2.4 mM palmitate. Therefore, we sought to demonstrate that cardiac function is equally improved by 1.2 mM palmitate, a plasma FA level that is similar to that found during the post-ischemic period (31). The comparison of contractile function between perfusing the neonatal heart with 0.4 and 1.2 mM palmitate demonstrated the importance of substrate supply to the neonatal heart. Furthermore, in the present study, similar palmitate oxidation rates were achieved at half the FA concentration (1.2 vs 2.4 mM palmitate) used in our previous study (4). This finding may represent a saturation of the FA oxidation pathway in the neonatal heart at 1.2 mM palmitate.

Increased FA oxidation rates occurred during both aerobic perfusion as well as reperfusion with 1.2 mM palmitate compared to 0.4 mM palmitate. However, cardiac output was not different between the two groups during aerobic perfusion supporting the concept of energy production capacity reserve. As cardiac function was not different under aerobic conditions, there may be a degree of oxygen wasting and inefficiency, which does not seem to be detrimental to the neonatal heart. The high fat-perfused neonatal heart may be less efficient during aerobic perfusion; however, a higher FA concentration improved post-ischemic functional recovery, as with prior studies (4). To add, if given only 0.4 mM palmitate, the neonatal heart is energy deficient during

reperfusion; so, increasing FA oxidation rates provides sufficient energy to recover contractile function. Therefore, the high fat-perfused heart is more efficient during post-ischemic recovery compared to a low-fat perfused heart.

Similarly, pyruvate supplementation in 0.4 mM palmitate-perfused 7-day-old rabbit hearts did not affect pre-ischemic, aerobic function despite increased PDH activity (32). In contrast, in an ATP-deficient state (eg. ischemia-reperfusion), pyruvate also improved post-ischemic functional recovery. As with FA, pyruvate supplementation demonstrates that an excess ATP production rate is vital to rescuing cardiac function and that a reserve metabolic capacity is present in spite of the metabolic inflexibility in the neonatal heart. An advantage that FA supplementation offers over pyruvate is that clinically, high circulating FA is readily achievable. Clinically ischemic-reperfused hearts, both in adults and neonates, are exposed to high circulating FA levels (31) and exogenous supplementation may not be necessary to achieve cardioprotection. While high FA may be detrimental to the adult heart during reperfusion (19,33), neonatal hearts may exploit the benefits of increased energy metabolite availability.

2.4.2 10 U/L insulin Improves Post-ischemic Cardiac Recovery Only in the Presence of 1.2 mM Palmitate

Relative to 0.1 U/L insulin treatment, supra-physiological insulin (10 U/L) improved the functional recovery of the 7-day-old rabbit heart during

reperfusion with 1.2 mM palmitate. 10 U/L insulin stimulation was oddly associated with an increased ATP production through augmented FA oxidation. Palmitate oxidation was not increased nor cardiac contractile recovery bettered in 10 U/L insulin-treated hearts in the presence of 0.4 mM palmitate and may be due to substrate limitation. Conversely, in the presence of 1.2 mM palmitate, the increased FA oxidation may be attributed to the associated unaltered ACC phosphorylation and increased CD36 translocation to increase substrate uptake for oxidation.

CD36 is a long chain FA (LCFA) transporter responsible for the bulk of LCFA transport into the rat cardiomyocyte (34). The majority of CD36 transporter is found in the recyclable endosomes, as with GLUT1, in contrast to GLUT4, which is concentrated in storage compartments (35). When activated, GLUT4s are translocated first to the recyclable endosome pool from the storage compartment and then to the plasma membrane; in contrast, CD36 is translocated directly from the recyclable pool (36). Insulin and contractile stimulation cause the translocation of both GLUT4 and CD36 transporters to the plasma membrane. Although the translocation of both transporters occurs simultaneously, it has also been demonstrated that the vesicles which contain and therefore regulate their translocation are different (37). Stienbusch et al (37) showed that insulin-stimulated GLUT4 and CD36 translocation are susceptible to differential inhibitory elements such as endosomal pH; hence, selective CD36

translocation may be possible apart from GLUT4 translocation. Here, in the neonatal rabbit heart model, we demonstrated that a supra-physiological insulin level can produce such effect that is associated with a selective increased in FA oxidation.

In the neonatal heart, supra-physiological insulin is implicated in cardioprotection on multiple regulatory steps of FA uptake. In the present study, mitochondrial FA uptake was not restricted as demonstrated similar rates of FA oxidation found between using 1.2 mM palmitate and to that in a prior study using 2.4 mM palmitate (4). Insulin was hypothesized to inhibit FA oxidation by decreasing AMPK phosphorylation and in turn inhibit ACC. AMPK phosphorylation was decreased in the presence of 10 U/L compared 0.1 U/L, but ACC phosphorylation was unchanged and may not have increased malonyl-CoA production. Although AMPK response to insulin is not blunted by high fat here, the overall FA metabolic response to insulin in the presence of high fat is similar to that found in adult mice where insulin does not inhibit FA oxidation (19).

Simultaneous to the decreased phosphorylation of AMPK, AKT phosphorylation and CD36 translocation were increased when 10 U/L insulin is present. This corroborates with the difference between insulin- and contraction-stimulated CD36 translocation owing to their differential regulation by AMPK (36). It further demonstrates that additional CD36 translocation may contribute to increased FA oxidation. In the immediate newborn period, plasma adiponectin levels elevate

simultaneous to decreased circulating insulin levels to prompt the metabolic maturation of the neonatal heart (13), which in part may owe to adiponectin's stimulation of CD36 translocation (38,39). CD36 translocation may be upregulated in the neonatal heart to enhance FA uptake for oxidation. Enhanced CD36 translocation is associated with supra-physiological insulin stimulation, here.

TG stores were not changed between 0.1 U/L and 10 U/L insulin treatments, it is likely that any increased FA uptake through CD36 was directed towards FA oxidation. Indeed, FA oxidation was increased in the 10 U/L insulin-treated group. Of interest is that the amount of TG present in these hearts are much lower than the values measured in 7-day-old hearts in a previous study (15). In the same study, the TG stores were compared between unperfused and 30-min aerobically perfused hearts to show that perfusion alone is able to decrease TG stores. Therefore, though TG values here are lower here, a possible explanation is that hearts in the current study were perfused for a longer period of time and subjected to the stress of ischemia-reperfusion, which is much more energy-demanding than aerobic perfusion. Moreover, this difference emphasizes the possibility that any increased FA uptake, is directed to increase FA oxidation as TG stores are at its minimum in these hearts. Overall, a disjoint is demonstrated in the AMPK-ACC signaling pathway whose decreased phosphorylation was expected to further inhibit FA oxidation. FA oxidation rates were augmented and

may have sufficiently surmounted the ischemia-reperfusion-induced energy deficit.

Unlike FA oxidation, glucose metabolism was unaltered in the presence of supra-physiological insulin. GLUT4 expression increases while that of GLUT1 decreases over the neonatal period (40). Oddly, excess insulin stimulation failed to increase GLUT4 translocation but was associated with increased CD36 present in the plasma membrane. A probable explanation is that GLUT4 translocation responds differently to 10 U/L insulin compared to CD36 translocation. In the diabetic heart, early insulin resistance and therefore in the presence hyperinsulinemia, CD36 translocation is increased while GLUT4 has yet to be impacted (41). Equally, the two substrate transporters are subjected to different vesicle trafficking mechanisms (37,42). The differential regulation of GLUT4 translocation may limit glucose uptake to maintain the low rates of glucose oxidation preventing the reciprocal inhibition on FA oxidation.

In summary, the present study has verified that elevating FA oxidation is cardioprotective to the neonatal heart. To clarify the misconception of insulin's detriments in the neonatal heart, supra-physiological insulin stimulation is cardioprotective whereby improved post-ischemic functional recovery is associated with increased FA oxidation rates. This insulin-associated increased FA oxidation is may be related to increased CD36 translocation. These findings help delineate the mechanism by which supra-physiological insulin is

cardioprotective in the neonatal heart, and may encourage its use in neonatal cardiac surgery. Although in adults, GIK cardioprotective effects remain controversial, supra-physiological insulin may be beneficial in the neonatal heart due to its metabolic immaturity.

2.5 Limitations

Although this study has disproven the hypothesis that insulin is detrimental to the ischemic-reperfused neonatal heart, the findings in this study demonstrate the potentials of insulin as a neonatal cardioprotective strategy. However, the full mechanism by which supra-physiological insulin improves functional recovery requires continued studies. Increased CD36 protein in the plasma membrane correlated to an increase in FA oxidation. We have demonstrated that several signaling molecules downstream of the insulin receptor have been elicited. Changes to AMPK phosphorylation is one way to differentiate between contractile versus insulin stimulated CD36 translocation. In order to differentiate the cause-and-effect relationship between insulin, myocardial contraction, and CD36 translocation, studies of differential cardiac pacing in the neonatal heart would be needed to demonstrate contractile-stimulated CD36 translocation. However, studies of such caliber are beyond the scope and aims of this study and would be best left for future investigations. Whether the increased CD36 in the plasma membrane is due to the 10 U/L insulin or increased contractility would require a comparison to hearts perfused similarly without the addition of

insulin. Furthermore, to validate the benefit insulin induces, pathway inhibition, such as by inhibited PI3-kinase or Akt phosphorylation would have better defined the role of insulin signaling in increasing FA oxidation.

Another limitation to this study is the inference that FA uptake was increased by increased CD36 translocation. Actual rates of FA uptake were not measured and the destination of FAs was not quantified. Although the TG stores are no different between the two groups at the end of reperfusion, it cannot preclude the possibility that TG stores were different prior to ischemia, which may contribute to the differences between insulin treatments. Other set of hearts that are aerobically perfused for only 30 min without an ischemic period as well as a set of hearts subjected to 30 min of aerobic perfusion followed by 30 min of ischemia and frozen prior to reperfusion should be prepared in future experiments to establish baseline, pre-ischemic signalling properties and TG amounts.

CPT-1 inhibition is major pathway by which FA oxidation is regulated. A drawback to this study is that, though palmitate oxidation rates and major regulators of malonyl-CoA production, such as AMPK and ACC were quantified, they serve only as surrogate markers of malonyl-CoA levels. As malonyl-CoA levels were not measured, it is difficult to determine the level of inhibition found in the respective experimental groups. Malonyl-CoA is a labile molecule sensitive to degradation and difficult to measure in frozen tissue stored for an extensive

period of time. Therefore, it is unfortunate that it is no longer possible to quantify malonyl-CoA in hearts from this study and must be part of a future study.

Lastly, though not a true limitation, it should be pointed out that the comparison of the 0 U/L insulin groups to 0.1 and 10 U/L groups was not made intentionally due to the limited clinical relevance of that comparison. Clinically, it is impossible to achieve 0 U/L insulin. Therefore, purpose of performing isolated heart perfusions in the absence of insulin is to demonstrate that insulin does not influence the impact of FA levels on post-ischemic functional recovery in neonatal hearts. However, it should be acknowledged that though changes in insulin levels had no impact on functional recovery in the presence of 0.4 mM palmitate, relative to 0 U/L insulin, 0.1 U/L was detrimental and is associated with impaired post-ischemic functional recovery. On the other hand, 10 U/L insulin restores post-ischemic functional recovery to levels found in the absence of insulin. Although, this demonstrates that physiological levels are detrimental to post-ischemic functional recovery, this finding is relative to a non-physiological unachievable state and was, therefore, not included in the discussion. Though several limitations are highlighted, this study has elucidated possible mechanisms by which supra-physiological insulin may benefit the ischemic-reperfused neonatal heart and emphasized a FA-centric cardiac

metabolism. However, future studies would be needed to further understand the underlying mechanisms to insulin treatment.

2.6 References

1. Allen BS. Pediatric myocardial protection: where do we stand? *J Thorac Cardiovasc Surg* 2004;128:11-3.
2. Bolling K, Kronon M, Allen BS, et al. Myocardial protection in normal and hypoxically stressed neonatal hearts: the superiority of hypocalcemic versus normocalcemic blood cardioplegia. *J Thorac Cardiovasc Surg* 1996;112:1193-200; discussion 1200-1.
3. Fallouh HB, Kentish JC, Chambers DJ. Targeting for cardioplegia: arresting agents and their safety. *Curr Opin Pharmacol* 2009;9:220-6.
4. Ito M, Jaswal JS, Lam VH, et al. High levels of fatty acids increase contractile function of neonatal rabbit hearts during reperfusion following ischemia. *Am J Physiol Heart Circ Physiol* 2010;298:H1426-37.
5. Wambolt RB, Lopaschuk GD, Brownsey RW, Allard MF. Dichloroacetate improves postischemic function of hypertrophied rat hearts. *J Am Coll Cardiol* 2000;36:1378-85.
6. Taniguchi M, Wilson C, Hunter CA, Pehowich DJ, Clanachan AS, Lopaschuk GD. Dichloroacetate improves cardiac efficiency after ischemia independent of changes in mitochondrial proton leak. *Am J Physiol Heart Circ Physiol* 2001;280:H1762-9.

7. Dyck JR, Hopkins TA, Bonnet S, et al. Absence of malonyl coenzyme A decarboxylase in mice increases cardiac glucose oxidation and protects the heart from ischemic injury. *Circulation* 2006;114:1721-8.
8. Dyck JR, Cheng JF, Stanley WC, et al. Malonyl coenzyme a decarboxylase inhibition protects the ischemic heart by inhibiting fatty acid oxidation and stimulating glucose oxidation. *Circ Res* 2004;94:e78-84.
9. Lopaschuk GD, Collins-Nakai RL, Itoi T. Developmental changes in energy substrate use by the heart. *Cardiovasc Res* 1992;26:1172-80.
10. Lopaschuk GD, Belke DD, Gamble J, Itoi T, Schonekess BO. Regulation of fatty acid oxidation in the mammalian heart in health and disease. *Biochim Biophys Acta* 1994;1213:263-76.
11. van der Vusse GJ, Glatz JF, Stam HC, Reneman RS. Fatty acid homeostasis in the normoxic and ischemic heart. *Physiol Rev* 1992;72:881-940.
12. Lopaschuk GD, Witters LA, Itoi T, Barr R, Barr A. Acetyl-CoA carboxylase involvement in the rapid maturation of fatty acid oxidation in the newborn rabbit heart. *J Biol Chem* 1994;269:25871-8.
13. Onay-Besikci A, Altarejos JY, Lopaschuk GD. gAd-globular head domain of adiponectin increases fatty acid oxidation in newborn rabbit hearts. *J Biol Chem* 2004;279:44320-6.

14. Makinde AO, Gamble J, Lopaschuk GD. Upregulation of 5'-AMP-activated protein kinase is responsible for the increase in myocardial fatty acid oxidation rates following birth in the newborn rabbit. *Circ Res* 1997;80:482-9.
15. Lopaschuk GD, Spafford MA. Energy substrate utilization by isolated working hearts from newborn rabbits. *Am J Physiol* 1990;258:H1274-80.
16. Hue L, Taegtmeyer H. The Randle cycle revisited: a new head for an old hat. *Am J Physiol Endocrinol Metab* 2009;297:E578-91.
17. Soltys CL, Kovacic S, Dyck JR. Activation of cardiac AMP-activated protein kinase by LKB1 expression or chemical hypoxia is blunted by increased Akt activity. *Am J Physiol Heart Circ Physiol* 2006;290:H2472-9.
18. Kovacic S, Soltys CL, Barr AJ, Shiojima I, Walsh K, Dyck JR. Akt activity negatively regulates phosphorylation of AMP-activated protein kinase in the heart. *J Biol Chem* 2003;278:39422-7.
19. Folmes CD, Clanachan AS, Lopaschuk GD. Fatty acids attenuate insulin regulation of 5'-AMP-activated protein kinase and insulin cardioprotection after ischemia. *Circ Res* 2006;99:61-8.
20. Fuller W, Eaton P, Medina RA, Bell J, Shattock MJ. Differential centrifugation separates cardiac sarcolemmal and endosomal

membranes from Langendorff-perfused rat hearts. *Anal Biochem* 2001;293:216-23.

21. Omar MA, Fraser H, Clanachan AS. Ischemia-induced activation of AMPK does not increase glucose uptake in glycogen-replete isolated working rat hearts. *Am J Physiol Heart Circ Physiol* 2008;294:H1266-73.
22. Folmes CD, Clanachan AS, Lopaschuk GD. Fatty acid oxidation inhibitors in the management of chronic complications of atherosclerosis. *Curr Atheroscler Rep* 2005;7:63-70.
23. Girard J, Ferre P, Pegorier JP, Duee PH. Adaptations of glucose and fatty acid metabolism during perinatal period and suckling-weaning transition. *Physiol Rev* 1992;72:507-62.
24. Onay-Besikci A. Regulation of cardiac energy metabolism in newborn. *Mol Cell Biochem* 2006;287:1-11.
25. Albacker TB, Carvalho G, Schricker T, Lachapelle K. Myocardial protection during elective coronary artery bypass grafting using high-dose insulin therapy. *Ann Thorac Surg* 2007;84:1920-7; discussion 1920-7.
26. Haider W, Benzer H, Schutz W, Wolner E. Improvement of cardiac preservation by preoperative high insulin supply. *J Thorac Cardiovasc Surg* 1984;88:294-300.

27. Svensson S, Berglin E, Ekroth R, Milocco I, Nilsson F, William-Olsson G. Haemodynamic effects of a single large dose of insulin in open heart surgery. *Cardiovasc Res* 1984;18:697-701.
28. Fan Y, Zhang AM, Xiao YB, Weng YG, Hetzer R. Glucose-insulin-potassium therapy in adult patients undergoing cardiac surgery: a meta-analysis. *Eur J Cardiothorac Surg* 2010.
29. Zhao YT, Weng CL, Chen ML, et al. Comparison of glucose-insulin-potassium and insulin-glucose as adjunctive therapy in acute myocardial infarction: a contemporary meta-analysis of randomised controlled trials. *Heart* 2010;96:1622-6.
30. Rabi D, Clement F, McAlister F, et al. Effect of perioperative glucose-insulin-potassium infusions on mortality and atrial fibrillation after coronary artery bypass grafting: a systematic review and meta-analysis. *Can J Cardiol* 2010;26:178-84.
31. Lopaschuk GD, Collins-Nakai R, Olley PM, et al. Plasma fatty acid levels in infants and adults after myocardial ischemia. *Am Heart J* 1994;128:61-7.
32. Saiki Y, Lopaschuk GD, Dodge K, Yamaya K, Morgan C, Rebeyka IM. Pyruvate augments mechanical function via activation of the pyruvate dehydrogenase complex in reperfused ischemic immature rabbit hearts. *J Surg Res* 1998;79:164-9.

33. Folmes CD, Sowah D, Clanachan AS, Lopaschuk GD. High rates of residual fatty acid oxidation during mild ischemia decrease cardiac work and efficiency. *J Mol Cell Cardiol* 2009;47:142-8.
34. Luiken JJ, Koonen DP, Willems J, et al. Insulin stimulates long-chain fatty acid utilization by rat cardiac myocytes through cellular redistribution of FAT/CD36. *Diabetes* 2002;51:3113-9.
35. Fischer Y, Thomas J, Sevilla L, et al. Insulin-induced recruitment of glucose transporter 4 (GLUT4) and GLUT1 in isolated rat cardiac myocytes. Evidence of the existence of different intracellular GLUT4 vesicle populations. *J Biol Chem* 1997;272:7085-92.
36. Schwenk RW, Luiken JJ, Bonen A, Glatz JF. Regulation of sarcolemmal glucose and fatty acid transporters in cardiac disease. *Cardiovasc Res* 2008;79:249-58.
37. Steinbusch LK, Wijnen W, Schwenk RW, et al. Differential regulation of cardiac glucose and fatty acid uptake by endosomal pH and actin filaments. *Am J Physiol Cell Physiol* 2010;298:C1549-59.
38. Palanivel R, Fang X, Park M, et al. Globular and full-length forms of adiponectin mediate specific changes in glucose and fatty acid uptake and metabolism in cardiomyocytes. *Cardiovasc Res* 2007;75:148-57.

39. Fang X, Palanivel R, Cresser J, et al. An APPL1-AMPK signaling axis mediates beneficial metabolic effects of adiponectin in the heart. *Am J Physiol Endocrinol Metab* 2010;299:E721-9.
40. Postic C, Leturque A, Printz RL, et al. Development and regulation of glucose transporter and hexokinase expression in rat. *Am J Physiol* 1994;266:E548-59.
41. Coort SL, Hasselbaink DM, Koonen DP, et al. Enhanced sarcolemmal FAT/CD36 content and triacylglycerol storage in cardiac myocytes from obese Zucker rats. *Diabetes* 2004;53:1655-63.
42. Schwenk RW, Dirkx E, Coumans WA, et al. Requirement for distinct vesicle-associated membrane proteins in insulin- and AMP-activated protein kinase (AMPK)-induced translocation of GLUT4 and CD36 in cultured cardiomyocytes. *Diabetologia* 2010;53:2209-19.

2.7 Figures

Figure 2-1: Neonatal Cardiac Function and Metabolism in 0.4 mM Palmitate or 1.2 mM Palmitate Without the Effects of Insulin. Cardiac output comparing the effects of 0.4 mM palmitate (n = 20) and 1.2 mM (n = 15) palmitate without the effect of insulin (0 U/L insulin) A). No significant differences are present during the first 30 minutes of aerobic perfusion. The hearts are then subjected to 30 minutes of global ischemia. 1.2 mM palmitate benefits the neonatal heart during reperfusion by increasing palmitate oxidation rates B); and therefore overall steady state ATP production C). Cardioprotective effect is apparent from 1.2 mM palmitate reperfusion. 1.2 mM palmitate performed with a significantly better function than those reperfused with 0.4 mM palmitate (*P<0.05).

Fig 2-1

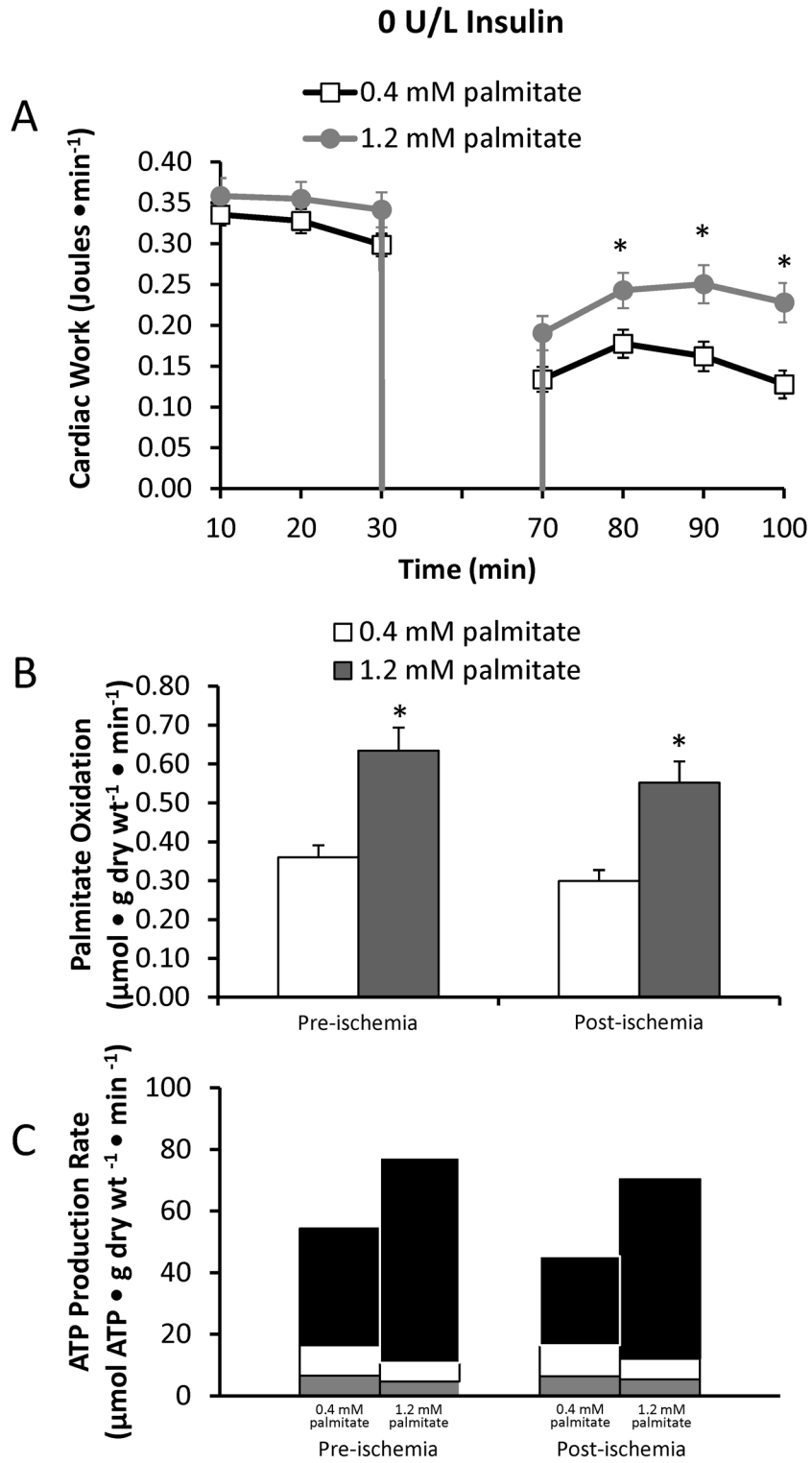


Figure 2-2: Neonatal Cardiac Function in 0.4 mM Palmitate or 1.2 mM Palmitate Treated with Either 0.1 or 10 U/L Insulin. Cardiac output comparing the effects of 0.1 U/L (n = 20) and 10 U/L (n = 8) insulin when 7-day-old rabbit hearts are perfused with 0.4 mM A) or 1.2 mM palmitate B). Insulin is added into the perfusate at 28 minutes into the aerobic perfusion, as indicated by the arrow. Insulin does not have an effect on cardiac function either in aerobic perfusion or in reperfusion (from 70 minutes to 100 minutes) in 0.4 mM palmitate, but 10 U/L is beneficial in 1.2 mM palmitate. * indicates significance between 0.1 and 10 U/L insulin (*P < 0.05). The arrow is the point at which insulin (0.1 or 10 U/L) was added to the perfusate, which is 2 min prior to ischemia.

Fig 2-2

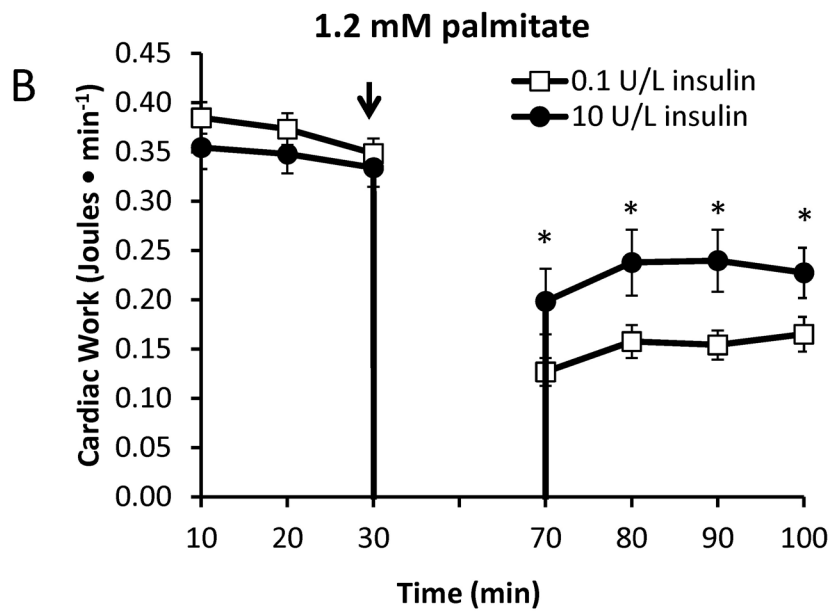
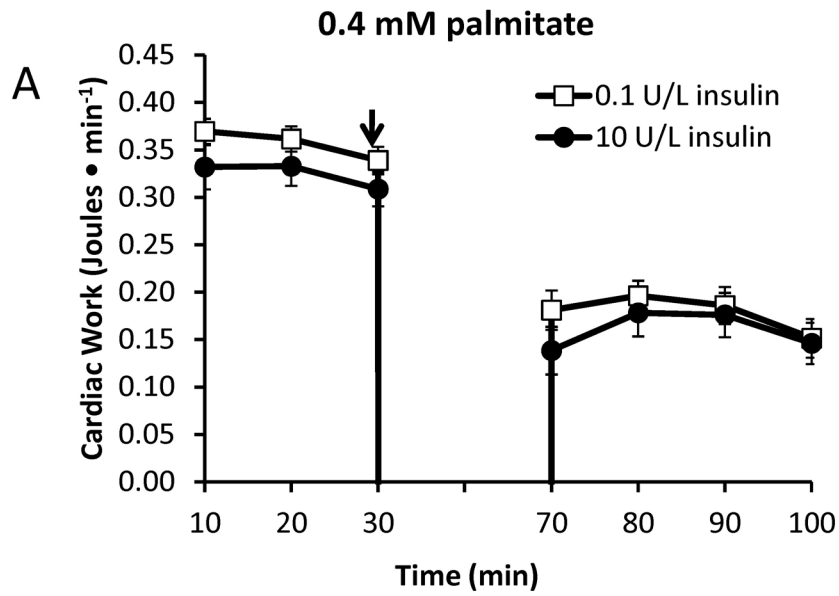


Figure 2-3: The Metabolic Effects of 0.1 and 10 U/L Insulin in Neonatal Hearts Perfused With 1.2 mM Palmitate. Insulin was added at 28 minutes into the aerobic perfusion and A) palmitate oxidation (\square -n = 8; \blacksquare -n = 5), B) glucose oxidation (\square -n = 4; \blacksquare -n = 6), and C) glycolysis (\square -n = 7; \blacksquare -n = 7) were assayed. D) Steady state ATP production rates were calculated from the metabolic rates above (\blacksquare -palmitate oxidation; \square -glucose oxidation; \blacksquare -glycolysis). Values represent means \pm SEM; * indicates significant difference between 0.1 and 10 U/L insulin groups (*P < 0.05).

Fig 2-3

1.2 mM palmitate

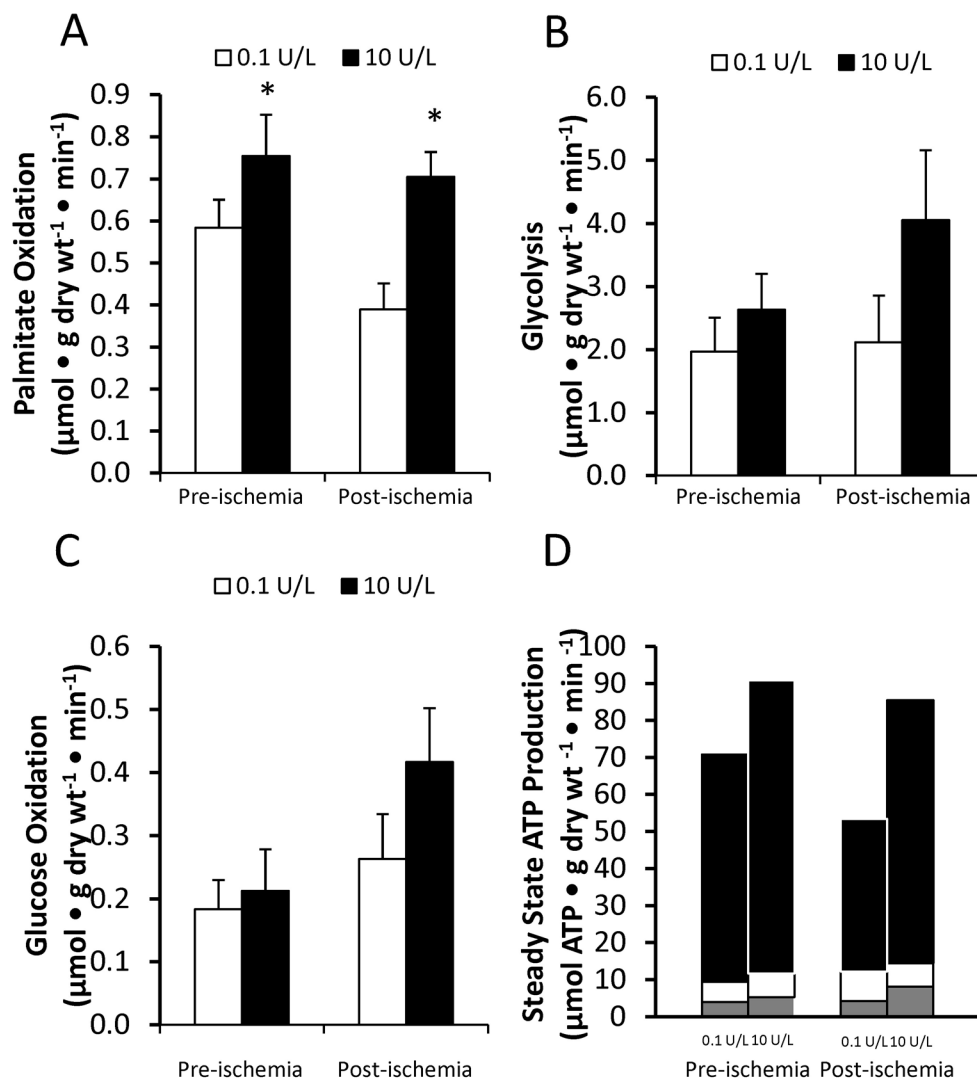


Figure 2-4: 10 U/L insulin Activates Akt and Inhibits AMPK Activation Without Affecting ACC Phosphorylation in 1.2 mM Palmitate-Perfused Hearts. 10 U/L insulin A) increases Akt (60 kDa) phosphorylation, B) inhibits AMPK (63 kDa) phosphorylation, C) but has no affect on ACC (265 kDa and 280 kDa) phosphorylation. D) Representative blots of Akt, AMPK, and ACC (all groups n \geq 4, *P < 0.05).

Fig 2-4

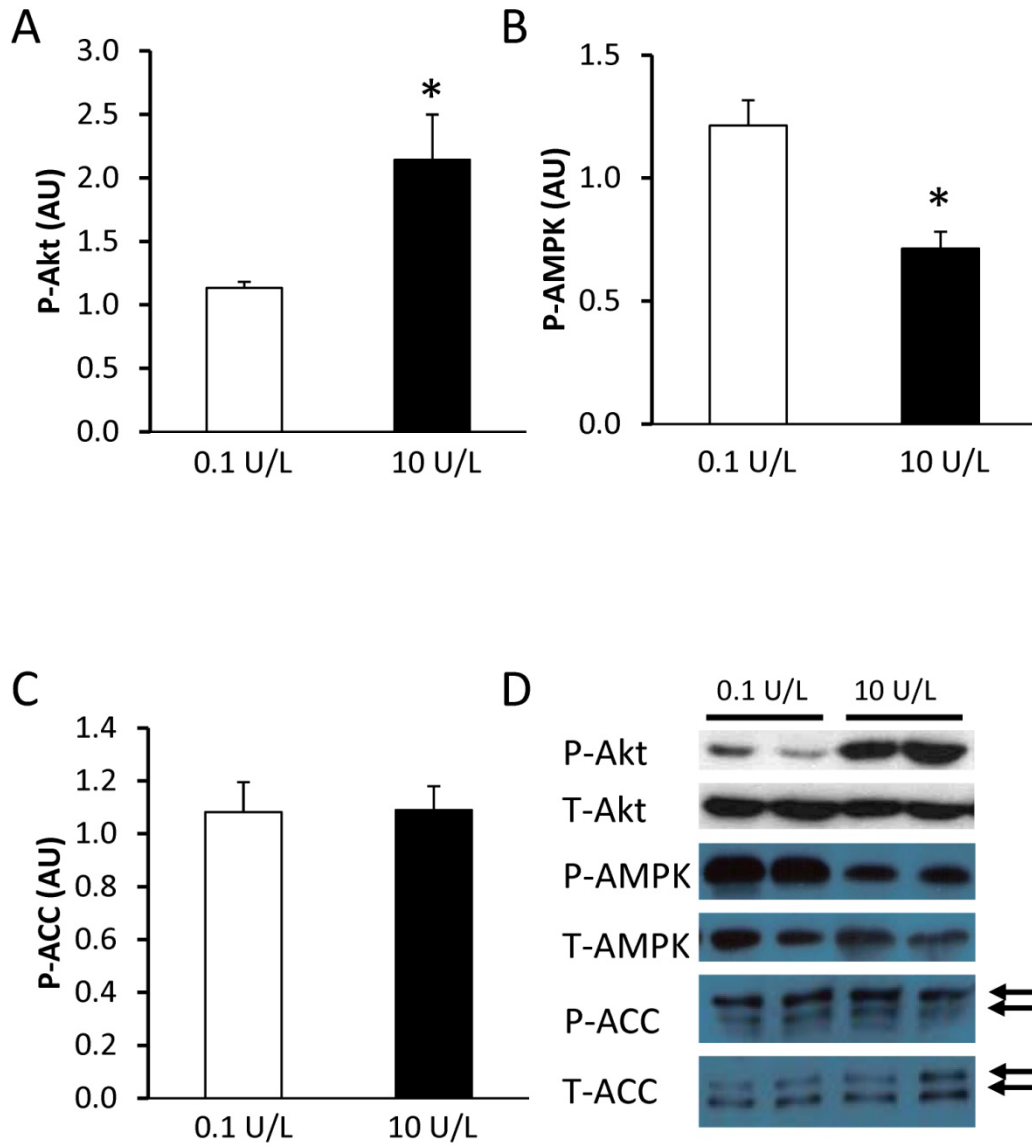
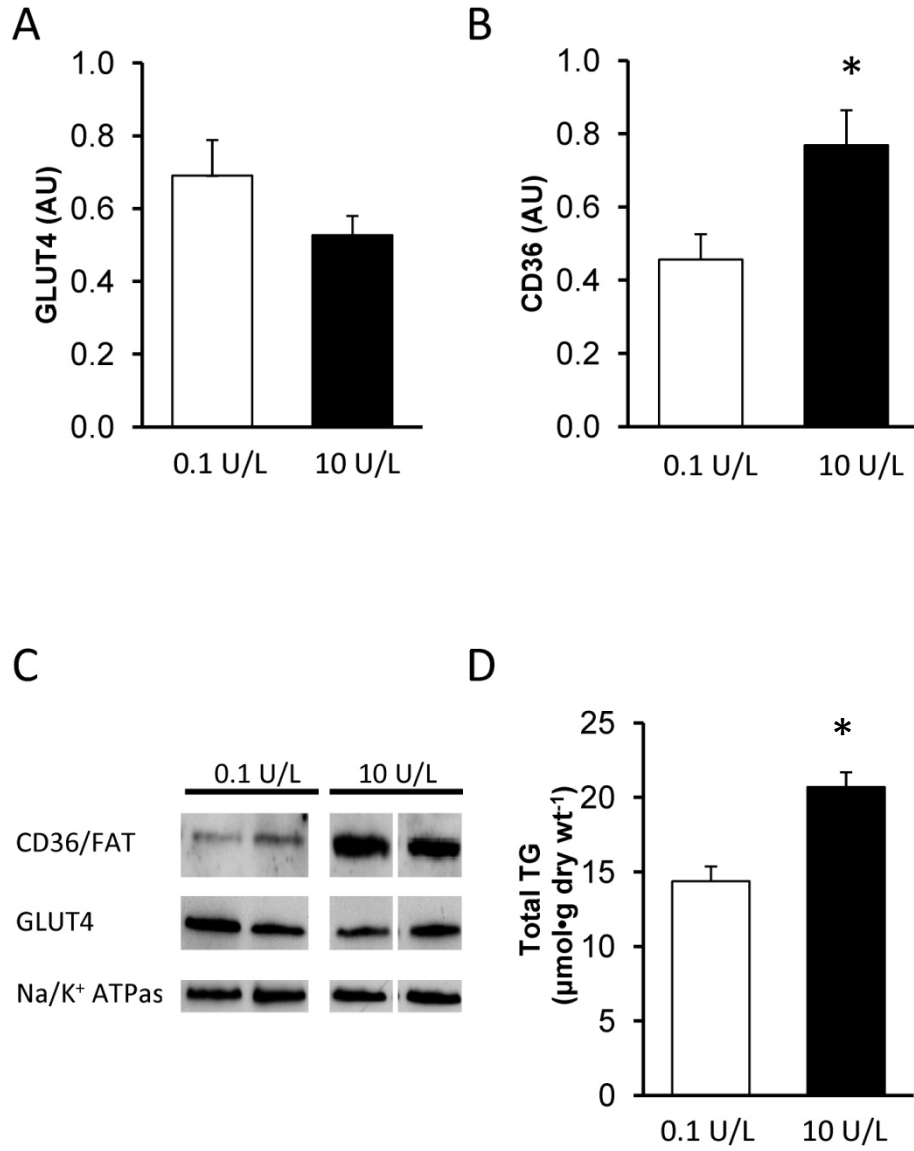


Figure 2-5: Cardiac Plasma Membrane CD36 is Increased in the Presence of 10 U/L Insulin Stimulation While Perfused with 1.2 mM Palmitate. 10 U/L insulin A) did not affect GLUT4 presence in the plasma membrane, but significantly increased B) CD36 levels. C) Representative blots of CD36, GLUT4, Na⁺/K⁺ ATPase (loading control) from the plasma membrane fraction. D) ventricular triacylglycerol (TG) contents was increased significantly in hearts treated with 10 U/L insulin compared to the 0.1 U/L treated hearts (all groups n ≥ 4, *P < 0.05).

Fig 2-5



2.8 Tables

Table 2-1: Comparison of rates of glycolysis and glucose oxidation when perfused with 0.4 mM or 1.2 mM palmitate

	0.4 mM palmitate		1.2 mM palmitate	
	Pre-ischemia	Post-ischemia	Pre-ischemia	Post-ischemia
Glycolysis	3.25 ± 0.45	3.20 ± 0.37	2.32 ± 0.43	2.69 ± 0.42
Glucose oxidation	333 ± 71	334 ± 63	202 ± 26	225 ± 32

All values are reported in $\mu\text{mol} \cdot \text{g dry wt}^{-1} \cdot \text{min}^{-1}$

Table 2-2: Average pre- and post-ischemia cardiac hemodynamic parameters

	0.1 U/L insulin		10 U/L insulin	
	Pre-ischemia	Post-ischemia	Pre-ischemia	Post-ischemia
Heart rate (beats•min ⁻¹)	238 ± 3	202 ± 6 [†]	244 ± 4	240 ± 5*
Coronary flow (mL•min ⁻¹)	10.7 ± 0.8	10.6 ± 0.8	11.5 ± 0.8	12.8 ± 0.8
Peak systolic pressure (mmHg)	25.0 ± 0.9	17.0 ± 1.1 [†]	25.2 ± 0.7	20.3 ± 0.4 [†] *

*vs 0.1 U/L; † vs pre-ischemic value, P<0.05

Table 2-3: Metabolic rates of hearts perfused with 0.4 mM palmitate treated with 0.1 or 10 U/L insulin

	0.1 U/L insulin		10 U/L insulin	
	Pre-ischemia	Post-ischemia	Pre-ischemia	Post-ischemia
Palmitate oxidation	384 ± 37	335 ± 46	448 ± 56	402 ± 55
Glycolysis	3.4 ± 0.8	4.5 ± 0.5	3.0 ± 0.6	3.3 ± 0.4
Glucose oxidation	0.30 ± 0.07	0.26 ± 0.03	0.36 ± 0.11	0.25 ± 0.08

All values are reported in $\mu\text{mol} \cdot \text{g dry wt}^{-1} \cdot \text{min}^{-1}$

Chapter 3
Neonatal Rabbit Aorto-Caval Shunt
Volume-Overload Cardiac
Hypertrophy Model

Neonatal Rabbit Aorto-Caval Shunt Volume-Overload Cardiac Hypertrophy

Model

Victoria H. Lam *BSc*, Tatsujiro Oka *MD, PhD*, Virgilio J Cadete *MSc*,

Ivan M. Rebeyka *MD, MSc*, and Gary D. Lopaschuk *PhD*

Cardiovascular Research Centre, Mazankowski Alberta Heart Institute, and
Departments of Pediatrics and Surgery, University of Alberta, Edmonton, Canada

Abbreviated title: Model of neonatal cardiac hypertrophy

Contribution:

Victoria HM Lam: Model A surgeries, model B development, data analysis,
primary authorship

Tatsjiro Oka: Model A development and surgery

Virgilio J Cadete: Model A development and surgery

Hypothesis:

If a shunt is created between the descending aorta and inferior vena cava (IVC)
in a neonatal rabbit, then blood will shunt across from the aorta into the IVC and
increase volume return causing volume-overload cardiac hypertrophy because of
the pressure gradient between the two vessels.

3.1 Introduction

It has been an ongoing debate as to whether the neonatal heart is more susceptible to ischemia-reperfusion injury compared to the adult heart. Intolerance of the neonatal heart to ischemia-reperfusion has been demonstrated by some studies (1-7). On the other hand, others have equally shown increased tolerance of the neonatal heart to ischemia-reperfusion (8-14) relative to that of the adult heart. The clinical relevance of this debate relates to the development of neonatal cardiac surgery for the correction of congenital heart defects (CHDs). During surgery, the neonatal heart must be arrested and therefore subjected to an obligatory period of ischemia in order to achieve the bloodless and motionless field of operation. These periods of ischemia can last for more than an hour (15). Cardioprotection is essential to successful post-ischemic recovery. Current post-surgical mortality rates remain considerable (~4%) despite superior technical skills and numerous factors, and can be attributed to poor cardioprotection (16-20).

A criticism of studies on ischemia-reperfused neonatal hearts is that these are normal hearts. CHDs disturb the cardiac hemodynamics causing a pressure- or volume-overload. Ventricular septal (VSD) and atrial septal defects (ASD) are the most prominent lesions that contribute to 29% and 21%, respectively, of all CHDs. These lesions and the resultant hemodynamic changes can lead to volume-overload cardiac hypertrophy. Cardiac hypertrophy in the adult heart

causes metabolic remodelling that reverts cardiac metabolism towards a more fetal-like profile. Similarly, in a neonatal piglet model of patent-ductus arteriosus, volume-overload cardiac hypertrophy was associated with a downregulation of regulatory elements of metabolic maturation (21). These findings suggested that the maturation of FA metabolism in these hearts were delayed. However, metabolic rates were not measurable in these hearts to validate these finding.

While the neonatal piglet model of patent ductus arteriosus is a highly relevant model of neonatal cardiac hypertrophy, in order to accurately quantify cardiac metabolism, a smaller animal that can be easily manipulated for acute and chronic studies is needed. Therefore, an aorto-caval shunt model was developed to increase volume-return to the right side of the heart and cause volume-overload cardiac hypertrophy.

3.2 Methods

3.2.1 Animals

The University of Alberta adheres to the principles developed by the Council for International Organizations of Medical Sciences and Medical Sciences and complies with Canadian Council of Animal Care guidelines in regards to the health and safety of animals used in biomedical research.

3.2.2 The Aorto-caval Shunt

An aorto-caval shunt was induced inferior to the renal blood vessels between the descending aorta and inferior vena cava (IVC) of 7-day-old New Zealand albino white rabbits (Vandermeer Rabbitry, Edmonton, Alberta) of either gender (90 - 200g). These rabbits were removed from maternal care after their maternal feeding and kept at room temperature as a litter while waiting for surgical procedure to be performed as follows, in a clean, non-sterile environment.

The 7-day-old rabbits were anesthetized with isoflurane (1-2%, oxygen flow rate of 2-3 ml/min). After the rabbit was unconscious, it was placed on a warming table of 37° C and isoflurane inhalation was continuous via a nose cone (4-5%, oxygen flow rate of 2-3 ml/min) to achieve a surgical plane of unconsciousness. The pup was then placed on its right lateral decubitus and its left flank shaved to expose the skin. 1% Iodine solution was applied to aseptically clean the surgical area. A left flank retroperitoneal incision was made using a sterile #10 scalpel blade to expose the descending aorta and the IVC (fig 3-1).

The descending aorta was clamped using a micro-clamp ~5 mm inferior to the renal blood vessels to cease downstream blood flow. An 18G needle at 1½ inch length was modified to form a 90° angle approximately 5 mm from the bevelled tip (fig 3-1). This modification permits ease of manoeuvring of the needle when puncturing the aorta and IVC. Model A (single puncture): Using the modified needle, the aorta was punctured below the micro-clamp and a through-and-

through is generated across the aorta to reach and puncture the IVC's adjacent wall (fig 3-1A). Model B (triple puncture): In a second group of animals, after the first through-and-through puncture was made as in model A, the needle was withdrawn from the hole connected to the IVC and the tip was placed caudally to the first puncture and a second and a third puncture were made (fig 3-1B). In model B, a total of 3 shunting holes were made between the aorta and IVC. In both models, the IVC was not subjected to a through-and-through. The needle was then carefully removed and a drop of cyanoacrylic glue was placed on the puncture site and let dry. As the glue dried, the micro-clamp was removed. Sham group: sham-operated animals were subjected to the peritoneal dissection and aortic clamping without puncturing the vessels with a needle. A drop of cyanoacrylic glue was placed at ~5 mm inferior to the renal blood vessels for 2 minutes and then removed. The sham animal is then sutured and allowed to recover as with the other two groups of animal.

Once hemostability was achieved, the peritoneum and skin layers were sutured separately using running stitches and 5-0 prolene. Iodine is applied on the sutured skin again. Isoflurane is ceased and the rabbits let to recover on the warming table (37° C) until they regain consciousness at which the recovered rabbit would be returned to its litter again. The rabbits were returned to the doe on the day of the surgery and iodine is applied to the doe's nose so that she may adapt to the new scent of its litter and continue to nurse them. The recovery of

the animals was monitored hourly for 24 hours to assure that no complications arose from the surgery.

3.2.3 Echocardiography Evaluation of the Aorta-Caval Shunt and of Cardiac Size and Function

One week after surgery, the rabbits were returned to the lab for evaluation by ultrasound and echocardiography. A timeline of the events is indicated in figure 3-2. The presence of an aorta-caval shunt was determined using color Doppler ultrasound at 7 and 13 days post-surgery. A 15 mHz probe, attached to the Acuson Sequoia 512 ultrasound imaging system was used (Siemens medical). Rabbits were anesthetised with gaseous isoflurane (1-2%, oxygen flow rate of 2-3 mL/min). After achieving unconsciousness, rabbits were placed on a warming table set at 37⁰C and continued on isoflurane (1-2%, oxygen flow rate of 2-3 mL/min) via a nose cone. The abdomen hair on the rabbit was removed with Nair® hair removing cream. Warmed ultrasound gel was applied to the abdomen and the probe is orientated longitudinally in order to capture flow direction of the aorta and IVC (fig 3-3). From this view, the diameter of the aorta and IVC were measured and often the patent shunt(s) was also visible (fig 3-3C and D). If and when the patent shunt is visible, the probe is turned 90⁰ to the longitudinal axis at the shunt to better visualize the shunting of blood from the aorta to the IVC (fig 3-3B). In this view, turbulence between the two vessels also verified the presence of a shunt.

The rabbit's chest was also cleared to skin with Nair® hair removing cream. Ultrasound gel was placed on the chest and probe was used to achieve a short and long-axis view from which the following measurements were made to assess cardiac hypertrophy (fig 3-4): left ventricular internal diameter (diastole) (LVIDd), right ventricular internal diameter (diastole) (RVIDd), right ventricular end-diastolic area, and ejection fraction (%EF).

Cardiac hypertrophy was also assessed by wet ventricular weights and normalized to body weight.

3.3 Results

3.3.1 Shunt Success Rates were Different Between the Two Models

With the two models of hypertrophy, model A produced a successful shunt at the rate of 18% while 68% of the shunts closed by 13 days after the surgery (table 3-1). On the other hand, 72% of the animals receiving model B shunt procedure had a persistent shunt 13 days after the surgery and shunt closer occurred at the rate of 13 % in these animals. Death rates in models A and B were similar between the two groups occurring at 14% and 15%, respectively. Pre-mature death was often attributed to intra-operative or peri-operative exsanguinations. Animals were terminated pre-maturely due to post-surgical complications. These complications include hindlimb ischemia, urinary incontinence, and diarrhea that were identified at the day of the first

echocardiography. In the course of the model development, these morbid conditions were lessened by decreasing aorta clamp time and minimizing the amount of cyanoacrylic glue applied.

3.3.2 Shunt Patency Detection by Ultrasound Increased IVC Diameter

Ultrasound of the abdominal vessels showed and increased volume to the IVC by its distension. The average IVC diameter in the sham group from model A is 2.84 ± 0.27 (table 3-2) and that from model B is 2.42 ± 0.15 mm (table 3-3). The two models developed were compared to their individual sham groups as the surgical procedures were performed at different times and by different surgeons between the two models and cannot be compared to each other. Nonetheless, the IVC from model A animals (4.62 ± 0.53 mm) were significantly greater than that from the sham group (Table 3-2, $P < 0.05$). Similarly model B shunt significantly increased the IVC diameter to 3.38 ± 0.11 mm (table 3-3, $P < 0.05$). Visualization of the shunt is demonstrated in figure 3-3 whereby model A (fig 3-3C) produced a single shunt and model B (fig 3-3D) produced two to three shunts. The enlarged IVCs are comparatively larger than the diameter of that found in the respective sham animals (fig 3-3A).

3.3.3 Volume-overload Cardiac Hypertrophy Resulted from the Shunt Procedure

Echocardiography, demonstrated in figure 3-4, showed bi-ventricular enlargement in shunted animals (table 3-2 and 3-3). The diastolic left ventricular

internal diameter (LVIDd) from models A (9.7 ± 0.2 mm) and B (8.7 ± 0.3 mm) were significantly increased compared to their respective shams (8.6 ± 0.1 and 7.83 ± 0.3 mm, respectively). As echocardiographic assessments were performed by differing operators between the two models, the assessment of the right ventricle RV were different. However, RV enlargement is present in both models. RV diastolic area (Area:d) was calculated for model A to demonstrate that RV was enlarged by increased volume return (46.9 ± 2.9 vs 34.4 ± 6.8 mm², $P < 0.05$). Similarly, in model B, RV internal diameter at diastole (RVID,d) was increased in the shunted animals (3.4 ± 0.1 vs 3.2 ± 0.2 mm, $P < 0.05$).

Despite the dilated ventricles, LV posterior wall (LVPW) was not increased in either model. Cardiac hypertrophy was also assessed by heart weight normalized to body weight (HW:BW). While body weight did not change between the shunted and sham groups, HW:BW were significantly increased in both models of hypertrophy (A: 6.6 ± 0.5 ; B: 4.7 ± 0.3) compared to the sham controls (A: 5.6 ± 0.4 ; B: 4.2 ± 0.1 , $P < 0.05$). However, of interest, is that while the shunt in model A did not alter ejection fraction (%EF) (60.3 ± 1.4 vs 57.6 ± 1.1 %), model B shunt decreased %EF significantly (67.4 ± 3.0 vs 75.4 ± 1.1 %, $P < 0.05$).

3.4 Discussion

Cardiac hypertrophy, though may develop secondary to a CHD, has been rarely studied in regards to cardiac metabolism and tolerance to ischemia-reperfusion. Although cardiac hypertrophy results in the newborn piglet model of ductus

arteriosus, the ability to quantify metabolism and validate the molecular changes was limited by the size of the heart. The rabbit heart model had been used extensively to study neonatal cardiac metabolism (22-29). Its size and ease of manipulation makes it convenient as an animal model to generate neonatal cardiac hypertrophy as well as to study its metabolism via the isolated working heart model. In the two neonatal models developed here, cardiac hypertrophy is reproducible by aorto-caval shunt(s) to cause volume-overload hypertrophy that increases the LV and RV internal diameters and increases HW:BW ratio.

The present neonatal volume-overload cardiac hypertrophy models are adaptations of a prior rat model. In the adult rat, a single needle puncture generating the aorto-caval shunt altered hemodynamics and produced sufficient cardiac hypertrophy (30). However, in the neonatal rabbit, by ultrasound assessment, it seemed that shunt closure was frequent in model A resulting in an 18% shunt patency rate. It is likely that the developing rabbit is highly resilient and is capable of healing the shunt. To add, as the rabbit grows in length and weight, the single shunt fistula may no longer be approximated and the shift between two vessels would occlude the fistula easily. Attempts of using a larger gauge needle or lengthen the amount of time the needle stays in the fistula failed to improve success rate of model A. It was not until three punctures into the IVC were attempted that shunt patency rates increased to 72%; hence, the production of model B. By ultrasound, this procedure readily produced two to three visible shunts between the two vessels. Model B decreased the rate of

shunt closure without affecting the morbidity/mortality rate. However, the mechanism by which the fistulas remained patent was not examined.

As stated, these two models were not produced during the same time period nor by the same surgeons. Consequently, the data gathered between the two groups cannot be statistically compared. Nonetheless, both models produced cardiac hypertrophy consistent with volume-overload hypertrophy whereby bi-ventricular dilation and increased heart weights were not accompanied by a thickening of the LVPW in model B. However, though the numerical values between the two models are incomparable, as differing echocardiographers performed the studies, model B seemed to cause systolic dysfunction while model A did not. Varying degrees of cardiac hypertrophy result from differing cardiac lesions; therefore, model B represents a more severe phenotype. It may be of interest to consider the two different techniques when examining varying types of CHDs and the degree to which they cause cardiac hypertrophy.

It should also be noted that the RV was examined by different means between the two models. RVIDd, though examined in model B, was not examined in model A. This is largely due to the experimental nature of measuring RVIDd in the 2D m-mode. Meanwhile, within the study of model A, the RV area:d was estimated instead. However, neither of these parameters are truly accurate in clinical studies (31). The study of both model was highly dependent on the precision of measurements and comparison to their respective control subjects.

These values are rarely attained in the human equivalent via 2D echocardiography as alternate modes of imaging are available to better capture RV parameters and functionality. These modes of imaging, such as 3D echocardiography or cardiac magnetic resonance imaging (CMR), are not readily accessible, even clinically. Therefore, little information in regards the prognostic value of the RVID is available. However, in the development of the volume-overload hypertrophy models, it is important to assess RV function and dilation as the initial increase in volume return enters into the right side of the heart. The model has a global impact and measuring only the LV would have limited the insight into the consequences of global volume-overload. Interestingly, the prognostic value RV assessment is becoming increasingly important. The RV's contribution to pathogenesis has been largely neglected as most attention is focused on LV function. RV assessment is growing in its importance as noted in several reviews (32-34). Its assessment is a challenge, as in models A and B, due to the anatomical location and position of the heart in the human let alone a rabbit. RV assessment remains limited due to anatomical and technological limitations. However, the evaluation of echocardiographic techniques and clinical relevance is beyond the scope of this study. In summary, by this technique, a neonatal cardiac hypertrophy model can be produced in a simple and consistent manner. This model could be applicable in the studies of pathological cardiac hypertrophy to examine the sole impact of cardiac hypertrophy on functionality.

3.5 Limitations

In the development of the neonatal volume-overload cardiac hypertrophy model, several limitations have arisen and should be considered in the evolution of this animal model. One limitation of this model is that although CHDs are intra-cardiac lesions, this present model of cardiac hypertrophy is produced by an extra-cardiac lesion. Therefore, this model is not a model of CHDs but rather a model of neonatal volume-overload cardiac hypertrophy that isolates the volume-overload hypertrophic aspect of complex CHDs for evaluation. This model, therefore, does not take into consideration the intra-cardiac hemodynamic difference between an intra-cardiac lesion versus an extra-cardiac lesion. For instance, an intra-cardiac lesion may cause a combination of pressure- and volume-overload that results in hypertrophy. Meanwhile, the resultant hypertrophy is molecularly and functionally different between that caused by pressure- versus volume-overload. Although hypertrophy may occur in both cases, the hemodynamic difference from an intra-cardiac lesion may cause molecular changes that are not appreciated in the present model. Therefore, when undergoing further molecular studies, as with any model, interpretation of the data must take into consideration that this model is not a true model of CHD.

Additionally, a major limitation in this study is that the models are not statistically comparable. This is apparent in the sham groups with significantly

differing %EF, LVIDd, body weight, and HW:BW ratios. This study was not designed to and does not have the power to statistically evaluate the efficacy of one method over the other. This study was meant to discuss the progression and evolution of surgical techniques to achieve volume-overload hypertrophy. The differences between sham groups can be accounted for by several factors. Temporal and technical factors contribute to the differences in surgical intervention as well as echocardiographic techniques. The two models were produced in series by two different surgeons/echocardiographers. This difference may be apparent in the echocardiographic data from sham animals. Despite the small SEM of several parameters (IVC, RV area, RVIDd, LVIDd, and LVPW), the mean averages are dramatically different between the two sham groups despite receiving the same sham surgery. Echocardiographic assessment is influenced by several factors including the technician, technique, and anesthesia. The echographic data from model A and B were attained by differing technicians. As this study is likely a first in demonstrating echocardiographic data for neonatal rabbits (14- and 21-day-old), no normative or historical data is available for comparison to validate echocardiographic techniques. To add, the finding here lend itself to conclude that baseline surgical techniques differ to impact both the sham and shunt procedures. Ideally, these technical differences would be controlled for by utilizing the same surgeon and echocardiographers.

One technical difference to note is the varying amounts of anesthesia, which depends on the size of the animal and susceptibility to anesthesia. Rabbits have

a relatively higher sensitivity to anesthesia (35). A high inter-rabbit variability of sensitivity to anesthesia further complicates the degree of anesthesia needed to attain the necessary echocardiogram. Although the rate of isoflurane and length of time of isoflurane anaesthesia was well controlled, the consequent impact on heart rate (HR) or respiratory rate was not quantified in either of the two models. As anaesthesia has a large impact on HR, monitoring HR during the course of anaesthesia and echocardiography would have added to normalize the echocardiographic data between the two models.

One way to control for differences in technique and anesthesia retrospectively is to compare the %EF or HR. Or to actively control for respiratory rate and/or HR. In these models, anesthesia was controlled mainly by subjective animal response in addition to the rate and time of flow. The %EF of the two models cannot be statistically compared as the values seem different in the two sham groups. %EF is the product of the stroke volume divided by the end diastolic volume. This parameter is highly influenced by HR. A higher HR would decrease stroke volume. Therefore, deep sedation would depress HR and elevated %EF. In model B, a high %EF relative to model A shams may be indicative of better cardiac function, but may also indicate a deeper state of anesthesia. Thus, HR would have normalized the data gathered from the two models and determine the origin of %EF changes. Unfortunately, an electrocardiogram (ECG) from which HR data may be easily derived, was not attainable in the rabbit model using the Sequoia system. Compared to a human ECG, animal ECGs are often done by

immobilizing the rabbit on a self-retaining board with electrodes embedded in the board. Although this system is meant to restrain the animal to prevent the animal's motion from disrupting the signal, it decreases the versatility of attaining an ECG. It is particularly difficult for a rabbit as its narrowed-shape chest limits upper limb extension and therefore prevents the animal from being placed at an anatomical position feasible for immobilization on the electrode board. In retrospect, such measurement may be attained if the rabbit is in a prone position and echocardiography is attained from underneath as the rabbit lies with sufficient contact with the electrodes on the board. Another method of retrospectively examine HR would have been to quantify HR from the M-mode images attained. It would be necessary to reanalyze each image to obtain an accurate HR. As data was accumulated over several years, re-analysis may be attainable, but not without challenge.

As the two models developed over a couple of years, it has been difficult to maintain the same breeding pair of animals. Although the supplier and breed remains the same, the neonatal rabbits used were from different does between model A and model B. The necessity to replace the doe that birthed the animals for model A was mainly due to old-age. Subsequently, animals for model B were, though still of the New Zealand white rabbit breed, from a different doe. It is likely that genetic variances may add to the differences between sham groups. In fact, significant body weight differences are noticeable between the two groups of shams despite being at the same age when weighted and receiving the

surgery. Differences in body weight would have also impacted the animals' response to anesthesia. Furthermore, the differences in body weight also impacts the differing HW:BW ratios. Of note, in model A, due to the high shunt closure rates at 14-days old during the first echocardiographic assessment, several of the animals originally receiving shunt surgery were deemed unsuccessful and added towards the sham group. Shunting during the interim between the surgery until the first echocardiography may have caused pathological cardiac hypertrophy despite closure of the shunt. However, pathological changes were not detected when evaluating the differences between sham animals and shunt animals of model A. Due to the higher shunt patency rate in model B, all sham animals received sham surgery and none of the animals had prior shunt surgery. Therefore, as animals from model A were later deemed as shams due to the loss of a patent shunt, the higher HW:BW ratio in model A sham group compared to that in model B may be the result of minor cardiac hypertrophy developing prior to the closure of the shunt. Although within model A, the cardiological differences between sham and shunt groups remain statistically significant and attributable to the presence or absence of a patent shunt, the shams may no longer be true shams as compared to model B's sham group.

In retrospect, normative or historical data, as mentioned, or additional quantifiable parameters would have added to establish congruency between the two sham groups. For instance, normal LVPW data, unavailable for model A,

would have helped verify that the hypertrophy is consistent with that of volume-overload hypertrophy. Model A's claim of volume-overload hypertrophy is therefore highly dependent enlarged intraventricular dimensions during diastole. Wall thickening, the hallmark of pressure-induced hypertrophy, is lacking in model A to rule out coincidental findings of pressure-induced hypertrophy. LVPW would be additional information that would aid to characterize this model as a volume-overload hypertrophy. Hence, as sham groups are characteristically different between the two models, it is difficult to assess their relative differences. In so, these limitations restrict the extent of this report to be able to only demonstrate and report the evolution of developing a neonatal model of volume-overload cardiac hypertrophy rather than to comparatively establish the models.

3.6 References

1. Magovern JA, Pae WE, Jr., Miller CA, Waldhausen JA. The immature and the mature myocardium. Responses to multidose crystalloid cardioplegia. *J Thorac Cardiovasc Surg* 1988;95:618-24.
2. Parrish MD, Payne A, Fixler DE. Global myocardial ischemia in the newborn, juvenile, and adult isolated isovolumic rabbit heart. Age-related differences in systolic function, diastolic stiffness, coronary resistance, myocardial oxygen consumption, and extracellular pH. *Circ Res* 1987;61:609-15.
3. Pridjian AK, Levitsky S, Krukenkamp I, Silverman NA, Feinberg H. Developmental changes in reperfusion injury. A comparison of intracellular cation accumulation in the newborn, neonatal, and adult heart. *J Thorac Cardiovasc Surg* 1987;93:428-33.
4. Watanabe H, Yokosawa T, Eguchi S, Imai S. Functional and metabolic protection of the neonatal myocardium from ischemia. Insufficient protection by cardioplegia. *J Thorac Cardiovasc Surg* 1989;97:50-8.
5. Wittnich C, Peniston C, Ianuzzo D, Abel JG, Salerno TA. Relative vulnerability of neonatal and adult hearts to ischemic injury. *Circulation* 1987;76:V156-60.

6. Wittnich C, Belanger MP, Bandali KS. Newborn hearts are at greater 'metabolic risk' during global ischemia--advantages of continuous coronary washout. *Can J Cardiol* 2007;23:195-200.
7. Hammel JM, Caldarone CA, Van Natta TL, et al. Myocardial apoptosis after cardioplegic arrest in the neonatal lamb. *J Thorac Cardiovasc Surg* 2003;125:1268-75.
8. Baker JE, Boerboom LE, Olinger GN. Age-related changes in the ability of hypothermia and cardioplegia to protect ischemic rabbit myocardium. *J Thorac Cardiovasc Surg* 1988;96:717-24.
9. Bove EL, Stammers AH. Recovery of left ventricular function after hypothermic global ischemia. Age-related differences in the isolated working rabbit heart. *J Thorac Cardiovasc Surg* 1986;91:115-22.
10. Bove EL, Stammers AH, Gallagher KP. Protection of the neonatal myocardium during hypothermic ischemia. Effect of cardioplegia on left ventricular function in the rabbit. *J Thorac Cardiovasc Surg* 1987;94:115-23.
11. Coles JG, Watanabe T, Wilson GJ, et al. Age-related differences in the response to myocardial ischemic stress. *J Thorac Cardiovasc Surg* 1987;94:526-34.

12. Jarmakani JM, Nakazawa M, Nagatomo T, Langer GA. Effect of hypoxia on mechanical function in the neonatal mammalian heart. *Am J Physiol* 1978;235:H469-74.
13. Nishioka K, Jarmakani JM. Effect of ischemia on mechanical function and high-energy phosphates in rabbit myocardium. *Am J Physiol* 1982;242:H1077-83.
14. Yano Y, Braimbridge MV, Hearse DJ. Protection of the pediatric myocardium. Differential susceptibility to ischemic injury of the neonatal rat heart. *J Thorac Cardiovasc Surg* 1987;94:887-96.
15. Minich LL, Atz AM, Colan SD, et al. Partial and transitional atrioventricular septal defect outcomes. *Ann Thorac Surg* 2010;89:530-6.
16. Welke KF, Diggs BS, Karamlou T, Ungerleider RM. Comparison of pediatric cardiac surgical mortality rates from national administrative data to contemporary clinical standards. *Ann Thorac Surg* 2009;87:216-22; discussion 222-3.
17. Allen BS. Pediatric myocardial protection: where do we stand? *J Thorac Cardiovasc Surg* 2004;128:11-3.
18. Allen BS, Barth MJ, Ilbawi MN. Pediatric myocardial protection: an overview. *Semin Thorac Cardiovasc Surg* 2001;13:56-72.

19. Bolling K, Kronon M, Allen BS, et al. Myocardial protection in normal and hypoxically stressed neonatal hearts: the superiority of hypocalcemic versus normocalcemic blood cardioplegia. *J Thorac Cardiovasc Surg* 1996;112:1193-200; discussion 1200-1.
20. Bolling K, Kronon M, Allen BS, Wang T, Ramon S, Feinberg H. Myocardial protection in normal and hypoxically stressed neonatal hearts: the superiority of blood versus crystalloid cardioplegia. *J Thorac Cardiovasc Surg* 1997;113:994-1003; discussion 1003-5.
21. Kantor PF, Robertson MA, Coe JY, Lopaschuk GD. Volume overload hypertrophy of the newborn heart slows the maturation of enzymes involved in the regulation of fatty acid metabolism. *J Am Coll Cardiol* 1999;33:1724-34.
22. Allah EA, Tellez JO, Yanni J, et al. Changes in the expression of ion channels, connexins and Ca²⁺-handling proteins in the sino-atrial node during postnatal development. *Exp Physiol* 2011;96:426-38.
23. Leung CH, Wang L, Fu YY, Yuen W, Caldarone CA. Transient mitochondrial permeability transition pore opening after neonatal cardioplegic arrest. *J Thorac Cardiovasc Surg* 2011;141:975-82.

24. Liu H, Cala PM, Anderson SE. Na/H exchange inhibition protects newborn heart from ischemia/reperfusion injury by limiting Na⁺-dependent Ca²⁺ overload. *J Cardiovasc Pharmacol* 2010;55:227-33.
25. Kitahori K, He H, Kawata M, et al. Development of left ventricular diastolic dysfunction with preservation of ejection fraction during progression of infant right ventricular hypertrophy. *Circ Heart Fail* 2009;2:599-607.
26. Ito M, Jaswal JS, Lam VH, et al. High levels of fatty acids increase contractile function of neonatal rabbit hearts during reperfusion following ischemia. *Am J Physiol Heart Circ Physiol* 2010;298:H1426-37.
27. Itoi T, Huang L, Lopaschuk GD. Glucose use in neonatal rabbit hearts reperfused after global ischemia. *Am J Physiol* 1993;265:H427-33.
28. Itoi T, Lopaschuk GD. The contribution of glycolysis, glucose oxidation, lactate oxidation, and fatty acid oxidation to ATP production in isolated biventricular working hearts from 2-week-old rabbits. *Pediatr Res* 1993;34:735-41.
29. Lopaschuk GD, Spafford MA. Energy substrate utilization by isolated working hearts from newborn rabbits. *Am J Physiol* 1990;258:H1274-80.
30. Garcia R, Diebold S. Simple, rapid, and effective method of producing aortocaval shunts in the rat. *Cardiovasc Res* 1990;24:430-2.

31. Mangion JR. Right ventricular imaging by two-dimensional and three-dimensional echocardiography. *Curr Opin Cardiol* 2010;25:423-9.
32. Mertens LL, Friedberg MK. Imaging the right ventricle--current state of the art. *Nat Rev Cardiol* 2010;7:551-63.
33. von Bardeleben RS, Kuhl HP, Mohr-Kahaly S, Franke A. Second-generation real-time three-dimensional echocardiography. Finally on its way into clinical cardiology? *Z Kardiol* 2004;93 Suppl 4:IV56-64.
34. Correale M, Ieva R, Manuppelli V, Rinaldi A, Di Biase M. Controversies in echocardiography: 2D vs 3D vs 4D. *Minerva Cardioangiol* 2009;57:443-55.
35. Gad SC. *Animal models in toxicology*. 2nd ed. Boca Raton: CRC/Taylor & Francis, 2007.

3.7 Figures

Figure 3-1: Schematic of the aorto-caval shunt models A and B. Model A: (1) The descending aorta (dAo) was punctured with a 20 gauge needle, penetrating the inferior vena cava (IVC). (2) The clamp was placed. (3) The needle was withdrawn and drop of cyanoacrylate glue was used to seal the aorta puncture point. (4) The clamp was removed. Model B: (5) The needle is withdrawn from just the IVC, but through the same hole in the aorta, two other holes are made before the hole is sealed as with (3) and (4).

Fig 3-1

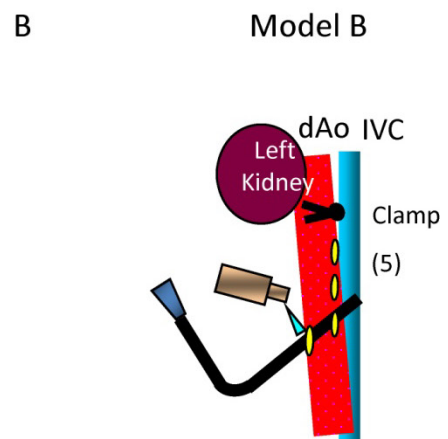
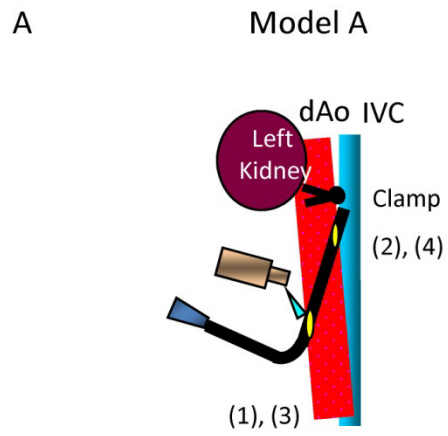


Figure 3-2: Timeline of events. Echocardiography (Echo)

Fig 3-2

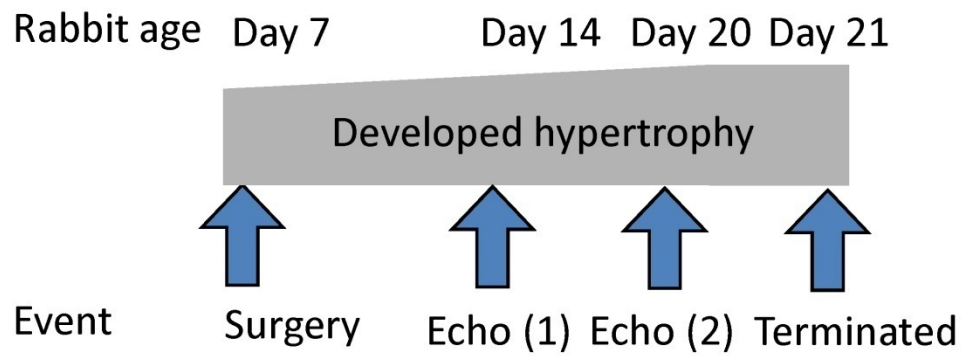
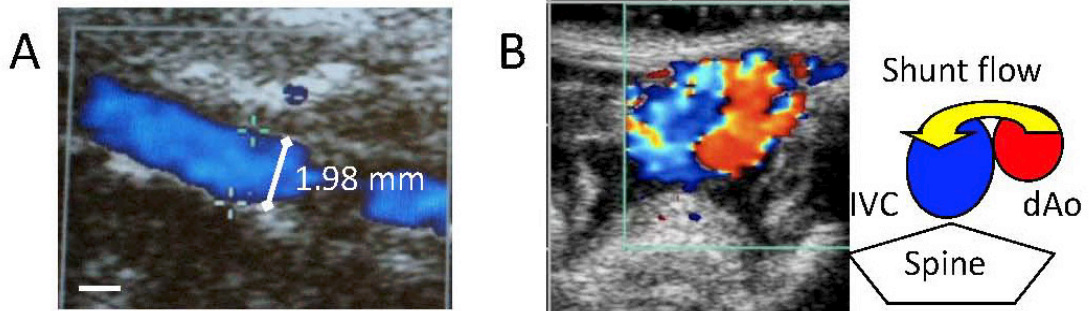
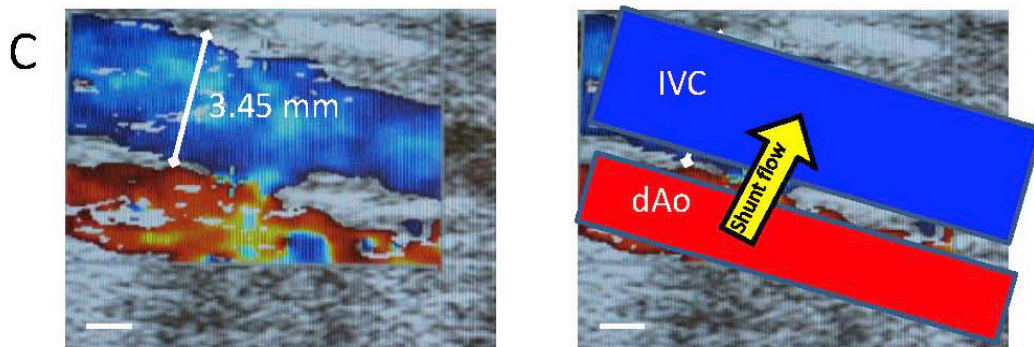


Figure 3-3: Ultrasound of the aorto-caval shunt. The size of the IVC is quantified in a A) sham animal. B) When the ultrasound probe is rotated 90° the shunt the shunt can also be seen to cause turbulence in the IVC. A longitudinal view of the descending aorta (dAo) and inferior vena cava (IVC) A) in model A where a single shunt is visible between the two vessels and in B) model B in which two shunts of the three made are visible between the two vessels. To the right of the ultrasound image is a graphical representation of the IVC, dAo, shunts, and direction of flow through the shunts.

Fig 3-3



Model A



Model B

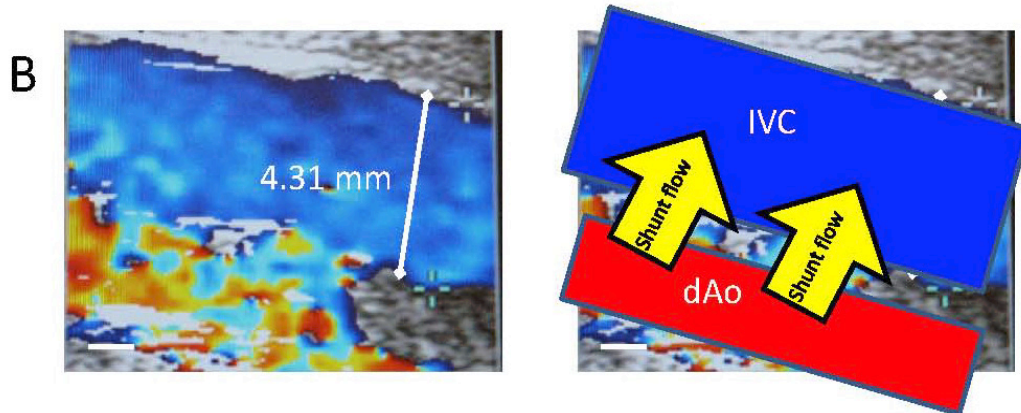
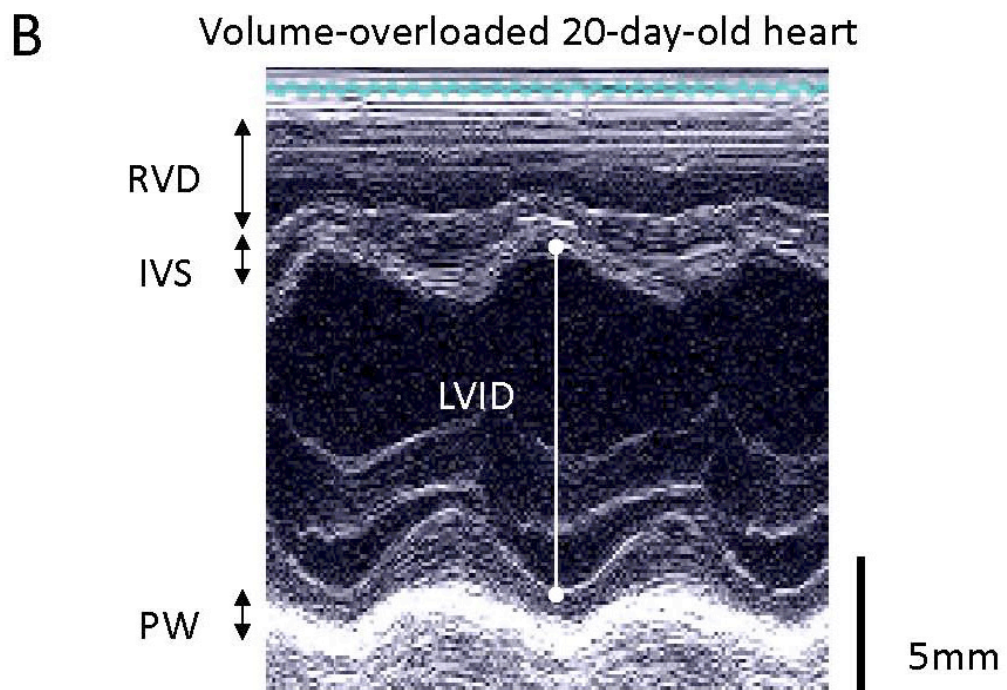
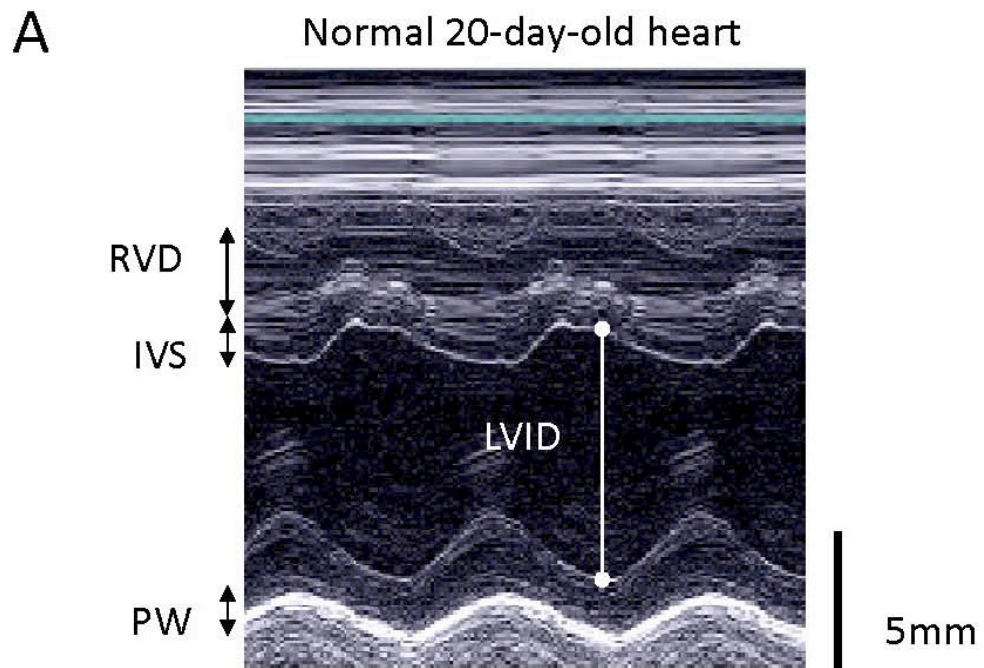


Figure 3-4: Representative M-mode images demonstrating the LVIDd of a A) normal 20-day old rabbit heart and B) that of a volume-overloaded heart are dramatically different.

Fig 3-4



3.8 Tables

Table 3-1: Success rates of aorto-caval shunt operation

	Model A		Model B	
	(single puncture)	%	(triple puncture)	%
Total number of surgeries	297		47	
Closed shunt				
Died/terminated	42	14	7	15

Table 3-2: Physical and Cardiac Parameters in 20-day-old rabbits with sham or model A (single puncture) aorto-caval shunt operation

	sham	shunt
Number of animals	12	11
IVC (mm)	2.84 ± 0.27	4.62 ± 0.53
RV Area:d (mm ²)	34.4 ± 6.8	46.9 ± 2.9 *
LVIDd (mm)	8.6 ± 0.1	9.7 ± 0.2 *
%EF	57.6 ± 1.1	60.3 ± 1.4
Body weight (g)	360 ± 18	338 ± 17
Heart weight (mg)	2060 ± 120	2390 ± 110 *
HW:BW (mg/g)	5.59 ± 0.37	6.64 ± 0.52 *

LV, left ventricle; RV, right ventricle; LVIDd, diastolic left ventricular internal diameter; %EF, ejection fraction; * indicates a significant difference (p<0.05) between sham and shunt. Values are the mean ± SEM

Table 3-3: Physical and Cardiac Parameters in 20-day-old rabbits with sham or model B (triple puncture) aorto-caval shunt operation

	Sham	Shunt
Number of animals	9	13
IVC (mm)	2.42 ± 0.15	3.38 ± 0.11*
RVIDd (mm)	3.1 ± 0.2	3.4 ± 0.1*
LVIDd (mm)	7.8 ± 0.3	8.7 ± 0.3*
LVPW (mm)	1.8 ± 0.1	1.7 ± 0.1
%EF	75.4 ± 1.1	67.4 ± 3.0*
Body Weight	422 ± 13	385 ± 28
Heart Weight (mg)	1703 ± 84	1881 ± 74
HW:BW (mg/g)	4.2 ± 0.10	4.7 ± 0.3*

IVC, inferior vena cava; RVIDd, right ventricular internal diameter during diastole in millimetre (mm); LVIDd, diastolic left ventricular internal diameter; LVPW, left ventricular posterior wall thickness; %EF, ejection fraction; HW:BW, heart weight to body weight ratio. * indicates a significant difference ($p < 0.05$) between sham and shunt. Values are the mean ± SEM

Chapter 4

Delayed Maturation of Fatty Acid β -Oxidation in Hypertrophied Neonatal Hearts Compromises Cardiac Energetics and Functional Recovery from Ischemia

**Cardiac Hypertrophy in the Newborn Delays the Maturation of Fatty Acid
β-Oxidation and Compromises Post-ischemic Functional Recovery**

Tatsujiro Oka*, Victoria H. Lam*, Liyan Zhang, Wendy Keung, Virgilio JJ. Cadete,
Victor Samokhvalov, Brandon A. Tanner, Donna L. Beker, John R Ussher, Alda
Huqi, Jagdip S. Jaswal, Ivan M. Rebeyka , Gary D. Lopaschuk

* The first authors contributed equally to this work.

Cardiovascular Research Centre, Mazankowski Alberta Heart Institute, and
Departments of Pediatrics and Surgery, University of Alberta, Edmonton, Canada

Abbreviated title: Cardiac hypertrophy compromises cardiac energetics

Contribution:

Tatsujiro Oka: Neonatal cardiac hypertrophy model surgery and
echocardiography, intellectual contribution, primary author

Victoria HM Lam: Neonatal cardiac hypertrophy model surgery and
echocardiography, bi-ventricular isolated working heart perfusions, Western
blot, data analysis, primary author

Liyan Zhang: PDH and MCD activity assays

Wendy Keung: Citrate synthase and βHAD activity assays, intellectual and
editorial contributions

Virgillio JJ Cadete: Neonatal cardiac hypertrophy model surgery, bi-ventricular
isolated working heart perfusion, intellectual contribution

Victor Samokhvalov: PPARα expression quantification

Brandon A Tanner: Western blot

Donna L Beker: Bi-ventricular isolated working heart perfusion

John R Ussher: Intellectual and editorial contribution

Alda Huqi: Western Blot

Jagdip S Jaswal: Intellectual and editorial contribution

Hypothesis:

If normal neonatal rabbit hearts undergo volume-overload hypertrophy, then its metabolism is expected to retain a fetal metabolic profile rather than mature into a FA oxidation-dependent metabolism. Increased HIF-1 α concomitant with decreased PPAR expression should contribute to retention of the fetal-like metabolic profile; and this metabolic profile would decrease the rates of ATP production causing an ATP deficiency that impedes post-ischemic functional recovery. These expected results are likely because in adult hearts, cardiac hypertrophy causes a reversion to a fetal-like metabolic profile

4.1 Introduction

One of every 100 children is born with a congenital heart defect. Cardiac hypertrophy can occur secondary to volume/pressure overload due to defects such as ventricular septal defects, atrial septal defects, or a patent ductus arteriosus representing 29, 21, and 10%, respectively, of all congenital heart diseases (1). These defects often undergo surgical repair that requires a motionless and bloodless field achieved by arresting the heart, which subjects the heart to a period of ischemia. Maturation of energy metabolism in the newborn heart is not complete until after birth. Therefore the response of the neonatal heart to ischemia may be different from the adult heart. Adding to that, hypertrophy may alter the normal course of metabolic maturation in the neonatal heart via changes in gene and protein expression. Thus, cardiac hypertrophy-related changes in cardiac energy metabolism in the neonatal heart may also impact the heart's tolerance to ischemia.

Shortly after birth, the heart rapidly develops the ability to metabolize fatty acids, while dramatically decreasing glycolytic rates (2-4). This metabolic transition occurs in many mammals including rabbits and pigs. In 1-day-old rabbit hearts, glycolysis contributes to nearly half of the total cardiac ATP production. By 7-days old, glycolysis contributes <10% of the hearts energy requirements (5,6). In contrast, in 1-day old rabbit hearts, fatty acid oxidation

provides <10% of total ATP production; by 7-day of age, it provides >50% (7,8). Decreased glycolysis following birth partly occurs by allosteric inhibition on upstream regulators due to increased fatty acid oxidation (4,6,9,10). Transcriptionally, decreased hypoxia-inducible factor-1 α (HIF-1 α) expression may also contribute to decreased glycolysis. HIF-1 α regulates expression of genes that favor anaerobic glycolysis. In normal cardiac maturation, HIF-1 α mRNA/protein levels drop (11), resulting in decreased glycolytic enzyme expression/activities (4,6,9). Simultaneously, increased acetyl-CoA from fatty acid oxidation inhibits pyruvate dehydrogenase (PDH), the first committed enzymatic step in glucose oxidation. Cardiac glucose oxidation rates remain low following birth due to low glycolysis and PDH activity (8,12,13).

In the adult heart, cardiac hypertrophy is associated with a reversion to a fetal metabolic profile (14,15) causing decreased fatty acid oxidation (16,17) and increased glycolytic rates (16,18,19). These metabolic changes correlate to altered expression/activity of key energy metabolic enzymes (20-24). While adult cardiac hypertrophy results in a fetal-like metabolic phenotype (25), the effect(s) of hypertrophy on the newborn heart, in the midst of a fetal-to-adult transition, is unclear. We previously showed that newborn cardiac hypertrophy in pig hearts delays the maturation of key fatty acid oxidation enzymes (26). However, the effects of hypertrophy on energy metabolic rates in the newborn heart has not been directly determined. Since energy substrate preference can

have profound impact on ischemic tolerance (27,28), it is important to understand the effect(s) of cardiac hypertrophy on energy substrate metabolism in the newborn heart.

To examine energy metabolism in hypertrophied newborn hearts, we developed a volume-overload hypertrophy model in newborn rabbit hearts. Our model produces bi-ventricular cardiac hypertrophy in 21-day-old rabbits, which is relevant to ventricular septal defects, atrial septal defects, and patent ductus arteriosus pathologies. Since systolic pressure in the right ventricle remains high in the perinatal period and decreases immediately after birth (13), our bi-ventricular model is particularly valid in correctly capturing the metabolic and functional changes in both ventricles that may occur during the development of hypertrophy. Using a bi-ventricular working heart preparation to measure cardiac function and metabolism, we show that the hypertrophied neonatal heart metabolism retains a fetal profile causing a severe decrease in overall cardiac energy production that compromises post-ischemic functional recovery.

4.2 Material and Methods

4.2.1 *Animals*

The University of Alberta adheres to the principles for biomedical research involving animals developed by the Council for International Organizations of Medical Sciences and complies with Canadian Council of Animal Care guidelines.

4.2.2 *Induction of volume-overload via production of an aorto-caval fistula in newborn rabbits*

7-day-old New Zealand White rabbits of either sex (90-200 g) were anesthetized with isoflurane (2%) via inhalation. Animals were placed on their right lateral, and a left flank retroperitoneal incision was made to expose the descending aorta and the inferior vena cava. The descending aorta was clamped with a micro-clamp 5 mm inferior to the renal blood vessels to cease downstream blood flow. The aorta was punctured with a 20 G needle tip below the micro-clamp and a through-and-through fistula generated across the aorta to reach and puncture the adjacent wall of inferior vena cava. The needle was then removed and a drop of cyanoacrylic glue was placed on the puncture site and allowed to dry, following which the micro-clamp was removed to restore blood flow. Following the surgical procedure animals were monitored for recovery hourly over a 24-hour period to assure there were no complications.

This produced a volume-overload leading to the development of bi-ventricular cardiac hypertrophy in 21-day old rabbits (table 4-1). All animal procedures were approved by the University of Alberta Health Sciences Animal Welfare and Policy Committee, which adheres to the principles for biomedical research involving animals developed by the Council for International Organizations of Medical Sciences and complies with Canadian Council of Animal Care guidelines.

4.2.3 Echocardiography

Transthoracic echocardiographic assessment was performed using a two dimensional / Doppler echocardiographic system (Acuson Sequoia 512 machine (Siemens medical solutions, Mountain View, CA) using a 15-Mhz probe on the day of 7 and 13 days after surgery. The left ventricular end-diastolic and systolic dimension, the right ventricular end-diastolic and systolic area, heart rate and shunt flow between the abdominal artery and vena cava were recorded. If the fistula between abdominal aorta and inferior vena cava persisted and cardiac hypertrophy developed, the animals were included in the hypertrophy group. All animals in which the shunt between the aorta and the inferior vena cava closed before day 7 after the surgery were defined as sham-operated animals.

4.2.4 Isolated Bi-ventricular Heart Perfusion Model

At 14 days post-surgery, 21-day-old rabbits were anesthetized with Na-pentobarbital (60 mg/kg body weight) and hearts were excised and cannulated and retrogradely (Langendorff) perfused with Krebs-Henseleit buffer (37⁰C, pH=7.4, gassed with 95 % O₂/5 % CO₂ mixture). During 15 minutes of retrograde perfusion, the superior vena cava (SVC), the left atria, and pulmonary artery were cannulated and the inferior vena cava was ligated. Left ventricular work was initiated at the end of the 15-minute retrograde perfusion by opening flow into the left atria and aortic afterload line and terminating the retrograde perfusion. Right ventricular load was added by opening SVC flow thereby producing a bi-ventricular working heart preparation. Hearts were subjected to 30 min left ventricular perfusion (clamped SVC cannula) followed by 30 min bi-ventricular perfusion (opened SVC cannula). Hearts were perfused with modified Krebs-Henseleit solution containing 2.5 mM Ca²⁺, 5.5mM glucose, 0.8 mM palmitate prebound to 3% bovine serum albumin, 0.5 mM lactate and 100 μU/mL insulin. The preload for the left and right atria were set at 12.5 mmHg and 7.5 mmHg, respectively. Left ventricular afterload was set at 35 mmHg and a right ventricular afterload at 4.5 mmHg. At the end of the perfusion protocols, left ventricular, right ventricular and septal tissues were separated and rapidly frozen in liquid N₂ and stored at -80⁰C for further biochemical analysis. Glycolysis, glucose oxidation, lactate oxidation, and palmitate

oxidation were measured as described (29,30). In some studies, hearts were subjected an initial 15 min left ventricular working heart, followed by 20 minutes of bi-ventricular perfusion, a 25 min period of isothermal, no-flow global ischemia followed by 30 minutes of bi-ventricular aerobic reperfusion.

ATP production rates from glycolysis, glucose oxidation, lactate oxidation and palmitate oxidation were calculated, using the values of 2 mol ATP per mol of glucose passing through glycolysis, 31 mol ATP per mol of glucose oxidized, 18 mol ATP per mol of lactate oxidized and 105 mol ATP per of palmitate oxidized. These numbers are derived based on using P/O ratios of 2.5 for NADH and 1.5 for FADH₂ (31,32).

4.2.5 Mechanical Measurements in Isolated Rabbit Bi-ventricular Working Heart

Heart rate and systolic and diastolic pressures were measured using a Gould P21 pressure transducer attached to the aortic and pulmonary outflow line. Left and right cardiac output and aortic and pulmonary flow were measured by using ultrasonic flow probes (Transonic T206) placed in the left atrial and SVC inflow line and aortic and pulmonary out flow line, respectively. Left and right ventricular work were calculated as (cardiac output • peak systolic pressure • 10⁻²) and served as continuous index of left and right ventricular mechanical function.

4.2.6 Tissue Sample Preparation for Immunoblot Analysis

Each sample of frozen ventricular tissue (~20 mg) was combined with homogenization buffer containing 50 mM Tris•HCl (pH 8 at 4°C), 1 mM EDTA, 10% (wt/vol) glycerol, 0.02% (wt/vol) Brij-35, 1 mM dithiothrietol (DTT), and protease and phosphatase inhibitors (Sigma) and homogenized for 30s using a Polytron Homogenizer. Samples were centrifuged at 800 g for 10 min. The supernatant was boiled in protein sample buffer solution (62.5 mM Tris-HCl, 6 M Urea, 10% glycerol, 2 % sodium dodecyl sulfate, 0.003 % bromophenol blue, and 5 % 2-betamercaptoethanol) for 5 min. Protein concentration of homogenates was determined using the Bradford protein assay kit (Bio-Rad) and normalized to 1 µg/µL to load onto the SDS-PAGE gel and ran as Dyck et al., 2000 (33).

4.2.7 Immunoblot Analysis

Denatured samples of heart tissue homogenate were subjected to SDS-PAGE and transferred to nitrocellulose membranes as previously described (33). Membranes were blocked in 10% fat-free milk for 1 hour and probed with anti-AMP-activated protein kinase (AMPK) (Cell Signaling Technologies), anti-phospho-threonine 172 AMPK (Cell Signaling Technologies), anti-MCD (University of Alberta), anti-HIF-1 α (Cell Signaling Technologies) (using nuclear fraction of cell homogenates), anti- α tubulin (Cell Signaling Technologies) (using nuclear fraction of cell homogenates), or anti-actin (Santa Cruz Biotechnology)

antibodies in 5% fatty acid-free BSA/PBS. After thoroughly washing, membranes are incubated in a peroxidase-conjugated goat anti-rabbit or anti-mouse secondary antibody in 5% fat-free milk/PBS. After further washing, antibodies were visualized using the enhanced chemiluminescence Western blot detection kit (Perkin Elmer) and quantified using Quantity One (4.4.0) software (Bio-Rad Laboratories).

4.2.8 Pyruvate Dehydrogenase Activity Assay

Pyruvate Dehydrogenase (PDH) activity was measured as in Constantin-Teodosiu et al., (34). For active PDH activity, frozen heart tissue (~20 mg) was homogenized in 1:10 buffer containing 200 mM sucrose, 50 mM KCl, 5 mM MgCl₂, 5 mM EGTA, 50 mM Tris HCl, 50 mM NaF, 5 mM dichloroacetate, and 0.1% Triton X-100 (pH 7.8). For total PDH activity, homogenization was done with 1:10 tissue to buffer, which contained 200 mM sucrose, 50 mM KCl, 5 mM MgCl₂, 5 mM EGTA, 50 mM Tris HCl, 10 mM glucose, and 4.5 U/mL hexokinase. *Active PDH activity.* Warm (37⁰C) assay buffer (150 mM Tris-HCl, 0.75 mM EDTA, 1.5 mM MgCl₂, 0.75 mM NAD⁺, 0.75 mM CoA grade 1, and 1.5 mM thiamine pyrophosphate) was added to samples. The reaction was initiated by the addition of pyruvate to a final concentration of 1 mM and incubated at room temperature (RT) for 10 min. The reaction was stopped with perchloric acid (80 mM). The acid was neutralized with KHCO₃. The samples were then centrifuged

at 10000 x g for 3 min. *Total PDH activity.* Samples were incubated with a pre-incubation reagent (200 mM sucrose, 50 mM KCl, 5 mM EGTA, 50 mM Tris-HCl, 24 mM CaCl₂, 600 mM MgCl₂, 125 mM dichloroacetic acid, 10 mM glucose, 18 U/mL hexokinase) added at a 1:20 dilution for 15 min at 37⁰C. Warm (37⁰C) assay buffer was added. The reaction was initiated with the addition of pyruvate/triton to a final concentration of 1 mM/0.003% tritonX-100 and incubated for 10 min at RT. Reactions were terminated with perchloric acid and centrifuged as above. Resulting supernatants from active and total samples were used to determine acetyl-CoA content as acetyl-CoA was converted to [¹⁴C]-citrate. [¹⁴C]-oxaloacetate was formed by reacting 50 mM (pH 7.8) HEPES, 2 mM EDTA, 2 mM α-ketoglutarate, 1.25 mM aspartate, and a total of 0.045 μCi of [¹⁴C]-aspartate catalyzed by glutamic-oxaloacetic transaminase (16.8 kU - 42kU) for 20 min at RT. To 200 μL aliquot of each sample was added dithiothreitol (0.83 mM) and CuSO₄-potassium acetate mixture (0.03 mM and 12 mM) and incubated for 30 min at RT. EDTA (4.6 mM, pH 7.4) was then added and mixture incubated for 5 min at RT. 20 μL of the [¹⁴C]-oxaloacetate reaction mixture was also added along with a total of 0.5 U of citrate synthase. The mixture was allowed to react for 20 min at RT and terminated with perchloric acid (60 mM) and cooled on ice for 10 min. The reaction was then neutralized with KOH (67 mM). EDTA (5.3 mM) was also added. The unreacted [¹⁴C]-oxaloacetate was removed by the reverse reaction whereby the oxaloacetate is reconverted to

aspartate with the addition of a glutamate/glutamic-oxalacetic transaminase solution (6.6 mM glutamate; 0.8-2.0 U glutamic-oxalacetic transaminase) incubated for 20 min at RT. 1 mL of Dowex slurry (1:2 w/v) was added to each reaction mixture and mixture vortexed every 10 min for 40 min. The mixture is then centrifuged at 3500 rpm for 5 min to separate out the Dowex beads. The supernatant was retrieved and added to scintillation fluid and radioactivity quantified via a scintillation counter. The amount of acetyl CoA was determined by comparison of acetyl CoA standard curves run in parallel in each experiment.

4.2.9 Citrate Synthase Activity Assay

According to the method from Seres (35), tissue homogenates were prepared as for immunoblot assays. The sample was added to the reaction mixture containing 92 mM Tris-HCl, 0.91 mM EDTA, and 0.91 mM MgCl₂, pH 8.2), 0.3 mM acetyl-CoA, and 0.1 mM dithionitrobenzoic acid (DNTB) to a final volume of 0.2 mL. Activity was spectrophotometrically quantified as the reaction occurred. Reaction was initiated with oxaloacetic acid (0.5 mM). Absorbance in the reaction is detected at 412 nm for 2 min. Citrate synthase activity was calculated with the following formula:

$$\text{activity} = \frac{[(\Delta A_{412}/\text{min}) \times 0.2 \text{ mL}]}{[13.6 \epsilon_{\text{for DNTB}} \times 0.552 \text{ path-length of 96 well plate used for measurement} \times \text{tissue wt}]}$$

4.2.10 β -hydroxyacyl CoA Dehydrogenase Activity Assay (β -HAD)

Tissue homogenates were prepared as described above (Tissue Sample Preparation for Immunoblot Analysis). The sample was added to a reaction mixture containing: 50 mM imidazole (pH 7.4) and 0.15 mM NADH. Acetoacetyl-CoA (0.1 mM) was added to initiate the reaction. The final volume of the reaction was 0.2 ml. Activity was quantified spectrophotometrically as the reaction occurred by measuring absorbance at 340 nm for 5 min.. β -HAD activity was calculated with the following formula.

$$\beta\text{-HAD activity} = \frac{[(\Delta A_{340}/\text{min}) \times 0.2 \text{ mL}]}{[6.22 \epsilon_{\text{for NADH}} \times 0.552 \text{ path-length of 96 well plate used for measurement} \times \text{tissue wt}]}$$

4.2.11 Malonyl-CoA Dehydrogenase (MCD) Activity Assay

Ventricular tissue samples were homogenized in a buffer containing 75 mM KCl, 20 mM sucrose, 10 mM HEPES, 1 mM EGTA, 20 mM NaF, and 5 mM protease inhibitor (Sigma). According to the established method found in (36,37), to initiate the MCD assay, heart homogenates were incubated in a 210- μ l assay buffer (0.1 M Tris, pH 8, 0.5 mM dithiothreitol, 1 mM malonyl-CoA) for 10 min at 37°C, in the presence or absence of NaF (50 mM) and NaPP_i (5 mM). Adding 40 μ L of perchloric acid (0.5 mM) stopped the reaction. The acid was neutralized

with 10 μl of 2.2 M KHCO_3 (pH 10) and centrifuged at 10,000 g for 5 min to remove precipitated proteins. Incubating heart sample with malonyl-CoA converted malonyl-CoA to acetyl-CoA, which was then combined with [^{14}C]oxaloacetate (0.17 $\mu\text{Ci/ml}$) to produce [^{14}C]citrate. *N*-ethylmaleimide was present in all reactions to remove excess CoA remaining in order to prevent the conversion of non-malonyl-CoA derived acetyl-CoA by other enzymes in the non-purified MCD assay sample in the latter stages of the reaction. Sodium glutamate (6.8 mM) and aspartate aminotransferase (0.533 $\mu\text{U}/\mu\text{l}$) were added to remove unreacted [^{14}C]oxaloacetate during a 20-min incubation at room temperature. A negative control of water, to which all reagents were added accordingly, was performed alongside samples to account for possible inhibitory effects of *N*-ethylmaleimide and alkylating effects of GOT. However, any inhibitory effect on MCD itself is not expected as *N*-ethylmaleimide was not added during the reaction whereby MCD converts malonyl-CoA to acetyl-CoA. The solution was then stirred in a 1:2 suspension of Dowex AG 50W-8X resin (100-200 mesh) and centrifuged at 400 g for 10 min. The supernatant fraction was counted for [^{14}C]citrate. An acetyl-CoA concentration standard curve was run with each experiment and used to quantify sample acetyl-CoA.

4.2.12 Peroxisome Proliferator Activated Receptor (PPAR) α mRNA Expression

PPAR α mRNA expression was determined by reverse transcription of total RNA followed by quantitative PCR (qPCR) analysis. Total RNA was extracted from 1-day old whole hearts and left and right ventricles of 7-, 21-day-old heart and 21-day old hypertrophied hearts, as above using TRI reagent (Qiagen) according to manufacturer's kit. RNA is then quantified spectrophotometrically at 260 nm. Reverse transcription was then performed on 1 μ g of total RNA using 100 IU of reverse transcriptase (Qiagen) with 100 ng of random hexanucleotide primers in a 20 μ L reaction volume. PCR cycles were then followed with 1 μ L of the reverse transcription product with 0.4 mmol/L of each dNTP, 25 pmol specific primers, PCR buffer, and 1.25 U of Taq DNA polymerase. 2 min of denaturation at 94 $^{\circ}$ C was followed by amplification of 30 cycles: 30s at 94 $^{\circ}$ C, 35 s at 53 $^{\circ}$ C, and 40 s at 72 $^{\circ}$ C, then maintained for 7 min at 72 $^{\circ}$ C. qPCR was then performed using 12.5 μ L Sybr-Green Jump Start Taq Readymix (Sigma-Aldrich), 5 μ L oligonucleotides, 7.5 μ L of cDNA. qPCR of ribosomal rRNA 18s was performed as the endogenous control.

Rabbit PPAR α primer sequence:

	Sequence	Start bp	Stop bp	Tm
Forward Primer	TGCACCCACTGTTGCAAGA	212	230	58
Reverse Primer	CGGCCTACCATCTCAGGAAA	274	255	59
Probe	ATCTACAGAGACATGTACTGAT	232	253	69

Eukaryotic 18S rRNA Endogenous Control (FAM[™] Dye/MGB Probe, Non-Primer Limited; Part Number: 4352930E)

4.2.13 Statistical analysis

Data are expressed as means \pm SEM. The significance of differences for multiple comparisons was estimated by one-way analysis of variance (ANOVA). If significant, selected data sets were compared by Bonferroni's multiple comparison test. The significance of differences between two groups was estimated by unpaired, two-tailed Student's *t*-test where appropriate. Differences were considered significant at $P < 0.05$.

4.3 Results

4.3.1 Establishing and Assessing Cardiac Hypertrophy by Echocardiography

An abdominal aorto-caval fistula was produced in 7-day old rabbits to increase volume returned to the right ventricle (RV). Aorto-caval fistula patency, thus volume-overload, was confirmed in 14-day and 20-day old rabbits utilizing color

Doppler echocardiography to demonstrate turbulent blood flow (fig 4-1A), which was absent in sham-operated animals. In volume-overload animals, at 20-days old, a significant increase in left-ventricular internal diameter (by 13%) (fig 4-1B-D, table 4-1), left ventricular (LV) volume (by 33%) (table 4-1), and end diastolic of RV area (by 36%) (table 4-1) was seen. Body weight was similar between the volume-overload and sham groups (table 4-1). In contrast, heart weight and heart weight to body weight ratio were significantly increased by 16% and 19%, respectively, in volume-overload compared to the sham group (table 4-1), indicative of cardiac hypertrophy. Heart rate, LV ejection fraction, and RV % fractional area change in 20-day old rabbits were similar between the two groups.

4.3.2 Aerobic Cardiac Function in Isolated Bi-ventricular Working Hearts

Control hearts were isolated from animals at 21 days of age subjected to sham surgery while hypertrophied hearts were isolated from animals in which volume-overload was produced secondary to a patent aorto-caval fistula. With aerobic bi-ventricular perfusion, cardiac hypertrophy did not alter cardiac function, consistent with *in vivo* echocardiographic studies. No differences in LV work (fig 4-2A) or cardiac output (fig 4-2C) were observed between hypertrophied and control hearts, regardless of left-ventricular or bi-ventricular mode. A trend toward a decrease in LV work and cardiac output was observed

in control hearts perfused in bi-ventricular mode; but the difference did not reach significance. LV stroke volume was also similar between hypertrophied and control groups when perfused in the left-ventricular mode. However, hypertrophied hearts had significantly increased LV stroke volume when perfused in the bi-ventricular mode (fig 4-2B). Heart rates were similar between hypertrophied and control hearts during left-ventricular perfusions, but were significantly increased in control hearts during the bi-ventricular perfusion (fig 4-2D).

4.3.3 Impact of Ischemia on Hypertrophied Hearts

Although cardiac hypertrophy did not affect bi-ventricular aerobic function compared to controls when perfused in 0.8 mM palmitate (fig 4-2 and table 4-2), it did affect functional recovery from ischemia (table 4-2). While the hypertrophied heart adapted to the volume-overload during aerobic perfusion, the ischemic-reperfusion recovery was only 52% of the function seen in the control hearts. The hearts exposed to 25 minutes of ischemia were given 1.2 mM palmitate rather than 0.8 mM as hypertrophied hearts cannot recover with 0.8 mM palmitate (data not shown). Therefore, 1.2 mM palmitate increases substrate availability in order to resolve differences in recovery between control and hypertrophied hearts. This significant functional decrease during recovery was accompanied by a corresponding increase in the AMP:ATP ratio in the RV.

Though an increase in AMP:ATP is present in the LV, the difference was insignificant. However, the significantly higher AMP:ATP in the RV compared to controls (table 4-2) may underlie the impaired ischemia-reperfusion recovery.

4.3.4 Metabolism in Aerobically-Perfused Hypertrophied Newborn Rabbit Hearts

Cardiac hypertrophy markedly decreased palmitate oxidation rates (by 57%) compared to controls during left-ventricular and bi-ventricular perfusions (Fig 4-3A). In contrast, glycolytic rates increased 246% and 172% during left-ventricular and bi-ventricular perfusion, respectively, in hypertrophied hearts (fig 4-3B). Glucose oxidation rates were similar in the two groups during left-ventricular perfusion. Hypertrophied hearts failed to increase glucose oxidation, whereas these rates increased to 148% in control hearts during bi-ventricular perfusion (fig 4-3D). Lactate oxidation rates were similar between the two groups (fig 4-3C). Active PDH activity was not diminished in LV or RV of hypertrophied versus controls (table 4-3). In fact, total PDH activity is increased in the RV.

In control hearts, fatty acid oxidation was the predominant ATP source providing >75% of ATP production in left-ventricular and bi-ventricular modes (table 4-3). Glucose oxidation was the second most important source of ATP (11-16%). Consistent with hypertrophy-altered energy metabolism, ATP production rates decreased by 42% and 38% in hypertrophied hearts compared to controls during

left-ventricular and bi-ventricular perfusion, respectively (fig 4-3E). Contribution of glycolysis increased in hypertrophied hearts to 27.2% (table 4-3). Overall decrease in ATP production, mainly due to the dramatic drop in fatty acid oxidation, suggests that volume-overload cardiac hypertrophy compromises cardiac energetics. In support of this, acetyl-CoA content, which increased with age in control hearts (1-21 days of age), did not increase in hypertrophied hearts (fig 4-3F).

4.3.5 Control of Fatty Acid Oxidation in Hypertrophied Hearts

Decreased malonyl CoA levels following birth is an important factor in normal maturational increase in cardiac fatty acid oxidation rates (38). Consistent with our previous reports (13,26), there was maturational increase in MCD activity during the neonatal period (1-21 days of age) in the LV and RV (fig 4-4A). This increase is attenuated in hypertrophied RVs. Interestingly, MCD activity and expression did not differ between hypertrophied and control LVs (fig 4-4B). While MCD expression did not differ between hypertrophied and control RV (fig 4-4B), MCD activity is significantly lower in hypertrophied RVs compared to control (fig 4-4A). Whereas malonyl-CoA content decreased in the LV of control hearts, this decrease was attenuated in hypertrophied hearts (fig 4-4C). Malonyl-CoA content decreased in the RV of hypertrophied and control hearts over the neonatal period (1-21 days of age). AMP-activated protein kinase

(AMPK) phosphorylation levels were assayed in RV and LV (fig 4-5). While no significant differences between the hypertrophied and control LVs and RVs were detected, RV phospho-AMPK increased in control hearts (21-day-old) versus 7-day old hearts ($p < 0.05$).

In the post-natal period, increased mitochondrial biogenesis increases mitochondrial TCA cycle activity and fatty acid oxidation capacity. Increases in TCA cycle enzyme activity, citrate synthase, occurred between 7- and 21-days of age in control hearts (table 4-4). Similarly, β -hydroxyacyl CoA dehydrogenase (β -HAD), a fatty acid β -oxidative enzyme, also increased in its activity. Hypertrophy reverted citrate synthase and β -HAD activities to that in 7-day-old control hearts (table 4-4).

4.3.6 HIF-1 α Expression and PPAR α Expression and Activity in Control and Hypertrophied Hearts

As with the normal maturational decrease in glycolysis (6), HIF-1 α expression decreased in neonatal RV, but not in the LV between 1- and 21-days of age (fig 4-6A). In hypertrophied hearts, HIF-1 α expression in RVs regressed to levels seen in the immediate newborn period (1- and 7-days). HIF-1 α expression did not change in the hypertrophied LV. In contrast, peroxisome proliferator activated receptor (PPAR) α , which activates the transcription of enzymes involved in fatty acid oxidation, showed reciprocal expression to that of HIF-1 α .

LV PPAR α mRNA expression remains low from 1 to 7-days old (1.6 ± 0.2 AU and 4.4 ± 1.2 AU, respectively) (fig 4-6B). By 21-days old, LV PPAR α mRNA expression increases dramatically to 26.6 ± 6.0 AU ($p < 0.05$ compared to 1- and 7-day-old hearts). Hypertrophy is associated with relatively lower PPAR α mRNA expression levels in the LV (1.9 ± 0.5 AU), levels seen in 1- and 7-day-old hearts. Hypertrophy has similar effect on RV PPAR α mRNA expression. RV PPAR α mRNA expression remains low in 1-, 7-, and to 21-days of age (1.6 ± 0.2 , 1.4 ± 0.2 , and 1.0 ± 0.1 AU, respectively). Hypertrophy is associated with significantly lower PPAR α mRNA levels in the RV at 0.4 ± 0.17 AU ($p < 0.05$).

4.4 Discussion

Newborn animal models of cardiac hypertrophy are limited and the direct effects of hypertrophy on energy substrate preference in the newborn heart are poorly understood. Cardiac hypertrophy is an ongoing remodeling process. This study has found a number of novel observations at a single time point of this remodeling process in the neonatal heart via the bi-ventricular working heart preparation. First, mild neonatal cardiac hypertrophy is not associated with significant alterations in aerobic cardiac function (*in vivo* or *in vitro*). However, the hypertrophy sufficiently altered neonatal cardiac energy metabolism including a substantial decrease in cardiac fatty acid oxidation rates and increase in glycolytic rates. Meanwhile, glucose and lactate oxidation do not increase in

response to the decreased fatty acid oxidation. This inflexibility in carbohydrate oxidation in response to lower fatty acid metabolic rates results in a decrease in overall ATP production in hypertrophied neonatal hearts. Cardiac energetics are compromised and therefore compromises recovery from ischemia.

Although the hypertrophied hearts produce ATP at a lower rate while performing the same amount of work as a normal heart, these changes are not compatible with ischemia-reperfusion. When subjected to ischemia, hypertrophied cardiac functional recovery is significantly hampered. Though some literature indicate that neonatal hearts are more ischemic tolerant (39), we demonstrate that the hypertrophied neonatal heart has less ischemic tolerance due to a metabolic deficit. This energy deficit is more apparent in the RV where the AMP:ATP is higher in hypertrophied neonatal hearts than controls. The difference illustrates the necessity of reserve energy production capacity. Hypertrophied neonatal hearts produce ATP at a lower rate than controls to perform the same amount of work, but the reserve ATP production capacity in controls enables it to better withstand ischemia and reperfusion insults. High fatty acid concentrations are cardioprotective to the ischemia-reperfused neonatal heart (40). Using 1.2 mM palmitate rather than 0.8 mM was an attempt to improve reperfusion recovery to better resolve differences between the two groups. With a defunct fatty acid oxidative pathway and undeveloped

alternative metabolic pathways, hypertrophied neonatal hearts, at 1.2 mM palmitate, still exhibited lower survival capacity. The lack of energy production reserve may be detrimental to a neonatal hypertrophied heart undergoing surgical correction of a congenital heart defect.

Cardiac fatty acid oxidation increases dramatically in the normal neonatal period (2-4). We found that hypertrophy is associated with markedly decreased fatty acid oxidation while glycolysis increased to recapitulate a fetal-like metabolic profile. In the adult heart, decreased fatty acid oxidation rates are reciprocated by increased glucose and lactate oxidation rates (27,28). In the neonatal heart, carbohydrate oxidation rates remain low until weaning (2). Hence, carbohydrate oxidation did not increase with the decreased fatty acid oxidation in hypertrophied hearts despite increased PDH expression. This lack of “metabolic flexibility” in hypertrophied neonatal hearts may compromise post-ischemic cardiac energetics, during which energy demands increase for successful recovery.

Malonyl-CoA regulates fatty acid oxidation in newborn and mature hearts. Decreased acetyl-CoA carboxylase (ACC) and high MCD expression/activity decrease malonyl-CoA levels in the immediate newborn to increase fatty acid oxidation (41). Although, ACC does participate in the final product of malonyl-CoA levels, this study focused on MCD and ACC was not examined. MCD

was chosen as prior studies demonstrated that ACC expression is not affected with maturation/age (38). To add, ACC is highly controlled by AMPK in normal cardiac maturation (41) as well as neonatal cardiac hypertrophy (26). Between 1- and 7-days of age, AMPK activity rises in the rabbit heart to phosphorylate and inhibit ACC and decrease ACC activity (41). In turn, contribution of ACC to the malonyl-CoA pool would decrease allowing for the increase in fatty acid oxidation. Although ACC activity was not further examined in these experiments, the analysis performed on AMPK is an indicator of ACC activity. The AMPK expression did not change between control and hypertrophied LV and RV and reflects on a likely lack of change to ACC activity. Therefore, focus was placed on MCD expression and activity as most responsible for malonyl-CoA level changes in the neonatal hearts.

PPAR α regulates MCD transcription (42-44). We demonstrate that with PPAR α changes, LV MCD expression also increases with age. However, though LV hypertrophy is associated with decreased PPAR α expression, MCD expression do not fall. This may be because transcriptional response to cardiac hypertrophy precedes protein level changes; in so, existing MCD must be degraded to decrease its protein levels.

On the other hand, RV MCD activity decreases with hypertrophy. Despite the decreased activity, RV malonyl-CoA levels do not change from controls.

Meanwhile, hypertrophied LV MCD activity, unchanged, is associated with a significant rise in malonyl-CoA levels compared to controls. This is further supported by the lower PPAR α mRNA levels in RV versus LV; thus, RV fatty acid oxidation pathway expression may be less. CPT-1 expression and activity were not assayed in this study. However, β -HAD, though not a rate-limiting step in FA oxidation, is a surrogate marker of FA oxidative capacity. When expressed at low levels, as indicated by a relatively lower activity in the hypertrophied LV, β -HAD may also limit the rate of FA oxidation. In contrast, its high expression and/or *in vitro* activity would not necessarily indicate an increase in FA oxidation rates, which is subject to other regulatory processes such as that of malonyl-CoA. Nonetheless, due to a lag between transcription and protein degradation, high malonyl-CoA levels may be needed to regulate continually high FA oxidation pathway in the LV. LV palmitate oxidation was low during aerobic perfusion and may be the primary contributor to total cardiac palmitate oxidation rates as rates did not change with adding RV work in bi-ventricular mode in both groups. Thus, RV palmitate oxidation occurs at a low, undetectable rate that requires little inhibitory signaling to decrease β -HAD activity. Meanwhile, hypertrophied LV's low palmitate oxidation rates primarily correlate to elevated malonyl-CoA levels.

As the heart matures, HIF-1 α expression declines, followed by a decreased dependence on glycolysis (11). Normal RVs showed this maturational decrease

in HIF-1 α expression. This decline is not replicated in the LV and so glycolytic enzymes may still be expressed early in life. The normally low glycolytic rates in the neonatal heart may result from allosteric inhibition rather than suppressed enzyme expression in the LV. In the hypertrophied LV, the elevated glycolytic rates reflect its release from inhibition from fatty acid oxidation rather than upregulated glycolytic pathway. In contrast, as with pressure-overload hypertrophy (27), hypertrophied RV HIF-1 α expression profile demonstrates the hypertrophy-recapitulated fetal profile.

MCD expression is under PPAR α regulation. Therefore, when PPAR α activity/expression decreases, so does MCD such as that found in PPAR α knock out mice (45). In contrast, when PPAR α activity is increased, as with stimulation with a PPAR α agonist, MCD mRNA expression increases (42). Now, HIF-1 α participates in a dynamic relationship with PPAR α . Intriguingly, the PPAR α gene contains a consensus motif that is under HIF-1 α transcriptional regulation (46). Upon hypoxia-induced HIF-1 α nuclear accumulation, HIF-1 α binding to the consensus sequence on the PPAR α gene is increased and PPAR α expression and binding activity is decreased. Additionally, HIF-1 α may also interrupt the interaction between PPAR α and the retinoid X receptor to prevent PPAR α -induced transcription (47). This increases lipid accumulation in cardiomyocytes and limits FA oxidation (47), an effect that may be attributed to elevated

malonyl-CoA content and decreased expression of MCD. Therefore, through its reciprocal interaction with PPAR α , HIF-1 α may influence MCD expression. Here, during normal cardiac metabolic maturation, malonyl-CoA levels decreased in the LV and the RV from 1-day to 21-days old alongside of increasing MCD expression and activity. In the LV, although HIF-1 α levels were not altered, PPAR α mRNA expression increased with normal maturation. In contrast, RV HIF-1 α levels decreased with normal aging and PPAR α mRNA expression was not altered. In the LV, MCD expression/activity may be influenced by changes in PPAR α mRNA expression alone. However, in the RV, the influence of HIF-1 α expression on the interaction of PPAR α activity may contribute to the changes in MCD expression without corresponding changes to PPAR α expression. Meanwhile, cardiac hypertrophy in the neonatal heart downregulates PPAR α mRNA expression in both the RV and LV, but its impact on MCD expression activity can only be appreciated in the RV. Although this finding is associated with an increased HIF-1 α expression relative to a control 21-day-old heart, whether HIF-1 α has a direct influence on MCD expression/activity is not defined by these experiments.

4.5 Conclusions

We demonstrate that volume-overloaded hypertrophied newborn hearts have lower fatty acid oxidation and higher glycolysis rates than controls. Increased

energy demands associated with modest elevations in cardiac work are met by a substantial increase in glucose oxidation rates only in control hearts. The hypertrophy-induced delayed metabolic maturation is detrimental to the ischemia-reperfused newborn heart, resulting in an impaired recovery of cardiac function. A diminished ability for ATP production may be detrimental to the stressed neonatal heart such as in surgical ischemia.

4.6 Limitations

Although our volume-overloaded hypertrophy model attempts to demonstrate the repercussions of uncorrected congenital heart defects at birth, our model is unable to mimic the exact clinical scenario. Children with ASDs, VSDs, and PDAs often are born with, or develop during neonatal life, a certain degree of volume-overloaded hypertrophy. Our model, however, is only instigated 7-days after birth. In the rabbit model, an array of change occurs in cardiac development within the first 7 days of life including metabolic and functional changes. Therefore, this model may not fully represent the extent of hypertrophied-related metabolic delays as opposed to a reversion of its metabolism to a more fetal-metabolic profile. On the other hand, the development of cardiac hypertrophy continues from birth throughout the neonatal period. This study captures a single critical developmental time point and also demonstrates the hypertrophy-postponed maturation of energy

metabolism. Therefore, further investigations may include similar assays at different developmental time points as the amount of hypertrophy is dependent on the quantity of stimulation as well as exposure to the stimulus.

Part of this study was to examine the impact of neonatal cardiac hypertrophy on tolerance to ischemia-reperfusion. Clinically, a neonatal heart would only be exposed to ischemia during surgery during which ischemia is induced in a controlled manner using cardioplegic solutions. In the present study, the neonatal hearts were subjected to an episode of ischemia most closely resembling that of ischemic heart disease which is a non-controlled ischemia without cardioplegic protection. However, with cardioplegia, neonatal rat hearts recover equally well compared to infant and adult rat hearts even after 40 min of ischemia (48). In neonatal rabbit hearts, cardioplegia, though found detrimental to the neonatal myocardium compared to adult hearts, produced a functional recovery of 86% after 2 hours of ischemia (49). Therefore, relative to uncontrolled ischemia, cardioplegia extends the neonatal heart's tolerance to ischemia. A controlled ischemia-reperfusion with cardioplegia would have been a closer simulation of when a neonatal heart would be exposed to ischemia, but the successful cardioprotection of the neonatal rabbit heart may decrease the sensitivity of the study to resolve functional differences between the experimental and control groups. In order to resolve differences between the two group, the hearts were exposed to a shorter period more severe ischemia to

illustrate the impact of ischemia alone on the hypertrophied hearts. To add, by decreasing the amount of time needed per heart perfused, this study was able to increase the number of animals per group to increase the precision of the results. Of interest, the isolated heart perfusions used palmitate as the sole FA substrate to evaluate fatty acid β oxidation, even though a variety of FA are metabolized in the heart. Palmitate (16:0) and oleate (18:1) are the most common fatty acids found in human circulation. Together, palmitate and oleate make up ~70% of total nonesterified FA (50,51). Several studies have evaluated the relative contributions of differing lengths of FA to FA metabolism. One such study demonstrate that short chain FA may compete for free CoA's and consequently inhibit long chain FA, oleate, oxidation leading to a decrease in the oleate's contribution to the pool of acetyl-CoA and malonyl-CoA without altering the absolute cellular amount of acetyl-CoA and malonyl-CoA (52). In contrast, oleate and palmitate are equally metabolized in the adult heart without preference for one or the other (53). In fact, though myocardial extraction of oleate may be relatively greater than that for palmitate (50), in healthy humans subjects, bodily oxidation rates of palmitate and oleate normalized to their plasma concentrations (54). Meanwhile, one study noted that at minimum of 20 minutes of hypoxia, the myocardium showed a preference for oleate oxidation relative to palmitate oxidation (53). In light of these previous studies, the present study selected palmitate as the sole long chain FA present in the

perfusate buffer for the isolated heart perfusions. This choice was so that competition between FAs would not interfere with nor convolute metabolic quantification; this is particularly important in a cardiac hypertrophy model in which FA metabolism was expected to change. However, exploring the impact of hypertrophy on oleate oxidation would be of interest in future studies as hypertrophy may represent a state of relative tissue hypoxia.

Another drawback to this study is that CPT-1 expression was not quantified. Multiple attempts were made to quantify changes to CPT-1 isoform expression via western blotting using rabbit heart tissues. Unfortunately, detecting the protein with the current commercially available L- and M-CPT-1 antibodies has been unsuccessful. Therefore, in order to overcome this obstacle, PPAR α expression was measured as it is a major regulator of expression of proteins involved in FA metabolism. As PPAR α expression decreases in hypertrophied hearts, it acts as a surrogate of decrease pan-expression of proteins involved in FA metabolism. Therefore, it is reasonable to infer that CD36, FATP1 and even CPT-1 itself are downregulated in these hearts. This would be in line with the observation that FA oxidation is lower in the hypertrophied hearts. Indeed, we did observe a decrease in the activity of β HAD, another FA oxidation related protein that is regulated by PPAR α . Thus, we have reason to believe that the decrease in fatty acid oxidation is a consequent of a general decrease in the expression of fatty acid oxidation related proteins, including CPT-1, CD36 and

FATP. However, assessing the expression and activities of these proteins would have been ideal and might be further considered in the future.

MCD, AMPK, and HIF-1 α expressions were evaluated in this study to highlight the key regulators of metabolism. Unfortunately, a major drawback encountered in these Western blots is the lack of appropriate loading controls. In these studies, actin was used; however, as actin content may also change with heart maturation of physiological hypertrophy as well as pathological hypertrophy, it is not an ideal loading control as demonstrated in the immunoblots (fig 4-4 and 4-5). In retrospect, an alternative loading control would be the ponceau-stained blots. Future comparative studies which cross age groups should consider this method as an alternative. As for HIF-1 α , a change in loading control was needed because HIF-1 α was not detected via immunoblots using whole cell lysate. As a result, nuclear fractionation concentrated nuclear contents sufficiently to detect HIF-1 α via immunoblotting. However, to our surprise, several nuclear proteins, such as laminin, TATA-binding protein, or histone, were not well detected in the immunoblots. This may be due to the antibodies that were used, which were raised in rabbits and were immunized against proteins or epitopes from rat or mice. Therefore, α -tubulin was used as a marker as the loading control. Although this protein is more commonly used as a cytoplasmic loading protein, as the nuclear fraction protocol was a nuclear fraction enrichment protocol, it is not unexpected to detect a cytoplasmic protein. In contrast, β -actin was difficult to

detect in these nuclear enriched fractions. Therefore, α -tubulin was used as the loading control against which HIF-1 α was compared.

Lastly, this study has largely focused on FA metabolism because of the dependence of the neonatal heart on FA oxidation and its dramatically altered rates associated with cardiac hypertrophy. Additionally, previous studies demonstrated the efficacy of FA supplementation in improving post-ischemic functional recovery. Rates of glycolysis increased dramatically with hypertrophy as well. Meanwhile, the mechanics of glucose metabolism has not been studied and merits further investigations in future studies to dissect.

4.7 References

1. Mangones T, Manhas A, Visintainer P, Hunter-Grant C, Brumberg HL. Prevalence of congenital cardiovascular malformations varies by race and ethnicity. *Int J Cardiol* 2009.
2. Girard J, Ferre P, Pegorier JP, Duee PH. Adaptations of glucose and fatty acid metabolism during perinatal period and suckling-weaning transition. *Physiol Rev* 1992;72:507-62.
3. Lopaschuk GD, Collins-Nakai RL, Itoi T. Developmental changes in energy substrate use by the heart. *Cardiovasc Res* 1992;26:1172-80.
4. Lopaschuk GD, Spafford MA. Energy substrate utilization by isolated working hearts from newborn rabbits. *Am J Physiol* 1990;258:H1274-80.
5. Julia P, Kofsky ER, Buckberg GD, Young HH, Bugyi HI. Studies of myocardial protection in the immature heart. III. Models of ischemic and hypoxic/ischemic injury in the immature puppy heart. *J Thorac Cardiovasc Surg* 1991;101:14-22.
6. Lopaschuk GD, Spafford MA, Marsh DR. Glycolysis is predominant source of myocardial ATP production immediately after birth. *Am J Physiol* 1991;261:H1698-705.

7. Itoi T, Huang L, Lopaschuk GD. Glucose use in neonatal rabbit hearts reperfused after global ischemia. *Am J Physiol* 1993;265:H427-33.
8. Makinde AO, Kantor PF, Lopaschuk GD. Maturation of fatty acid and carbohydrate metabolism in the newborn heart. *Mol Cell Biochem* 1998;188:49-56.
9. Bristow J, Bier DM, Lange LG. Regulation of adult and fetal myocardial phosphofructokinase. Relief of cooperativity and competition between fructose 2,6-bisphosphate, ATP, and citrate. *J Biol Chem* 1987;262:2171-5.
10. Thrasher JR, Cooper MD, Dunaway GA. Developmental changes in heart and muscle phosphofructokinase isozymes. *J Biol Chem* 1981;256:7844-8.
11. Nau PN, Van Natta T, Ralphe JC, et al. Metabolic adaptation of the fetal and postnatal ovine heart: regulatory role of hypoxia-inducible factors and nuclear respiratory factor-1. *Pediatr Res* 2002;52:269-78.
12. Itoi T, Lopaschuk GD. Calcium improves mechanical function and carbohydrate metabolism following ischemia in isolated Bi-ventricular working hearts from immature rabbits. *J Mol Cell Cardiol* 1996;28:1501-14.

13. Onay-Besikci A, Campbell FM, Hopkins TA, Dyck JR, Lopaschuk GD. Relative importance of malonyl CoA and carnitine in maturation of fatty acid oxidation in newborn rabbit heart. *Am J Physiol Heart Circ Physiol* 2003;284:H283-9.
14. Depre C, Shipley GL, Chen W, et al. Unloaded heart in vivo replicates fetal gene expression of cardiac hypertrophy. *Nat Med* 1998;4:1269-75.
15. Razeghi P, Young ME, Alcorn JL, Moravec CS, Frazier OH, Taegtmeyer H. Metabolic gene expression in fetal and failing human heart. *Circulation* 2001;104:2923-31.
16. Allard MF, Schonekess BO, Henning SL, English DR, Lopaschuk GD. Contribution of oxidative metabolism and glycolysis to ATP production in hypertrophied hearts. *Am J Physiol* 1994;267:H742-50.
17. El Alaoui-Talibi Z, Guendouz A, Moravec M, Moravec J. Control of oxidative metabolism in volume-overloaded rat hearts: effect of propionyl-L-carnitine. *Am J Physiol* 1997;272:H1615-24.
18. Schonekess BO, Allard MF, Henning SL, Wambolt RB, Lopaschuk GD. Contribution of glycogen and exogenous glucose to glucose metabolism during ischemia in the hypertrophied rat heart. *Circ Res* 1997;81:540-9.

19. Wambolt RB, Henning SL, English DR, Dyachkova Y, Lopaschuk GD, Allard MF. Glucose utilization and glycogen turnover are accelerated in hypertrophied rat hearts during severe low-flow ischemia. *J Mol Cell Cardiol* 1999;31:493-502.
20. van der Vusse GJ, van Bilsen M, Glatz JF. Cardiac fatty acid uptake and transport in health and disease. *Cardiovasc Res* 2000;45:279-93.
21. van Bilsen M, Smeets PJ, Gilde AJ, van der Vusse GJ. Metabolic remodelling of the failing heart: the cardiac burn-out syndrome? *Cardiovasc Res* 2004;61:218-26.
22. Kelly DP. PPARs of the heart: three is a crowd. *Circ Res* 2003;92:482-4.
23. Finck BN, Lehman JJ, Barger PM, Kelly DP. Regulatory networks controlling mitochondrial energy production in the developing, hypertrophied, and diabetic heart. *Cold Spring Harb Symp Quant Biol* 2002;67:371-82.
24. Barger PM, Kelly DP. Fatty acid utilization in the hypertrophied and failing heart: molecular regulatory mechanisms. *Am J Med Sci* 1999;318:36-42.
25. Sambandam N, Lopaschuk GD, Brownsey RW, Allard MF. Energy metabolism in the hypertrophied heart. *Heart Fail Rev* 2002;7:161-73.

26. Kantor PF, Robertson MA, Coe JY, Lopaschuk GD. Volume overload hypertrophy of the newborn heart slows the maturation of enzymes involved in the regulation of fatty acid metabolism. *J Am Coll Cardiol* 1999;33:1724-34.
27. Choi YH, Cowan DB, Nathan M, et al. Myocardial hypertrophy overrides the angiogenic response to hypoxia. *PLoS One* 2008;3:e4042.
28. Stanley WC, Recchia FA, Lopaschuk GD. Myocardial substrate metabolism in the normal and failing heart. *Physiol Rev* 2005;85:1093-129.
29. Barr RL, Lopaschuk GD. Direct measurement of energy metabolism in the isolated working rat heart. *J Pharmacol Toxicol Methods* 1997;38:11-7.
30. Lopaschuk GD, Wambolt RB, Barr RL. An imbalance between glycolysis and glucose oxidation is a possible explanation for the detrimental effects of high levels of fatty acids during aerobic reperfusion of ischemic hearts. *J Pharmacol Exp Ther* 1993;264:135-44.
31. Salway JG. *Metabolism at a glance*. 3rd ed. Malden, Mass.: Blackwell Pub., 2004.
32. Hinkle PC. P/O ratios of mitochondrial oxidative phosphorylation. *Biochim Biophys Acta* 2005;1706:1-11.

33. Dyck JR, Berthiaume LG, Thomas PD, et al. Characterization of rat liver malonyl-CoA decarboxylase and the study of its role in regulating fatty acid metabolism. *Biochem J* 2000;350 Pt 2:599-608.
34. Constantin-Teodosiu D, Cederblad G, Hultman E. A sensitive radioisotopic assay of pyruvate dehydrogenase complex in human muscle tissue. *Anal Biochem* 1991;198:347-51.
35. Srere P. Citrate synthase. *Methods Enzymol* 1969:3-5.
36. Sambandam N, Steinmetz M, Chu A, Altarejos JY, Dyck JR, Lopaschuk GD. Malonyl-CoA decarboxylase (MCD) is differentially regulated in subcellular compartments by 5'AMP-activated protein kinase (AMPK). Studies using H9c2 cells overexpressing MCD and AMPK by adenoviral gene transfer technique. *Eur J Biochem* 2004;271:2831-40.
37. Dyck JR, Barr AJ, Barr RL, Kolattukudy PE, Lopaschuk GD. Characterization of cardiac malonyl-CoA decarboxylase and its putative role in regulating fatty acid oxidation. *Am J Physiol* 1998;275:H2122-9.
38. Lopaschuk GD, Witters LA, Itoi T, Barr R, Barr A. Acetyl-CoA carboxylase involvement in the rapid maturation of fatty acid oxidation in the newborn rabbit heart. *J Biol Chem* 1994;269:25871-8.

39. Wittnich C. Age-related differences in myocardial metabolism affects response to ischemia. Age in heart tolerance to ischemia. *Am J Cardiovasc Pathol* 1992;4:175-80.
40. Ito M, Jaswal JS, Lam VH, et al. High levels of fatty acids increase contractile function of neonatal rabbit hearts during reperfusion following ischemia. *Am J Physiol Heart Circ Physiol* 2010;298:H1426-37.
41. Makinde AO, Gamble J, Lopaschuk GD. Upregulation of 5'-AMP-activated protein kinase is responsible for the increase in myocardial fatty acid oxidation rates following birth in the newborn rabbit. *Circ Res* 1997;80:482-9.
42. Lee GY, Kim NH, Zhao ZS, Cha BS, Kim YS. Peroxisomal-proliferator-activated receptor alpha activates transcription of the rat hepatic malonyl-CoA decarboxylase gene: a key regulation of malonyl-CoA level. *Biochem J* 2004;378:983-90.
43. Lehman JJ, Kelly DP. Transcriptional activation of energy metabolic switches in the developing and hypertrophied heart. *Clin Exp Pharmacol Physiol* 2002;29:339-45.

44. Rimbaud S, Sanchez H, Garnier A, et al. Stimulus specific changes of energy metabolism in hypertrophied heart. *J Mol Cell Cardiol* 2009;46:952-9.
45. Campbell FM, Kozak R, Wagner A, et al. A role for peroxisome proliferator-activated receptor alpha (PPARalpha) in the control of cardiac malonyl-CoA levels: reduced fatty acid oxidation rates and increased glucose oxidation rates in the hearts of mice lacking PPARalpha are associated with higher concentrations of malonyl-CoA and reduced expression of malonyl-CoA decarboxylase. *J Biol Chem* 2002;277:4098-103.
46. Narravula S, Colgan SP. Hypoxia-inducible factor 1-mediated inhibition of peroxisome proliferator-activated receptor alpha expression during hypoxia. *J Immunol* 2001;166:7543-8.
47. Belanger AJ, Luo Z, Vincent KA, et al. Hypoxia-inducible factor 1 mediates hypoxia-induced cardiomyocyte lipid accumulation by reducing the DNA binding activity of peroxisome proliferator-activated receptor alpha/retinoid X receptor. *Biochem Biophys Res Commun* 2007;364:567-72.

48. Yano Y, Braimbridge MV, Hearse DJ. Protection of the pediatric myocardium. Differential susceptibility to ischemic injury of the neonatal rat heart. *J Thorac Cardiovasc Surg* 1987;94:887-96.
49. Baker JE, Boerboom LE, Olinger GN. Age-related changes in the ability of hypothermia and cardioplegia to protect ischemic rabbit myocardium. *J Thorac Cardiovasc Surg* 1988;96:717-24.
50. Rothlin ME, Bing RJ. Extraction and release of individual free fatty acids by the heart and fat depots. *J Clin Invest* 1961;40:1380-6.
51. Kaijser L, Ericsson M, Walldius G. Myocardial turnover of plasma free fatty acids during angina pectoris induced by atrial pacing. *Clin Physiol* 1988;8:267-86.
52. Bian F, Kasumov T, Jobbins KA, et al. Competition between acetate and oleate for the formation of malonyl-CoA and mitochondrial acetyl-CoA in the perfused rat heart. *J Mol Cell Cardiol* 2006;41:868-75.
53. DeGrado TR, Kitapci MT, Wang S, Ying J, Lopaschuk GD. Validation of 18F-fluoro-4-thia-palmitate as a PET probe for myocardial fatty acid oxidation: effects of hypoxia and composition of exogenous fatty acids. *J Nucl Med* 2006;47:173-81.

54. Wisneski JA, Gertz EW, Neese RA, Mayr M. Myocardial metabolism of free fatty acids. Studies with ¹⁴C-labeled substrates in humans. *J Clin Invest* 1987;79:359-66.

4.8 Figures

Figure 4-1: Aorto-caval Fistula Validation and Volume-Overload Cardiac Hypertrophy Assessment. A) Schematic view of aorto-caval fistula, descending aorta (dAo), inferior vena cava (IVC) and Color-flow Doppler echocardiography confirms the fistula flow. Transthoracic echocardiography of B) normal left ventricles from sham-operated animals and C) volume-overloaded animals with a dilated left ventricle. D) Correlation between body weight and diastolic left ventricular internal diameter (LVIDd) measured by M-mode. Right ventricular diameter (RVD), interventricular septal thickness (IVS), posterior wall (PW), left ventricular internal diameter (LVID)

Fig 4-1

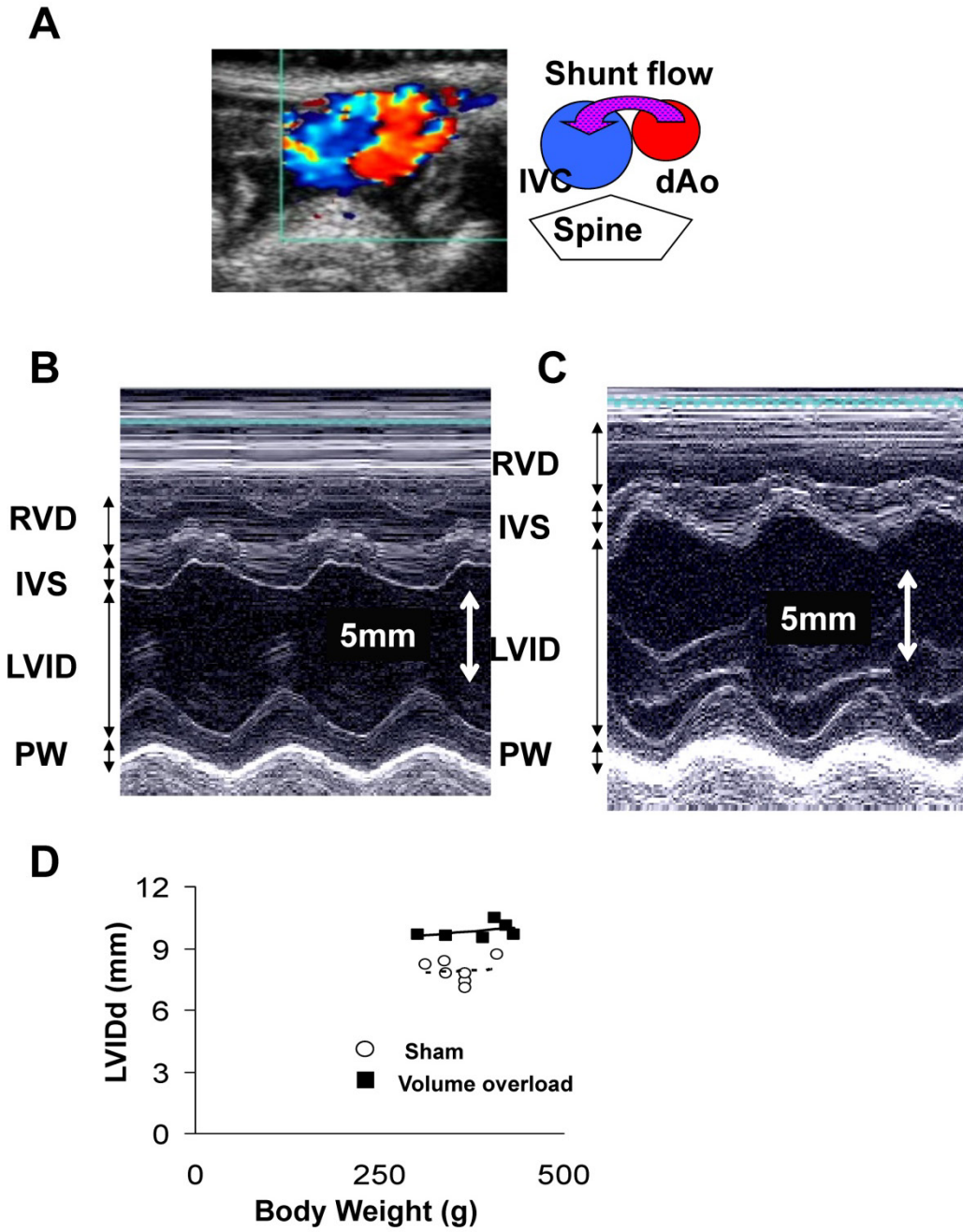


Figure 4-2: Comparison of 21-day-old control and hypertrophy LV cardiac functions during 30 min aerobic left ventricular followed by 30 min bi-ventricular perfusion. A) LV work (n=32 and n=16 for control and hypertrophy, respectively). B) LV cardiac output. C) Heart rate. D) LV stroke volume. The values represent means \pm SEM. Differences were determined using a one-way ANOVA with Bonferroni post hoc test. * $P < 0.05$, significantly different from left ventricular perfusion. † $P < 0.05$, significantly different from corresponding 21-day-old control group.

Fig 4-2

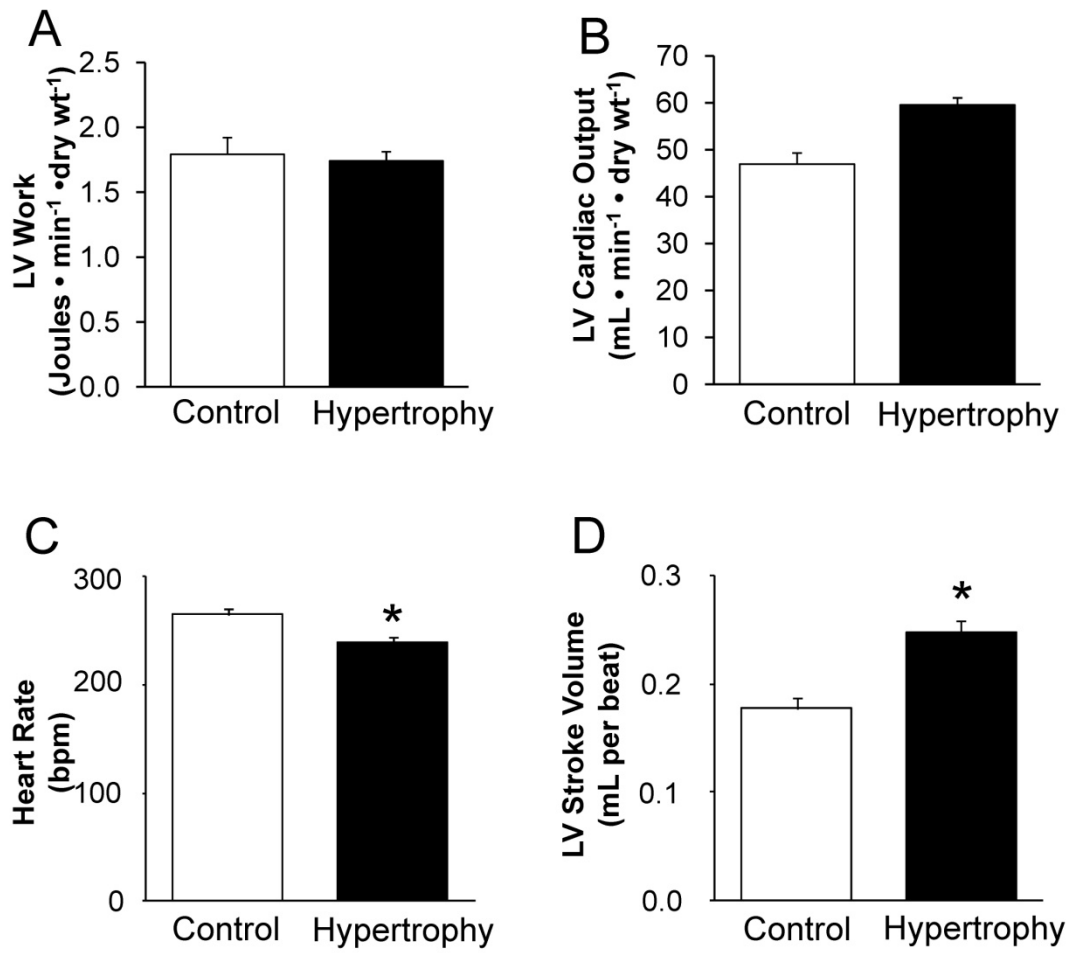


Figure 4-3: Metabolic Effects of Neonatal Volume-Overload Cardiac Hypertrophy. Steady state rates of A) palmitate oxidation (n=7 and n=5 for control and hypertrophy hearts, respectively), B) glycolysis (n=35 and n=6, respectively), C) lactate oxidation (n=14 and n=9, respectively), and D) glucose oxidation (n=22 and n=4, respectively). (□-rates obtained in LV mode. ■- rates obtained in bi-ventricular mode). E) Calculated steady state ATP production rate. F) Acetyl-CoA content LV and RV of in 1-, 7-, and 21-day-old controls versus 21-day-old hypertrophied hearts. Values represent means ± SEM. Differences were determined using one-way ANOVA with Bonferroni post hoc test. * $P < 0.05$, significantly different from the value in left ventricular perfusion in 21-day-old controls. † $P = 0.058$ vs the value in left ventricular perfusion in hypertrophy hearts.

Fig 4-3

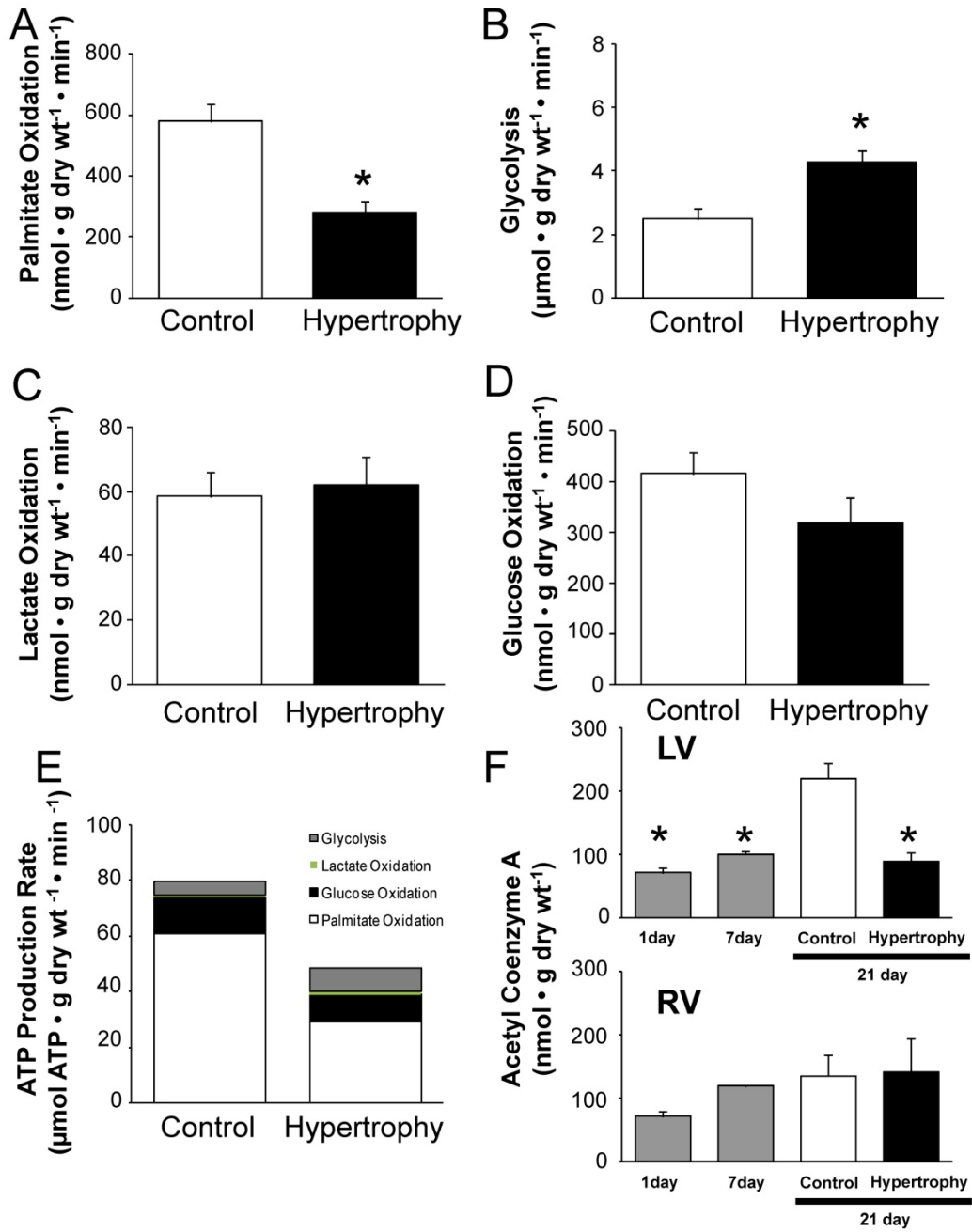


Figure 4-4: MCD Expression and Activity and Malonyl-CoA Levels in Control and Hypertrophied Neonatal Hearts. A) MCD activity and B) expression, and C) malonyl-CoA content in LV and RV from 1-, 7-, and 21-day-old control versus 21-day-old hypertrophied hearts. Values are means \pm SEM (n=5). Differences were determined using one-way ANOVA with Bonferroni post hoc test. * $P < 0.05$ Significantly different from 21-day-old controls.

Fig 4-4

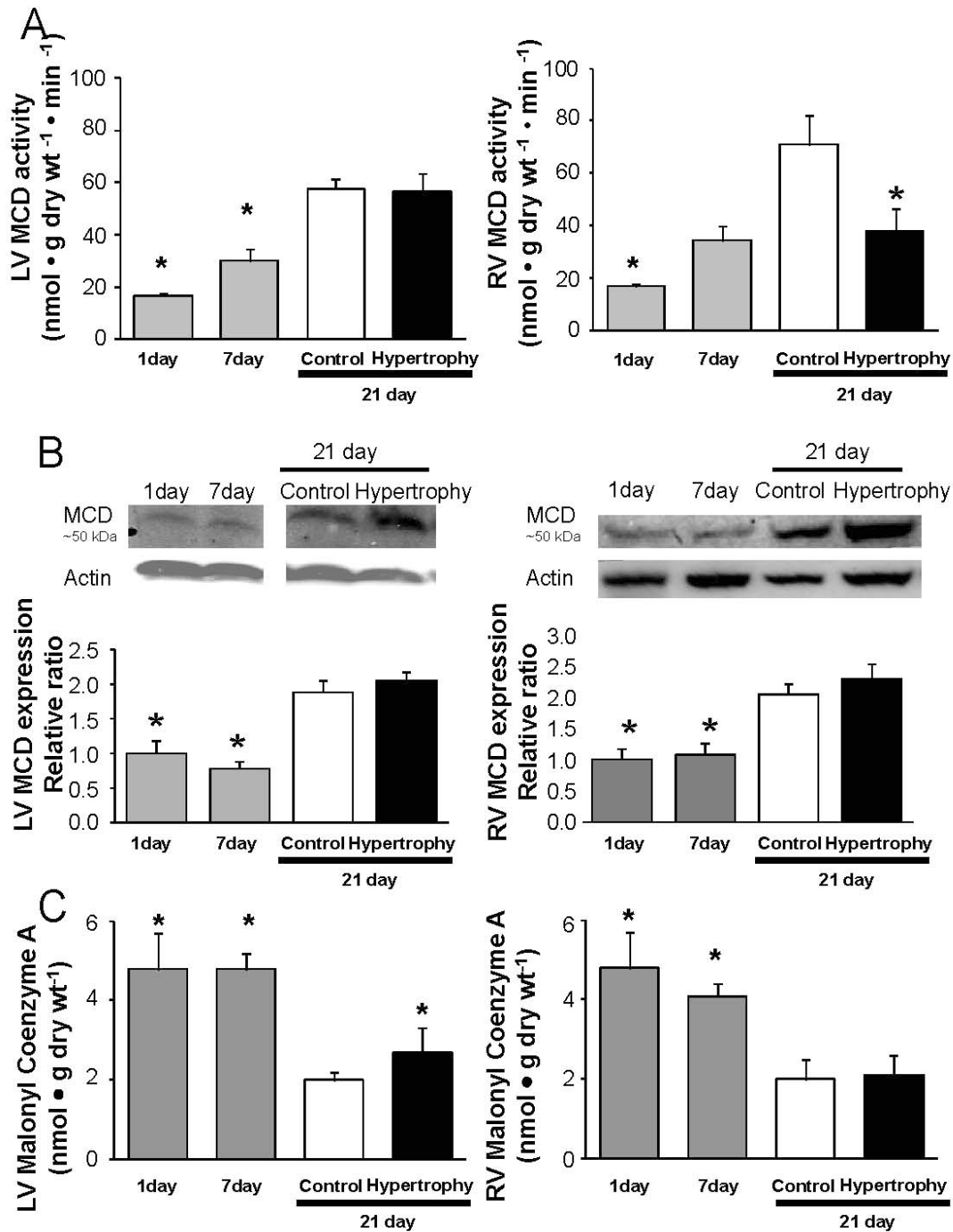


Figure 4-5: AMPK expression and phosphorylation do not change in hypertrophied hearts compared to controls in left (LV) or right (RV) ventricles. This finding is represented by relative ratios of phosphorylated AMPK (P-AMPK) to total AMPK (T-AMPK) and their corresponding representative western immunoblots above. * $P < 0.05$ Significantly different from 21-day-old controls.

Fig 4-5

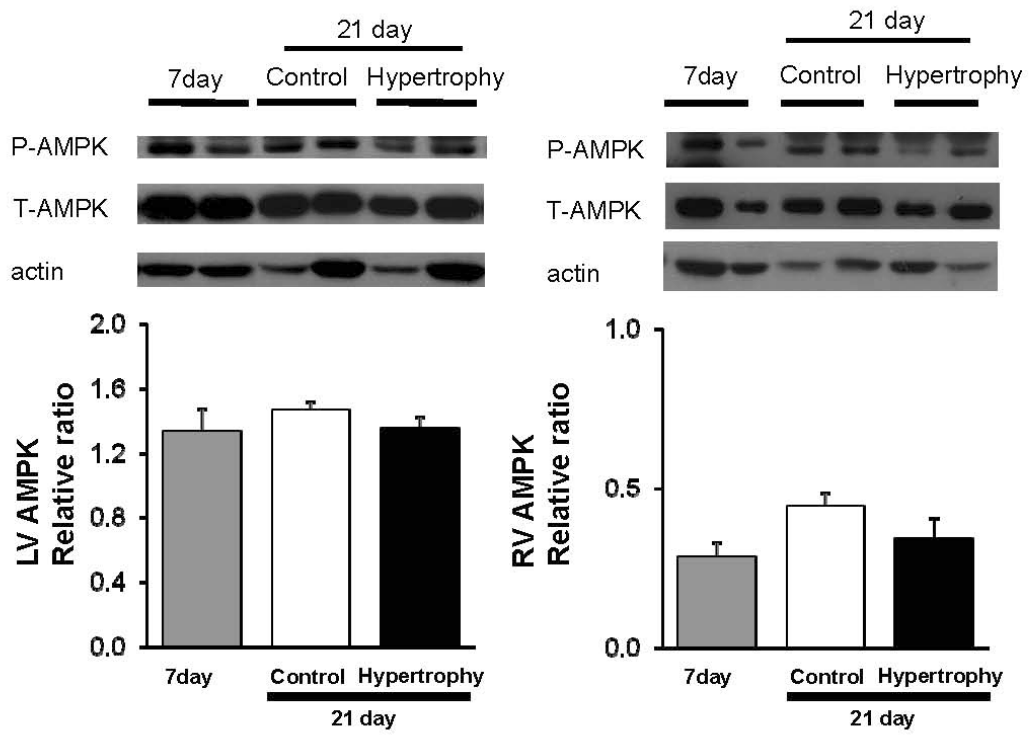


Figure 4-6: Cardiac HIF- α expression and PPAR α activity change with age and hypertrophy. A) HIF-1 α expression decreases with age. In hypertrophied hearts, LV and RV tissues express HIF-1 α levels at that of 1-day-old hearts. B) PPAR α mRNA expression measured relatively to 18s protein in arbitrary units (AU) increases with age (day 1 and 21) in RV and LV while hypertrophy decreases expression significantly. * $P < 0.05$ as compared with 21-day-old controls.

Fig 4-6

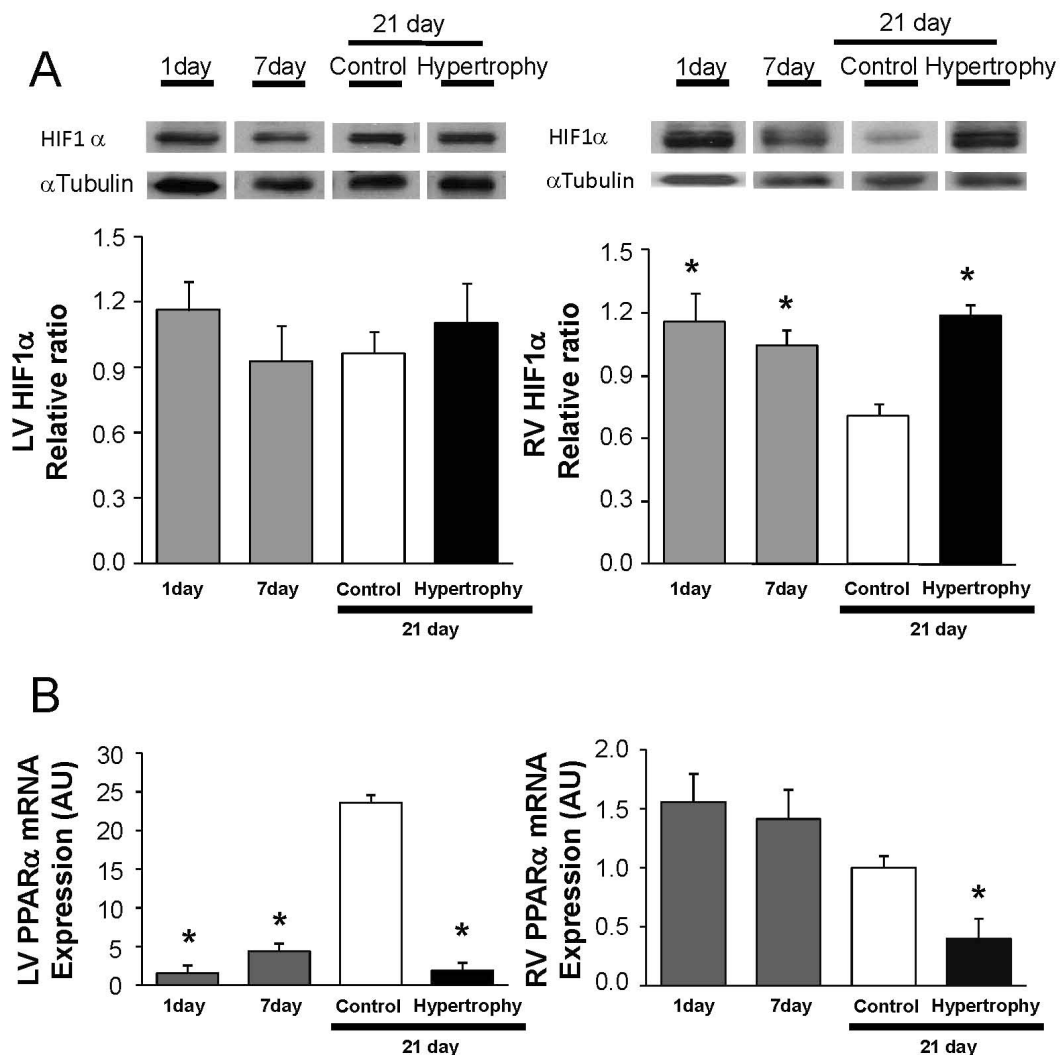
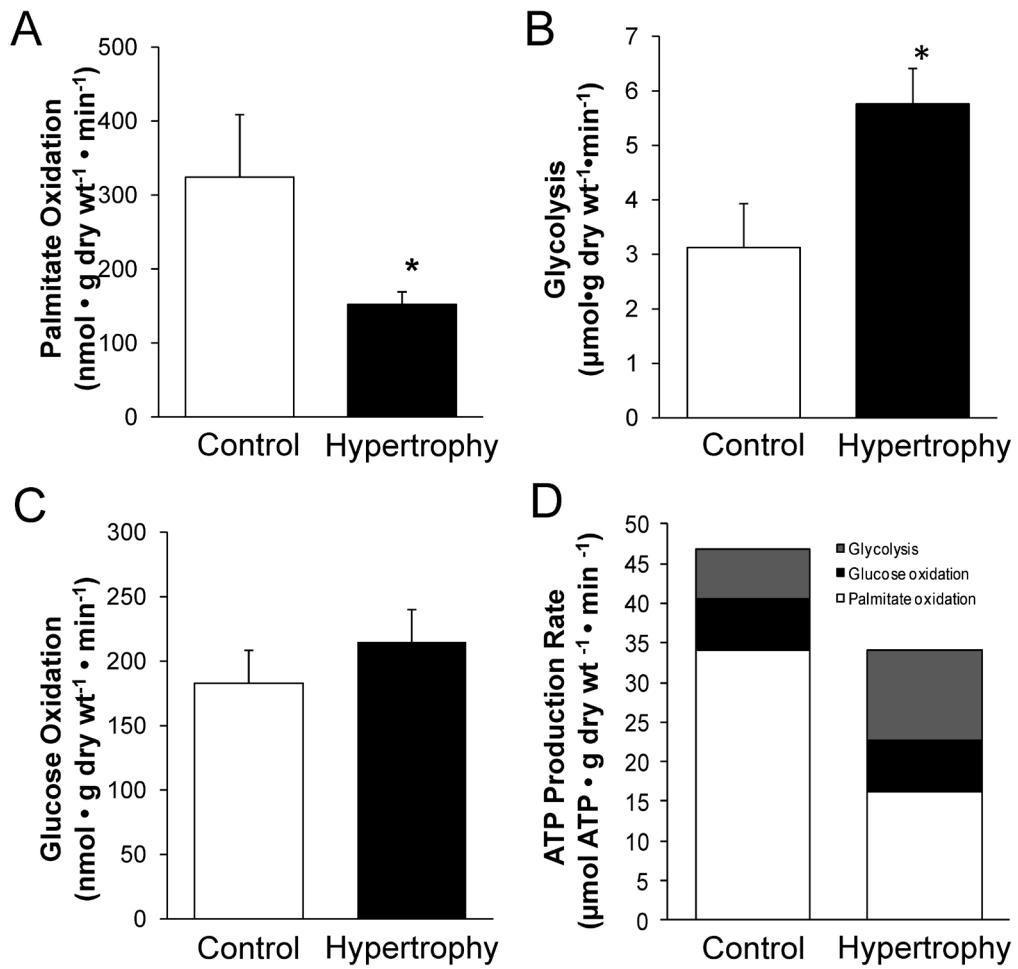


Figure 4-7: Post-Ischemic Metabolic Rates From Control (□) and Hypertrophied (■) Hearts Subjected to 25 minutes of Ischemia. A) Steady state rates of palmitate oxidation (n=9 and n=14 for control and hypertrophied hearts, respectively); B) glycolysis (n=8 and n=8, respectively); C) glucose oxidation (n=7 and n=11, respectively). D) Calculated steady state ATP production rate. Values represent means \pm SEM; * P <0.05 vs control.

Fig 4-7



4.8 Tables

Table 4-1: Physical and Cardiac Parameters in 20-day-old control and hypertrophy rabbits

	control	hypertrophy
Number of animals	12	11
Body weight (g)	360 ± 18	338 ± 17
Heart weight (g)	2.06 ± 0.12	2.39 ± 0.11 *
HW / BW (mg/g)	5.59 ± 0.37	6.64 ± 0.52 *
Heart Rate (bpm)	316 ± 6	305 ± 5
Left Ventricle		
LVIDd (mm)	8.6 ± 0.1	9.7 ± 0.2 *
LV Vol:d (mm ³)	406 ± 17	538 ± 20 *
Stroke volume (mm ³)	234 ± 11	323 ± 10 *
%EF	57.6 ± 1.1	60.3 ± 1.4
LV Vol / BW	1.17 ± 0.05	1.62 ± 0.11 *
Right Ventricle		
RV Area:d (mm ²)	34.4 ± 6.8	46.9 ± 2.9 *
RV %FAC	39.2 ± 4.5	39.3 ± 4.5
RV Area:d / BW	0.096 ± 0.005	0.129 ± 0.008 *

Rabbits from the control group underwent sham operation at 7 days of age.

Rabbits from the hypertrophy group underwent aorto caval fistula operation at 7

days of age. LVIDd, diastolic left ventricular internal diameter; LV Vol:d, left ventricular

volume; %EF, ejection fraction; %FAC, %fractional area change. *indicates a significant

difference (p<0.05) between sham and shunt. Values are the mean ± S.E.M.

Table 4-2: Cardiac function and corresponding ATP:AMP ratios in 21-day-old control and hypertrophy hearts under aerobic bi-ventricular perfusion or ischemic reperfusion

21-day-old	Aerobic Perfusion		Ischemia Reperfusion	
	Control	Hypertrophy	Control	Hypertrophy
Bi-ventricular Aerobic work	18.42±0.33	18.21±0.55	20.70±1.03	18.13±1.03
Reperfusion	-	-	17.69±1.20	9.25±0.98*
LV AMP:ATP	0.051±0.004	0.078±0.015*	0.052±0.009	0.077±0.006
RV AMP:ATP	0.084±0.019	0.095±0.015	0.067±0.009	0.149±0.031*

All cardiac functional work was normalized between RV and LV and measured as $HRx(AoPSP+ PVPSP) \times 10^3$ (mmHg • ml • min⁻¹ • 10⁻²). Aerobic hearts were perfused in 0.8 mM palmitate (n=32 and n=16 for control and hypertrophy, respectively) while hearts subjected to 25 min of ischemia were perfused in 1.2 mM palmitate (n=5 and n=5 for control and hypertrophy, respectively). Data is reported as group mean's ± SEM. * indicates a significant difference ($P<0.05$) vs control.

Table 4-3: Percent contribution to ATP production

		Palmitate	Glucose		Lactate
		Oxidation	Oxidation	Glycolysis	Oxidation
Control	Left Ventricle	80.5	11.5	6.7	1.3
	Bi-ventricular	76.4	16.2	6.2	1.2
Hypertrophy	Left Ventricle	51.5	19.1	27.2	2.2
	Bi-ventricular	59.9	20.3	17.5	2.3

Percent contribution to ATP production from palmitate oxidation, glucose oxidation, glycolysis, and lactate oxidation during left ventricular and bi-ventricular perfusion in 21-day-old hypertrophy and control hearts. Palmitate oxidation is the predominant source of ATP contributing the greatest portion. However, in hypertrophied hearts, palmitate oxidation provides proportionally less ATP than control hearts. Glucose oxidation ATP contribution seconds to the proportion from palmitate oxidation. While glycolysis and lactate oxidation contribute minimally to total ATP in control hearts, glycolysis is markedly increased in hypertrophied hearts. Glycolysis makes a greater contribution to total ATP production in the hypertrophied hearts.

Table 4-4: PDH, citrate synthase and β HAD activity in 1-day, 7-day, 21-day control and 21-day hypertrophy

			1 day	7day	21 days	
					Control	Hypertrophy
PDH activity (nmol•gwt wt ⁻¹ •min ⁻¹)	LV	Total	1.12±0.13	0.75±0.07*	1.40±0.0	1.06±0.06
		Active	0.45±0.1	0.57±0.03*	0.88±0.0	0.80±0.06
		(Ratio)	0.48±0.0	0.69±0.05†	0.63±0.0	0.81±0.09
	RV	Total		1.05±0.07	1.22±0.0	1.60±0.06
		Active		0.43±0.10	0.47±0.1	0.78±0.09
		(Ratio)		0.46±0.11	0.48±0.1	0.49±0.05
Citrate Syntase (μ mol•gwt wt ⁻¹)	LV		6.7± 1.0*	7.1±0.8*	13.6±1.0	10.4±1.7†
	RV			8.9±0.9	9.4±1.6	12.4±1.3
β HAD (μ mol•gwt wt ⁻¹)	LV		0.33±0.1	0.71±0.06*	1.44±0.1	1.18±0.13
	RV			0.75±0.11*	1.12±0.0	0.79±0.04

Pyruvate dehydrogenase (PDH), hydroxyacyl dehydrogenase (HAD), LV left ventricle, RV right ventricle, wt weight, Data are group means \pm SEM. * indicates a significant difference ($P<0.05$) vs. sham; † indicates significant difference ($P<0.05$) vs 1 day; ‡ indicates significant difference ($P<0.05$) vs 7 day.

Chapter 5
Activating Peroxisome Proliferator -
Activated Receptor α Prevents Post-
Ischemic Contractile Dysfunction in
the Hypertrophied Neonatal Heart

Activating PPAR α Prevents Post-Ischemic Contractile Dysfunction in the Hypertrophied Neonatal Heart

Victoria H. Lam *BSc*, Alda Huqi *MD*, Brandon A. Tanner, Wendy Keung *PhD*, Jagdip S. Jaswal *PhD*, Ivan M. Rebeyka *MD, MSc*, and Gary D. Lopaschuk *PhD*

Cardiovascular Research Centre, Mazankowski Alberta Heart Institute, and Departments of Pediatrics and Surgery, University of Alberta, Edmonton, Canada

Abbreviated title: Cardiac hypertrophy compromises cardiac energetics

Contribution:

Victoria HM Lam: Neonatal cardiac hypertrophy model surgery and echocardiography, bi-ventricular isolated working heart perfusions, Western blot, TG quantification, enzyme activity assays, data analysis, primary author

Alda Huqi: Western Blot

Brandon A Tanner: Western blot

Wendy Keung: intellectual and editorial contributions

Jagdip S Jaswal: Intellectual and editorial contribution

Hypothesis:

Since neonatal cardiac hypertrophy downregulates the heart's enzymatic capacity to metabolize FA causing a deficit in ATP production rates that is detrimental to post-ischemic contractile recovery, GW7647, a PPAR α agonist, is expected to upregulate the expression the FA oxidation pathway. In so, FA oxidation and ATP production rates would increase ATP available to overcome the energy deficit related to cardiac hypertrophy during ischemia-reperfusion

5.1 Introduction

Unlike adult cardiovascular disease, rarely is there an alternative to surgical correction for neonatal congenital heart defects (CHDs). Such surgical repair is a lengthy process which requires the neonatal heart be arrested subjecting the heart to global ischemic periods of more than an hour (1). The length of ischemic exposure corresponds to the degree of post-ischemic injury and consequent contractile dysfunction in pediatric patients (2-4). Despite advances in surgical skills and techniques (5, 6), insufficient cardioprotection continues to contribute greatly to post-surgical mortality (7-11). Contractile dysfunction, which manifests in up to 20% of these patients (12), is the most common cause of post-surgical death (13-15).

Altered cardiovascular hemodynamics due to the structural CHD often causes secondary cardiac hypertrophy. We have recently demonstrated in a model of volume-overload hypertrophy that neonatal cardiac hypertrophy retains a fetal-like metabolic profile (unpublished data). Although *in vivo* and *in vitro* baseline/aerobic function are normal, we showed that the hypertrophied neonatal heart recovers to only 52% of the post-ischemic function of sham-operated 21-day-old hearts. The diminished contractile recovery was attributed to a deficit in energy production on account of a retained fetal metabolic profile.

As part of this fetal metabolic profile, like adult cardiac hypertrophy, peroxisome proliferator agonist receptor (PPAR) α expression decreased relative to a normal

neonatal heart. This transcription factor controls the expression of genes involved in fatty acid (FA) metabolism, from FA uptake, transport, to oxidation. These target genes include lipoprotein lipase (LPL) (16-18), CD36/FA translocase (19), carnitine palmitoyl-transferase (CPT)-1 (20-23), and malonyl-CoA decarboxylase (MCD) (23, 24). Simultaneously, PPAR α activates the expression of pyruvate dehydrogenase kinase (PDK) 4, which phosphorylates and inhibits pyruvate dehydrogenase, the first committed step to pyruvate oxidation (23). Therefore, altered PPAR α expression also impacts on glucose metabolism.

Hypoxia-inducible factor (HIF)- α is a transcription factor controlling the transcription of key glucose metabolic enzymes such as GLUT1 (25), lactate dehydrogenase (LDH)-A (26, 27), Phosphofructose kinase (PFK)-2 (28) and monocarboxylate transporter (MCT)-4 (29, 30). As PPAR α expression/activity correlate reciprocally to HIF-1 α expression/activity, glucose metabolism is further regulated by PPAR α through its relationship with HIF-1 α , which is downregulated by an increase in PPAR α expression. In PPAR α overexpressing mice, the FA oxidation pathway is upregulated while glucose transport and glycolytic pathways are downregulated (31, 32).

During the normal neonatal period, the heart rapidly matures to metabolize FAs and derives most of its needed ATP from FA oxidation with minor contributions from glycolysis and lactate oxidation (33-38). During maturation PPAR α is upregulated in the heart (39, 40). Due to its high dependence on FA oxidation,

high fat perfusion of the neonatal heart increases its tolerance to ischemia-reperfusion in normal 7-day-old rabbit hearts (41). This phenomenon contrasts the detriments of FA oxidation in the adult heart in which increased FA oxidation inhibits glucose oxidation to perpetuate injurious acidosis during reperfusion (42). In the hypertrophied neonatal heart, as FA oxidation is downregulated due to decreased PPAR α expression/activity, it is incompletely compensated by increased glycolysis. In turn, despite a high-fat perfusion, post-ischemic functional recovery is a fraction to that of a normal heart (unpublished data).

Although excessive PPAR α activity in normal hearts causes cardiac toxicity and cardiac hypertrophy (43, 44), the administration of rosiglitazone, a PPAR γ agonist, averted cardiac hypertrophy in adult high-fat diet-induced cardiac hypertrophy (45). In rats, a PPAR α agonist inhibited the progression from hypertrophy to heart failure following coronary artery ligation (46). Others have demonstrated the prevention of cardiac hypertrophy increases survival of adult animal models of pathological cardiac hypertrophy (47, 48).

GW7647 is a PPAR α agonist that upregulates the components of the FA metabolic pathway. Since neonatal cardiac hypertrophy downregulates PPAR α expression, and consequently the heart's enzymatic capacity to metabolize FA, we hypothesize that chronic treatment with GW7647 would increase FA oxidation in hypertrophied neonatal hearts to increase ATP synthesis and availability to overcome the energy deficit. Consequently, the restored ATP

producing capacity will improve post-ischemic functional recovery. In this study, a previously established volume-overload neonatal cardiac hypertrophy model is administered GW7647 for two weeks after the induction of volume-overload to demonstrate that increased FA oxidation improves the hypertrophied heart's tolerance to ischemia-reperfusion.

5.2 Material and Methods

5.2.1 Animals

The University of Alberta adheres to the principles for biomedical research involving animals developed by the Council for International Organizations of Medical Sciences and complies with Canadian Council of Animal Care guidelines.

5.2.2 Induction of Volume-overload via Production of an Aorto-caval Fistula in Neonatal Rabbits and GW7647 Treatment

The aorto-caval fistula was produced as described previously (chapter 3, Model B). New Zealand White rabbits of either sex (7-day-old, 90-200 g) were anesthetized with inhaled isoflurane (2%). A left flank retroperitoneal incision was made to expose the descending aorta and the inferior vena cava. The descending aorta was clamped with a micro-clamp inferior to the renal blood vessels to cease blood flow. The aorta was punctured once with a 20 G needle tip below the micro-clamp and 3 through-and-through fistulas were generated across the aorta and inferior vena cava (IVC). The needle was then removed and

a drop of cyanoacrylic glue was placed on the puncture site, following which the micro-clamp was removed to restore blood flow. Following the surgical procedure animals were monitored for recovery over a 24-hour period. This produced a volume overload bi-ventricular cardiac hypertrophy in 21-day old rabbits (table 1).

From 1 day post-surgery (8-days old) until 14 days post-surgery (day of working heart perfusion), rabbits are given an intraperitoneal injection of GW7647 (EC_{50} = 6 nmol/L for PPAR α and 1.1 μ mol/L for PPAR γ (49) Cayman Chemical) twice a day (3 mg/kg/day) dissolved in DMSO and diluted with normal saline or the vehicle. Echocardiography was performed on post-surgical days 7 and 13 as previously established.

5.2.3 Isolated Bi-ventricular Heart Perfusion Model

As with previous perfusion, post-surgery, 21-day-old rabbits were anesthetized with Na-pentobarbital (60 mg/kg body weight) and hearts were excised and cannulated and retrogradely (Langendorff) perfused with Krebs-Henseleit buffer (37⁰C, pH=7.4, gassed with 95 % O₂/5 % CO₂ mixture). During 15 minutes of retrograde perfusion, the superior vena cava (SVC), the left atria, and pulmonary artery were cannulated and the IVC was ligated. Left ventricular (LV) work was initiated at the end of the 15-minute retrograde perfusion by opening flow into the left atria and aortic afterload line and perfused as LV working model for 15 min. Right ventricular (RV) load was added by opening SVC flow. The heart is

perfused as a bi-ventricular working preparation for 20 min followed by 25 min of global, no flow, normothermic ischemia (fig 5-1A). Bi-ventricular reperfusion for 30 min followed. Hearts were perfused with modified Krebs-Henseleit solution containing 2.5 mM Ca^{2+} , 5.5mM glucose, 1.2 mM palmitate prebound to 3% bovine serum albumin, 0.5 mM lactate and 100 $\mu\text{U}/\text{mL}$ insulin. The preload for the left and right atria were set at 12.5 mmHg and 7.5 mmHg, respectively. LV afterload was set at 35 mmHg and a RV afterload at 4.5 mmHg. At the end of the perfusion protocols, LV, RV, and septal tissues were separated and rapidly frozen in liquid N_2 and stored at -80°C for further biochemical analyses. Glycolysis, glucose oxidation, lactate oxidation, and palmitate oxidation were measured as described (42, 50). For further details, please refer to section 4.2 material and methods.

5.2.4 Tissue Sample Preparation for Immunoblot Analysis

Frozen ventricular tissue (~20 mg) was homogenized in homogenization buffer (containing 50 mM Tris•HCl (pH 8 at 4°C), 1 mM EDTA, 10% (wt/vol) glycerol, 0.02% (wt/vol) Brij-35, 1 mM dithiothrietol (DTT), and protease and phosphatase inhibitors (Sigma)). Samples were then homogenized for 30s using a Polytron Homogenizer. Samples were centrifuged at 800 g for 10 min. The supernatant was boiled at 95°C in protein sample buffer solution (62.5 mM Tris-HCl, 6 M Urea, 10% glycerol, 2 % sodium dodecyl sulfate, 0.003 % bromophenol blue, and 5 % 2-betamercaptoethanol) for 5 min. Protein concentration of homogenates

was determined using the Bradford protein assay kit (Bio-Rad) and normalized to 1 µg/µL to load into the SDS-PAGE gel and separated by molecular weight (51). The separated proteins were then electrophoretically transferred onto a nitrocellulose membrane, which was probed with primary antibodies against malonyl-CoA decarboxylase (MCD), HIF-1 α (nuclear), phospho-acetyl-CoA carboxylase (P-ACC), total-ACC (T-ACC), adipose triglyceride lipase (ATGL), Akt, and GLUT4.

5.2.5 PPAR α mRNA Expression

PPAR α mRNA expression was determined by reverse transcription of total RNA followed by quantitative PCR (qPCR) analysis. Total RNA was extracted from the LV and RV of 21-day-old heart and 21-day old hypertrophied hearts (GW7647-treated and non-treated), as above using TRI reagent (Qiagen) according to manufacturer's kit. RNA is then quantified spectrophotometrically at 260 nm. Reverse transcription was then performed on 1 µg of total RNA using 100 IU of reverse transcriptase (Qiagen) with 100 ng of random hexanucleoties primers in a 20 µL reaction volume. PCR cycles were then followed with 1 µL of the reverse transcription product with 0.4 mmol/L of each dNTP, 25 pmol specific primers, PCR buffer, and 1.25 U of Taq DNA polymerase. 2 min of denaturation at 94 $^{\circ}$ C was followed by amplification of 30 cycles: 30s at 94 $^{\circ}$ C, 35 s at 53 $^{\circ}$ C, and 40 s at 72 $^{\circ}$ C, then maintained for 7 min at 72 $^{\circ}$ C. qPCR was then performed using 12.5 µL Sybr-Green Jump Start Taq Readymix (Sigma-Aldrich), 5 µL oligonucleotides, 7.5

μ L of cDNA. qPCR of ribosomal rRNA 18s was performed as the endogenous control.

5.2.6 Triacylglycerol (TG) Quantification

20 mg of frozen tissue sample was homogenized in 20x chloroform:methanol (2:1) mixture for 30 sec. 0.2X the volume of methanol was then added and sample vortexed well before the samples were centrifuged for 10 min at 3500 rpm. The supernatant was collected and its volume recorded. To this supernatant, 0.2X the volume of 0.04% CaCl_2 was added and allowed to separate into 2 phases. Samples were then centrifuged again at 2400 rpm for 20 min. The upper phase was removed and the bottom phase was washed three times with 150 μ L of pure solvent (chloroform, methanol, and water mixture) added to the bottom phase and centrifuged again at 2400 rpm for 20 min. The upper phase was removed and 50 μ L of methanol was added to the lower phase and sample was heated to 60⁰C and dried under a stream of N_2 gas. Once dried, sample was re-dissolved in 50 μ L of 3:2 tertbutyl alcohol:triton X-100/methyl alcohol (1:1) mixture and left overnight. TG concentrations were determined by a Wako Triglyceride M kit on the following day.

5.2.7 Carnitine Palmitoyl Transferase-1 (CPT-1) Activity Assay

Frozen cardiac tissue was homogenized as above and centrifuged at 15000xg for 30 min with supernatant removed. Pellets with the mitochondrial fraction were

reconstituted with 30 μ L of buffer containing 75 mM KCl, 20 mM sucrose, 10 mM HEPES, 1 mM EGTA (pH 7.5). A protein assay was performed, as above for western blots. To 100 μ g of the mitochondrial fraction 37.5 μ L of 1 mM palmitol-CoA (dissolved in 25 mM KH_2PO_4 , pH 5.3) and 250 μ L of incubation buffer (150 mM KCl, 100 mM mannitol, 50 mM HEPES [pH 7.3], 4 mM NaCN, 0.4 mM EGTA, 1 mM dithiothreitol) was added. Samples were incubated for 3 min. 10 μ L of 10 mM L-carnitine with L-[methyl- ^3H] carnitine (1/100 dilution) is added and incubated for 6 min, during which the reaction is linear. The reaction is stopped with 100 μ L of concentrated HCl. 1.4 mL 1-butanol saturated water is then added and an additional 1 mL of 1-butanol is added to extract the radiolabelled ^3H -palmitoyl-carnitine, samples vortexed and centrifuged for 7 min at 3500 rpm. Extraction was repeated twice and 500 μ L of each sample is subjected to scintillation counting.

5.3 Results

5.3.1 The Effects of GW7647 Treatment

Through an aorto-caval shunt, volume returning to the right side of the heart was increased to induce a volume-overload hypertrophy. In order to verify that an increased volume return occurred in animals that received shunt surgery, color Doppler ultrasound was used to examine the abdominal IVC and aorta. The physical shunt was readily visualized as verified by communication from the aorta to the IVC which generated turbulent flow. The flexibility and lack of

musculature of the IVC allowed the increased volume return to distend the IVC which significantly increased IVC diameter in shunted animals (vehicle-: 3.38 ± 0.11 mm and GW7647-treated: 3.53 ± 0.09 mm) when compared to sham-operated, control animals (2.42 ± 0.15 mm, $P < 0.05$) (table 5-1). Elaborated in table 5-1, 2D echocardiography showed that LV (LVIDd) and RV (RVIDd) internal diameters during diastole were increased in the two groups receiving shunt surgery compared to sham-operated, control animals. The increased internal diameter indicates global cardiac volume-overload. As the LV posterior wall (LVPW) is not thickened, these findings in the shunted animals are consistent with eccentric cardiac hypertrophy. Furthermore, while body weight were comparable across the three groups of animals, heart to body weight (HW:BW) ratio is significantly greater in the two shunt-operated groups (vehicle-: 4.7 ± 0.3 ; GW7647-treated: 4.8 ± 0.2 ; and control: 4.2 ± 0.1 , $P < 0.05$) and further illustrates the extent of cardiac hypertrophy. LV, septum, and RV weight to body weights are also reported in table 5-1.

EF% is decreased significantly in the vehicle-treated hypertrophied hearts (67.4 ± 3.0) compared to the sham-operated animals (75.4 ± 1.1 , $P < 0.05$). GW7647 treatment did not alter the physical parameters (IVC diameter, RVIDd, LVIDd, LVPW, and HW:BW) of hypertrophied hearts (table 5-1). However, EF% of the hypertrophied hearts was improved by the GW7647 treatment (76.5 ± 2.5 %).

5.3.2 GW7647 Rescues Post-ischemic Cardiac Dysfunction in Hypertrophied Hearts

Our lab has found that cardiac hypertrophy in the neonatal rabbit heart diminishes post-ischemic functional recovery associated with an energy deficit (unpublished data). Although aerobic LV function (unpublished data) or bi-ventricular function were no different between hypertrophied (vehicle- or GW7647-treated) and normal hearts, post-ischemic functional recovery is severely diminished in hypertrophied hearts (fig 5-1B). The percent recovery (fig 5-1C) of hypertrophied hearts is significantly less than that of control hearts ($56.4 \pm 8.9\%$ vs $80.2 \pm 4.7\%$, respectively). GW7647 treatment restored functional recovery (fig 5-1A and B) of hypertrophied hearts ($83.6 \pm 6.4\%$) to levels seen in control hearts without affecting aerobic function prior to the ischemic episode.

5.3.3 GW7647 Increased ATP Production Rates

Neonatal cardiac hypertrophy is associated with marked decreased FA oxidation rates and increased glycolytic rates as compared to age-matched control hearts (fig 5-2A and C); but rates of glucose oxidation are unaltered (fig 5-2B). Due to increased rates of glycolysis, and without equally increased glucose oxidation rates, H^+ s were produced in excess. In aerobic perfusion (pre-ischemia), excessive H^+ production (fig 5-2D) did not seem to affect cardiac function. However, during ischemia-reperfusion, unable to oxidize glucose or FA, the

hypertrophied heart relied on glycolysis at rates which persists into reperfusion (fig 5-2C). Uncoupled from glucose oxidation, H^+ production from increased glycolysis rates was exacerbated during post-ischemic reperfusion (fig 5-2D).

GW7647 is an agonist that increases PPAR α activity and hence increases the transcription of enzymes involved in FA metabolism. Improved functional recovery of hypertrophied neonatal hearts by treating with GW7647 was associated with increased rates of FA oxidation (fig 5-1A and 5-2A). These rates of FA oxidation were accompanied by decreased rates of glycolysis (fig 5-2C) with no changes to glucose oxidation rates (fig 5-2B). The increased ability to oxidize FA persisted during post-ischemic reperfusion. As rates of glycolysis were suppressed, H^+ production rates were significantly decreased to lower H^+ load (fig 5-2D).

Hypertrophied hearts had an ATP production deficit as indicated by decreased steady state ATP production rates at pre- and post-ischemia, compared to control hearts (fig 5-3A). ATP production rates were elevated, mainly from FA oxidation, by GW7647 treatment of hypertrophied hearts. GW7647 also increased pre- and post-ischemic tricarboxylic acid cycle (TCA) activity (fig 5-3B) when compared to vehicle-treated hypertrophied and control hearts.

5.3.4 GW7647 Altered Gene Transcription

Cardiac hypertrophy significantly decreased LV PPAR α mRNA expression by 32% ($P < 0.05$, fig 5-4A). However, unlike the LV, RV PPAR α expression was increased by 78% in hypertrophied hearts ($P < 0.05$). GW7647 increases PPAR α activity and is not expected to alter PPAR α expression directly; so, while GW7647 did not affect LV PPAR α expression, compared to controls, GW7647 increased RV expression by 20% ($P < 0.05$).

HIF-1 α expressional changes, on the other hand, have been negatively associated with PPAR α expression/activity. As hypertrophy decreased LV PPAR α expression, HIF-1 α protein expression was significantly increased compared to controls (fig 5-4B). Hypertrophy also significantly increased RV HIF-1 α expression compared to controls regardless of relative PPAR α expression. Overall, elevated HIF-1 α protein levels corroborate with elevated glycolysis rates in hypertrophied hearts (fig 5-2C). GW7647 is associated with significantly decreased LV HIF-1 α expression in hypertrophied hearts compared to levels found in vehicle-treated hypertrophied hearts. These levels are similar to those found in control hearts (fig 5-4B). RV HIF-1 α was not affected by GW7647 treatment compared to vehicle-treated hypertrophied or control hearts.

5.3.5 GW7647 Removed CPT-1 Inhibition in Hypertrophied Hearts

The total CPT-1 activity was assayed and represents CPT-1 uninhibited activity (fig 5-5A). This uninhibited, total CPT-1 activity may be correlated to total expression as well. Cardiac hypertrophy did not alter LV or RV CPT-1 expression/activity (1.14 ± 0.09 and $1.67 \pm 0.13 \mu\text{mol}\cdot\text{mg}^{-1}\cdot\text{min}^{-1}$, respectively) compared to control hearts (0.9 ± 0.13 and $1.75 \pm 0.21 \mu\text{mol}\cdot\text{mg}^{-1}\cdot\text{min}^{-1}$, respectively). GW7647 treatment of hypertrophied hearts is associated with significantly increased total CPT-1 activity in both LV and RV (1.55 ± 0.20 and $1.93 \pm 0.11 \mu\text{mol}\cdot\text{mg}^{-1}\cdot\text{min}^{-1}$, respectively) compared to control and vehicle-treated hypertrophied hearts (fig 5-5A).

LV malonyl-CoA levels were not altered by hypertrophy in vehicle-treated hearts compared to control hearts (fig 5-5B), but GW7647 treatment decreased its levels (fig 5-5B). On the other hand, malonyl-CoA levels were significantly increased in the hypertrophied RV which GW7647 treatment also normalized back to control levels.

Malonyl-CoA levels are the result of the balance between acetyl-CoA carboxylase (ACC) synthesis and malonyl-CoA decarboxylase (MCD) degradation. MCD protein levels did not change in the LV between the three groups (fig 5-6A). Therefore, changes to malonyl-CoA levels are likely dependent on ACC expression/activity. LV hypertrophy did not increase ACC expression or phosphorylation compared to control hearts (fig 5-6B) correlating to the

unaltered malonyl-CoA levels in the hypertrophied LV compared to control hearts (fig 5-5A). However, in the presence of normal MCD expression, total ACC expression of the LV was significantly decreased in the GW7464-treated hearts when compared to vehicle-treated hypertrophied hearts. This finding corroborated with low LV malonyl-CoA levels in GW7647-treated hearts.

Contrary to the LV, hypertrophy significantly decreased RV MCD expression compared to control hearts (fig 5-6A). In spite of simultaneous decreased T-ACC expression (fig 5-6B), malonyl-CoA levels are significantly elevated in these hearts when compared to controls. On the other hand, GW7647, though not to control levels, is associated with restored MCD expression to exceed that of vehicle-treated hypertrophied hearts. To add, T-ACC levels remained significantly decreased in the RV with GW7647 compared to vehicle.

5.3.6 Intracellular Triacylglycerol (TG) Storage Altered by Hypertrophy and GW7647 treatment

In the hypertrophied neonatal hearts, LPL mRNA is significantly down-regulated compared to controls (fig 5-7A). GW7647 did not significantly alter LV LPL transcription in hypertrophied hearts. In contrast, RV LPL mRNA transcription did not differ between control and hypertrophied hearts. However, GW7647 increased LPL mRNA expression in the RV (fig 5-7A).

In the presence of hypertrophy, both the LV and RV have significantly decreased ATGL protein expression compared to control hearts (fig 5-7B). This correlated to elevated TG content in hypertrophied hearts (fig 5-7C) compared to controls. In the LV, with GW7647, increased FA oxidation rates correlated to significantly increased ATGL expression and decreased TG stores. On the other hand, RV ATGL expression did not increase and remained at levels similar to those in vehicle-treated hypertrophied hearts (fig 5-7B). However, TG storage was decreased with GW7647 treatment (fig 5-7C). Therefore, different mechanisms govern TG pool dynamics between the LV and RV, but less FA are being stored as TG with GW7647 treatment compared to vehicle-treated hypertrophied hearts.

5.3.7 Glucose Uptake and Metabolism

Glucose metabolism can be regarded in two parts: glycolysis and oxidative phosphorylation. Both parts are dependent on glucose uptake, governed by GLUT1 and GLUT4 translocation. In adult cardiac hypertrophy, in which insulin resistance develops, GLUT4 is downregulated relative to GLUT1 expression (52). Similarly, GLUT4 expression is downregulated in the hypertrophied neonatal RV, but not in the LV, when compared to controls (fig 5-8A). GLUT1 expression is upregulated in the hypertrophied LV and RV (fig 5-8B). Therefore, a reciprocal relationship between GLUT4 and GLUT1 expression is maintained in the RV whereby when GLUT4 was downregulated, GLUT1 expression increased (fig 5-8B). GW7647 treatment, though maintained elevated GLUT1 expression in the

LV, downregulated its expression in the RV simultaneous to an increase in RV GLUT4 expression. LV GLUT4 expression is not altered with GW7647 treatment.

GLUT4 translocation, though not examined in these hearts, is determined by the propensity of the insulin signalling pathway. Insulin signals GLUT4 translocation via AKT. AKT expression is significantly increased in the LV of hypertrophied hearts but unaltered in the RV compared to control hearts (fig 5-8C). Downstream to Akt signalling, although not statistically significant, there was a trend towards decreased AMPK phosphorylation in hypertrophied LV (fig 5-8D). A statistically significant decreased in P-AMPK is apparent in the RV. GW7647 treatment did not alter the LV AKT expression, but increased P-AMPK. Interestingly, GW7647 is associated with upregulated AKT expressions in the RV compared to vehicle-treated hypertrophied hearts, but P-AMPK did not increase significantly with GW7647 treatment.

Glucose uptake signalling aside, glucose oxidation is directly affect by GW7647 treatment because as PPAR α activity is increased, PDK4 expression is expected to elevate and modulate glucose metabolism as part of the Randle cycle. Glucose oxidation rates did not change throughout the ischemia-reperfusion protocol. This phenomenon is likely due to the metabolic immaturity of these neonatal hearts (53, 54). The insulin signalling pathway is still developing in the heart at this time point. The immature glucose metabolic pathway in the neonatal heart is apparent in PDH expression. In spite of hypertrophy-related decrease in LV

active PDH activity (fig 5-9A), glucose oxidation rates were no different from that of control hearts (fig 5-2B). RV active PDH activity remained at similar levels in hypertrophied hearts compared to controls. Therefore, regardless of the impact GW7647 has on altered PDK4 expression (fig 5-9C) and PDH activity, glucose oxidation, at such low rates, cannot be altered by PDK4 expression/activity. Nonetheless, GW7647 does increase PDK4 expression, non-significantly in the LV, but significantly in the RV as compared to the control hearts.

5.4 Discussion

In addition to the normal adaptations to *ex-utero* hemodynamics, a CHD causes pathological hemodynamic stress. Therefore, neonatal cardiac hypertrophy may develop secondary to a CHD. The coinciding altered cardiac metabolism was previously demonstrated to cause an energy deficiency that deters appropriate recovery during ischemia reperfusion. In the present study, the administration of GW7647, a PPAR α agonist, 1) normalized and improved post-ischemic recovery of hypertrophied neonatal hearts. 2) The rescued phenotype was associated with increased FA oxidation and decreased glycolysis. 3) These metabolic changes are associated with altered allosteric and expressional control of the FA metabolic pathway.

5.4.1 The Hypertrophied Neonatal Heart and Tolerance to Ischemia-Reperfusion

Whether neonatal hearts are more tolerant of ischemia-reperfusion injury relative to an adult heart has been a topic of debate for over three decades, but often the models examined are normal hearts and cannot be compared to the clinical correlate. Yet, several studies on normal neonatal hearts demonstrate that improving post-ischemic recovery is possible (41, 55). In this neonatal model of cardiac hypertrophy, hypertrophy decreases tolerance to ischemia-reperfusion and may be attributed to a decrease in ATP availability that is rectified in the present study by GW7647 therapy. Simultaneously, cardiac hypertrophy is also associated with excessive H^+ production that may have contributed to poorer post-ischemic recovery.

Hypertrophy downregulates PPAR α expression in the neonatal heart to produce a similar metabolic profile to that of PPAR α null mice. Both glucose oxidation and glycolysis increase in the PPAR α null mice, while palmitate oxidation rates decrease significantly compared to WT controls (56, 57). Yet, hearts from these PPAR α null mice are more tolerant of an ischemic episode (57). Apart from species differences, contrasting responses to ischemia may be largely related to an energy deficit associated with age-related metabolic maturity and juxtaposing cardiac hypertrophy. Unlike the adult hearts, TCA activity is decreased in hypertrophied neonatal hearts as acetyl-CoA production lost from decreased FA oxidation was not compensated for by upregulated glucose oxidation. In

contrast, in the adult mice, although percent contribution to the TCA cycle from FA and glucose oxidation change dramatically, the total acetyl-CoA produced did not change. This compensatory mechanism is found in the normal heart as well (36).

The immediate newborn heart is largely dependent on glycolysis (34) and switches to a dependence on FA oxidation in the newborn period (33) as rates of glucose oxidation remain low (58). Cardiac hypertrophy magnifies this metabolic inflexibility found in the neonatal heart that may contribute to poor post-ischemic recovery. GW7647 may be cardioprotective as it prevents the loss of ability to metabolize FA and helps overcome the deficit in producing sufficient ATP during reperfusion. In fact, GW7647 increases TCA cycle activity and ATP production rates to levels exceeding those of the normal neonatal heart. Now, the increased ATP production rates may represent a degree of ATP wasting during aerobic perfusion as cardiac function is not different between the two groups (fig 5-1B). However, during reperfusion, increased ATP production rates may be necessary for the improved functional recovery derived from GW7647.

An ATP production deficit is detrimental because poor contractile recovery is, in part, due to diversion of ATP to non-contractile purposes of rectifying the post-ischemic ionic imbalance instigated by acidosis. Wittnich et al demonstrated that H^+ production is higher in the normal neonatal heart compared to the adult heart and that its buffering capacity is weaker as well (59). Although the

mechanisms of increased H^+ production and its impact on functional recovery were not assessed, it was assumed more detrimental relative to an adult heart. In fact, normal 7-day-old rabbit hearts are more tolerant to ischemia with a 87% post-ischemic functional recovery compared to an adult heart, which recovered to only 47% (60). In contrast to normal hearts, the mismatched elevated rates of glycolysis to low rates of glucose oxidation in hypertrophied hearts augments H^+ production in neonatal hearts. Therefore, this clinically-relevant hypertrophy model may help illustrate the detriments of acidosis and ischemia in the neonatal heart. To add, these high baseline H^+ production rates are further amplified by ischemia. GW7647 did not alter overall glucose oxidation or pre-ischemic H^+ production rates, but FA oxidation rates were increased and paralleled to decreased post-ischemic rates of glycolysis thereby decreasing post-ischemic H^+ production. In adult hearts, high fat perfusions inhibit glucose oxidation more so than glycolysis (42). As neonatal hearts are less able to oxidize glucose owing to its underdeveloped pyruvate oxidative capacity, increased FA oxidation rates seem to inhibit glycolysis more so than pyruvate oxidation. Therefore, unlike the detriments of high fat in adult hearts, high FA oxidation rates increase ATP availability for functional recovery to rectify the ionic imbalance as well as inhibit H^+ production from glycolysis in the neonatal heart.

Hence, GW7647 treatment produced two metabolic advantages to offset ischemia-reperfusion injury: 1) by increasing ATP production capacity through increasing FA oxidation and 2) depressed rates of glycolysis and H^+ production.

5.4.2 GW7647 Normalizes the Regulatory Pathway on FA Oxidation in Hypertrophied Neonatal Myocardium

FA metabolism maturation in the neonatal heart is partially driven by increased substrate availability from dietary FA in milk (35). Simultaneously, PPAR α mRNA increases over the neonatal period (61). FAs are PPAR α -activating ligands and the coinciding increase in FA concentrations to PPAR α expression upregulates the FA metabolic pathway. Indeed, increased FA oxidation rates occur simultaneously to increased MCD activity (53), CPT-1 activity (53) and expression (62), and CPT-2 activity (62). Mitochondrial FA uptake is therefore increased to accelerate FA oxidation in the neonatal period. In hypertrophied neonatal heart, this developmental transition does not seem to occur.

In hypertrophied neonatal hearts, although LV PPAR α mRNA markedly decreases compared to controls, RV PPAR α levels are actually elevated. As with the biochemical profile of PPAR α null mice and adult hypertrophied hearts (56, 63, 64), malonyl-CoA levels remain high in the LV. Despite elevated PPAR α mRNA, malonyl-CoA levels are elevated in the RV. However, total CPT-1 activity remains constant between hypertrophied and normal hearts. Accordingly, MCD nor ACC expression changed in these hypertrophied LVs but MCD expression decreased significantly as with ACC inactivation in the hypertrophied RV. Therefore, in the RV, though malonyl-CoA synthesis may decrease by decreased active ACC, it is likely that degradation decreased sufficiently to maintain elevated malonyl-CoA

levels to inhibit CPT-1 and consequently, FA oxidation. This demonstrates that though the metabolic switch in the hypertrophied myocardium is closely tied to PPAR α expression/activity in adult hearts, a discrepancy is present in the neonatal heart between the LV and RV (65, 66). Nonetheless, an increase in acute inhibition of CPT-1 FA transport is present in both the LV and RV as malonyl-CoA contents are elevated. However, the chronic changes are apparent only in the RV. The resulting energy deficit is similar to that found in adult PPAR α null mice; and likewise, the energy deficit did not affect aerobic function (67).

Metabolic remodelling in the hypertrophied hearts, though increases aerobic efficiency, also decreases ability to compensate and generate sufficient ATP in response to additional stress. PPAR α knockout mice do not have myocardial hypertrophy, but when subjected to stimuli, the cardiac dysfunction in these mice is intensified (68-70). Overexpressing GLUT1 compensated for the downregulated FA metabolism in these PPAR α null mice; consequently, ischemic stress tolerance was restored. Neonatal cardiac hypertrophy treated with GW7647 had normalized functional response to additional stress. In GW7647-treated hearts, PPAR α expression does not increase dramatically, but the expected increase in PPAR α activity is linked to restored the energy deficit by decreasing malonyl-CoA and upregulating FA oxidation. In the hypertrophied LV, lowered malonyl-CoA levels are attributed to a downregulation of ACC expression while MCD expression is unaffected. Therefore, malonyl-CoA may be produced at a lower rate relative to controls and vehicle-treated hypertrophied

hearts. In contrast, RV malonyl-CoA levels decrease due to increased MCD expression with little effect on ACC, which would increase malonyl-CoA degradation while rates of synthesis remains constant.

These findings support the notion that LV and RV metabolism are different (71). MCD and ACC expressions may differ between the two ventricles, but elevated malonyl-CoA remains the key effector regulating FA metabolism in the neonatal heart in both ventricles. Bi-ventricular perfusion was an attempt to resolve the metabolic difference between two ventricles, but this set up merely assessed global cardiac metabolism to improve upon the physiological relevance compared to the LV working heart preparation (50). RV metabolism is dependent on that of the LV so that the measurements of individual ventricular metabolic rates remain unattainable at this time. Until the metabolism of individual ventricles can be resolved, differing metabolic rates between the two ventricles cannot be measured. Suggestions that either ventricle is more susceptible to dysfunction (71) still cannot be validated. In fact, equally elevated levels of malonyl-CoA suggest that FA oxidation in both ventricles could be equally inhibited. What is clear is that the restored expression of the metabolic pathway and its regulatory components (MCD and ACC) is associated with normalized cardiac metabolism and improved post-ischemic functional recovery.

5.4.3 GW7647 Altered FA Uptake and Utilization

In hypertrophied rat hearts treated with WY-14643, a PPAR α agonist, PPAR α -regulated genes were upregulated (72) similarly to findings in the present study. Although in the *ex vivo* working heart, PPAR α agonism decreased aerobic contractile function, these rat hearts were perfused with only 0.4 mM oleate. Here, GW7647 increased the hypertrophied neonatal hearts' ability to extract both exogenous and endogenous FA for the increased FA metabolism. At rest, much of the FAs taken up into cardiomyocytes are not immediately oxidized but rather diverted into myocardial TG stores before redirected for oxidation (73). The size of TG stores is determined by the rate of FA uptake and synthesis into TG and the rate of TG hydrolysis. The heart acquires FA from circulating non-esterified albumin-bound FA and FA from the hydrolysis of TGs associated in plasma lipoproteins. The latter reaction is governed by LPL expression.

ATGL has been suggested as the rate-limiting step in the first step of TG hydrolysis into diacylglyceride and one FA and is responsible for basal TG degradation (74, 75). Aside from adipose tissue, ATGL is also expressed in the adrenals, testis, skeletal, and cardiac muscle (76, 77). In the neonatal hypertrophied hearts, ATGL is significantly decreased in both ventricles. While TG levels remain constant in the RV, the decreased ATGL expression correlates to increase TG levels in the LV. This correlates to a decreased ability to mobilize fat stores despite the increased energy demands of ischemia-reperfusion.

Like TG levels, RV LPL mRNA expression did not change in hypertrophied hearts, yet it decreases in the hypertrophied LV. Low LPL expression in the native RV may be due to lower energy demands requiring less substrate compared to the LV. Therefore, when RV is hypertrophied, as cardiac metabolism becomes more dependent on glycolysis, at a pre-existing low level, LPL expression may not be altered. Overall, substrate availability may remain limited as the enzyme required to derive the needed FA is expressed at a low rate.

LV ATGL levels and RV LPL levels increased while LV and RV TG stores decreased under GW7647 treatment compared to vehicle-treated hearts. Although the extracellular expulsion of LPL is required for it to increase exogenous FA extraction, only LPL mRNA levels were examined here. Increased LPL mRNA expression may increase the GW7647-treated hearts' ability to extract FA from circulation to increase substrate availability of FA oxidation. Overall FA cycling in the TG pool normalized to that of control RV and LV when hearts were treated with GW7647. This shows an increased cycling of extracellular FA into the endogenous pool. Studies of extracellular LPL concentration/activity and serum free FA would be needed to verify increased extracellular activity and uptake in neonatal rabbits. However, in mice, GW7647 significantly decreased serum free FA levels (78). To add, in order to prevent substrate limitation, the neonatal hearts were perfused with 1.2 mM palmitate. In WY-14643-treated hypertrophied hearts, heart may have been substrate-limited even during aerobic working hearts perfusions using only 0.4 mM oleate bound to 3% BSA (72), which limited

its aerobic function in contrast findings in the present study. Therefore, it is reasonable to suggest that increased FA oxidation rates are associated with appropriate increased intra- and extra-cellular FA extraction in hypertrophied hearts treated with GW7647.

5.4.4 GW7647 Suppresses HIF-1 α and Downstream Effectors

In contrast to FA metabolism, glycolysis was downregulated by GW7647. PPAR α expression is reciprocally related to HIF-1 α expression (79, 80). To no surprise, neonatal cardiac hypertrophy upregulates HIF-1 α , particularly in the RV. HIF-1 α upregulates enzymes involved in the glycolytic pathway as well as enzymes which inhibit glucose oxidation. Specifically, HIF-1 α upregulates pyruvate dehydrogenase kinase 1 (PDK1) to phosphorylate and inhibit PDH and ultimately block glycolytic products from entering the TCA cycle (81, 82). In hypertrophied neonatal hearts, decreased LV active PDH activity was found despite a decrease in PDK4 mRNA expression. GW7647 treatment maintained the levels of active PDH activity in the LV, with no changes to the RV, but decreases total PDH expression/activity. In the GW7647-treated hypertrophy LV, PDK4 mRNA levels did not significantly change, but in the RV, it was upregulated compared to normal hearts. Therefore, possible mechanisms by which GW7647 decreases glycolysis is via 1) PPAR α 's dynamic relationship with HIF-1 α and 2) PPAR α -upregulated inhibitory enzymes, such as PDK4. However, as glucose oxidation is natively low, it remains low regardless of PDK4 expression. The disjoint between

altered PDH expression/activity exemplifies the immaturity of the pyruvate oxidation pathway in the neonatal heart. This finding is validated by previous findings of a gradual increase in citrate synthase activity between 1, 7, and 21 days of age in the rabbit heart both in the LV and RV (unpublished data). However, the exact mechanism that limits pyruvate oxidation in the neonatal heart has yet to be fully elucidated. From this study, PDH does not appear to be rate-limiting to pyruvate oxidation in the neonatal heart.

Increased HIF-1 α caused cardiac steatosis via upregulating the HIF-1 α -PPAR γ axis, a suggested molecular mechanism that accounts for the integration of glycolysis and TG synthesis in cardiomyopathy-related steatosis (79). In models of adult cardiac hypertrophy, cardiac steatosis correlates to increased apoptosis (83, 84). Despite overlapping functions, a difference between PPAR γ and PPAR α is that PPAR γ is associated with TG synthesis, while PPAR α is associated with FA oxidation. In the hypertrophied neonatal heart, TG accumulation occurs in the LV while remaining the same as normal hearts in the RV. Whether TG accumulation adds to the *in vivo* systolic dysfunction, although not explored here, has been hypothesized to physically interrupt contractile function. *In vivo* cardiac function was salvaged with GW7647 treatment, which also caused a decreased TG accumulation in both the LV and the RV. The decrease in intra-myocardial lipids has been shown to improve contractile function (85). Therefore, as with adults, decreased TG accumulation seems to benefit the hypertrophied neonatal heart.

To what extent TG accumulation harms the vehicle-treated hypertrophy heart was not explored in this study, but would be of great interest to understand.

5.4.5 GW7647 Effects on Cardiac Hypertrophy and Implications on Cardiac Surgery

GW7647 corrected the altered metabolism and improves IR tolerance but have no affect on the course of cardiac hypertrophy. Similarly, adult hLpL^{GPI} transgenic mice treated with rosiglitazone had lowered ANP and BNP levels and a normal cardiac lipid profile, but the cardiomyopathy was not reverted (86). Permanently LAD-ligated rats treated with a PPAR δ agonist also had normalized cardiac lipid profiles and energy metabolism, yet cardiac dysfunction was still present (87). In the present study, GW7647 treatment improved *in vivo* cardiac function by restoring ejection fraction, but it did not alter the course of cardiac remodelling in the continued presence of a volume-overload. Unlike the adult heart where damage is permanent, when the physical CHD is surgically corrected, remodelling will occur to adapt to the altered hemodynamic. Energy metabolism should evolve after energy demand changes. Therefore, surgical correction is expected to alter, or perhaps, correct the metabolic derangement in the hypertrophied heart as cardiomyocytes remodel after the improved hemodynamics.

However, prior to surgery, the hypertrophied neonatal heart is energy deficient and less tolerant to added stress. Limited perioperative cardioprotection remains

a major contributor to mortality following surgical repair of CHDs (7, 9). Contractile dysfunction manifests in 20% of pediatric patients following CHD surgery (12), and is the most common cause of post-surgical death (13, 14). Inotropic support stimulates cardiac contractility at the expense of depleting acetyl-CoA at rates that exceed the hearts ability to regenerate it (54). In normal neonatal rabbit hearts, the energy demands in response to an inotrope cardiostimulation are met by an increase in both glucose and FA metabolism (54). Since neonatal hypertrophied hearts are in an energy deficient state, it is likely that inotrope therapy would detrimentally exacerbate the energy deficit leading to dire states. Hearts from adult PPAR α null mice are unable to compensate when challenged with an increased workload (56, 67). As with adults (88), the necessity of corrective surgery for CHDs in children is a predictor of morbidity/mortality(89). When PPAR α -null mice simultaneously over-expressed GLUT1, glucose uptake and oxidation were upregulated and the rescue phenotype surmounted the inability to respond to increased workload (67). However, neonatal hearts have a preference for FA over glucose oxidation (55). Aside from protection against IR injury, GW7647 treatment of the hypertrophied heart may increase a hypertrophied heart's tolerance to inotrope support that may be required for non-metabolic heart failure. It would be interesting to further examine energy economy of hypertrophied hearts when challenged with an inotrope and whether GW7647 treatment would improve its response to curb the morbidity/mortality associated with its use. Therefore,

acute GW7647 treatment is an appealing option to overcome the temporary limitations of surgery and cardiac hypertrophy in the immediate reperfusion period as well as for peri-operative treatments of cardiac dysfunction.

5.5 Conclusion

Neonates with CHDs often develop secondary cardiac hypertrophy. Here and previously, we have demonstrated that neonatal cardiac hypertrophy causes the retention of the fetal metabolic profile. Furthermore, we have demonstrated that this glycolysis-dependent metabolism, an energy deficient state, is incompatible with ischemia-reperfusion and decreases post-ischemic functional recovery significantly compared to control hearts. GW7647 upregulates FA oxidation and suppresses glycolysis to increase ATP production capacity, to improve post-ischemic functional recovery to levels seen in a normal heart. The restoration of normal cardiac metabolism was associated with upregulated expression of key enzymes in the FA oxidation pathway as well as those involved in the regulation of malonyl-CoA to prevent CPT-1 inhibition. Therefore, GW7647 may be a viable acute peri-operative treatment for neonates undergoing corrective cardiac surgery.

5.6 Limitations

Although the study was performed to the best of our abilities and based on current knowledge of neonatal cardiac hypertrophy, the limitations should be

acknowledged. The isolated working heart model is of particular limitation to this study. GW7647 was systemically administered for 14 days, but the end point was an *ex vivo* study of cardiac metabolism. While functional recovery from ischemia improved with the GW7647 treatment, the global impact of this agonist was not assayed. Although these animals do not have significant weight changes, it would have been of interest to examine GW7647's effect on muscle and liver metabolism as well as blood lipid levels. In the isolated heart model, systemic circulation and global influence are removed; however, clinically, as a child's heart recovers from ischemia, the circulating metabolites and hormones would influence cardiac functional recovery as well. Circulating fatty acid levels, potentially impacted by peripheral effects of GW7647, would also influence metabolic and subsequently functional recovery from ischemia. While the isolated working heart model demonstrates cardiac metabolic changes in isolation, it would be of interest to explore *in vivo* factors such as serum FFA levels, peripheral TG storage, and plasma hormonal levels in order to understand the global influence of GW7647 in the neonate animal.

The rabbit model is a hurdle to attaining protein expression profile. Numerous antibodies are raised in rabbit hosts, which increases the cross reactivity of the antibody. Monoclonal antibodies appear to produce better results. Monoclonal antibodies originate from a reaction to a single epitope of an antigen of interest. Therefore, these antibodies are highly specific. The likelihood of the monoclonal antibody cross reacting with proteins with similar binding sides decreases as

opposed to polyclonal antibodies. Polyclonal antibodies, though raised against the same antigen, are derived from pooling antibodies from several sources. These antibodies may react to different epitopes. While these antibodies have increased sensitivity to the antigen compared to a monoclonal antibody, its specificity decreases. In fact, polyclonal antibodies may have an increased chance of cross reacting to another protein that may share a similar sequence. Alternatively, when possible, antibodies raised in mice or rats were used.

However, certain proteins remained non-amenable to Western blotting. Therefore, in attempts to elucidate a more detailed metabolic and expressional profile in these hearts, mRNA expression was also evaluated. In light of the limitations of RT-PCR, in combination with other evidence, this study attempted to illustrate the impact of cardiac hypertrophy on neonatal heart metabolism and the effects of PPAR α agonism. In order to provide further evidence to validate mRNA expressional data, it would be preferred to demonstrate the same changes in another animal model from which protein expression can be easily demonstrated.

Enzyme activity was another method this study pursued. In contrast to the primary study on neonatal cardiac hypertrophy in chapter 4, this present study assayed CPT-1 activity to illustrate cardiac hypertrophy on CPT-1 expressional changes via uninhibited activity assay. This method overcame the limitation of CPT-1 Western blotting. Thus, enzyme activity assays were a means to

overcoming limitations of antibody availability and tissue compatibility. However, as enzyme activity assays are much more complicated and time consuming, the present study was limited by number of assays that may be performed in a timely fashion. To add, of these assays, numerous of them are surrogate markers and remain quite artificial. For instance, for CPT-1 activity, the present study was unable to determine the degree of inhibition it undergoes from mal-CoA. CPT-1 is not irreversibly inhibited by mal-CoA, which is labile and prone to degradation during the processing of the tissue for protein extraction. Therefore, this assay determined only the total, uninhibited, CPT-1 activity *in vitro*. Nonetheless, future studies using the same animal model should find enzyme activity assays an asset.

This study partly dissected the glucose and FA transport in the hypertrophied and GW7647-treated hypertrophied neonatal hearts via the expression patterns of LPL, GLUT1, GLUT4. Although the findings are interesting, the translocation of these proteins was not assayed. The results demonstrated the chronic impact of hypertrophy and GW7647 agonism, but the whether hypertrophy or GW7647 treatment impacts the acute translocation process is an aspect not examined. As the translocation of these proteins play an important part to their efficacy, further investigation into their transport would elucidate a more meaningful role in their expressional changes.

5.7 References

1. Minich LL, Atz AM, Colan SD, Sleeper LA, Mital S, Jagers J, Margossian R, Prakash A, Li JS, Cohen MS, Lacro RV, Klein GL, Hawkins JA, Pediatric Heart Network I 2010 Partial and transitional atrioventricular septal defect outcomes. *Ann Thorac Surg* 89:530-536.
2. Molina Hazan V, Gonen Y, Vardi A, Keidan I, Mishali D, Rubinshtein M, Yakov Y, Paret G 2010 Blood lactate levels differ significantly between surviving and nonsurviving patients within the same risk-adjusted Classification for Congenital Heart Surgery (RACHS-1) group after pediatric cardiac surgery. *Pediatr Cardiol* 31:952-960.
3. Basaran M, Sever K, Kafali E, Ugurlucan M, Sayin OA, Tansel T, Alpagut U, Dayioglu E, Onursal E 2006 Serum lactate level has prognostic significance after pediatric cardiac surgery. *J Cardiothorac Vasc Anesth* 20:43-47.
4. Cheifetz IM, Kern FH, Schulman SR, Greeley WJ, Ungerleider RM, Meliones JN 1997 Serum lactates correlate with mortality after operations for complex congenital heart disease. *Ann Thorac Surg* 64:735-738.
5. Allen BS 2004 Pediatric myocardial protection: a cardioplegic strategy is the "solution". *Semin Thorac Cardiovasc Surg Pediatr Card Surg Annu* 7:141-154.
6. Durandy Y 2008 Pediatric myocardial protection. *Curr Opin Cardiol* 23:85-90.

7. Allen BS 2004 Pediatric myocardial protection: where do we stand? *J Thorac Cardiovasc Surg* 128:11-13.
8. Allen BS, Barth MJ, Ilbawi MN 2001 Pediatric myocardial protection: an overview. *Semin Thorac Cardiovasc Surg* 13:56-72.
9. Bolling K, Kronon M, Allen BS, Ramon S, Wang T, Hartz RS, Feinberg H 1996 Myocardial protection in normal and hypoxically stressed neonatal hearts: the superiority of hypocalcemic versus normocalcemic blood cardioplegia. *J Thorac Cardiovasc Surg* 112:1193-1200; discussion 1200-1191.
10. Bolling K, Kronon M, Allen BS, Wang T, Ramon S, Feinberg H 1997 Myocardial protection in normal and hypoxically stressed neonatal hearts: the superiority of blood versus crystalloid cardioplegia. *J Thorac Cardiovasc Surg* 113:994-1003; discussion 1003-1005.
11. Welke KF, Diggs BS, Karamlou T, Ungerleider RM 2009 Comparison of pediatric cardiac surgical mortality rates from national administrative data to contemporary clinical standards. *Ann Thorac Surg* 87:216-222; discussion 222-213.
12. Butler TL, Egan JR, Graf FG, Au CG, McMahon AC, North KN, Winlaw DS 2009 Dysfunction induced by ischemia versus edema: does edema matter? *J Thorac Cardiovasc Surg* 138:141-147, 147 e141.
13. Caputo M, Modi P, Imura H, Pawade A, Parry AJ, Suleiman MS, Angelini GD 2002 Cold blood versus cold crystalloid cardioplegia for repair of

- ventricular septal defects in pediatric heart surgery: a randomized controlled trial. *Ann Thorac Surg* 74:530-534; discussion 535.
14. Modi P, Suleiman MS, Reeves B, Pawade A, Parry AJ, Angelini GD, Caputo M 2004 Myocardial metabolic changes during pediatric cardiac surgery: a randomized study of 3 cardioplegic techniques. *J Thorac Cardiovasc Surg* 128:67-75.
 15. Imura H, Caputo M, Parry A, Pawade A, Angelini GD, Suleiman MS 2001 Age-dependent and hypoxia-related differences in myocardial protection during pediatric open heart surgery. *Circulation* 103:1551-1556.
 16. Staels B, Schoonjans K, Fruchart JC, Auwerx J 1997 The effects of fibrates and thiazolidinediones on plasma triglyceride metabolism are mediated by distinct peroxisome proliferator activated receptors (PPARs). *Biochimie* 79:95-99.
 17. Simpson HS, Williamson CM, Olivecrona T, Pringle S, Maclean J, Lorimer AR, Bonnefous F, Bogaievsky Y, Packard CJ, Shepherd J 1990 Postprandial lipemia, fenofibrate and coronary artery disease. *Atherosclerosis* 85:193-202.
 18. Desager JP, Horsmans Y, Vandenplas C, Harvengt C 1996 Pharmacodynamic activity of lipoprotein lipase and hepatic lipase, and pharmacokinetic parameters measured in normolipidaemic subjects receiving ciprofibrate (100 or 200 mg/day) or micronised fenofibrate (200 mg/day) therapy for 23 days. *Atherosclerosis* 124 Suppl:S65-73.

19. Bonen A, Campbell SE, Benton CR, Chabowski A, Coort SL, Han XX, Koonen DP, Glatz JF, Luiken JJ 2004 Regulation of fatty acid transport by fatty acid translocase/CD36. *Proc Nutr Soc* 63:245-249.
20. Brandt JM, Djouadi F, Kelly DP 1998 Fatty acids activate transcription of the muscle carnitine palmitoyltransferase I gene in cardiac myocytes via the peroxisome proliferator-activated receptor alpha. *J Biol Chem* 273:23786-23792.
21. Mascaro C, Acosta E, Ortiz JA, Marrero PF, Hegardt FG, Haro D 1998 Control of human muscle-type carnitine palmitoyltransferase I gene transcription by peroxisome proliferator-activated receptor. *J Biol Chem* 273:8560-8563.
22. van der Lee KA, Vork MM, De Vries JE, Willemsen PH, Glatz JF, Reneman RS, Van der Vusse GJ, Van Bilsen M 2000 Long-chain fatty acid-induced changes in gene expression in neonatal cardiac myocytes. *J Lipid Res* 41:41-47.
23. Muoio DM, Way JM, Tanner CJ, Winegar DA, Kliewer SA, Houmard JA, Kraus WE, Dohm GL 2002 Peroxisome proliferator-activated receptor-alpha regulates fatty acid utilization in primary human skeletal muscle cells. *Diabetes* 51:901-909.
24. Lee GY, Kim NH, Zhao ZS, Cha BS, Kim YS 2004 Peroxisomal-proliferator-activated receptor alpha activates transcription of the rat hepatic

- malonyl-CoA decarboxylase gene: a key regulation of malonyl-CoA level. *Biochem J* 378:983-990.
25. Morissette MR, Howes AL, Zhang T, Heller Brown J 2003 Upregulation of GLUT1 expression is necessary for hypertrophy and survival of neonatal rat cardiomyocytes. *J Mol Cell Cardiol* 35:1217-1227.
 26. Bishop SP, Altschuld RA 1970 Increased glycolytic metabolism in cardiac hypertrophy and congestive failure. *Am J Physiol* 218:153-159.
 27. Taegtmeyer H, Overturf ML 1988 Effects of moderate hypertension on cardiac function and metabolism in the rabbit. *Hypertension* 11:416-426.
 28. Minchenko O, Opentanova I, Caro J 2003 Hypoxic regulation of the 6-phosphofructo-2-kinase/fructose-2,6-bisphosphatase gene family (PFKFB-1-4) expression in vivo. *FEBS Lett* 554:264-270.
 29. Ullah MS, Davies AJ, Halestrap AP 2006 The plasma membrane lactate transporter MCT4, but not MCT1, is up-regulated by hypoxia through a HIF-1 α -dependent mechanism. *J Biol Chem* 281:9030-9037.
 30. Evans RK, Schwartz DD, Gladden LB 2003 Effect of myocardial volume overload and heart failure on lactate transport into isolated cardiac myocytes. *J Appl Physiol* 94:1169-1176.
 31. Finck BN, Han X, Courtois M, Aimond F, Nerbonne JM, Kovacs A, Gross RW, Kelly DP 2003 A critical role for PPAR α -mediated lipotoxicity in the pathogenesis of diabetic cardiomyopathy: modulation by dietary fat content. *Proc Natl Acad Sci U S A* 100:1226-1231.

32. Hopkins TA, Sugden MC, Holness MJ, Kozak R, Dyck JR, Lopaschuk GD 2003 Control of cardiac pyruvate dehydrogenase activity in peroxisome proliferator-activated receptor- α transgenic mice. *Am J Physiol Heart Circ Physiol* 285:H270-276.
33. Lopaschuk GD, Collins-Nakai RL, Itoi T 1992 Developmental changes in energy substrate use by the heart. *Cardiovasc Res* 26:1172-1180.
34. Lopaschuk GD, Spafford MA, Marsh DR 1991 Glycolysis is predominant source of myocardial ATP production immediately after birth. *Am J Physiol* 261:H1698-1705.
35. Girard J, Ferre P, Pegorier JP, Duee PH 1992 Adaptations of glucose and fatty acid metabolism during perinatal period and suckling-weaning transition. *Physiol Rev* 72:507-562.
36. Onay-Besikci A, Sambandam N 2006 Malonyl CoA control of fatty acid oxidation in the newborn heart in response to increased fatty acid supply. *Can J Physiol Pharmacol* 84:1215-1222.
37. Makinde AO, Gamble J, Lopaschuk GD 1997 Upregulation of 5'-AMP-activated protein kinase is responsible for the increase in myocardial fatty acid oxidation rates following birth in the newborn rabbit. *Circ Res* 80:482-489.
38. Lopaschuk GD, Witters LA, Itoi T, Barr R, Barr A 1994 Acetyl-CoA carboxylase involvement in the rapid maturation of fatty acid oxidation in the newborn rabbit heart. *J Biol Chem* 269:25871-25878.

39. Panadero M, Herrera E, Bocos C 2000 Peroxisome proliferator-activated receptor-alpha expression in rat liver during postnatal development. *Biochimie* 82:723-726.
40. Skarka L, Bardova K, Brauner P, Flachs P, Jarkovska D, Kopecky J, Ostadal B 2003 Expression of mitochondrial uncoupling protein 3 and adenine nucleotide translocase 1 genes in developing rat heart: putative involvement in control of mitochondrial membrane potential. *J Mol Cell Cardiol* 35:321-330.
41. Ito M, Jaswal JS, Lam VH, Oka T, Zhang L, Beker DL, Lopaschuk GD, Rebeyka IM 2010 High levels of fatty acids increase contractile function of neonatal rabbit hearts during reperfusion following ischemia. *Am J Physiol Heart Circ Physiol* 298:H1426-1437.
42. Lopaschuk GD, Wambolt RB, Barr RL 1993 An imbalance between glycolysis and glucose oxidation is a possible explanation for the detrimental effects of high levels of fatty acids during aerobic reperfusion of ischemic hearts. *J Pharmacol Exp Ther* 264:135-144.
43. Engle SK, Solter PF, Credille KM, Bull CM, Adams S, Berna MJ, Schultze AE, Rothstein EC, Cockman MD, Pritt ML, Liu H, Lu Y, Chiang AY, Watson DE 2010 Detection of left ventricular hypertrophy in rats administered a peroxisome proliferator-activated receptor alpha/gamma dual agonist using natriuretic peptides and imaging. *Toxicol Sci* 114:183-192.

44. Duan SZ, Ivashchenko CY, Russell MW, Milstone DS, Mortensen RM 2005 Cardiomyocyte-specific knockout and agonist of peroxisome proliferator-activated receptor-gamma both induce cardiac hypertrophy in mice. *Circ Res* 97:372-379.
45. Ren L, Li Y, Tang R, Hu D, Sheng Z, Liu N 2010 The inhibitory effects of rosiglitazone on cardiac hypertrophy through modulating the renin-angiotensin system in diet-induced hypercholesterolemic rats. *Cell Biochem Funct* 28:58-65.
46. Linz W, Wohlfart P, Baader M, Breitschopf K, Falk E, Schafer HL, Gerl M, Kramer W, Rutten H 2009 The peroxisome proliferator-activated receptor-alpha (PPAR-alpha) agonist, AVE8134, attenuates the progression of heart failure and increases survival in rats. *Acta Pharmacol Sin* 30:935-946.
47. Ichihara S, Obata K, Yamada Y, Nagata K, Noda A, Ichihara G, Yamada A, Kato T, Izawa H, Murohara T, Yokota M 2006 Attenuation of cardiac dysfunction by a PPAR-alpha agonist is associated with down-regulation of redox-regulated transcription factors. *J Mol Cell Cardiol* 41:318-329.
48. Asai T, Okumura K, Takahashi R, Matsui H, Numaguchi Y, Murakami H, Murakami R, Murohara T 2006 Combined therapy with PPARalpha agonist and L-carnitine rescues lipotoxic cardiomyopathy due to systemic carnitine deficiency. *Cardiovasc Res* 70:566-577.

49. Brown PJ, Stuart LW, Hurley KP, Lewis MC, Winegar DA, Wilson JG, Wilkison WO, Ittoop OR, Willson TM 2001 Identification of a subtype selective human PPARalpha agonist through parallel-array synthesis. *Bioorg Med Chem Lett* 11:1225-1227.
50. Barr RL, Lopaschuk GD 1997 Direct measurement of energy metabolism in the isolated working rat heart. *J Pharmacol Toxicol Methods* 38:11-17.
51. Dyck JR, Berthiaume LG, Thomas PD, Kantor PF, Barr AJ, Barr R, Singh D, Hopkins TA, Voilley N, Prentki M, Lopaschuk GD 2000 Characterization of rat liver malonyl-CoA decarboxylase and the study of its role in regulating fatty acid metabolism. *Biochem J* 350 Pt 2:599-608.
52. Rosenblatt-Velin N, Lerch R, Papageorgiou I, Montessuit C 2004 Insulin resistance in adult cardiomyocytes undergoing dedifferentiation: role of GLUT4 expression and translocation. *FASEB J* 18:872-874.
53. Onay-Besikci A, Campbell FM, Hopkins TA, Dyck JR, Lopaschuk GD 2003 Relative importance of malonyl CoA and carnitine in maturation of fatty acid oxidation in newborn rabbit heart. *Am J Physiol Heart Circ Physiol* 284:H283-289.
54. Jaswal JS, Lund CR, Keung W, Beker DL, Rebeyka IM, Lopaschuk GD 2010 Isoproterenol stimulates 5'-AMP-activated protein kinase and fatty acid oxidation in neonatal hearts. *Am J Physiol Heart Circ Physiol* 299:H1135-1145.

55. Saiki Y, Lopaschuk GD, Dodge K, Yamaya K, Morgan C, Rebeyka IM 1998 Pyruvate augments mechanical function via activation of the pyruvate dehydrogenase complex in reperfused ischemic immature rabbit hearts. *J Surg Res* 79:164-169.
56. Campbell FM, Kozak R, Wagner A, Altarejos JY, Dyck JR, Belke DD, Severson DL, Kelly DP, Lopaschuk GD 2002 A role for peroxisome proliferator-activated receptor alpha (PPARalpha) in the control of cardiac malonyl-CoA levels: reduced fatty acid oxidation rates and increased glucose oxidation rates in the hearts of mice lacking PPARalpha are associated with higher concentrations of malonyl-CoA and reduced expression of malonyl-CoA decarboxylase. *J Biol Chem* 277:4098-4103.
57. Sambandam N, Morabito D, Wagg C, Finck BN, Kelly DP, Lopaschuk GD 2006 Chronic activation of PPARalpha is detrimental to cardiac recovery after ischemia. *Am J Physiol Heart Circ Physiol* 290:H87-95.
58. Itoi T, Lopaschuk GD 1993 The contribution of glycolysis, glucose oxidation, lactate oxidation, and fatty acid oxidation to ATP production in isolated biventricular working hearts from 2-week-old rabbits. *Pediatr Res* 34:735-741.
59. Wittnich C, Su J, Boscarino C, Belanger M 2006 Age-related differences in myocardial hydrogen ion buffering during ischemia. *Mol Cell Biochem* 285:61-67.

60. Murashita T, Borgers M, Hearse DJ 1992 Developmental changes in tolerance to ischaemia in the rabbit heart: disparity between interpretations of structural, enzymatic and functional indices of injury. *J Mol Cell Cardiol* 24:1143-1154.
61. Steinmetz M, Quentin T, Poppe A, Paul T, Jux C 2005 Changes in expression levels of genes involved in fatty acid metabolism: upregulation of all three members of the PPAR family (alpha, gamma, delta) and the newly described adiponectin receptor 2, but not adiponectin receptor 1 during neonatal cardiac development of the rat. *Basic Res Cardiol* 100:263-269.
62. Brown NF, Weis BC, Husti JE, Foster DW, McGarry JD 1995 Mitochondrial carnitine palmitoyltransferase I isoform switching in the developing rat heart. *J Biol Chem* 270:8952-8957.
63. Leone TC, Weinheimer CJ, Kelly DP 1999 A critical role for the peroxisome proliferator-activated receptor alpha (PPARalpha) in the cellular fasting response: the PPARalpha-null mouse as a model of fatty acid oxidation disorders. *Proc Natl Acad Sci U S A* 96:7473-7478.
64. Muoio DM, MacLean PS, Lang DB, Li S, Houmard JA, Way JM, Winegar DA, Corton JC, Dohm GL, Kraus WE 2002 Fatty acid homeostasis and induction of lipid regulatory genes in skeletal muscles of peroxisome proliferator-activated receptor (PPAR) alpha knock-out mice. Evidence for compensatory regulation by PPAR delta. *J Biol Chem* 277:26089-26097.

65. Barger PM, Brandt JM, Leone TC, Weinheimer CJ, Kelly DP 2000 Deactivation of peroxisome proliferator-activated receptor-alpha during cardiac hypertrophic growth. *J Clin Invest* 105:1723-1730.
66. Sack MN, Disch DL, Rockman HA, Kelly DP 1997 A role for Sp and nuclear receptor transcription factors in a cardiac hypertrophic growth program. *Proc Natl Acad Sci U S A* 94:6438-6443.
67. Luptak I, Balschi JA, Xing Y, Leone TC, Kelly DP, Tian R 2005 Decreased contractile and metabolic reserve in peroxisome proliferator-activated receptor-alpha-null hearts can be rescued by increasing glucose transport and utilization. *Circulation* 112:2339-2346.
68. Holness MJ, Smith ND, Bulmer K, Hopkins T, Gibbons GF, Sugden MC 2002 Evaluation of the role of peroxisome-proliferator-activated receptor alpha in the regulation of cardiac pyruvate dehydrogenase kinase 4 protein expression in response to starvation, high-fat feeding and hyperthyroidism. *Biochem J* 364:687-694.
69. Panagia M, Gibbons GF, Radda GK, Clarke K 2005 PPAR-alpha activation required for decreased glucose uptake and increased susceptibility to injury during ischemia. *Am J Physiol Heart Circ Physiol* 288:H2677-2683.
70. Watanabe K, Fujii H, Takahashi T, Kodama M, Aizawa Y, Ohta Y, Ono T, Hasegawa G, Naito M, Nakajima T, Kamijo Y, Gonzalez FJ, Aoyama T 2000 Constitutive regulation of cardiac fatty acid metabolism through

- peroxisome proliferator-activated receptor alpha associated with age-dependent cardiac toxicity. *J Biol Chem* 275:22293-22299.
71. Quaglietta D, Belanger MP, Wittnich C 2008 Ventricle-specific metabolic differences in the newborn piglet myocardium in vivo and during arrested global ischemia. *Pediatr Res* 63:15-19.
 72. Young ME, Laws FA, Goodwin GW, Taegtmeyer H 2001 Reactivation of peroxisome proliferator-activated receptor alpha is associated with contractile dysfunction in hypertrophied rat heart. *J Biol Chem* 276:44390-44395.
 73. Swanton EM, Saggerson ED 1997 Effects of adrenaline on triacylglycerol synthesis and turnover in ventricular myocytes from adult rats. *Biochem J* 328 (Pt 3):913-922.
 74. Haemmerle G, Lass A, Zimmermann R, Gorkiewicz G, Meyer C, Rozman J, Heldmaier G, Maier R, Theussl C, Eder S, Kratky D, Wagner EF, Klingenspor M, Hoefler G, Zechner R 2006 Defective lipolysis and altered energy metabolism in mice lacking adipose triglyceride lipase. *Science* 312:734-737.
 75. Zechner R, Kienesberger PC, Haemmerle G, Zimmermann R, Lass A 2009 Adipose triglyceride lipase and the lipolytic catabolism of cellular fat stores. *J Lipid Res* 50:3-21.
 76. Lake AC, Sun Y, Li JL, Kim JE, Johnson JW, Li D, Revett T, Shih HH, Liu W, Paulsen JE, Gimeno RE 2005 Expression, regulation, and triglyceride

- hydrolase activity of Adiponutrin family members. *J Lipid Res* 46:2477-2487.
77. Kershaw EE, Hamm JK, Verhagen LA, Peroni O, Katic M, Flier JS 2006 Adipose triglyceride lipase: function, regulation by insulin, and comparison with adiponutrin. *Diabetes* 55:148-157.
78. Yue TL, Bao W, Jucker BM, Gu JL, Romanic AM, Brown PJ, Cui J, Thudium DT, Boyce R, Burns-Kurtis CL, Mirabile RC, Aravindhan K, Ohlstein EH 2003 Activation of peroxisome proliferator-activated receptor-alpha protects the heart from ischemia/reperfusion injury. *Circulation* 108:2393-2399.
79. Krishnan J, Suter M, Windak R, Krebs T, Felley A, Montessuit C, Tokarska-Schlattner M, Aasum E, Bogdanova A, Perriard E, Perriard JC, Larsen T, Pedrazzini T, Krek W 2009 Activation of a HIF1alpha-PPARGamma axis underlies the integration of glycolytic and lipid anabolic pathways in pathologic cardiac hypertrophy. *Cell Metab* 9:512-524.
80. Narravula S, Colgan SP 2001 Hypoxia-inducible factor 1-mediated inhibition of peroxisome proliferator-activated receptor alpha expression during hypoxia. *J Immunol* 166:7543-7548.
81. Kim JW, Tchernyshyov I, Semenza GL, Dang CV 2006 HIF-1-mediated expression of pyruvate dehydrogenase kinase: a metabolic switch required for cellular adaptation to hypoxia. *Cell Metab* 3:177-185.

82. Papandreou I, Cairns RA, Fontana L, Lim AL, Denko NC 2006 HIF-1 mediates adaptation to hypoxia by actively downregulating mitochondrial oxygen consumption. *Cell Metab* 3:187-197.
83. Listenberger LL, Schaffer JE 2002 Mechanisms of lipoapoptosis: implications for human heart disease. *Trends Cardiovasc Med* 12:134-138.
84. Dyntar D, Eppenberger-Eberhardt M, Maedler K, Pruschy M, Eppenberger HM, Spinass GA, Donath MY 2001 Glucose and palmitic acid induce degeneration of myofibrils and modulate apoptosis in rat adult cardiomyocytes. *Diabetes* 50:2105-2113.
85. Zhou YT, Grayburn P, Karim A, Shimabukuro M, Higa M, Baetens D, Orci L, Unger RH 2000 Lipotoxic heart disease in obese rats: implications for human obesity. *Proc Natl Acad Sci U S A* 97:1784-1789.
86. Vikramadithyan RK, Hirata K, Yagyu H, Hu Y, Augustus A, Homma S, Goldberg IJ 2005 Peroxisome proliferator-activated receptor agonists modulate heart function in transgenic mice with lipotoxic cardiomyopathy. *J Pharmacol Exp Ther* 313:586-593.
87. Jucker BM, Doe CP, Schnackenberg CG, Olzinski AR, Maniscalco K, Williams C, Hu TC, Lenhard SC, Costell M, Bernard R, Sarov-Blat L, Steplewski K, Willette RN 2007 PPARdelta activation normalizes cardiac substrate metabolism and reduces right ventricular hypertrophy in congestive heart failure. *J Cardiovasc Pharmacol* 50:25-34.

88. Sudarsanam TD, Jeyaseelan L, Thomas K, John G 2005 Predictors of mortality in mechanically ventilated patients. *Postgrad Med J* 81:780-783.
89. Gaies MG, Gurney JG, Yen AH, Napoli ML, Gajarski RJ, Ohye RG, Charpie JR, Hirsch JC 2010 Vasoactive-inotropic score as a predictor of morbidity and mortality in infants after cardiopulmonary bypass. *Pediatr Crit Care Med* 11:234-238.

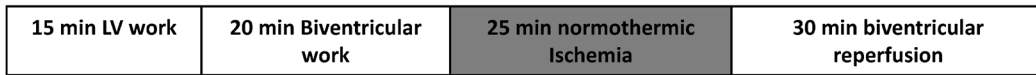
5.8 Figures

Figure 5-1: Bi-ventricular Perfusion of 21-day-old Rabbit Hearts. A) Schematic of the perfusion protocol. B) Normalized LV and RV functions based on (HR x (AoPSP + PVPSP)) demonstrating the effects of hypertrophy (triangle, n = 13) and hypertrophy treated with GW7647 (grey circle, n = 8) compared to control (open circle, n = 20) when given 25 min of global no flow ischemia. C) Percent recovery comparing functional recovery after 30 min reperfusion to post-ischemic function at 35 min. Hypertrophy decreased LV and RV function during 30 min reperfusion, significantly $*(P<0.05)$, when compared to control hearts. GW7647 reverts the decreased function caused by hypertrophy during reperfusion.

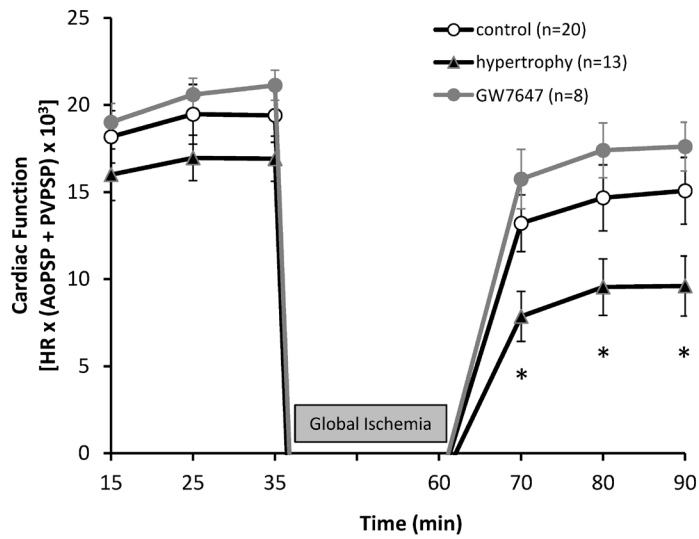
Fig 5-1

A

Fig 5-1



B



C

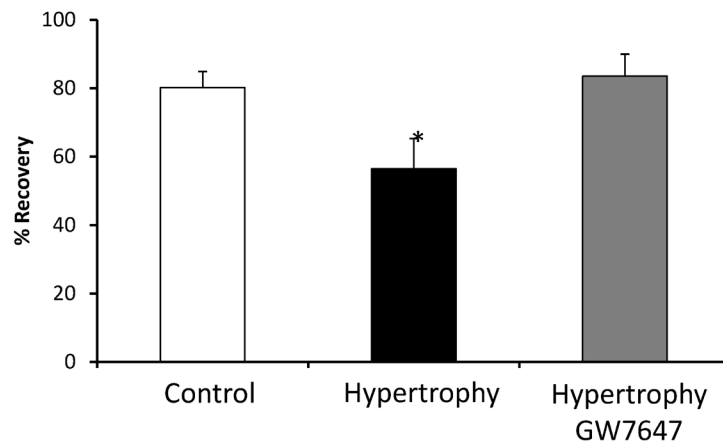


Figure 5-2: Pre-Ischemic and Post-ischemic Metabolic Rates Measured During Bi-ventricular Isolated Heart Perfusions. A) cardiac hypertrophy (■, n = 16) decreases pre-ischemic and post-ischemic palmitate oxidation rates when compared to control animals (□, n = 13, p < 0.05). GW7647 treatment (■, n = 24) recovers the palmitate oxidation rates in hypertrophied hearts to levels seen in control hearts. B) Hypertrophied hearts (n = 11) had increased pre-ischemia glycolysis rates. Control (n = 16) and hypertrophied (n = 11) hearts had elevated post-ischemic glycolytic rates, but GW7647-treated hypertrophied hearts (n = 9) did not have altered glycolytic rates from pre-ischemia. C) Neither pre-ischemia or post-ischemia glucose oxidation rates change in normal (n = 7), cardiac hypertrophy (n = 11), or GW7647-treated cardiac hypertrophy animals (n = 5). D) Calculated proton production using the formula (H^+ production = $2 \times (\text{average rate of glycolysis}) - (\text{rate of glucose oxidation})$). H^+ production rates are significantly higher during post-ischemic recovery compared to the pre-ischemic rates in control, hypertrophy, and hypertrophy treated with GW7647 hearts. * compared to pre-ischemia or post-ischemia control, ‡ compared to pre-ischemia or post-ischemia hypertrophy, † compared to the pre-ischemia value within the same treatment group, P<0.05

Fig 5-2

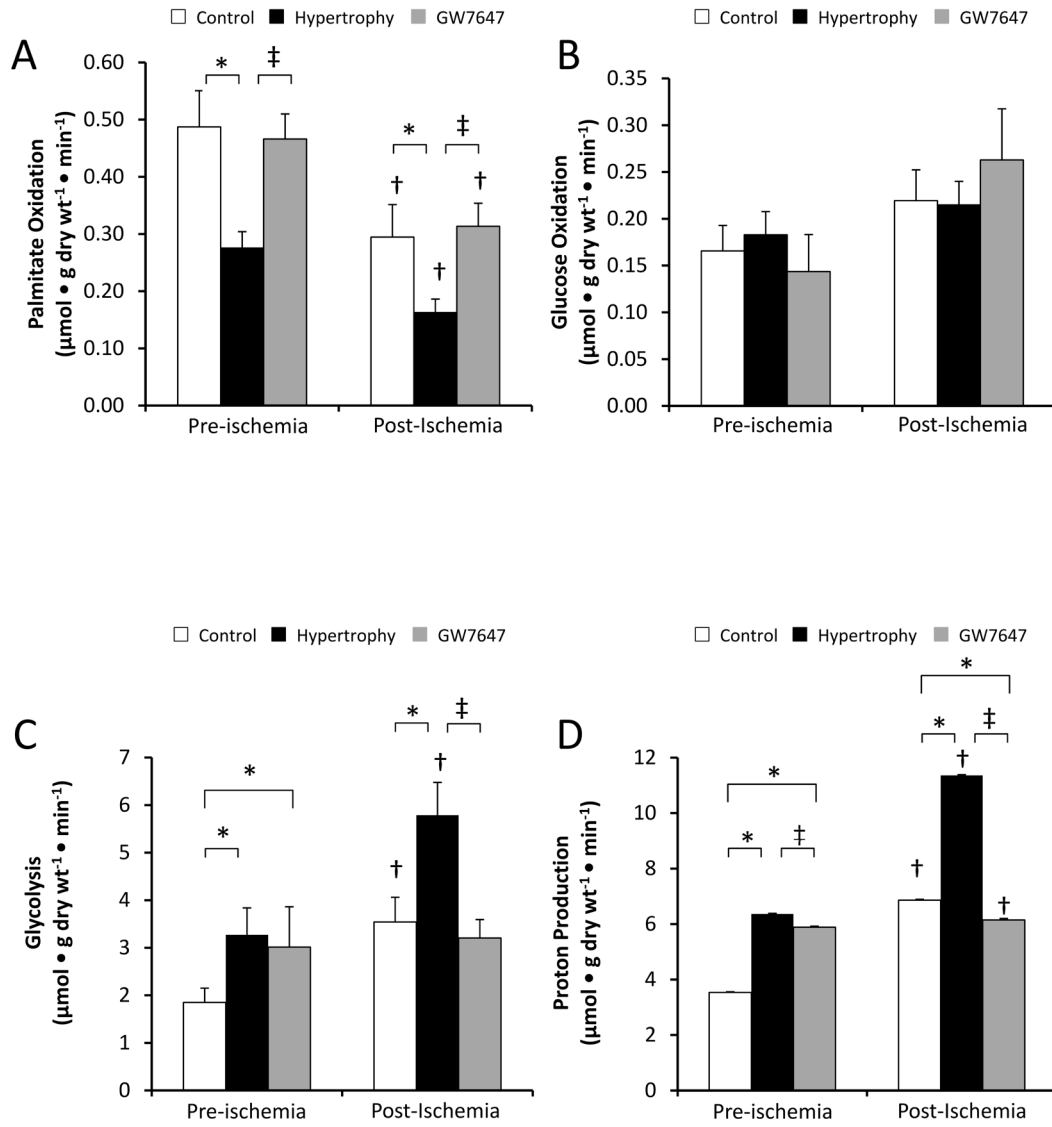
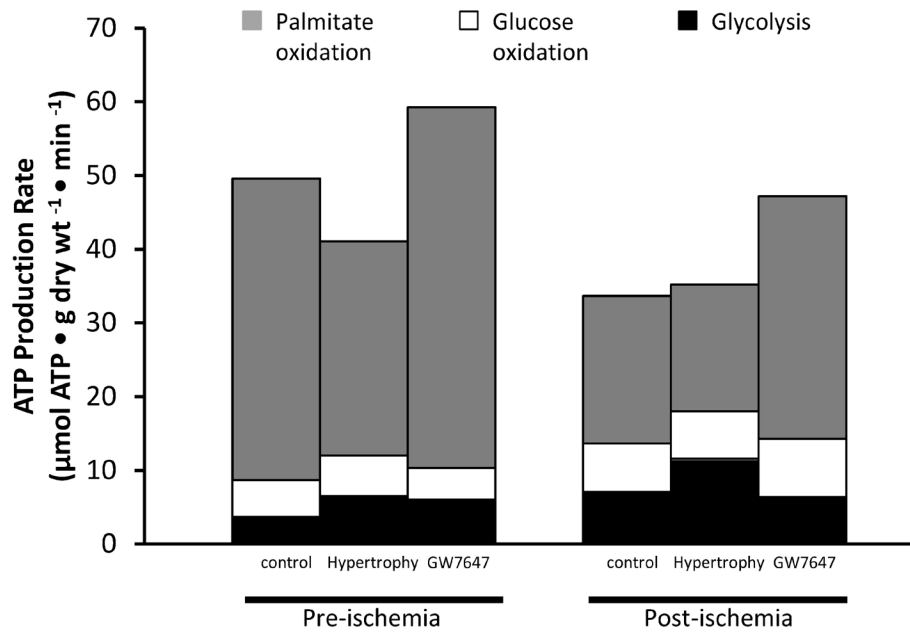


Figure 5-3: Calculated Steady State ATP and Acetyl-CoA Production Rates of Control, Hypertrophied, and GW7647-Treated Hypertrophied Hearts. A) Calculated steady state ATP production rates from palmitate oxidation (■, 105 mol ATP per of palmitate oxidized), glucose oxidation (□, 31 mol ATP per mol of glucose oxidized), and glycolysis (■, 2 mol ATP per mol of glucose passing through glycolysis); and B) calculated acetyl-CoA contribution to tricarboxylic (acid) cycle from glucose oxidation (□, 2 mol of acetyl-CoA per mol glucose oxidized) and palmitate oxidation (■, 8 mol of acetyl-CoA per mol of palmitate oxidized) during pre- and post-ischemia for control, hypertrophy, and hypertrophy treated with GW7647 compound hearts.

Fig 5-3

A



B

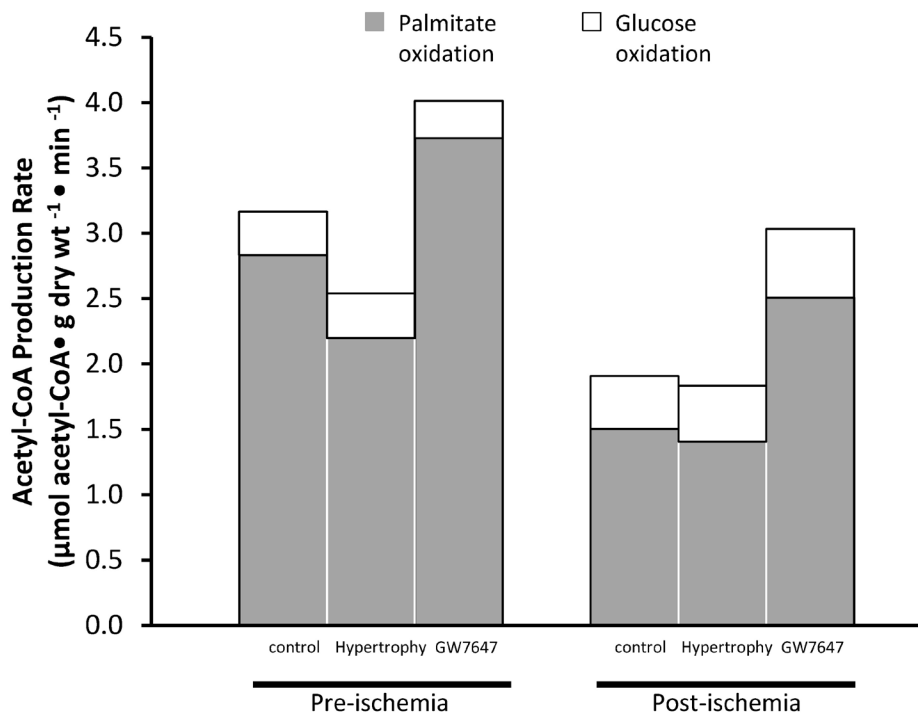


Figure 5-4: Expression of PPAR α and HIF-1 α in Control, Hypertrophied, and GW7647-Treated Hypertrophied Hearts. A) Relative PPAR α mRNA expression normalized to 18s expression and B) relative HIF-1 α protein expression in the LV and RV of control, hypertrophy, and GW7647 treated hypertrophied hearts. Arbitrary unit (AU); *compared control, † compared to the hypertrophy, P<0.05

Fig 5-4

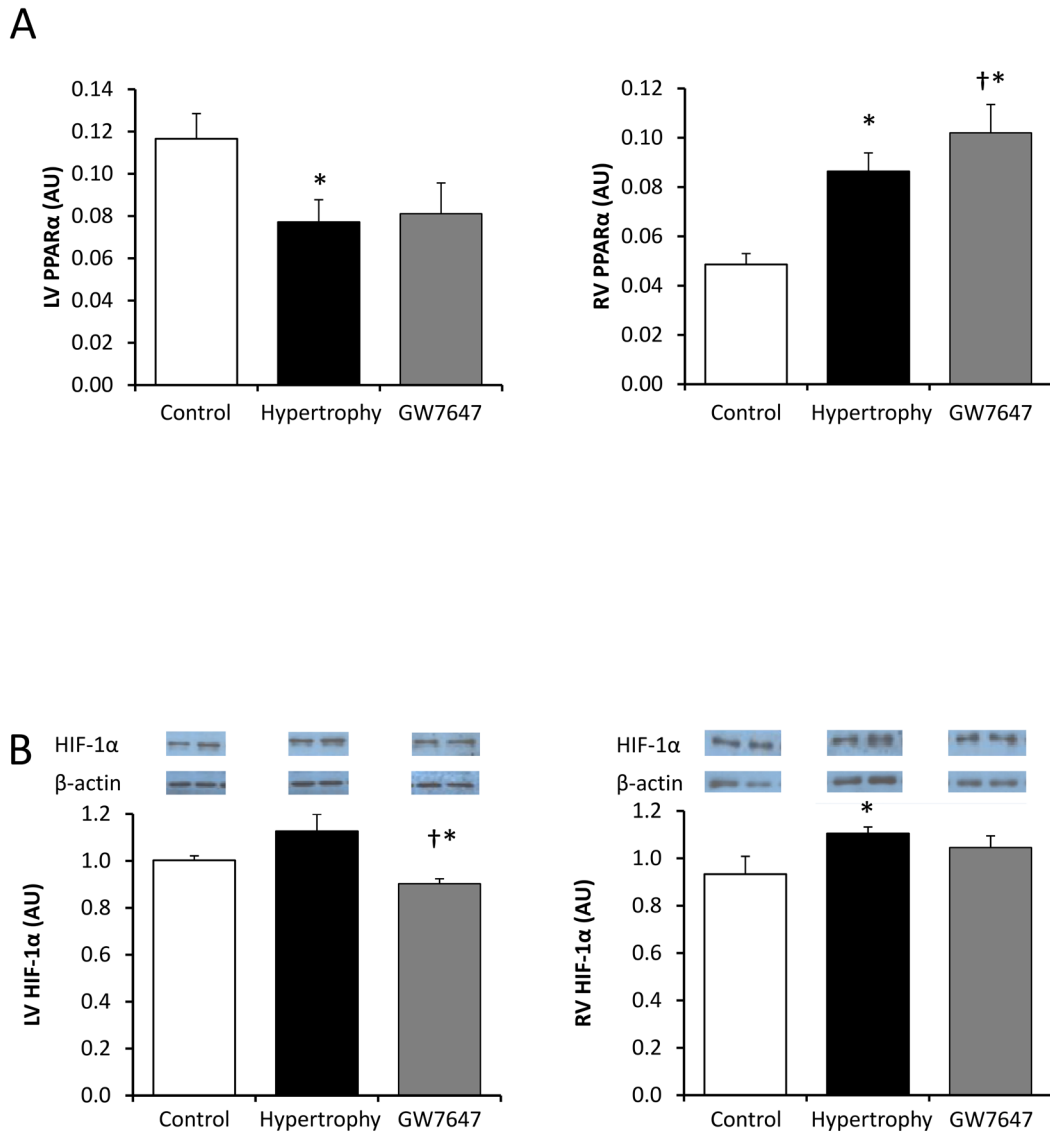


Figure 5-5: GW7647 Removes CPT-1 Inhibition in Hypertrophied Hearts. A) GW76474 (■) increases total LV and RV CPT-1 activity in hypertrophied hearts compared to control (□) and untreated hypertrophied hearts (■). B) LV and RV malonyl-CoA levels are decreased by GW7647 treatment of hypertrophied hearts. *compared control, † compared to the hypertrophy, P<0.05

Fig 5-5

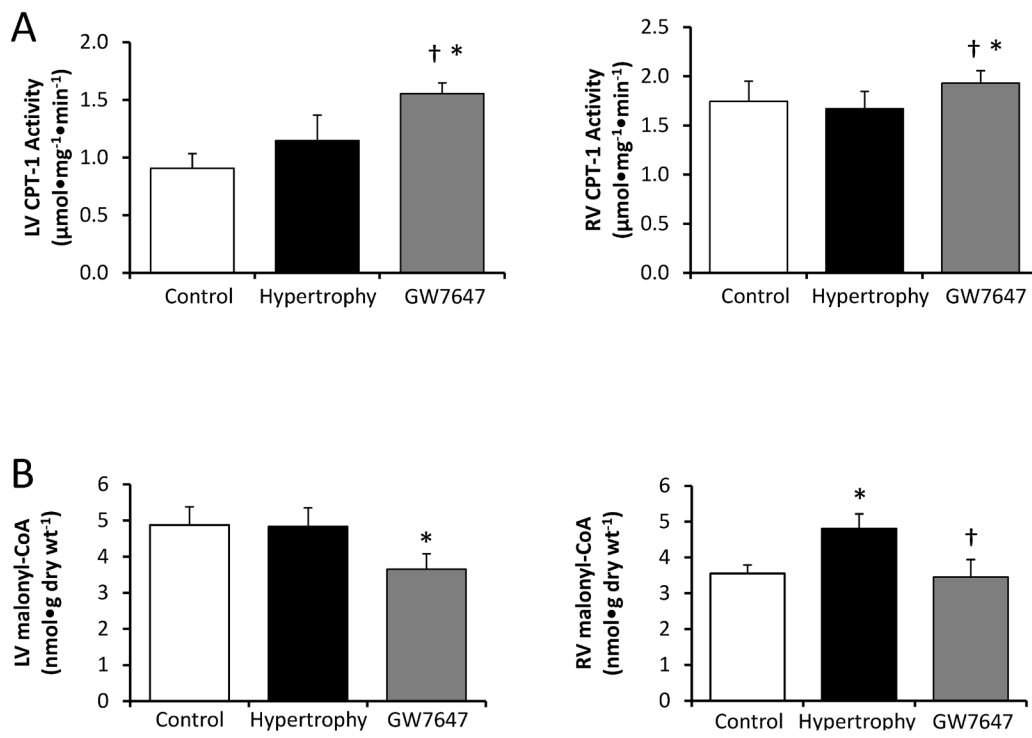


Figure 5-6: Malonyl-CoA Levels are Reflective of Collective Changes in MCD and ACC. A) MCD protein concentrations expressed in relative ratios to α -tubulin (arbitrary units, AU) and B) relative protein expression of total ACC (T-ACC, \square), phospho-ACC (P-ACC, \blacksquare), and C) phospho:total ACC ratio. Arbitrary unit (AU); *compared control, † compared to the hypertrophy, $P < 0.05$

Fig 5-6

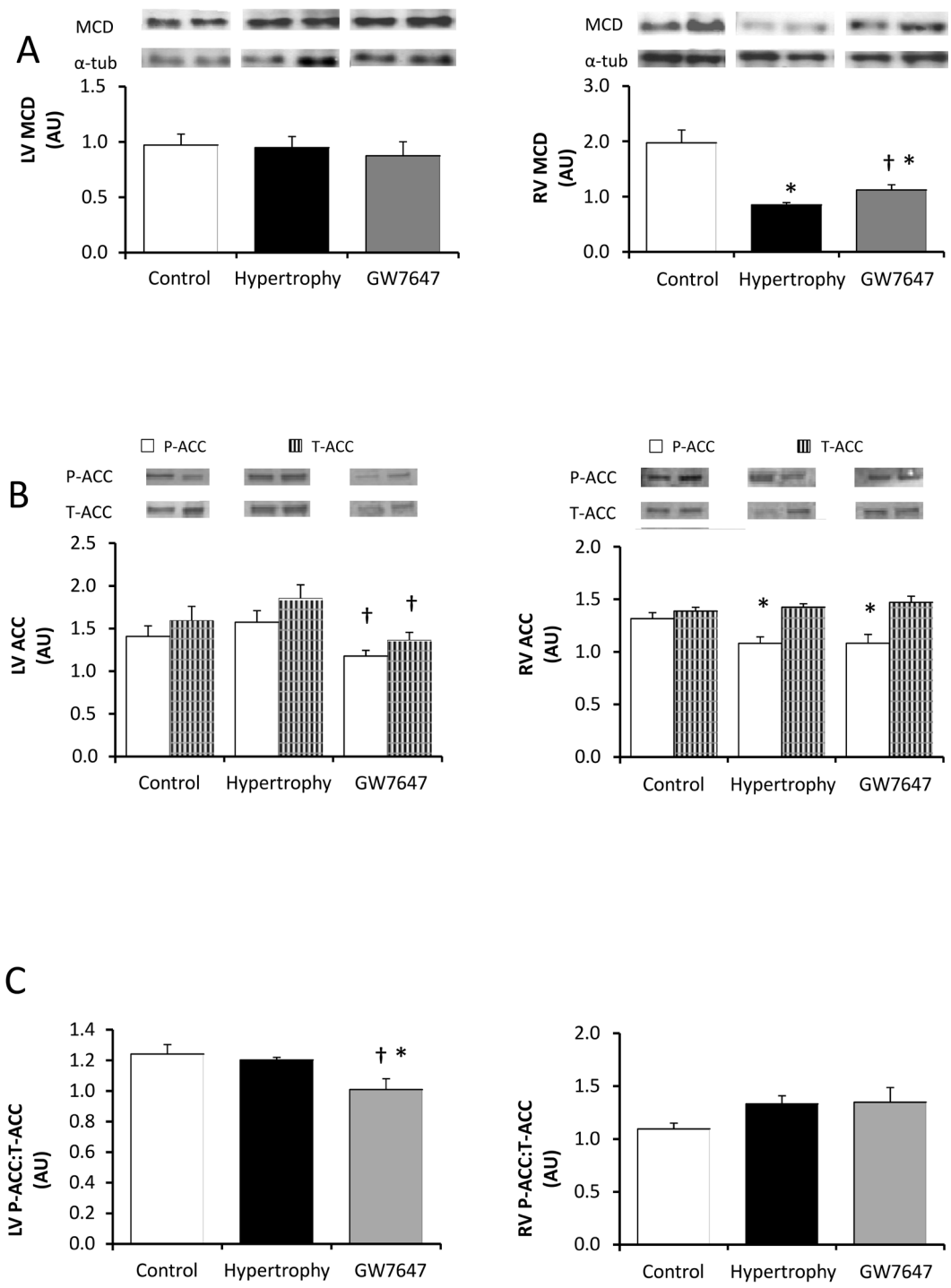


Figure 5-7: GW7647 Decreases Triacylglycerol Pools in the LV and RV Relative to Altered Enzyme Expression. A) Relative mRNA expression of CD36 normalized to 18s and B) relative ATGL protein expression change reflect the C) size of triacylglycerol pools in the LV and RV. Arbitrary unit (AU);*compared control, † compared to the hypertrophy, P<0.05

Fig 5-7

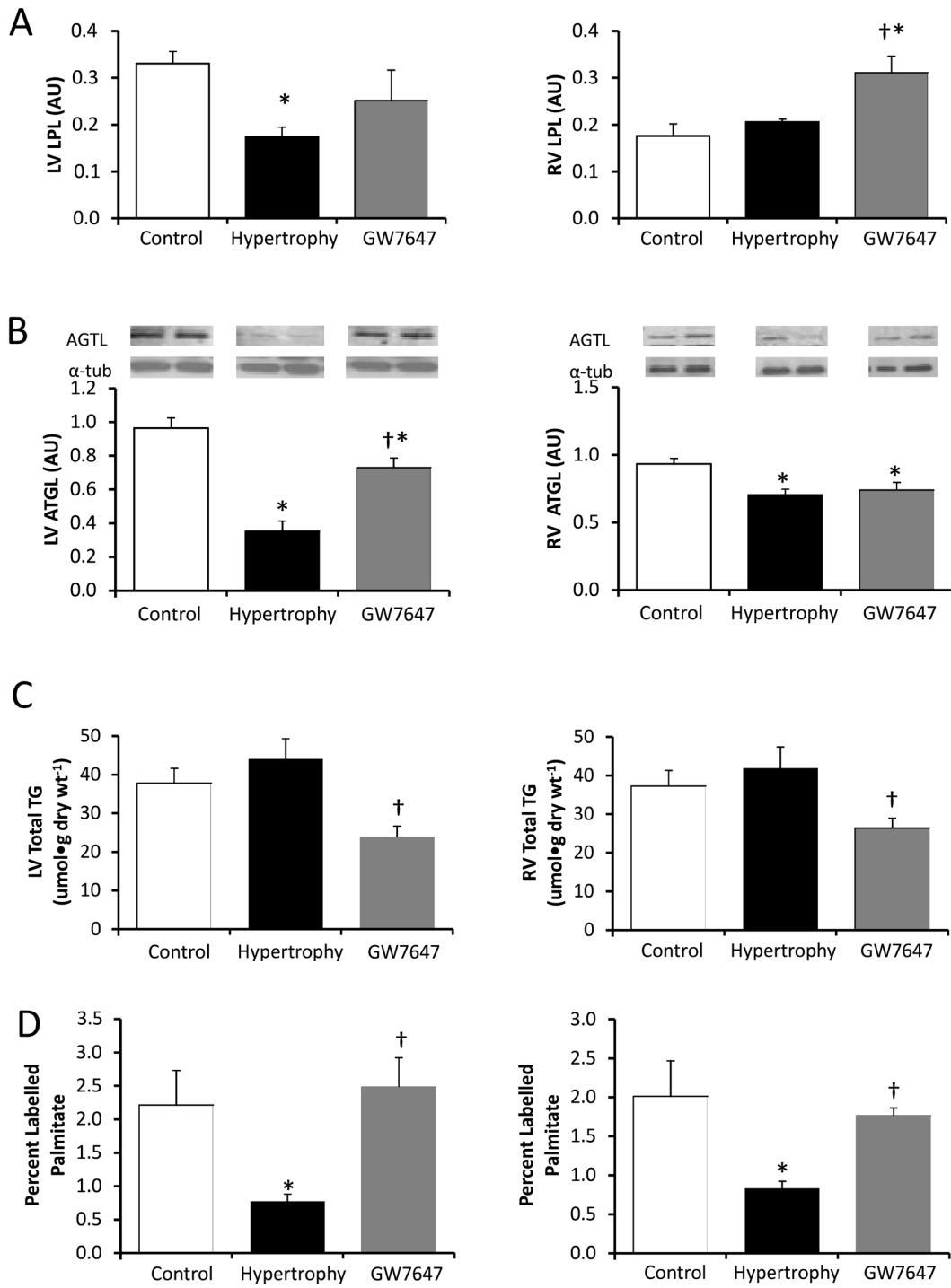


Figure 5-8: Effects of Hypertrophy and GW7647 Treatment on Regulators of Glucose Metabolism in the LV and RV in Control, Hypertrophied, and GW7647-Treated Hypertrophied Hearts. A) Relative GLUT4 , B) GLUT1, C) AKT protein expressions, and D) phospho:total AMPK ratio in the LV and RV to show changes to the insulin-glucose uptake axis. Arbitrary unit (AU);*compared control, † compared to the hypertrophy, P<0.05

Fig 5-8

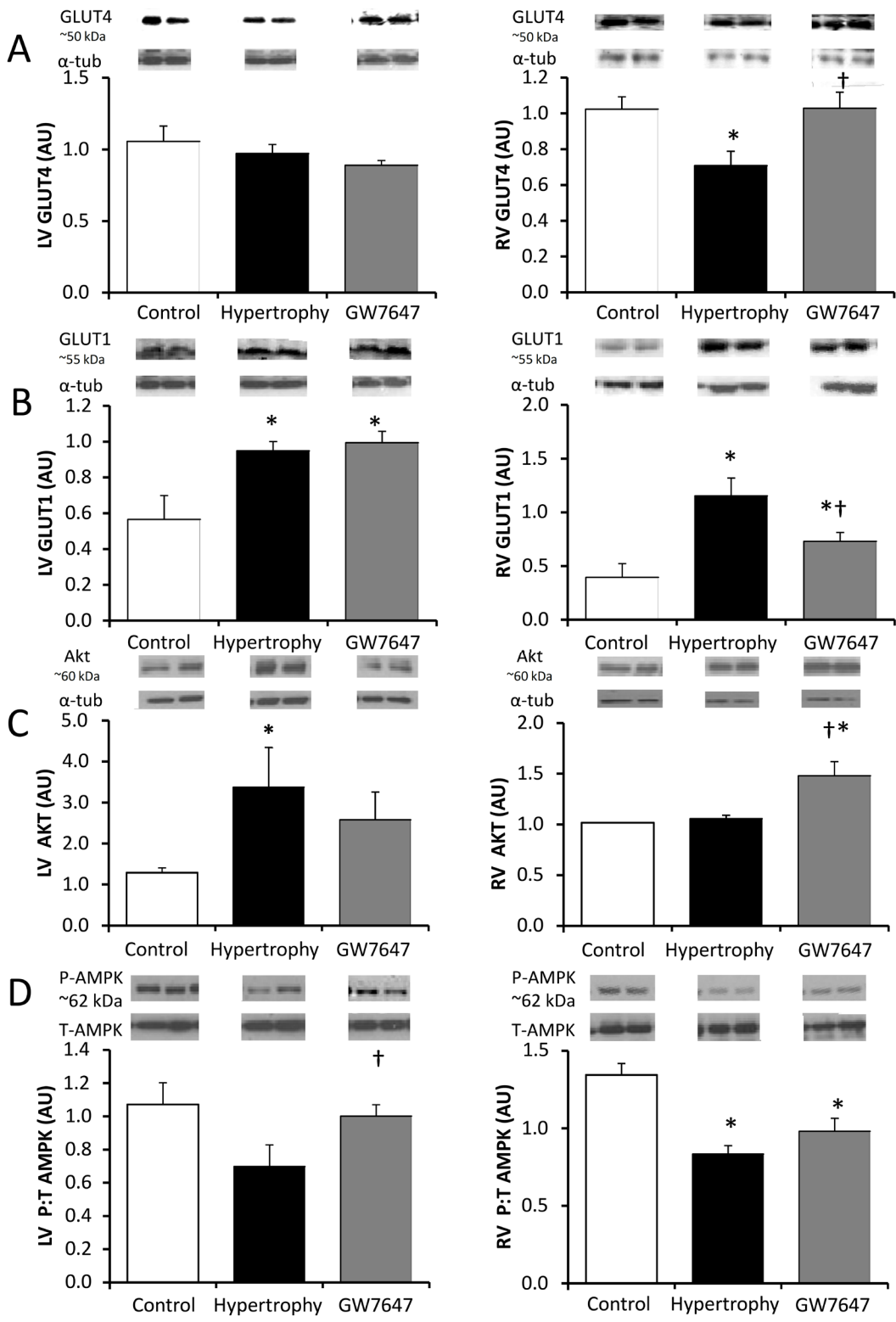
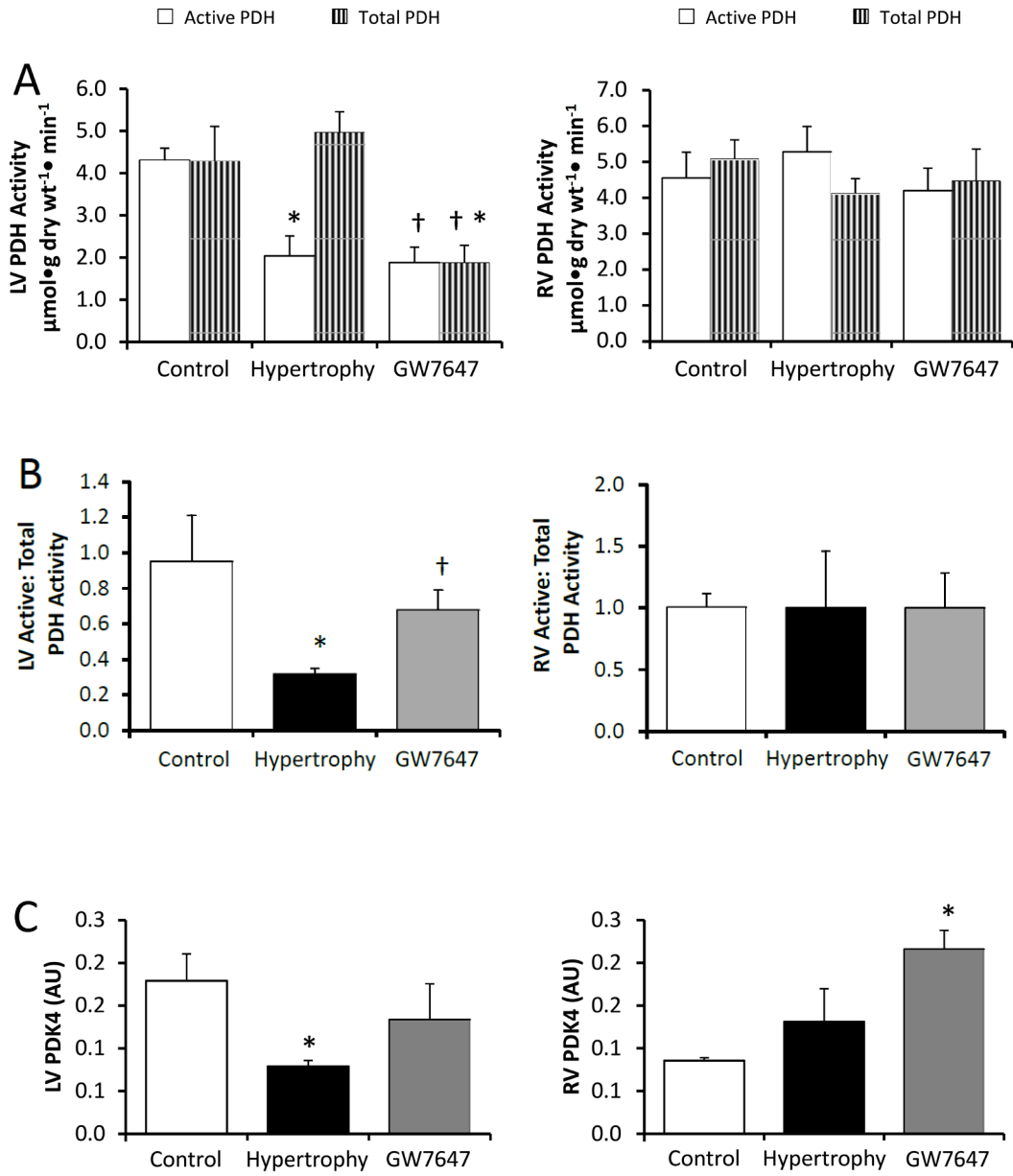


Figure 5-9: The Rate-Limiting Step to Glucose Oxidation is Controlled by PDH Activity. A) Active PDH activity (\square), total PDH activity (\blacksquare), B) active:total PDH activity ratio and D) relative PDK4 mRNA expression normalized to 18s. Arbitrary unit (AU);*compared control, † compared to the hypertrophy, $P < 0.05$

Fig 5-9



5.9 Tables

Table 5-1: Physical and Cardiac Parameters in vehicle- or GW7647-treated 20-day-old rabbits with of sham or aorto-caval fistula operation

	Sham	Hypertrophy	GW7647
n	9	13	7
IVC (mm)	2.42 ± 0.15	3.38 ± 0.11*	3.53 ± 0.09*
RVIDd (mm)	3.15 ± 0.16	3.42 ± 0.11*	3.71 ± 0.13*
LVIDd (mm)	7.83 ± 0.31	8.74 ± 0.28*	8.79 ± 0.31*
LVPW (mm)	1.76 ± 0.09	1.66 ± 0.07	1.84 ± 0.11
%EF	75.4 ± 1.1	67.4 ± 3.0*	76.5 ± 2.5†
Body Weight	422 ± 13	385 ± 28	422 ± 11
HW:BW (mg/g)	4.2 ± 0.10	4.7 ± 0.3*	4.8 ± 0.2*
LV:BW (mg/g)	1.85 ± 0.07	1.93 ± 0.11	2.12 ± 0.08*
SEP:BW (mg/g)	1.52 ± 0.07	1.60 ± 0.11	1.66 ± 0.06
RV:BW (mg/g)	0.86 ± 0.03	1.07 ± 0.09*	1.02 ± 0.04*

Diameter of the inferior vena cava (IVC) in millimetres (mm); right ventricular internal diameter during diastole (RVIDd); left ventricular internal diameter during diastole (LVIDd); left ventricular posterior wall thickness (LVPW); percent ejection fraction (%EF); body weight (BW); left ventricle (LV); septum (SEP); right ventricle (RV); * vs control; † vs hypertrophy; P>0.05.

Chapter 6

General Discussion

Pediatric cardiac surgery is a 20th century accomplishment (1,2) and has evolved over the past 100 or so years. During this development, although the principle defect causing the abnormal hemodynamics could be corrected, morbidity and mortality remained high. These corrective surgeries often require the neonatal heart to be arrested and exposed to ischemia to achieve the bloodless/motionless field of operation. These periods of ischemia can often exceed an hour. Post-surgical functional recovery depends not only on optimal intra-operative cardioprotection and techniques, peri-operative interventions are also vital (3-8). Post-surgical contractile dysfunction can manifest in up to 20% of pediatric patients following CHD surgery (9), and is the most common cause of post-surgical death (10,11). ~4% of mortality from pediatric cardiac surgery can be attributed to poor cardioprotection (5,12-15). Furthermore, post-surgical contractile dysfunction is largely related to ischemia. Several reports have demonstrated that prolonged ischemia increases lactate release, which in turn, correlates to higher rates of mortality and morbidity (16-20). Metabolic manipulation is a novel approach to reduce post-ischemic injury. It has been predominantly targeted against adult cardiac ischemia-reperfusion injury. Neonatal hearts are also subjected to ischemia-reperfusion during corrective surgery. However, as even the normal neonatal cardiac metabolism differs dramatically from that of the adult heart, the metabolic approach to cardioprotection in the neonatal heart may differ from that of the adult.

Furthermore, CHD may induce cardiac hypertrophy-related metabolic changes that further alter cardioprotective strategies employed in the neonatal heart.

6.1 Increasing FA Oxidation Improved Normal Neonatal Cardiac Post-ischemic Contractile Recovery

The prominence of FA oxidation in the developing neonatal myocardium has been demonstrated in several studies (21-24). This maturational dependence occurs as malonyl-CoA levels decline in the newborn period to release the inhibition on CPT-1 (23) and FA substrate supply increases from nursing (25); meanwhile, glucose metabolism contribute less to ATP production. To these findings, our studies of cardiac maturation adds that rabbit LV and RV MCD expression and activity also increased during the neonatal period between 1 to 21 days of age (fig 4-4). This further degraded and lowered malonyl-CoA levels in both ventricles to prevent the inhibition of CPT-1. Although a previous study did demonstrate the decline in malonyl-CoA levels in a 6-week-old rabbit heart, these rabbits are closer to an adolescent animal and falls neither in the neonatal period nor adulthood (26). With 21-day-old rabbit hearts, the normal dramatic decline in malonyl-CoA is apparent by three weeks of age. The rapid maturation of FA oxidation and decrease in glycolysis can be correlated to an increased PPAR α expression and reciprocal decreased HIF-1 α expression to illustrate the changes in transcriptional control that accompany these metabolic changes (fig 4-6).

With these changes to the neonatal heart, it was therefore surprising to find that supra-physiological levels of insulin stimulate FA oxidation further rather than the hypothesized inhibition of FA oxidation through decreasing AMPK and ACC phosphorylation. The combined product of high fat (1.2 mM palmitate) that caused a disjoint between AMPK and ACC signalling and the increased plasma membrane CD36 was linked to the improved post-ischemic contractile recovery in the neonatal heart. Whether other cardioprotective pathways were elicited to increase contractile function and therefore drive an increase in FA oxidation require further studies. However, as demonstrated previously, (22,27) as well as here, lowered steady state ATP production rates in the neonatal heart is associated with worsen post-ischemic recovery. This energy deficit can be rescued by increasing FA oxidation (22) or pyruvate oxidation (28). In contrast, dichloroacetate (DCA) was unable to improve contractile recovery (27). It was thought that though glucose oxidation rates were increased from basal rates in the 7-day-old rabbit heart, the increased rates were incomparable to those in the 6-week-old rabbit heart, in which DCA did improve contractile recovery (27). Therefore, the authors suggested that the increased glucose oxidation rates remained insufficient to the amount of ATP needed in the post-ischemic period.

DCA, at the dosage used, may not have sufficiently stimulated glucose oxidation, but pyruvate supplementation has been shown to improve post-ischemic contractile function in neonatal rabbit hearts (28). Although in this latter study, no substrate metabolic rates were assessed, PDH activity was increased

significantly in the presence of pyruvate. The malate/aspartate shuttle capacity decreases dramatically in the neonatal period (29) to minimize anapleurotic flux in the neonatal heart. Therefore, assuming minimal anapleurotic flux, it may be said that increased glucose oxidation rates achieved by DCA stimulation was only a fifth of the PDH activity caused by pyruvate supplementation when glucose oxidation is equated to PDH activity stoichiometrically (27,28). Although DCA was unable improve contractile recovery, increasing glucose oxidation, such as by pyruvate supplementation, represents a method of metabolic manipulation to improve neonatal post-ischemic recovery. However, augmenting FA oxidation offers further advantage over increasing glucose oxidation rates as post-ischemic circulating FAs are elevated, which exposes the myocardium to high FA levels (30). Furthermore, whether strict peri-operative glycemic control increases post-operative morbidity and mortality has been controversial (31-35). Therefore, augmenting FA oxidation is a viable cardioprotective strategy for neonatal cardiac ischemia.

6.2 A Model of Neonatal Cardiac Pathological Hypertrophy

Surgical intervention to correct CHDs necessitated the need to understand neonatal cardiac ischemia and reperfusion. However, a drawback persists in that most studies used normal neonatal hearts not subjected to pathological remodelling. Pathological cardiac hypertrophy can develop secondary to CHDs. According to Health Canada and the Heart and Stroke Foundation, CHDs are the

most common structural anomalies with an incidence of 1 in 100 newborns (36). Globally, 1 million children are born with a CHD (37). Of the various CHDs, ventricular septal (VSD) and atrial septal defects (ASD) are the most prominent representing 29% and 21% of all CHDs, which can lead to volume-overload cardiac hypertrophy (38).

Adult cardiac hypertrophy reverts cardiac metabolism towards a fetal-like metabolic profile dependent largely on glycolysis (39,40). This reversion is due to a decrease in oxidative phosphorylation. In a neonatal piglet model of patent ductus arteriosus, volume-overload resulted in cardiac hypertrophy accompanied by a decrease in AMPK expression corresponding to continually high ACC activity despite maturation (41). Normally, AMPK expression and activity increases during the neonatal period and corresponds to high rates of FA oxidation (42). ACC activity as well as malonyl-CoA levels remained higher in these hypertrophied hearts suggesting that FA oxidation rates were likely suppressed and the maturation of cardiac metabolism was delayed. However, metabolic rates were not assayed in these hearts. Therefore, a relevant model of neonatal cardiac hypertrophy is vital to elucidate the underlying mechanism involved in the remodelling process as well as whether cardiac metabolism was actually affected.

This neonatal cardiac hypertrophy model here most closely represents CHDs with left-to-right lesions such as ASD, VSD, and large patent ductus arteriosus

(43). VSDs and ASDs may stand alone or be a part of more complex malformations and is therefore difficult to standardize hypertrophy. As ASDs and VSDs are the most prominent CHDs, this model is applicable to a large portion clinical cases. Furthermore, as minor ASDs and VSDs may close spontaneously, practitioners often would choose to delay surgical intervention. However, the continuous volume overload during this wait time may generate cardiac hypertrophy. Moreover, should the child require surgery despite the wait, the surgeon may be operating on a hypertrophied heart. A model of neonatal cardiac hypertrophy may be useful to elucidate the metabolic and molecular aspects of newborn heart hypertrophy in order to ensure operational safety and success.

However, this model is not without limitations. Inducing the fistula at 7-days postnatally is not true to a CHD as a degree of maturation has taken place. However, newborn rabbits are not fully mature until after weaning (12 weeks). Furthermore, in rabbit hearts, maturational metabolic remodelling continues even into 10 and 14 days after birth (24). This model, hence, is a model that interrupts the maturational process, but produces relevant cardiac hypertrophy and metabolic remodelling.

A second limit is where the aorto-caval fistula is not a cardiac defect as it is an extra-cardiac lesion. As with many peripheral pressure and volume overload cardiac hypertrophy models (44,45), our volume overload model generates

sufficient volume overload hypertrophy. However, this design prevents it from representing a specific type of CHD, rather, it represents the aspect of volume-overload hypertrophy common to multiple defects such as atrio-ventricular septal defects (AVSD). With AVSD as an example, although the present model lacks the valvular defects associated with AVSD, the biventricular hypertrophy is present and an important aspect to understand as it may be the cause for a 27% post-op LV dysfunction in a multi-center study (46). Furthermore, mortality rates from AVSD alone remain between 8.7 to 21.7% (47,48). Studying cardiac hypertrophy and metabolism in isolation from complex defects permits a wide-application of the model as well as unconfounding understanding of hypertrophic cardiac metabolism.

In addition to the animal model of neonatal cardiac hypertrophy, the metabolism and cardiac function were assessed using a bi-ventricular working heart model. This model allows flow through and therefore functional assessment of both the LV and the RV. This is crucial in understanding the neonatal heart because fetal circulation is dependent on the RV. Hemodynamic changes at birth increase pressure and flow to the LV so that the systemic circulation becomes dependent on the LV rather than the RV. However, in volume-overload hypertrophy, increase volume return to the RV alters its post-natal response. In fact, in the present model of neonatal cardiac hypertrophy, bi-ventricular hypertrophy occurs. Hence, assessing global function and metabolism

becomes a more accurate and holistic approach to understanding hypertrophy cardiac metabolism.

6.3 Neonatal Cardiac Hypertrophy Alters Cardiac Metabolism

Although much emphasis is placed on neonatal cardiac FA oxidation, cardiac hypertrophy is associated with a retained fetal-metabolic profile in the neonatal myocardium. The decreased rates of FA oxidation are reciprocated with increased rates of glycolysis. These changes involve both chronic and acute mechanisms.

In both studies from chapters 4 and 5, chronic changes in metabolism originated in changes in the transcriptional control of cardiac metabolism in both the LV and RV, namely reciprocal changes in PPAR α and HIF-1 α . These transcriptional changes diverted the normal maturation towards a more glucose-centered metabolism. Consistent with adult cardiac hypertrophy, these hypertrophic neonatal hearts had notably higher rates of glycolysis accompanied by increased GLUT1 expression and downregulated GLUT4 expression (fig 5-8). Meanwhile, without changes to rates of glucose oxidation, total PDH activities in both studies were decreased in the LV and increased in the RV in chapter 4 but was not changed in chapter 5 (table 4-4 and fig 5-9). The diversity in results may be due to a number of factors including the severity of hypertrophy. To add, these studies examine only one time point in the course of the development of hypertrophy and may not have captured at time point when the changes have

occurred in both models. Nonetheless, in the latter study, LV PDK4 expression was found decreased and corresponded to decreased PDH phosphorylation. This transcriptional change is due to a decreased expression of PPAR α in the hypertrophied heart as PPAR α regulates PDK4 expression (49,50).

The decreased inhibition did not result in changes in glucose oxidation rates and is likely a product of further inhibition on glucose oxidation by other mechanisms not examined here. One possibility is that hypertrophy outstrips a heart of its circulatory supply to cause a relative hypoxic state. This partly contributes to the upregulation of HIF-1 α in hypertrophied hearts. In a relatively hypoxic environment, the heart downregulates its oxidative phosphorylation capacity, including both glucose and FA oxidation, without affecting PDH activity or expression. Alternatively, the finding that glucose oxidation rates remain the same between sham-operated and control hearts suggests that a portion of the glucose oxidation pathway has yet to mature. In comparison, in adult PPAR α null mice, although rates of FA oxidation are significantly downregulated causing a dramatic decrease in its contribution to the acetyl-CoA pool, glucose oxidation is upregulated to compensate for the loss and therefore the total amount of acetyl-CoA is no different in these PPAR α null mice compared to wild type mice (51). Therefore, the dichotomous phenotypes between the adult heart and the neonatal heart suggests that an element of the Randle cycle has yet to mature in the neonatal heart in order that glucose oxidation increases to compensate for lost acetyl-CoA contributions from FA oxidation.

Of the acute regulatory signals, malonyl-CoA has been shown to strongly correlate to rates FA oxidation in myocardium (26,52-54). Though malonyl-CoA inhibition is a type of acute metabolic control, as the expression of the enzymes involved in malonyl-CoA metabolism were changed, a somewhat chronic response resulted in these studies. The aerobic perfusion of the hypertrophied neonatal heart showed no change to cardiac function, but overall steady state ATP production rates were decreased (chapters 4 and 5). This was attributed to increased malonyl-CoA levels in the LV while having no measurable effect on RV malonyl-CoA levels (fig 4-4). When not challenged with added load, this new equilibrium between ATP supply and demand in the two ventricles seems to sustain aerobic work. However, RV malonyl-CoA levels were later found increased in the vehicle-treated IR-perfused hypertrophied hearts in chapter 5. The later study of cardiac hypertrophy also showed signs of *in vivo* cardiac dysfunction with a lowered %EF (Table 5-1) compared to that in chapter 4 (Table 4-1). The differences *between in vivo* cardiac function suggest that when RV malonyl-CoA levels are also increased alongside of that of the LV, systolic dysfunction may result. This possibility is juxtaposed to normal maturation during which the RV is involuting as the LV grows increasingly dominant. To what degree the two ventricles rely on each other was not explored in these studies, but the results presented here suggest that a change in RV acute metabolic control in conjunction to that found in the LV is associated *in vivo* systolic dysfunction.

A second difference between the two studies that may account for the discrepancy is that the latter study was an analysis of hearts subjected to ischemia and reperfusion that may have altered the demands on individual ventricles. In a study of neonatal piglet hearts, differences in metabolic intermediates as well as enzymatic activities were found between the LV and RV in aerobically and ischemia-reperfused perfused hearts (55). Studies in chapters 4 and 5 further emphasize the metabolic differences between the two ventricles, even though the metabolic rates cannot be differentiated between the two ventricles. Despite metabolic differences, the interdependence between the two ventricles amounts to global cardiac dysfunction when challenged with ischemic stress. The rescue treatment with GW7647 involved augmenting malonyl-CoA removal in both ventricles. Incidentally, these changes were achieved by differing mechanisms between the two ventricles.

6.4 Rescuing the Ischemic-Reperfused Neonatal Heart

Previous studies as well as chapter 5 have demonstrated that metabolic manipulation is a viable therapy for normal neonatal heart subjected to ischemic reperfusion (22,28). However, hypertrophied neonatal hearts, a more likely clinical scenario compared to normal hearts, has demonstrated a deranged metabolic profile that may or may not respond to substrate supplementation. These hypertrophied neonatal hearts have lowered ability to oxidize FA and non-compensatory glucose metabolism, despite elevated rates of glycolysis. In

chapter 4, the hypertrophied neonatal heart was unable to recover from ischemia when perfused with only 0.8 mM palmitate; yet, when given 1.2 mM palmitate, these hearts were able to recover. Although FA supplementation improves function recovery, supplementation alone is insufficient as functional recovery of the hypertrophied neonatal heart is only a fraction of that of a normal heart supplemented with FA. Due to the non-compensatory rates of glucose metabolism and post-surgically elevated circulating FA levels, restoring the FA oxidation capacity in these hypertrophied hearts is a clinically-relevant therapeutic option.

GW7647, a PPAR α agonist, was expected to increase PPAR α activity without altering PPAR α expression. Interestingly, while that remained true for the hypertrophied LV, in the RV, PPAR α expression was further increased by GW7647 treatment relative to the vehicle-treated hearts. In contrast, others have shown that chronic PPAR α activation downregulates PPAR α expression in spite of increased expression of target genes (56). In the present study, downstream mRNA, activity, or expression of target genes were upregulated and include: CPT-1 (shown by increased total CPT-1 activity), MCD, LPL, and PDK4. Furthermore, to the best of knowledge, this study showed for the first time an upregulation of AGTL is associated with PPAR α activation. Whether or not AGTL is a target gene of PPAR α requires further exploration. Nonetheless, GW7647 treatment restored the expression of key components to FA metabolism in the hypertrophied neonatal heart.

The restored capacity to mobilize, uptake, and oxidize FA proved beneficial to the ischemia-reperfused hypertrophied neonatal heart at relevant FA levels (1.2 mM palmitate). Functional improvements were evident as post-ischemic functional recovery was restored to normal levels despite the persistent cardiac hypertrophy. The accompanied metabolic profile of increased rates of FA oxidation and decreased rates of glycolysis suggests that the functional improvements are due to increased FA utilization and a consequent suppression of glycolysis. However, in order to definitively determine the effects of PPAR α agonism, it would be prudent to define the effects GW7647 through inhibition studies to demonstrate that when PPAR α or elements of the PPAR α transcriptional complex which would include the receptor, retinoid X receptor (RXR), and its co-activator, PGC-1 α , are downregulated, the effects of GW7647 are lost.

From these studies, restoration of FA oxidation capacity can become a key component to rescuing the hypertrophied neonatal heart from ischemic-reperfusion injury that occurs during cardiac surgery. Although PPAR α agonism does not prevent cardiac hypertrophy in the neonatal heart, as an interim treatment, PPAR α agonism may be a method to improve surgical outcome. Whether this treatment prolongs survival or improve survival would require further studies and understanding of long term effects.

6.5 Conclusion

Unlike adult cardiac hypertrophy whereby the instigating pathology is unlikely to be corrected, neonatal cardiac pathological lesions may be surgically corrected and normal hemodynamics restored. This model demonstrates that hypertrophy secondary to a physical lesion can, alone, alter cardiac metabolism in the neonatal heart. In adult cardiac hypertrophy, modifying cardiac metabolism improves post-ischemic functional recovery. In fact, PPAR γ agonist reverses hypertrophy in the adult heart. Whether correcting the CHD and normalization hemodynamics would normalize metabolism in the neonatal heart, has not been explored. However, this question implicates the importance of these studies on hypertrophied neonatal cardiac hypertrophy.

However, in the interim between surgical correction and immediate post-surgical recovery, the neonatal myocardium is subjected to several hurdles that can potentially be metabolically modified: 1) hypertrophy-related altered cardiac metabolism that is associated with less tolerance to added stress, 2) surgical ischemia, and 3) inotrope challenge/support.

In both normal neonatal hearts and hypertrophied neonatal hearts, a FA-centered metabolism has been clearly demarcated in these studies. A decreased tolerance to ischemia-reperfusion is associated with decreased ability to metabolize FA in these neonatal hearts. In contrast, acute or chronic treatments to augment FA oxidation rates are associated with improved post-ischemic

recovery. These studies demonstrate that by increasing rates of FA oxidation, limitations to ATP production are surmounted. Therefore, metabolic manipulation of FA oxidation potentially provides peri-operative cardioprotection and buffering for added stress, which would increase energy demands.

6.6 Future directions

Studies of the biochemistry and anatomy of the neonatal heart has produced a wealth of knowledge that aids the development of cardioprotective strategies for pediatric cardiac surgery. However, little is known of neonatal cardiac hypertrophy and its impact on surgical cardioprotective strategies and survival. A clinically relevant model of neonatal cardiac hypertrophy was developed in these studies to commence a new generation of neonatal cardiac ischemic-reperfusion studies. However, these studies only represent a small fraction of the applicable knowledge needed to improve surgical outcome. Areas such as drug use and their interaction with a hypertrophied neonatal heart have yet to be explored.

For instance, to prompt further studies of drug use in neonatal hearts, these studies have shown that contrary to the hypothesis, supra-physiological levels of insulin is cardioprotective to the ischemia-reperfused neonatal heart. However, the study was performed in normal 7-day-old rabbit hearts and caused an increase in FA oxidation. While evidence to claim that improved post-ischemic recovery is driven by an increase in FA oxidation, it would be of interest to test

such hypothesis with hypertrophied neonatal hearts. As these hearts have downregulated FA metabolic components, supra-physiological levels of insulin may fail to increase FA oxidation. Should the benefits of insulin be related to its ability to augment FA oxidation, hypertrophied hearts may not demonstrate an equal response to supra-physiological levels of insulin. Of interest, however, is that long-term benefits of high-dose insulin has been demonstrated in adult hearts (57). An acute dose of supra-physiological level insulin was administered as part of a glucose-insulin-potassium regiment after a percutaneous coronary intervention (PCI). At 6 months follow-up, patients treated with the high dose GIK showed improved cardiac function, cardiac index, and lessened cardiac remodelling. Therefore, the application of insulin in hypertrophied neonatal hearts may be of interest as an immediate treatment as well as its chronic outcomes.

In addition to insulin, cardio-stimulants, such as isoproterenol or dobutamine, are often used during the peri-surgical period. However, as they are cardio-stimulatory, they increase energy demands. In a study of the effects of isoproterenol on neonatal hearts, rates of both FA oxidation and glucose metabolism are increased so that the rate of acetyl-CoA consumption exceeds the rates at which it can be generated (58). Therefore, as energy demand increases by these cardio-stimulatory agents, it would not be surprising if in hypertrophied hearts, these agents are detrimental. The decreased ATP producing capacity would limit the efficacy of cardio-stimulation whether

metabolism drives cardiac function as an energy deficit would result. This possible detriment is emphasized by the correlation that increased inotropic support is associated with poor post-surgical outcome and high mortality rates (59). Validating these clinical findings by dissecting the molecular mechanisms underlying the detriments of inotrope support in a clinically-relevant model of neonatal cardiac hypertrophy seems appropriate.

Further understanding of the realities of neonatal cardiac hypertrophy and its treatment beyond surgical correction of the CHD will better define the treatment approach for neonatal patients.

6.7 References

1. Waldhausen JA. The early history of congenital heart surgery: closed heart operations. *Ann Thorac Surg* 1997;64:1533-9.
2. Baum VC. Pediatric cardiac surgery: an historical appreciation. *Paediatr Anaesth* 2006;16:1213-25.
3. Allen BS. The clinical significance of the reoxygenation injury in pediatric heart surgery. *Semin Thorac Cardiovasc Surg Pediatr Card Surg Annu* 2003;6:116-27.
4. Allen BS. Pediatric myocardial protection: a cardioplegic strategy is the "solution". *Semin Thorac Cardiovasc Surg Pediatr Card Surg Annu* 2004;7:141-54.
5. Allen BS, Barth MJ, Ilbawi MN. Pediatric myocardial protection: an overview. *Semin Thorac Cardiovasc Surg* 2001;13:56-72.
6. Amark K, Berggren H, Bjork K, et al. Blood cardioplegia provides superior protection in infant cardiac surgery. *Ann Thorac Surg* 2005;80:989-94.
7. Durandy Y. Pediatric myocardial protection. *Curr Opin Cardiol* 2008;23:85-90.
8. Hammon JW, Jr. Myocardial protection in the immature heart. *Ann Thorac Surg* 1995;60:839-42.

9. Butler TL, Egan JR, Graf FG, et al. Dysfunction induced by ischemia versus edema: does edema matter? *J Thorac Cardiovasc Surg* 2009;138:141-7, 147 e1.
10. Caputo M, Modi P, Imura H, et al. Cold blood versus cold crystalloid cardioplegia for repair of ventricular septal defects in pediatric heart surgery: a randomized controlled trial. *Ann Thorac Surg* 2002;74:530-4; discussion 535.
11. Modi P, Suleiman MS, Reeves B, et al. Myocardial metabolic changes during pediatric cardiac surgery: a randomized study of 3 cardioplegic techniques. *J Thorac Cardiovasc Surg* 2004;128:67-75.
12. Welke KF, Diggs BS, Karamlou T, Ungerleider RM. Comparison of pediatric cardiac surgical mortality rates from national administrative data to contemporary clinical standards. *Ann Thorac Surg* 2009;87:216-22; discussion 222-3.
13. Allen BS. Pediatric myocardial protection: where do we stand? *J Thorac Cardiovasc Surg* 2004;128:11-3.
14. Bolling K, Kronon M, Allen BS, et al. Myocardial protection in normal and hypoxically stressed neonatal hearts: the superiority of hypocalcemic versus normocalcemic blood cardioplegia. *J Thorac Cardiovasc Surg* 1996;112:1193-200; discussion 1200-1.

15. Bolling K, Kronon M, Allen BS, Wang T, Ramon S, Feinberg H. Myocardial protection in normal and hypoxically stressed neonatal hearts: the superiority of blood versus crystalloid cardioplegia. *J Thorac Cardiovasc Surg* 1997;113:994-1003; discussion 1003-5.
16. Basaran M, Sever K, Kafali E, et al. Serum lactate level has prognostic significance after pediatric cardiac surgery. *J Cardiothorac Vasc Anesth* 2006;20:43-7.
17. Cheifetz IM, Kern FH, Schulman SR, Greeley WJ, Ungerleider RM, Meliones JN. Serum lactates correlate with mortality after operations for complex congenital heart disease. *Ann Thorac Surg* 1997;64:735-8.
18. Hannan RL, Ybarra MA, White JA, Ojito JW, Rossi AF, Burke RP. Patterns of lactate values after congenital heart surgery and timing of cardiopulmonary support. *Ann Thorac Surg* 2005;80:1468-73; discussion 1473-4.
19. Siegel LB, Dalton HJ, Hertzog JH, Hopkins RA, Hannan RL, Hauser GJ. Initial postoperative serum lactate levels predict survival in children after open heart surgery. *Intensive Care Med* 1996;22:1418-23.
20. Munoz R, Laussen PC, Palacio G, Zienko L, Piercey G, Wessel DL. Changes in whole blood lactate levels during cardiopulmonary bypass for surgery

for congenital cardiac disease: an early indicator of morbidity and mortality. *J Thorac Cardiovasc Surg* 2000;119:155-62.

21. Lopaschuk GD, Spafford MA. Differences in myocardial ischemic tolerance between 1- and 7-day-old rabbits. *Can J Physiol Pharmacol* 1992;70:1315-23.
22. Ito M, Jaswal JS, Lam VH, et al. High levels of fatty acids increase contractile function of neonatal rabbit hearts during reperfusion following ischemia. *Am J Physiol Heart Circ Physiol* 2010;298:H1426-37.
23. Onay-Besikci A, Sambandam N. Malonyl CoA control of fatty acid oxidation in the newborn heart in response to increased fatty acid supply. *Can J Physiol Pharmacol* 2006;84:1215-22.
24. Onay-Besikci A, Campbell FM, Hopkins TA, Dyck JR, Lopaschuk GD. Relative importance of malonyl CoA and carnitine in maturation of fatty acid oxidation in newborn rabbit heart. *Am J Physiol Heart Circ Physiol* 2003;284:H283-9.
25. Girard J, Ferre P, Pegorier JP, Duee PH. Adaptations of glucose and fatty acid metabolism during perinatal period and suckling-weaning transition. *Physiol Rev* 1992;72:507-62.

26. Lopaschuk GD, Witters LA, Itoi T, Barr R, Barr A. Acetyl-CoA carboxylase involvement in the rapid maturation of fatty acid oxidation in the newborn rabbit heart. *J Biol Chem* 1994;269:25871-8.
27. Itoi T, Huang L, Lopaschuk GD. Glucose use in neonatal rabbit hearts reperfused after global ischemia. *Am J Physiol* 1993;265:H427-33.
28. Saiki Y, Lopaschuk GD, Dodge K, Yamaya K, Morgan C, Rebeyka IM. Pyruvate augments mechanical function via activation of the pyruvate dehydrogenase complex in reperfused ischemic immature rabbit hearts. *J Surg Res* 1998;79:164-9.
29. Scholz TD, Koppenhafer SL, tenEyck CJ, Schutte BC. Ontogeny of malate-aspartate shuttle capacity and gene expression in cardiac mitochondria. *Am J Physiol* 1998;274:C780-8.
30. Lopaschuk GD, Collins-Nakai R, Olley PM, et al. Plasma fatty acid levels in infants and adults after myocardial ischemia. *Am Heart J* 1994;128:61-7.
31. Scohy TV, Golab HD, Egal M, Takkenberg JJ, Bogers AJ. Intraoperative glycemic control without insulin infusion during pediatric cardiac surgery for congenital heart disease. *Paediatr Anaesth* 2011.
32. Bell C, Hughes CW, Oh TH, Donielson DW, O'Connor T. The effect of intravenous dextrose infusion on postbypass hyperglycemia in pediatric patients undergoing cardiac operations. *J Clin Anesth* 1993;5:381-5.

33. Aouifi A, Neidecker J, Vedrinne C, et al. Glucose versus lactated Ringer's solution during pediatric cardiac surgery. *J Cardiothorac Vasc Anesth* 1997;11:411-4.
34. Verhoeven JJ, Hokken-Koelega AC, den Brinker M, et al. Disturbance of glucose homeostasis after pediatric cardiac surgery. *Pediatr Cardiol* 2011;32:131-8.
35. Moga MA, Manhiot C, Marwali EM, McCrindle BW, Van Arsdell GS, Schwartz SM. Hyperglycemia after pediatric cardiac surgery: impact of age and residual lesions. *Crit Care Med* 2011;39:266-72.
36. Canadian Perinatal Surveillance System. Congenital anomalies in Canada : a Perinatal Health Report, 2002. [Ottawa, Ontario]: Minister of Public Works and Government Services Canada, 2002.
37. Tchervenkov CI, Jacobs JP, Bernier PL, et al. The improvement of care for paediatric and congenital cardiac disease across the World: a challenge for the World Society for Pediatric and Congenital Heart Surgery. *Cardiol Young* 2008;18 Suppl 2:63-9.
38. Mangones T, Manhas A, Visintainer P, Hunter-Grant C, Brumberg HL. Prevalence of congenital cardiovascular malformations varies by race and ethnicity. *Int J Cardiol* 2010;143:317-22.

39. Lorell BH, Grossman W. Cardiac hypertrophy: the consequences for diastole. *J Am Coll Cardiol* 1987;9:1189-93.
40. Razeghi P, Young ME, Alcorn JL, Moravec CS, Frazier OH, Taegtmeyer H. Metabolic gene expression in fetal and failing human heart. *Circulation* 2001;104:2923-31.
41. Kantor PF, Robertson MA, Coe JY, Lopaschuk GD. Volume overload hypertrophy of the newborn heart slows the maturation of enzymes involved in the regulation of fatty acid metabolism. *J Am Coll Cardiol* 1999;33:1724-34.
42. Makinde AO, Gamble J, Lopaschuk GD. Upregulation of 5'-AMP-activated protein kinase is responsible for the increase in myocardial fatty acid oxidation rates following birth in the newborn rabbit. *Circ Res* 1997;80:482-9.
43. Park MK. *Pediatric cardiology for practitioners*. 5th ed. Philadelphia, PA: Mosby/Elsevier, 2008.
44. Friehs I, Cao-Danh H, Nathan M, McGowan FX, del Nido PJ. Impaired insulin-signaling in hypertrophied hearts contributes to ischemic injury. *Biochem Biophys Res Commun* 2005;331:15-22.
45. Friehs I, del Nido PJ. Increased susceptibility of hypertrophied hearts to ischemic injury. *Ann Thorac Surg* 2003;75:S678-84.

46. Minich LL, Atz AM, Colan SD, et al. Partial and transitional atrioventricular septal defect outcomes. *Ann Thorac Surg* 2010;89:530-6.
47. Dodge-Khatami A, Herger S, Rousson V, et al. Outcomes and reoperations after total correction of complete atrio-ventricular septal defect. *Eur J Cardiothorac Surg* 2008;34:745-50.
48. Al-Hay AA, MacNeill SJ, Yacoub M, Shore DF, Shinebourne EA. Complete atrioventricular septal defect, Down syndrome, and surgical outcome: risk factors. *Ann Thorac Surg* 2003;75:412-21.
49. Wu P, Inskeep K, Bowker-Kinley MM, Popov KM, Harris RA. Mechanism responsible for inactivation of skeletal muscle pyruvate dehydrogenase complex in starvation and diabetes. *Diabetes* 1999;48:1593-9.
50. Abbot EL, McCormack JG, Reynet C, Hassall DG, Buchan KW, Yeaman SJ. Diverging regulation of pyruvate dehydrogenase kinase isoform gene expression in cultured human muscle cells. *FEBS J* 2005;272:3004-14.
51. Hopkins TA, Sugden MC, Holness MJ, Kozak R, Dyck JR, Lopaschuk GD. Control of cardiac pyruvate dehydrogenase activity in peroxisome proliferator-activated receptor-alpha transgenic mice. *Am J Physiol Heart Circ Physiol* 2003;285:H270-6.

52. Saddik M, Gamble J, Witters LA, Lopaschuk GD. Acetyl-CoA carboxylase regulation of fatty acid oxidation in the heart. *J Biol Chem* 1993;268:25836-45.
53. Cook GA, Lappi MD. Carnitine palmitoyltransferase in the heart is controlled by a different mechanism than the hepatic enzyme. *Mol Cell Biochem* 1992;116:39-45.
54. Hall JL, Lopaschuk GD, Barr A, Bringas J, Pizzurro RD, Stanley WC. Increased cardiac fatty acid uptake with dobutamine infusion in swine is accompanied by a decrease in malonyl CoA levels. *Cardiovasc Res* 1996;32:879-85.
55. Quaglietta D, Belanger MP, Wittnich C. Ventricle-specific metabolic differences in the newborn piglet myocardium in vivo and during arrested global ischemia. *Pediatr Res* 2008;63:15-9.
56. Yue TL, Bao W, Jucker BM, et al. Activation of peroxisome proliferator-activated receptor-alpha protects the heart from ischemia/reperfusion injury. *Circulation* 2003;108:2393-9.
57. Li Y, Zhang L, Zhang H, et al. High-dose glucose-insulin-potassium has hemodynamic benefits and can improve cardiac remodeling in acute myocardial infarction treated with primary percutaneous coronary

intervention: From a randomized controlled study. *J Cardiovasc Dis Res* 2010;1:104-9.

58. Jaswal JS, Lund CR, Keung W, Beker DL, Rebeyka IM, Lopaschuk GD. Isoproterenol stimulates 5'-AMP-activated protein kinase and fatty acid oxidation in neonatal hearts. *Am J Physiol Heart Circ Physiol* 2010;299:H1135-45.
59. Gaies MG, Gurney JG, Yen AH, et al. Vasoactive-inotropic score as a predictor of morbidity and mortality in infants after cardiopulmonary bypass. *Pediatr Crit Care Med* 2010;11:234-8.